Spring 5-2020

Sedimentary Dynamics and Water Quality in Floodplains of the Lower Mississippi River near Natchez, Mississippi, during the 2018 and 2019 Floods

Jansen Costello

SEDIMENTARY DYNAMICS AND WATER QUALITY IN FLOODPLAINS OF THE LOWER MISSISSIPPI RIVER NEAR NATCHEZ, MISSISSIPPI, DURING THE 2018 AND 2019 FLOODS

by

Jansen D. Costello

A Thesis
Submitted to the Graduate School,
the College of Arts and Sciences
and the School of Biological, Environmental, and Earth Sciences
at The University of Southern Mississippi
in Partial Fulfillment of the Requirements
for the Degree of Master of Science

Approved by:

Dr. Franklin T. Heitmuller, Committee Chair
Dr. Davin Wallace
Dr. Paul F. Hudson
Dr. T. Markham Puckett

May 2021

Published by the Graduate School

ABSTRACT

The Lower Mississippi River (LMR) near Natchez, Mississippi, experienced intervals of major flooding during the 2018 and 2019 water years. While federal agencies sample sediment and water quality in the main LMR channel, little is known about sedimentary dynamics, water quality, and nutrient concentrations of the overbank water column within the embanked LMR floodplain. These data are needed to support ecological floodplain restoration efforts and provide context for downstream concerns including sediment delivery to coastal zones and hypoxia in the Gulf of Mexico.

This study monitored the overbank flood pulses and associated sediment deposition along the LMR embanked floodplain during water years 2018 and 2019. Between March and May 2018, the LMR at Natchez flooded with a maximum stage of 17.41 m (57.12 ft), qualifying as the 5th highest crest on record. The river receded but remained above normal stages through September when another rise pushed the river above action stage through January 2019, when the river exceeded flood stage through July resulting in a new flood duration record (212 days to date) and a maximum stage of 17.65 m (57.91 ft) on March 12th (third highest on record). Measured depths of the water column above the floodplain surface ranged from 2.60 to 7.75 m during the crest. Flow velocities measured at a 1.22 m depth across the floodplain ranged from 0.07 to 1.06 m/s.

Floodplain surface deposits were sampled in October 2017 and September 2018 before the onset of flood events; these were analyzed for grain size, organic matter (OM) content, magnetic susceptibility (MS), and total carbon (C) and adsorbed nutrients (N, P). Flood water and suspended sediment of the overbank water column were sampled during the 2019 flood (March and June), which included in situ measurements of temperature,

pH, dissolved oxygen, and total dissolved solids. Suspended sediments in bottled samples were analyzed for concentration (SSC), grain size, carbon, and nutrients. Water in bottled samples was analyzed for dissolved phosphorus and nitrite-nitrate.

Overbank sediment properties in different hydrologic and geomorphological settings vary with proximity to the main channel. Floodplain surface and suspended sediments decrease in grain size (D50) as distance increases from the LMR channel. Generally, OM, C, N, and P increase with a decrease in grain size. An increase in suspended sediment concentrations and larger in grain size are directly correlated with an increase in overbank flow velocity and increased turbidity.

Using analysis of covariance (ANACOVA) (with D50 as the covariant), OM, C, and nutrients were statistically higher with distance from the LMR channel; OM, C, and nutrients were statistically higher in backswamps and swales relative to the other subenvironments. Subenvironment classifications (levee, backswamp, meander scroll) had a stronger correlation to grain size than grouping the data by year. When the data was grouped by year, little significance was found using ANACOVA.

Overbank water quality samples in 2019 were very similar among sampling sites during the same sample trip (i.e., same time). However, most parameters including temperature, pH, and dissolved carbon and nutrients were greater in June than March because of both seasonal influences and event hysteresis. Due to hysteresis peaks, suspended sediment concentration, nitrate plus nitrite, and phosphorus had peak values after the peak stage height, with no peak concentrations corresponding with maximum stage height. In both March and June, suspended sediment, phosphorus and nitrite-nitrate were lower than corresponding values in the LMR main channel.

ACKNOWLEDGMENTS

I am highly gratified to be able to thank the following people for all their help and support throughout these last two years in order to fully complete my thesis project to its fullest potential. First of all, this project wouldn't be what it is today without the dedication of my advisor Dr. Frank Heitmuller who constantly was there for guidance, support, encouragement, and much needed knowledge. I would also like to offer my sincere thanks to my committee members: Dr. Davin Wallace, Dr. Paul F. Hudson, and Dr. T. Markham Puckett. I wish to extend my gratitude to Dr. Kuehn and Dr. Halvorson (lab members, lab equipment, and guidance), Kent Ozment (sediment collection, field safety, etc.), Samuel Munoz (sample collection), and Dr. Schaefer (jon boat, etc.).

Much gratitude is needed for the to the School of Biological, Environmental and Earth Sciences and School of Ocean Sciences and Engineering at Stennis Space Center for equipment and instruments used. I also convey my gratitude to my sources of funding including: GSA (grant), Nature Conservancy (grant), and Dr. Paul Hudson (stage sensors). I am also thankful to the research permit from St. Catherine Creek, U.S. Fish & Wildlife Service (field study) , and the landowner MR. Jerry Edwards.

Lastly, much love and dedication from my family, especially my mom, dad, aunt, cousins, and friends. Without them behind me this project would not be to the caliber it is today.

TABLE OF CONTENTS

LIST OF TABLES

LIST OF ILLUSTRATIONS

LIST OF ABBREVIATIONS

GCP	ground control points
GOM	Gulf of Mexico
LMR	Lower Mississippi River
LMV	Lower Mississippi Valley
MS	Mississippi
OM	organic matter
PT	pressure transducer
SCCNWR	ST. CATHERINE CREEK NATIONAL WILDLIFE REFUGE
SE	subenvironment
SS	suspended sediment
V	velocity

CHAPTER I INTRODUCTION

Rivers are an essential part of the hydrologic cycle and transport water, sediment, and dissolved constituents from terrestrial sources to oceans, lakes, and ephemeral basins. River flows widely vary from low discharges during drought conditions to overbank floods. Daily average flows can fluctuate depending upon climatic variables in the watershed. It has been recognized that flow variability is essential to maintain morphologic equilibrium of river channels (Leopold et al., 1964), effectively transport sediment (Wolman and Miller, 1960), and support healthy aquatic and riparian ecosystems (Junk et al., 1989; Poff et al., 1997). Of particular relevance to this study is the connectivity between large rivers and surrounding floodplains during major flood events, including overbank transport and depositional processes along heavily impacted embanked (i.e., flood-control levees / dikes) rivers.

This study investigates overbank sedimentary characteristics and selected water quality parameters along the embanked Lower Mississippi River (LMR) floodplain in Adams and Wilkinson counties, Mississippi, in association with large flood events in 2018 and 2019. Sampling locations in the floodplain varied with respect to distance from the main channel and included different depositional sub-environments (i.e., natural levee, meander scroll, backswamp). The study design supported a better understanding of sediment exchange from the channel to the floodplain and will identify changes to water quality, including carbon and nutrients, across the floodplain.

The two water years between October 1st, 2017 and September 30th, 2019 included two large historic flood events. The flood of 2018 started on March 1st and continued for 68 days above the flood stage of 14.63 m (48 ft) at Natchez, MS

(03/01/2018 – 5/8/2018). This flood had a maximum stage of 17.41 m (57.12 ft), qualifying as the fifth highest crest on record at Natchez (03/18/2018). Again in 2019, the LMR rose above flood stage between January and August (01/05/2019 – 08/05/2019) resulting in a new flood duration record (212 days) with a maximum stage of 17.65 m (57.91 ft) on March 12th (third highest historic crest) at Natchez. The only two floods in recorded history that surpassed those in 2018 and 2019 at Natchez occurred in 1937 and 2011 (U.S. Army Corps of Engineers, 2020).

A refined knowledge of the effects of Mississippi River flooding will advance our understanding of sediment, carbon, and nutrient delivery to passive continental margins; and facilitate efforts to re-establish ecosystem services in the floodplain, prevent flood disasters, ameliorate coastal land loss in Louisiana, and reduce offshore hypoxia.

1.1 RESEARCH QUESTIONS

1.1.1 QUESTION 1

Are floodplain sediments deposited in various floodplain sub-environments (i.e., natural levees, meander scrolls, backswamps) different from each other (i.e., grain size, composition)? Are overbank sediment deposit characteristics similar before and after the 2018 flood?

1.1.2 QUESTION 2

Does floodplain topography result in spatially unequal flood durations and stages during the rising and falling limbs of the flood hydrograph? Do hydrograph patterns differ in all study locations, including LMR main channel locations?

1.1.3 QUESTION 3

Are water quality (including dissolved carbon, nitrogen, and phosphorus) and

suspended sediment (including concentration; grain size; and adsorbed carbon, nitrogen, and phosphorus) different during the 2019 flood event (samples collected in March and June) within the overbank water column? Does the concentration of carbon, nitrogen, and phosphorous differ between soluble and adsorbed forms? Are suspended sediment characteristics, water temperature, and selected water-quality parameters (including carbon, nitrogen, and phosphorus) across the embanked floodplain during the 2019 flood comparable to contemporaneous values in the main river channel? How do these parameters vary across embanked floodplains during large overbank floods? Is water temperature directly associated with dissolved carbon and nutrients in the overbank water column?

1.2 HYPOTHESES

1.2.1 HYPOTHESIS 1

Overbank sediment deposit characteristics will differ according to depositional sub-environment and proximity to the main channel (Saucier, 1994; Heitmuller et al., 2017). Relatively coarse sands and silts are associated with natural levees and, to a lesser extent, meander scroll ridges, whereas fine silts and clays are associated with backswamps and meander scroll swales. Grain size will be coarser for sediments deposited by the 2018 flood because of its relatively high magnitude relative to floods during the preceding 5 years (presumed to be the sources of floodplain surface sediments that were sampled in October 2017). Sorting should remain the same for a given median grain size within a particular sub-environment. Sorting will decrease with less floodplain space for lateral deposition, especially in constricted embanked floodplain locations (Hudson et al., 2008). Organic matter content will be greater in pre-flood samples and

magnetic susceptibility will correspond to lithology of the contributing tributary watershed(s) in flood (Saucier, 1994; Heitmuller et al., 2017).

Overbank sediment deposition depends on the magnitude, duration, and shape of the flood hydrograph. A high-magnitude flood will result in deposition of sand in close proximity to the main channel (Middelkoop and Asselman, 1998). The pattern and timing of flood recession has a large influence on depositional patterns as well. Flood deposits should only consist of silty clay beyond more than 50 to 100 meters from the natural levee (Middelkoop and Asselman, 1998).

Nutrients (nitrogen and phosphorus) adsorbed to sediments deposited during the flood of 2018 (suspended sediment) will have a similar adsorption and sequester rates than that of sediments from previous flood years (Schramm et al., 2009). Floodplain vegetation and decomposition will remain at low levels until the flood water has receded and is fully drained (Bonyongo and Mubyana, 2004). The sediment that was previously deposited will have decreased levels of nutrients because of consumption by the vast amount of vegetation and microbial activity active in the floodplain (Bonyongo and Mubyana, 2004). For a given depositional sub-environment (similar grain sizes (silt, sand, etc.)), nutrient levels will be constant within sediment from the same flood (Bonyongo and Mubyana, 2004).

1.2.2 HYPOTHESIS 2

The timing of inundation on the rising limb and drainage on the receding limb will effect the overall hydrographic pattern of the 2018 and 2019 flood. Pertaining to floodplain topography, areas that are “blocked” off from the LMR as opposed to areas that have direct access to the main channel will have higher flood stages. Rosenqvist et

al. (2002) shows a contrast in duration of flooding within different sub-environments and locations with proximity to a meander on the Jaú River. Stage height will remain constant once the stage is high enough, then everything is submerged and, of course, a uniform water-surface (and downstream slope) is achieved.

1.2.3 HYPOTHESIS 3

During the two water sampling periods (March and June 2019), water quality and suspended-sediment characteristics will differ depending on the timing of the flood hydrograph (i.e., hysteresis). Suspended-sediment loads have been found to be high during the winter and early spring (for large discharge events) along the LMR (Mossa, 1989). Therefore, suspended sediment concentrations during the 2019 flood should be greater during March than June.

Suspended sediment concentration and grain size in the overbank water column will be less than in the main channel. Concentration and grain size in the overbank water column will decrease as overbank flow distance from the main channel increases due to roughness imparted by submerged vegetation, topography, and associated deposition (Pizzuto, 1987).

Selected water quality values (dissolved constituents) will remain similar across the floodplain with overbank flow distance from the main channel. These values will include decreases in pH (organic acid contributions) and dissolved oxygen (mg/L), and increases in conductivity (mS/cm) and inorganic forms of carbon (%), nitrogen (%), and phosphorus (%) in association with direct additions from the floodplain (Bonyongo and Mubyana, 2004).

Nitrogen will gradually decrease with prolonged durations of inundation. Because the 2019 flood was the longest duration in recorded history along the LMR, there should be a large amount of nitrogen sequestration into the soil and adsorbed to suspended sediment. Soil is the main sink for nitrogen removal during times of overbank flow. However, soil was found to be a source for phosphorus instead of a sink (Schramm et al., 2009). Particulate phosphorus, adsorbed to suspended sediment, makes up 68% of total phosphorus during flooding periods (Schramm et al., 2009). Water temperatures above 17 ^{O}C and prolonged flood durations will increase nitrogen and phosphorus uptake as organism activity increases, including planktonic communities that will sequester, remove, and utilize these nutrients (Schramm et al., 2009).

1.3 SCOPE OF WORK

Table 1.1 *Research trips to the study areas*

[NWR, National Wildlife Refuge; C, carbon; N, nitrogen; P, phosphorus; m, meters; m/s; meters per second; °C, degrees Celsius; mg/L, milligrams per liter; µs/cm, microsiemens per centimeter; ppt, parts per thousand; mV, millivolts; µg/l, micrograms per liter]

Research Trip	Study Areas	Purpose	Lab Analysis
10/15/2017 – 10/20/2017	St. Catherine Creek NWR; Loch Leven and Artonish Lake area	Collect floodplain surface sediment samples and install water level & temperature sensors	Physical size, organic matter, magnetic susceptibility, color, nutrient analysis (C, N, and P)
9/8/2018 – 9/10/2018	St. Catherine Creek NWR; Artonish Lake area	Collect floodplain surface sediment, collect a vertical section of flood sediment	Physical size, organic matter, magnetic susceptibility, color, nutrient analysis (C,N, and P)
3/10/2019 – 3/13/2019	St. Catherine Creek NWR: Sibley Unit, Cloverdale Unit, and Artonish Lake area and Fort Adams	Collect water quality data and water samples for lab analysis	Depth (m), velocity (m/s), turbidity, temperature (°C), dissolved oxygen (% and mg/l), conductivity (µs/cm), total dissolved solids (mg/l), salinity (ppt), pH, oxidation reduction potential (mV), suspended sediment, physical size, nutrient analysis (phosphorus (µg/l), nitrite-nitrate (µg/l), and ammonia (µg/l))
6/21/2019 – 6/23/2019	St. Catherine Creek NWR: Sibley Unit, Cloverdale Unit, and Artonish Lake area and Fort Adams	Collect water quality data and water samples for lab analysis	Depth (ft.), velocity (m/s), turbidity, temperature (°C), dissolved oxygen (% and mg/l), conductivity (µs/cm), total dissolved solids (mg/l), salinity (ppt), pH, oxidation reduction potential (mV), suspended sediment, physical size, nutrient analysis (phosphorus (µg/l), nitrite-nitrate (µg/l), and ammonia (µg/l))

CHAPTER II – LITERATURE REVIEW

2.1 RIVER AND FLOODPLAIN CHARACTERISTICS (SEDIMENT DEPOSITION)

2.1.1 MEANDERING ALLUVIAL RIVER SYSTEMS AND FLOODPLAINS

Meandering alluvial rivers ~~laterally~~ migrate through previously deposited sediments within a valley bounded by considerably older, resistant lithologic units. A floodplain is the region that is inundated when the river channel rises in stage above a specific height and laterally transfers water and sediment into adjacent areas. Deposition of alluvium (unconsolidated sediment) occurs during times of inundation. High-magnitude flood events (low-frequency flood) exert a considerable impact upon the floodplain due to transportation of large amounts of sediment (Wolman and Miller, 1960). Flood events can alter floodplain morphology and landforms on a seasonal basis (Wolman and Gerson, 1978). Within the floodplain, a majority of deposition and sometimes erosion, occurs during times of inundation (dry periods have low rates of deposition) (Saucier, 1994).

In a meandering river floodplain, variable rates of deposition and erosion are dependent on proximity to the channel and hydraulic patterns established by the sinuous channel course (Saucier, 1994; Hudson and Heitmuller, 2003). A large flood event deposits a new layer of sediment throughout the floodplain, with some areas receiving more sediment than others. During the 1973 flood along the Lower Mississippi River (LMR), an average of 53 cm of sediment was deposited on the natural levee; in comparison, only a minute amount was deposited in backswamps distal from the main channel (Kesel et al., 1974). The actively migrating channel and associated pattern of

flood deposition creates a sequence of overbank areas: natural levee (crest), levee backslope, backswamp (flood basin), meander scroll (ridge and swale topography), and valley wall (bluff line) (Saucier, 1994).

2.1.2 MEANDERING RIVER FLOODPLAIN PROCESSES

Active channels are where the main discharge of the river occurs. Perennial flow is characteristic of large rivers in humid regions, whereas seasonal flow variability is common depending upon climatic patterns and conditions. A meandering channel will migrate because of cutbank erosion and point bar deposition, which progressively results in floodplain consumption and floodplain development (migration and deposition of sediment) for decades to centuries in an alluvial valley. Channel migration correlates to river competence and channel gradients throughout the fluvial regime (Fisk, 1944). Throughout the Holocene, the LMR has migrated and its floodplain has been altered regularly (Coleman, 1966). The pattern of migration is visible by the positions of abandoned channels, natural levees, and crevasse splays within former meander belts. (Farrell, 1987).

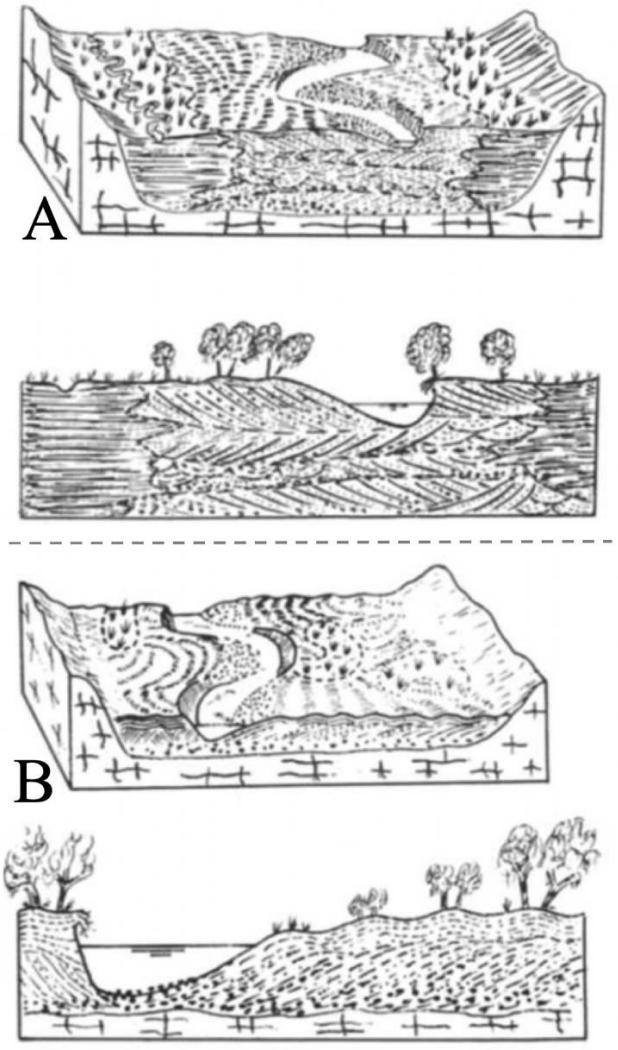

Figure 2.1 *Representation of a the different classifications of floodplains (edited from Nanson and Croke, 1992). Diagram A is a lateral migration/backswamp floodplain and diagram B is a lateral migration/scrolled floodplain.*

2.1.2.2 POINT BARS

Point bars are depositional features of a meander belt in which sediment is deposited on the convex side of the river channel. Characteristics of these convex features include coarse-grained sediment (sand and silt), relatively low turbulence, and slow velocity. More specifically, these conditions result in submerged dunes in the adjacent stream channel due to helical flow, which migrate in shallow water as transverse bars and

sand waves (Saucier, 1994). Through time, a vertical sequence of sedimentation was found. The pattern in the lithology was found to have a fining upwards pattern of sedimentary structures as the bar grows vertically (Bluck, 1971).

Point bars usually form during high stream stages (annual floods) as lateral migration is activated. The larger the flood (higher velocity, load, sediment size, etc.), the more rapid the deposition and migration of a point bar. During high-flow events, cutbanks erode through bank caving processes and resupply sediment into the channel, which eventually can be deposited along a downstream point bar (Saucier, 1994).

2.1.2.3 RIVER CUTOFF

As a result of channel migration through time, meanders often become abandoned because of a change in the flow direction and position of the main channel. This happens through two different styles: “neck cutoffs” and ”chute cutoffs” (Saucier, 1994). A “neck cutoff” is formed when two active meander bends become too close to each other and a breach is created at their intersection, producing a new main channel and an abandoned channel segment (Saucier, 1994). Farrell (1987) showed the neck cutoff of the MSR that occurred between 1200 YRS.B.P and present (Figure 2.2)(Farrell, 1987). A “chute cutoff” occurs when a major flood event erodes and scours across a sloping point bar through a major swale (Saucier, 1994). These two processes differ in that neck cutoffs occur more rapidly and more frequently, whereas development of a “chute cutoff” takes decades and happens less frequently due to the rarity of major flood events.

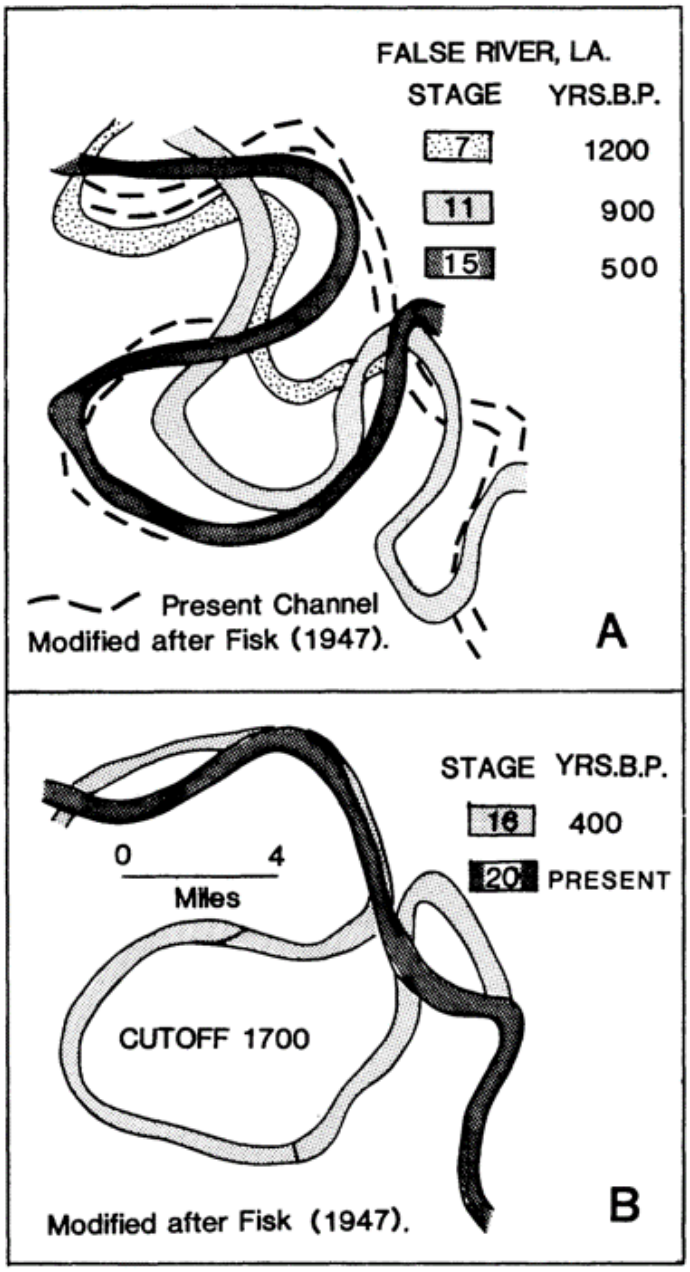

Figure 2.2 *Migratory pattern of the MSR with a neck cutoff taking place in 1700 CE (Farrell, 1987).*

Once the channel is abandoned, neck cutoffs will deposit sand bars at its upper and lower arms, creating an oxbow lake (Saucier, 1994). Oxbow lakes are not directly connected (no river throughflow) to the main channel; however, small batture channels allow flow between locations during low stages. During high stages, water is transferred

from the main channel to the oxbow lake. Deposition within oxbow lakes is influenced by three factors: points of inflow, flow patterns, and lake morphology (Cooper and McHenry, 1989). Because oxbow lakes are disconnected from the main channel, larger sediment (sand and coarse silt) no longer reaches the abandoned channels during regular conditions (Saucier, 1994). Therefore, oxbow lakes slowly fill through time with fine-grained sediment resulting in sediment wedges or clay plugs. Once filled with clay, the abandoned channel is classified as a fresh water marsh or swamp. In some cases, continuous migration and meandering of the main channel will either maintain a constant connection to the oxbow lake creating a dense swamp forest, or even reconnect to the lake, recreating the main channel. If the main channel migrates a considerable distance from the abandoned channel, the oxbow can become a relatively deep, semi-permanent water body through time (Saucier, 1994).

2.1.3 DEPOSITIONAL SUBENVIRONMENTS

2.1.3.1 NATURAL LEVEES

A natural levee is an accumulation of sediment on the banks of a river, creating a relatively high ridge that borders a channel and separates it from the distal floodplain (Saucier, 1994). Natural levees develop from progressive deposition of suspended sediment, commonly ranging in grain size from medium sand to silt. On the cutbank side of the meander, the levee crest is better developed and more mature, in comparison to the point bar side (Allen, 1965; Saucier, 1994). Depending on the meander morphology, natural levees are wider as curvature decreases (Hudson and Heitmuller, 2003). Throughout a meander bend sequence, the levees alternate sides depending on the cutbank position (Fisk, 1947; Iseya and Ikeda, 1989). In proximity to the main channel,

cutbanks erode and undercut natural levees resulting in older and steeper levees. On the opposite side, the point bar extends through deposition and new levees are created.

During floods, water and sediment from the main channel can overtop the levee and inundate the floodplain, or breach the levee to create a new temporary route through a crevasse. Breaches in the levee form a fan-shaped deposit of relatively coarse sand and silt on the landward side of the breach (a crevasse splay deposit). Natural levees affect the amount of water and sediment reaching the distal floodplain and routes of inundation during flood periods (Brierley, 1997). For the majority of the year, however, and even during minor floods, the natural levee remains dry.

Varying levels of overbank hydraulic energy during a flood results in different grain sizes of sediments deposited in a floodplain. The closer the proximity to the stream, the larger the grain size and amount of sediment that is deposited (Fisk, 1944,1947; Farrell, 1987). Consequently, natural levees include larger grain sizes compared to distal floodplain environments. Sediment deposited on the levee will always be finer grained than in the active channel and coarser grained than the distal floodplain (Miall, 1985; Collinson, 1996; Hudson and Heitmuller, 2003). The backslope of the levee gradually transitions into lower parts of the floodplain. Size and height are directly influenced by the time allotted for deposition or age of the levee (Saucier, 1994). Consequently, the older the levee, the larger the dimensions it has. Hudson and Heitmuller (2003) documented a positive relationship between drainage area, sediment load, and levee size in a basin-scale model along the meandering Pánuco River and tributaries in Mexico. The average dimensions of levees along the LMR were 4.57 m (15 ft) high and 3.22-4.83 km

(2-3 miles) wide (Saucier, 1994; Brierley et al., 1997). As sediment size decreases toward the coast, the levee size decreases and becomes more fine-grained (Kolb, 1962).

2.1.3.2 FLOOD BASIN / BACKSWAMPS

Backswamps are the lowest areas (depressions) of a floodplain between meander belts and natural levee slopes (meander scrolls, alluvial valley walls, or terrace scarps) (Saucier, 1994; Aslan and Autin, 1999). The terms "flood basin" and "backswamp" are used interchangeably. These areas are inundated during a flood and remain ponded during the flood recession due to few drainage outlets for the flood water. This creates swamps (fresh water) and small sloughs (Aslan and Autin, 1999). Backswamp deposits are dominated by fine silts and clays that slowly settle out of suspension (Coleman, 1966; Farrell, 1987). Natural levees sequester the relatively coarse-grained suspended sediment and preclude sands from reaching backswamps except through crevasse channels. Backswamp clay deposits inhibit vertical drainage and trap water for months (seasons) throughout the year (Saucier, 1994). If water is extensive and predominant for long durations, the area could be considered a flood basin lake. However, the water supply is usually variable, with water being present for several months and then dry for the remainder of the year. The variability of water levels and flood durations creates a harsh environment that limits permanent vegetation to hydrophytic trees such as bald cypress (*Taxodium distichum*) and tupelo (*Nyssa sylvatica*) in the Lower Mississippi Valley (LMV).

In the study region near Natchez, it is estimated that there are ~18.3 m (60 ft) of clay (with sand and silt lenses) out of ~40 m of alluvial sediment (Fisk, 1944; Fisk, 1947)

deposited above older glacial outwash (Hudson et al., 2013). These sediments have been dated to be as old as 10,000 yr. BCE (McFarlan, 1961).

2.1.3.3 MEANDER SCROLLS

Meander scrolls are arcuate planform features representing the historical lateral migration patterns of a river across its alluvial valley. Meander scroll areas are characterized by semi-parallel topographic ridges and swales that corresponded to the direction of channel migration (Gagliano and van Beek, 1970; Saucier, 1994) (Figure 2.3). The ridges consist of relatively coarse sediments of the former natural levee position, whereas the swales are the lower parts of the point bar, in some instances a former chute channel, and is filled with relatively fine-grained sediment (Saucier, 1994). The sequential nature of ridges and swales indicates pulses of channel migration that occur during high-magnitude flows (e.g., flood events). A higher amount of clay gets deposited compared to sand during periods of crevassing and avulsion in depressions (swales) (Kraus and Aslan, 1993; Willis and Behrensmeyer, 1994). Meander scroll areas play an important role during flood events, where they act as pathways for inundation. When the flood recedes, water collected in the swales facilitates fine-grained particles (i.e., clays) to settle.

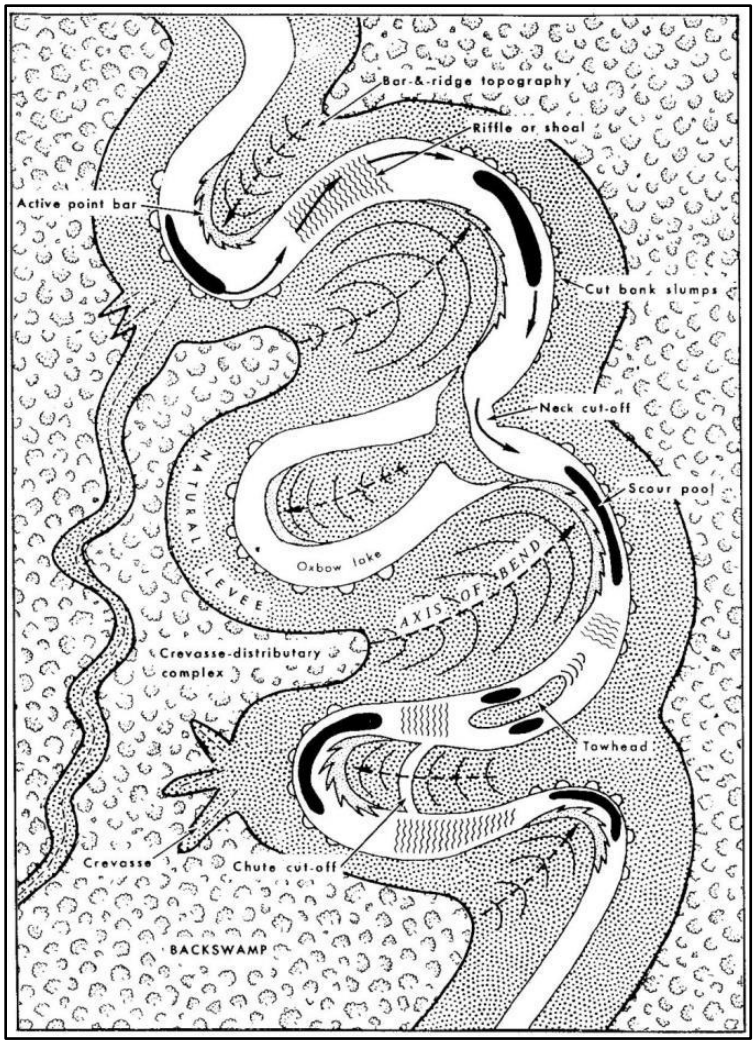

Figure 2.3 *A schematic representation of a meandering river migration pattern, including cutoffs and meander scrolls (Gagliano and van Beek, 1970).*

In local depressions within the floodplain, a 50 to 100 percent increase in sediment deposition will be shown when compared to higher elevated areas (ridges) (Middelkoop and Asselman, 1998). However, lateral variations will exist throughout the floodplain, with areas of ponding having a higher effective deposition of suspended sediment (Walling and He, 1998). Deposition in low topographic areas will have a maximum accumulation during low floods, but with a longer duration (Middelkoop and Asselman, 1998).

2.1.4 CREVASSE SPLAYS

A meander belt crevasse is a channelized gap of water flow that forms due to a breach in a levee. These diversions of ~~a~~ water from a river can also occur in proximal coastal and lacustrine basins, but this discussion will focus on floodplain crevasse splays (North and Davidson, 2012; Yuill et al., 2016). Crevasse splays are thin layers of sediment deposits (minideltas) in the flood plain (Saucier, 1994). The "crevasse" is the actual breach of the bank or levee and the "splay" is the sediment that is deposited during inundation (Welder, 1959; Pizzuto, 1987; Cahoon et al., 2011; Fagherazzi et al., 2015). The sediment transport mechanism is similar to a delta system in which fine sediment (clay) is located at the furthest extent of the plume. The actual location of the crevasse will contain relatively coarse sediment.

Crevasses are small (~1/4 mi) in comparison to the natural levee itself (Saucier, 1994). They often form during multiple events, over multiple years, creating incremental series of patterns. However, during large flood events, large crevasse splays can form at once. Along the False River, a crevasse splay formed, with seven main crevasses creating the entirety of the splay (Figure 2.4) (Farrell, 1987). Crevasses typically do not last long because they quickly fill up with coarse sediment. The three factors that will terminate a crevasse splay are: loss of hydraulic energy, reduction of flow depth, and/or increased hydraulic roughness (Kleinhans et al., 2008, 2013; Sloff and Mosselman, 2012). As transport capacity and bed slope decline, the crevasse aggrades and backfills to the main channel, leading to closure (Coleman, 1969; Roberts, 1997).

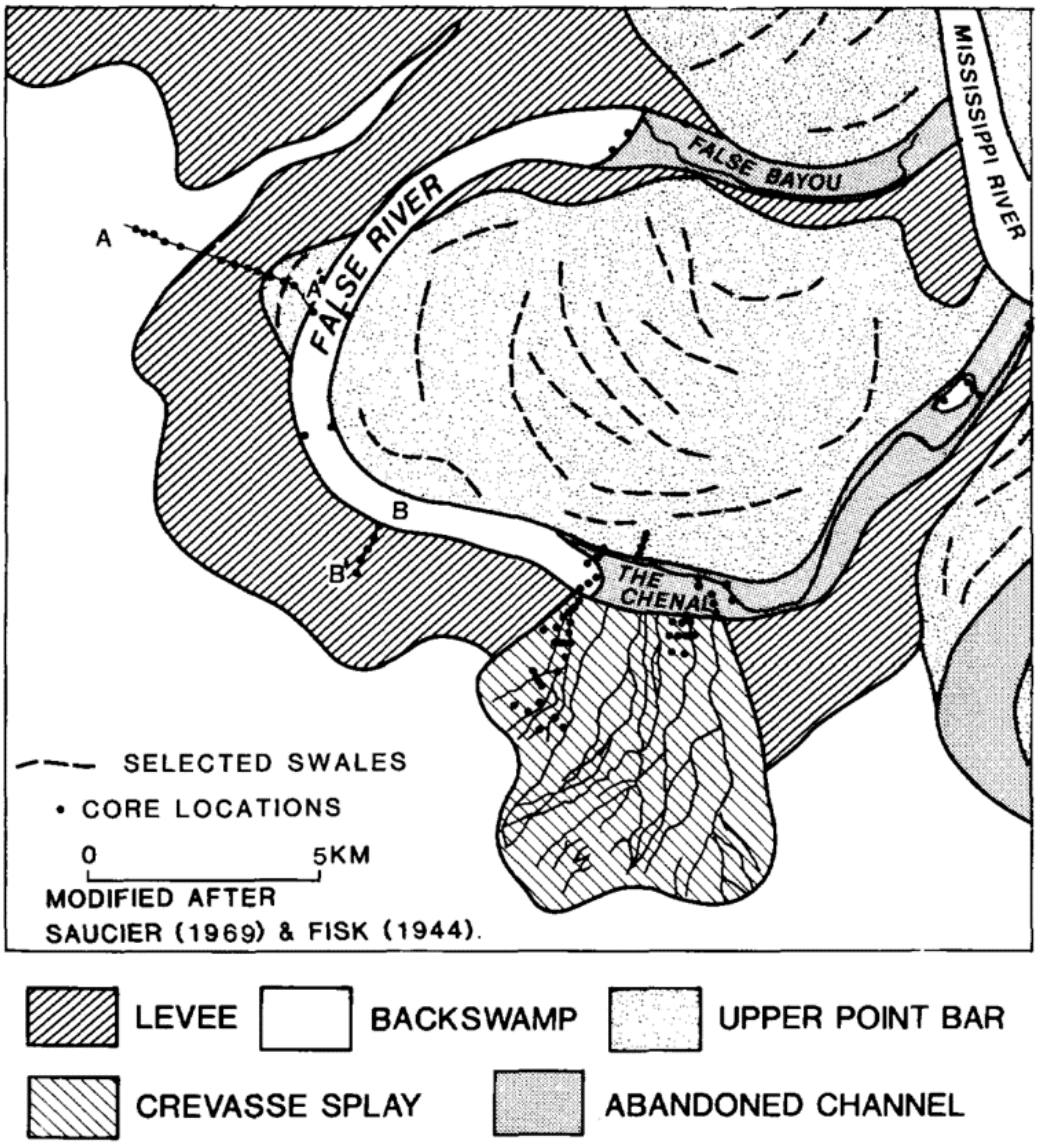

Figure 2.4 *A schematic representation of crevasse splay on the False River, and oxbow lake of the Lower Mississippi River. (Farrell, 1987).*

2.1.5 NUTRIENTS SEQUESTRATION

Nutrients are a large part of the health of a river floodplain. Floodplains are important material sinks for rivers to help reduce the amount of nutrients being transported downstream. This nutrient uptake often occurs during periods of flooding (Pinay et al., 1992). River channels have low nutrient retention rates (transporting most of their load downstream), making nutrient sequestration in the floodplains even more

imperative (Alexander et al., 2000). Nutrients are processed well in floodplain wetlands due to their natural processes of oxidation-reduction interfaces, high rates of decomposition and productivity, and high nutrient loading rates (Noe and Hupp, 2005). Floodplain wetlands are also great locations for nursery grounds for fisheries, regional biodiversity, riverine metabolism, and a trophic base in landscapes (Welcomme, 1979; Brinson et al., 1981; Salo et al., 1986; Cuffney, 1988; Junk et al., 1989; Meyer et al., 1997).

Nitrogen and phosphorous sequestration can only readily occur during specific temperature, oxygen levels, and water conditions. Nitrate will turn into nitrous oxide or mineral nitrogen through microorganisms releasing gas as a waste product (Forshay and Stanley, 2005). Phosphorus is scarce during aerobic conditions, but increases during periods of flooding where anaerobic conditions take place (Brady and Weil, 1999). This increase in phosphorous occurs due to the dissolution and reduction of iron phosphates, release of clay-bound phosphates, and dissolution of ion and aluminum phosphates (Gambrell and Patrick, 1978).

Nutrient sequestration can also occur by the biota of the living organisms in the floodplain during times of inundation. For aquatic biota (excluding fish) the two main types of organisms that drive the sequestration are primary producers and biofilm organisms attached to vegetation in the water column. The primary producers (phytoplankton and other photosynthesizing microbes) will uptake the most nutrients during times of increased temperature, long flooding durations (retention time), and a low amount of inorganic turbidity (Schramm et al., 2009). Once deceased these organisms will be incorporated in the sediment. However, biofilm organisms attached to wetland

plants work together to remove nutrients from the soil (plants) and within the water column (biofilm organisms). These organisms have a relatively long lifespan and continue to sequester after the flood water has receded. The nutrients from the biofilm organisms are consumed by invertebrates as a final route within the floodplain (Schramm et al., 2009). Additionally, flood duration has a large influence on fish feeding and growth rates. Studies have shown a positive relationship between production of floodplain fish and extent of inundation (Gutreuter et al., 1999; Schramm et al., 2000; Schramm and Eggleton, 2006).

Noe and Hupp (2005) found an average of nutrient accumulation measurements to be: carbon between 61 to 212 $g \cdot m^{-2} \cdot yr^{-1}$, nitrogen between 3.5 to 13.4 $g \cdot m^{-2} \cdot yr^{-1}$, and phosphorus between 0.2 to 4.1 $g \cdot m^{-2} \cdot yr^{-1}$ for the eight floodplains collected in Chickahominy River (urban), Mattaponi River (forested), and Pocomoke River (agricultural) over a six-year time of deposition.

Schramm et al., (2009) found rates of nitrogen sequestration by aquatic ecosystems and soils to be between 542 and 976 kg nitrogen ha^{-1}. Soil is by far the most efficient part of the floodplain that sequesters the nutrients for nitrogen, whereas soil was found to be a source rather than a sink for phosphorous Schramm et al., (2009) has shown soil to be efficient in both present and historic data (Figure 2.5).

Source	Present Hydrograph		Historic Hydrograph	
	Nitrogen, kg ha^{-1}	Phosphorus, kg ha^{-1}	Nitrogen, kg ha^{-1}	Phosphorus, kg ha^{-1}
Soil	542	−150	976	−150
Water column and wetlands biota	6	1	58	13
Fish	3	1	5	2
Total	551	−148	1039	−135

Figure 2.5 *Amounts of nitrogen and phosphorus (estimated) during March 15th till May 15th in the MSR floodplain during times of inundation, for both "present" (2003) and "historic" (1988) hydrographs (Schramm et al., 2009).*

2.2 CLIMATE AND FLOODING IN THE MISSISSIPPI RIVER BASIN (FLOOD CHARACTERISTICS)

2.2.1 PRECIPITATION AND SNOW COVER

Climate in the Mississippi River basin is a dominant influence on flooding and, thus, floodplain formation. Sediment deposition in the floodplain is contingent on the source area and timing of precipitation, associated flood patterns along the LMR and tributaries. Since the start of the 20th century, streamflow, temperature, and precipitation has increased throughout the United States (Lettenmaier et al., 1994; Karl et al., 1996). Previous investigations have reported increases in temperature (exceeding previously recorded maximum temperatures) and precipitation across the United States during the 20th Century (Angel and Huff, 1997; Groisman et al., 2003), which have resulted in snowmelt occurring earlier in the Spring alongside enhanced rainfall intensity (Cayan et al., 2001; Changnon, 2001; Groisman et al., 2001). An increase in snow melt/retreat is directly correlated to a decrease in spring snow-cover, creating earlier spring (summerlike) conditions (Cayan et al., 2001; Groisman et al., 2001). From 1901-1994 a rise in daily precipitation events (>2 inches) has increased by 20% (Angel and Huff, 1997). Thunderstorm activity connected to an increased cumulonimbus clouds coverage, is an effect of intense changes in snow cover (Changnon, 2001). The aforementioned climate changes have resulted in increased streamflow and flooding in the Mississippi River basin (Lettenmaier et al., 1994; Karl et al., 1996; Knox, 2000; Groisman et al., 2003).

2.2.2 AIR MASSES AND JET STREAM

Air masses and jet flows along the U.S. have a large effect on flooding in the UMV. When a tropical air mass comes in contact with the jet stream axis in the UMV, the high precipitable water vapor in the air mass will create large precipitation events (Knox, 2000). Tropical air masses flow north from the GOM, whereas the cold air masses originate in the Arctic region. This combination of air masses creates large precipitation events allowing for large floods to form (Knox, 2000).

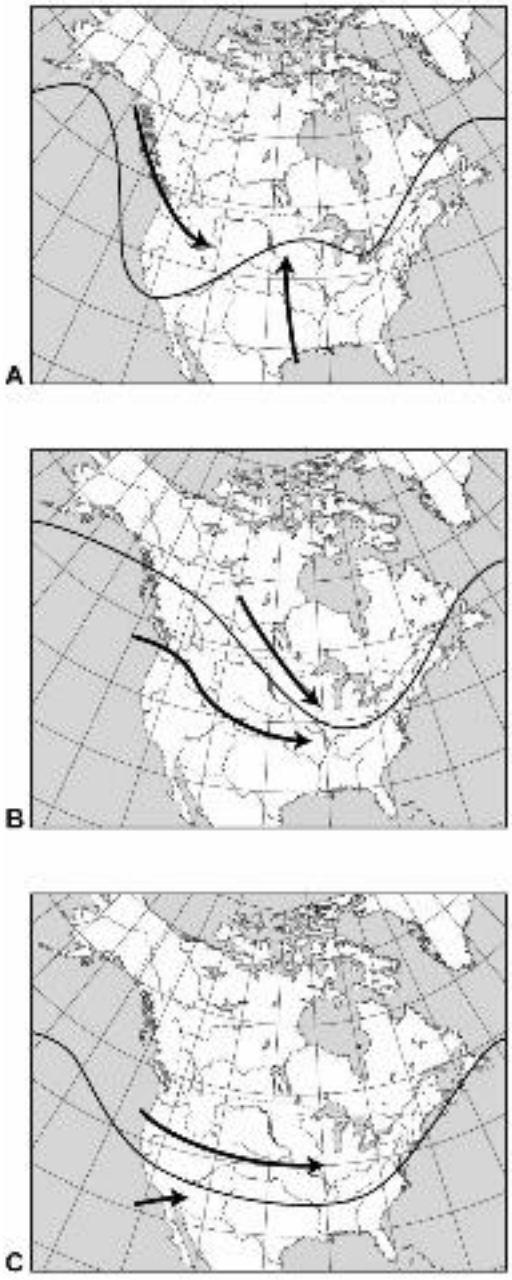

Figure 2.6 *Pathways of air masses (black arrows) and jet stream locations (black line) across the continental United States. Map A shows the two climate patterns that are positively correlated with large flood evens in the UMV. Map B and C climate patterns have a negative correlation to large flood events in the UMV (Knox, 2000).*

2.2.3 ATLANTIC MULTIDECADAL OSCILLATION

Climate patterns (65 to 80-year cycle) of the Atlantic Multidecadal Oscillation (AMO) influence the flooding of the LMR. AMO cycles last for periods of ~twenty

years. The previous patterns of AMO were 1860–1880 and 1940–1960 of warm phases of AMO, while during 1905–1925 and 1970–1990 there were cool phases of AMO (Kerr, 2000). Due to the influences on the climate during AMO phases, the Mississippi River's outflow can be affected by ±10% between wet/dry AMO phases (Enfield et al., 2001) (Figure 2.7).

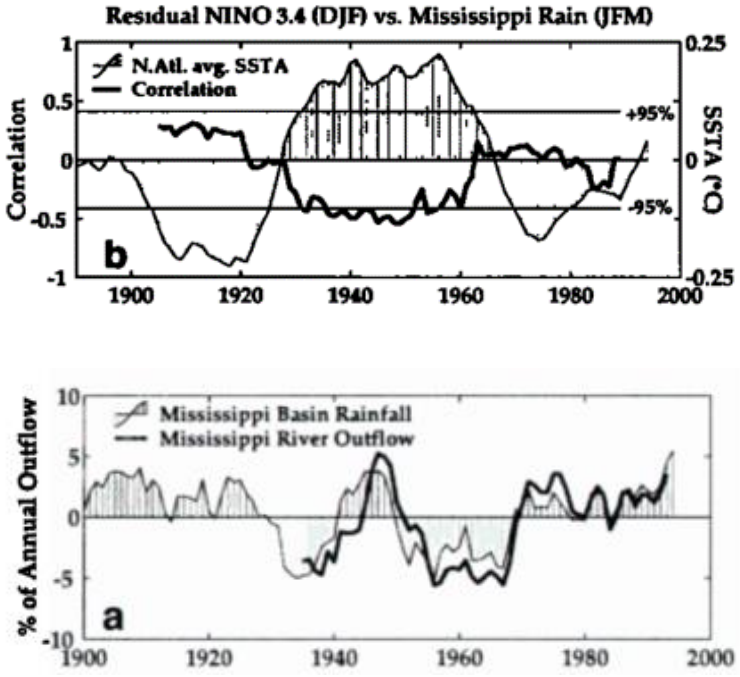

Figure 2.7 *AMO and NINO-3.4 (NINO-3.4 is the SSTA index for December to February) effects the climate (precipitation) of the MSR region for the years 1900-2000 (top) (Enfield et al., 2001). Mean outflow of the MSR in comparison to MSR basin precipitation (bottom) (Enfield et al., 2001).*

E1 Niño-Southern Oscillation (ENSO) cycles influence large events like flooding to smaller daily influences i.e., outflows rates on the MSR. Flood pulses resulting from ENSO cycles have been shown to affect the connectivity of oxbow lakes. Lake stages of oxbow lakes in Cuero and Victoria, Texas, were directly correlated to discharge of the Guadalupe River (Hudson et al., 2012). Seasonal precipitation changes (between summer and winter) and El Niño condition were associated with an increase in connectivity of the

river and oxbow, as well as an increase in lake levels (Hudson et al., 2012), whereas during La Niña periods, there was a lack of floodplain/oxbow connectivity and a decrease in alluvial water table (Hudson et al., 2012).

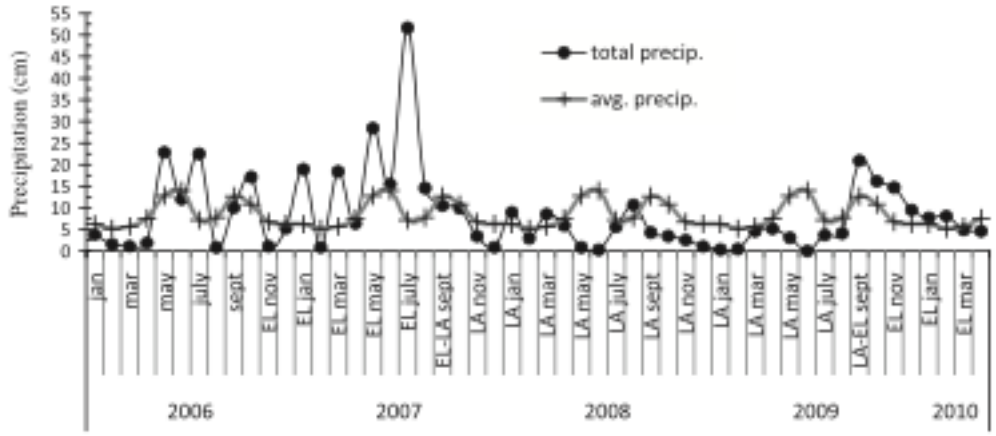

Figure 2.8 *Precipitation data for the Guadalupe basin at Victoria, Texas (LA- La Niña) (EL- El Niño) (Hudson et al., 2012).*

Region number	Subregion	*P* (mm)				
		90	95	99	99.7	99.9
1	Northwest	15	20	35	45	55
2	Missouri River basin	15	20	35	50	65
3	Upper Mississippi	20	25	45	65	80
4	Northeast	20	30	50	65	80
5	California and Nevada	20	30	50	65	80
6	Southwest	15	20	35	45	55
7	South	30	40	75	105	130
8	Midwest	25	35	60	80	100
9	Southeast	30	45	75	105	130
	48-states average	*20*	*30*	*50*	*70*	*90*

Changes in the twentieth century		Changes in the past 50 yr	
Mean precipitation	↑	all the left and	
Min temperature	↑	Spring max temperature	↑
Mean streamflow	↑	Spring snow cover in the west	↓
Heavy and very heavy rains in the east	↑	Cloudiness (total, low, Cb)	↑
High streamflow events in the east	↑	Near-surface humidity	↑
Wet conditions in the Mississippi River basin	↑	Evaporation	↑
Dry conditions in the Southwest	↑	Near-surface wind speed	↓

Figure 2.9 *Average daily precipitation values of differing percentiles from 90-99.9 (heavy rain to extreme rain events) of different regions throughout the conterminous United States (Groisman et al., 2003) followed by different aspects of the hydrologic cycle through time (Groisman et al., 2003).*

2.2.4 FLOODING TYPES/ORIGINS

Two types of floods have been recorded for the Upper Mississippi and Missouri Rivers: snowmelt floods and rainfall floods. Olsen et al. (1999) report that snowmelt floods do not increase as they flow downstream (i.e., floods of 1965 and 1969), whereas rainfall floods increase considerably as they travel downstream (i.e., floods of 1973, 1993, and 1995). Flood events that occur in March-April were found to be snowmelt floods, where May-September are rainfall floods (Olsen et al., 1999). However, rainfall events often support floods during a large snowmelt year due to increased baseflow and soil moisture (Olsen et al., 1999). Figure 2.10 shows the top five record flood events in the UMV since the 1950's with the annual discharge of the MSR at St. Paul, MN (Knox, 2000). An increase in discharge and flooding can be seen since the 1950's.

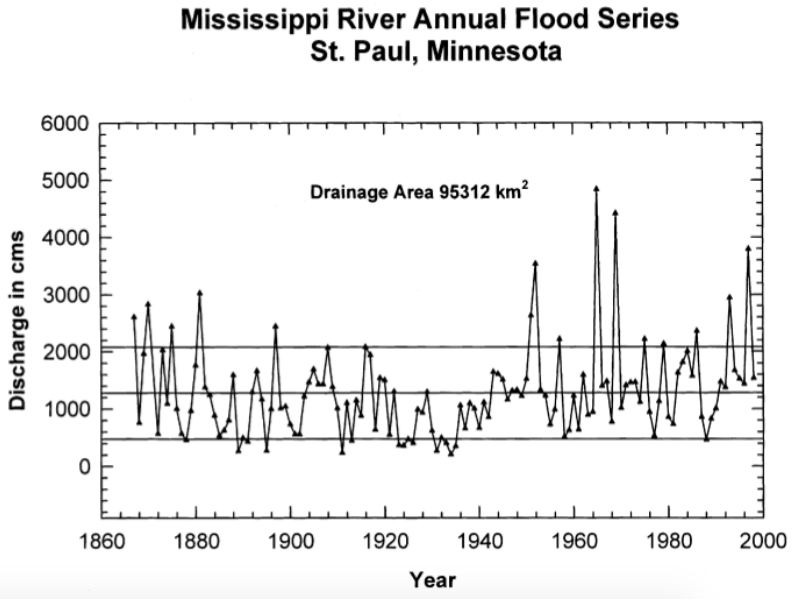

Figure 2.10 *The annual maximum floods for the UMR at St. Paul, MN. The middle line is the average discharge (m^3/s), with the upper and lower line being the one standard deviation. An increase in large flood events is shown occurring after 1950 (Knox, 2000).*

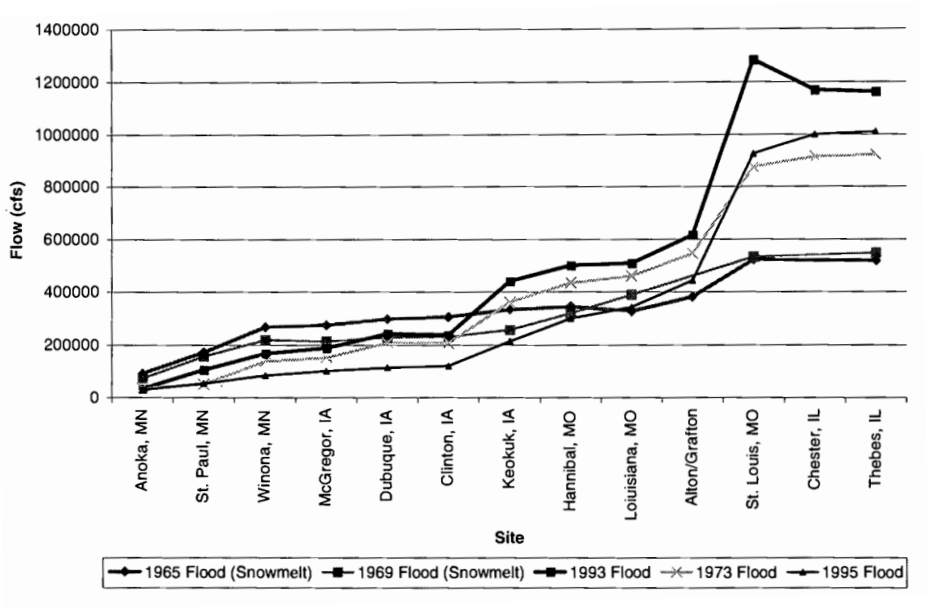

Figure 2.11 *Five large flood events (1965, 1969, 1993, 1973, and 1995), that were caused due to snowmelt events and/or rain events (Olsen et al., 1999).*

2.2.5 REDUCTION OF SUSPENDED SEDIMENT & ASSOCIATED LAND LOSS IN COASTAL LOUISIANA

Riparian and coastal wetlands are ecosystems of low relief that are defined by a hydroperiod of saturation for durations that ensure anaerobic conditions. Wetlands are sites of low-energy deposition of fine-grained sediments and organic matter, although major floods and coastal storms can transport coarser sediment to these areas. Sensitivity to external inputs results in wetlands being a high priority for environmental monitoring and conservation. Forty percent of the wetlands in the United States are located in the Mississippi deltaic plain (Bourne, 2000; Coleman et al., 2008). A total economic value of coastal wetlands has been estimated between $10,000 to $20,000 $ha^{-1}yr^{-1}$ (Costanza et al., 1997).

Wetlands in Louisiana are directly influenced by the amount of sediment transported to them by the LMR. Land loss and regression of these wetlands is a major

concern along the Gulf Coast, due to the lack of sediment. Horowitz (2010) documents an overall decline of flow-weighted sediment within the Mississippi River basin. During the past 25 years suspended sediment concentrations have declined due to a limited supply rather than a reduced discharge (Horowitz, 2010). Meade and Moody (2010) stated that the Missouri-Mississippi River system has converted to a supply-limited system from a transport-limited system, which now only transports 145 million metric tons per year in comparison to 400 million metric tons before the 20th century. Anthropogenic controls of sediment availability to the coastal zone are correlated to a lack of floodplain connectivity and deltaic sedimentation. This decrease was found not only to be from dams, but meander cutoffs, river-training structures, bank revetments, diversion channels, artificial levees, and other structures.

Kesel (2003) attributed degradation of the MSR channel to the lack of floodplain connectivity and associated reductions of sediment from the river. Before human modifications, the major source of sediment was derived from bank caving. Channel bars have exceeded pre-modification periods that engineers had previously expected. After a decreased use of artificial engineering, a direct correlation of sediment storage and river connectivity of sediments into the flood plains was studied. However, most of the influences of anthropogenic controls on the river, including sediment supply, are irreversible. Artificial levees have caused the amount of water and sediment pathways into the flood plain to decrease (>90 percent) (Kesel, 2003).

The Mississippi deltaic plain has been actively depositing sediment for the last 12,000 years (Blum and Roberts, 2009), with a 1–4 cm/yr rate of sediment deposition that has been inferred for the previous hundreds of years (Shen et al., 2015). In recent years,

the sediment load from the Mississippi River has decreased by fifty percent (Gagliano et al., 1981). Twenty five percent of the Mississippi deltaic plain wetlands have eroded, at an approximate rate of $100 km^2 yr^{-1}$, within the last few hundreds of years. (Blum and Roberts, 2009). By 2100, the deltaic plain will have lost 10,000–13,500 km^2 of land area. It would take 18 to 24 billion tons of sediment to sustain the delta. Blum and Roberts (2009), however, claim there are many methods and possibilities of restoring sediment to the coastal zone. However, because of sea level rise (Church et al., 2001), land loss is irreversible.

Allison et al. (2012) documents retention of suspended sediment along both the Mississippi and Atchafalaya rivers. Around 44%-48% of suspended sediment (larger sand?) is lost from the Mississippi River and 80% of sand from the Red River at the Old River Control (Blum and Roberts, 2009, Syvitski et al., 2009; Allison et al, 2012) is lost. An overall increasing trend between 1992 and 2003 of channel aggradation moving downstream from the Old River Control is due to the loss in sediment from above.

2.2.6 NUTRIENT TRANSPORT & GULF OF MEXICO HYPOXIA

Nutrients (i.e., nitrogen, phosphorus) that bypass the floodplain and are flushed downstream will contribute to eutrophication and associated hypoxia in the Gulf of Mexico, commonly referred to as the Gulf of Mexico Hypoxic Zone (GOMHZ). Eutrophication leads to an excess reproduction of algae, which consume large levels of oxygen, resulting in a hypoxic zone (lack of oxygen). The primary nutrient driving the hypoxic events is nitrogen, which fuels the growth of algal blooms, microorganisms, and organic matter below the pycnocline (Scavia et al., 2003). The respiring organisms that consume this organic material deplete oxygen more rapidly than it is replenished. During

hypoxic events, dissolved oxygen concentrations decline to 2 mg L^{-1} or less. Normal levels of oxygen in the GOM are typically ~8 mg L^{-1} (Rabalais et al., 2001). At levels less than 2 mg L^{-1}, mortality of fish and shrimp results in cessation of commercial fishing (Pavela et al., 1983; Leming and Stuntz 1984; Renaud, 1986). The hypoxic zone has previously expanded to ~20,000 km^2, with a length of 600 km west from the mouth of the Mississippi River (Rabalais et al., 2002).

An increase in nitrogen (N) and phosphorus (P) have been anthropogenically introduced in excess amounts due to agricultural fertilizers, wastewater (detergents), oxidized nitrogen from fossil fuels, and nitrogen fixation in legumes (Peierls et al., 1991; Howarth et al., 1996). An increase by a factor of 2–3 of both total inorganic N and reactive P was found between 1960 and 1987 (Turner and Rabalais, 1991). However, flood amplitudes along the Mississippi River have not been linked to magnitudes of the hypoxic events (Pokryfki and Randall, 1987; Justic´ et al., 1993; Rabalais et al., 1996; Wiseman et al., 1997).

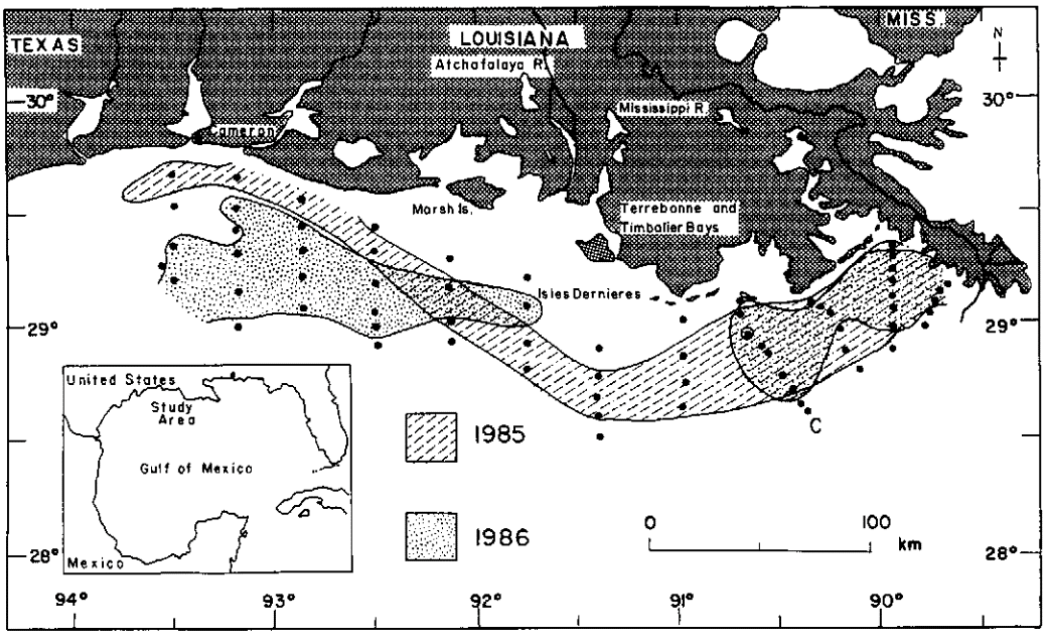

Figure 2.12 *Maps of the area in the GOM that contain less than 2 mg 1^{-1} of dissolved oxygen (hypoxic zones) (shown in gray). The years of hypoxia are 1985 (shaded with dashes) and 1986 (shaded with dots) (Rabalais et al.,1991).*

Two hypoxic events occurred during this study's time period. The 2019 GOMHZ was the eighth largest area (mapped) hypoxic zones in the GOM (since the 1985 record started). However, during 2018, the GOMHZ was the fourth smallest mapped (area).

2.2.7 FLOOD OF 2011

To date the largest flood on record for the Natchez area is the 2011 flood, which was the largest recorded discharge in North American history (Heitmuller et al., 2017). This flood reached a maximum stage height of 18.88 m (61.95 ft) at the Natchez gauge on May 19, 2011 (NOAA, 2020). The maximum discharge for the LMR reached 65,978 m^3/s (in Vicksburg) (Welch and Barnes, 2013). In comparison, the 1973 flood discharge peaked at 55,558 m^3/s and the estimated 1927 discharge peaked at 69,999 m^3/s (Costa and Jarrett, 2008; USGS, 2016; Heitmuller et al., 2017) The 2011 flood resulted in damages of $3.2 billion to infrastructure and agricultural loss (Camillo, 2012).

Studies have been made on the relationship between the 2011 flood and sedimentary characteristics of overbank flood deposits, including along the LMR in different depositional sub-environments of the embanked floodplain. Heitmuller et al. (2017) documented an average sediment deposition of 13.8 cm along natural levee crests, 0.9 cm on meander scrolls, and 0.3 cm in backswamps. The event-based sedimentation rates were less than those documented for a similar flood in 1973 (Kesel et al., 1974), which is possibly because the flood source in 2011 did not include sediment-rich inputs from the Missouri River subbasin (Heitmuller et al., 2017). Further, the sediment deposited in 2011 was relatively coarse compared to 1973, indicating that the finer sediment was possibly washed further downstream. The sedimentation rate during the 2011 flood within the Mississippi River basin accounted for 35–88% of the annual deposition amount (Khan et al., 2013).

2.3 LOWER MISSISSIPPI VALLEY

2.3.1 LMV HYDROLOGIC AND GEOLOGIC SETTING

The Mississippi River contributes 90% of fresh water and sediment to the Gulf of Mexico, and changes to its flood regime and sediment load affect processes in the coastal zone (Rabalais et al., 1996). The boundaries of the LMV are defined by its northern extent near Cape Girardeau, Missouri, and the Gulf of Mexico to the south (Saucier, 1994). More specifically, the LMV begins at the confluence of the Mississippi River and the Ohio River at Cairo, Illinois (northern limit) and is laterally delimited by the bluffs separating the valley from coastal plain uplands of Paleogene age (eastern boundary) (Saucier, 1994). However, there is no distinct western boundary because valleys of principal tributaries merge with the LMV.

The LMV is separated into 6 basins: Western Lowlands, St. Francis Basin, Yazoo Basin, Arkansas Lowland, Boeuf Basin, and the Tensas Basin (Saucier, 1994). Each basin is separated by minor topographic highs (or the LMR itself). For example, the Tensas Basin is primarily enclosed by the mouth of the Arkansas River, mouth of the Red River, Macon Ridge, and the southern extent of Sicily Island (Saucier, 1994). Sedimentologically, the LMV mainly consists of Pleistocene valley-train sands and Holocene meander belts, backswamps, and associated deltaic and chenier plains (Saucier, 1994; Aslan and Autin, 1999). Figure 2.13 shows an example of the geology of the MSR and its floodplain in Baton Rouge, LA. The LMV can be separated into two geomorphic categories: the alluvial plain and the deltaic plain (Autin et al., 1991). The width of the LMV ranges from 30 to 100 km (Aslan and Autin, 1999).

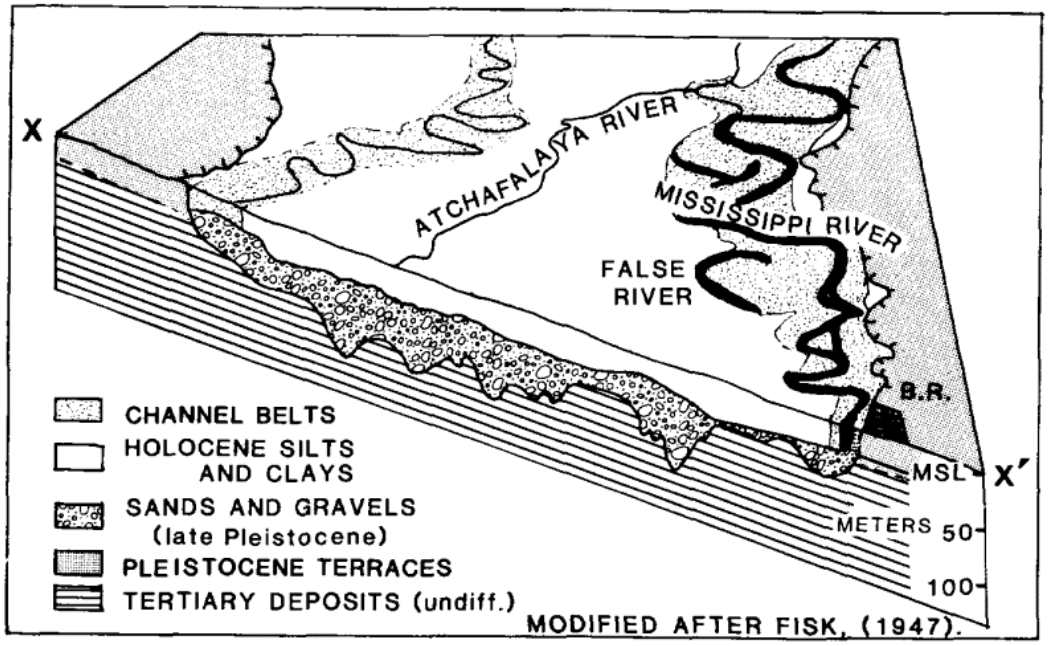

Figure 2.13 *Geologic cross sections (X-X') showing the LMV near Baton Rouge, LA (Farrell, 1987). This is a representation of what is typically found in a MSR floodplain.*

2.3.2 FLOODPLAIN DEPOSITION STYLES

Floodplain sub-environments in the LMV are dynamic because depositional and erosional mechanisms shift locations as the river migrates. There are three primary geologic controls associated with floodplain dynamics: (i) quantity and physical characteristics of sediment, (ii) sediment transportation pathway, and (iii) environmental setting (e.g., floodplain lake, forest, swamp, slopes) (Saucier, 1994). Depositional sub-environments rarely reach a level of equilibrium and/or maturity because of the shifting nature of these controlling factors. Alongside the natural floodplain dynamics of alluvial meandering rivers, several unique attributes must be considered along the LMR because of historical human controls.

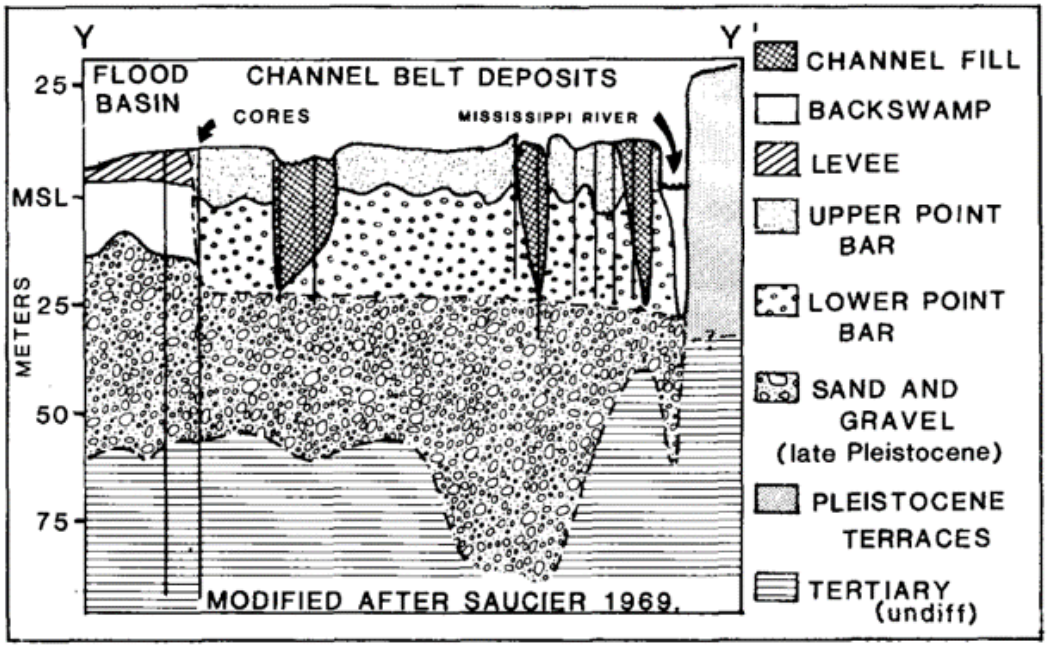

Figure 2.14 *A geologic cross section (Y-Y') the MSR floodplain with the main river channel (right) and ending with the flood basin (left) (Farrell, 1987).*

The classification of floodplains is organized by the stream's power and sediment character. Each stream has an ability to entrain sediment by transportation and the erosional resistance that forms their floodplains. The three main classifications of

floodplains are high-energy (non-cohesive), medium-energy (non-cohesive), and low-energy (cohesive floodplains). The LMR is classified under a high-energy system. According to Nanson and Croke (1992) the LMV floodplain is described as a B3, B3b and B3c floodplain. The classification of B3 floodplain consists of meandering river (lateral-migration) and the b is a scrolled floodplain (lateral migration) and the c is a backswamp floodplain (lateral migration) (Nanson and Croke, 1992).

2.3.3 EMBANKED FLOODPLAIN

Embanked floodplains are located between artificial flood-control levees and the active river channel. Embanked floodplain systems, like that along the LMR, require a more focused understanding of overbank processes. Techniques to help understand the embanked floodplain along the LMR include event-based sedimentation, more accurately model flooding, effectively manage natural resources, and support of riparian ecosystems.

Floodplain geomorphology will differ depending on the degree of flood management. Flood management techniques that are readily used along the LMR include groins, dikes, cutoffs, and bank protection. At embanked floodplains, the creation of oxbow lakes by artificial cutoffs have fundamentally adjusted floodplain geomorphology since 1936. The 1928 Mississippi Rivers & Tributaries Act renovating these features into wetlands (Hudson, et al, 2008). The sediments of river cutoffs include the bedrock of the channel bed and clayey within the backswamps.

Figure 2.15 *Section of the MSR where the meanders of the MSR have previously been cutoff. Embankment has occurred along locations of neck cutoff creating oxbow lakes. The northern-most oxbow is Lake Saint John and the southern cutoff is the Giles Cutoff (Google, 2020).*

2.3.4 CHANNEL-FLOODPLAIN CONNECTIVITY

An understanding of overbank processes along the embanked LMR floodplain requires an assessment of the hydrologic connectivity of the area. Hydrologic connectivity encompasses the frequency, magnitude, duration, and timing of connection between a river to its floodplain and how different parts of the system are affected, including various ecological functions. Efforts to increase hydrologic connectivity between the main channel and overbank environments are being considered along the

Mississippi River to improve riparian habitats and floodplain ecosystem services, including flood storage and nutrient sequestration. A refined knowledge of flood inundation and floodplain sedimentation will improve new river and flood management strategies for various societal and ecological benefits. It is vital that continuous measurements of Mississippi River stage heights and sedimentation rates during flood events be recorded, because these variables are perpetually adjusting to autogenic and allogenic controls such as climate, sea level, neotectonics, ground subsidence, and response to historical river engineering projects.

The connectivity of a channel-floodplain systems is highly dependent on the flow regime of the river ~~is~~ and sources of alteration (e.g., reservoir release schedules, flood spillway activation, human consumption). Magnitude, frequency, duration, timing, and rate of change of hydrologic conditions are the five factors that make up a flow regime (Poff, 1997). For the LMR, the main source of alteration includes flood-control levees, channelization, and spillway activation. According to Poff (1997), the hydrologic change in the LMR is a reduction of overbank flows associated with the geomorphic response of channel restriction (downcutting), floodplain erosion and deposition impediments, and a decrease in channel migration. However, this anticipated scenario doesn't fully account for other effects, including downstream translation of sediment waves or loss of sediment transport capacity in the vicinity of major diversion structures (Knox and Latrubesse, 2016).

For this study, high-magnitude flood events inundate the majority of the embanked floodplain, thus affecting all sub-environments. During low discharge events (normal flows) a majority of LMR environments are not inundated, excluding areas of

low topography that occur below flood stage (continuous season flows) (e.g., swales) (Hudson et al., 2013).

2.3.5 ANTHROPOGENIC CONTROLS

The United States government mandates that commercial waterways are maintained by the U.S. Army Corps of Engineers, in order to protect the security and economy associated with large rivers through control and navigation (Smith and Winkley, 1996). Natural processes and geomorphological adjustments along the LMR have been considerably influenced and changed by human activities, including upstream dams, flood-control levees, and various channel "improvements". Some of these modifications were done to enhance existing natural processes or protect lives and properties affected by flooding. However, after years of subsequent research along the LMR and other rivers similarly changed anthropogenically, it is now known that negative effects of these engineered features occur as well.

In 1879 – 1931 bank protection measures, including introduction of impermeable materials, were started as the first anthropogenic control along the Mississippi River (Moore, 1972; Smith and Winkley, 1996). In 1927, a catastrophic flood resulted in massive damages and loss of life, and initiated an unprecedented effort to control future flood events. By 1973, flood-control levees up to 12 m high were constructed along in the LMV (Smith and Winkley, 1995). Additionally, diversions including the Bonnet Carré and Morganza spillway structures were constructed to redirect large volumes of water during floods and reduce the pressure on levee systems (Camillo, 2012). Dams and reservoirs along tributaries were built to decrease downstream stages along the Mississippi River. Consequently, the deposition upstream will cause a decline of channel

gradient linked to diminishing channel connectivity (Smith and Winkley, 1996). Artificial cutoffs between 1929–1989 have shortened the MSR by 331 km (207 miles) (Smith and Winkley, 1996). Installations of concrete mattresses (revetments) to prevent bank erosion were followed by construction of dikes and groins. Two types of dikes (permeable and impermeable) have been placed in "fields" to adjust sediment and flow direction at differing angles along the channel. It has been concluded that impermeable dikes are more effective, especially when placed at locations with high natural rates of sediment deposition (Anding, 1968).

Relatively new techniques of river engineering like dredging have been implemented along the LMR to offset mid-channel bar development and channel-bed aggradation. However, dredging is only beneficial for areas that require an increase in depth for transportation (Smith and Winkley, 1996).

CHAPTER III – STUDY AREA

The Mississippi River drainage basin is the 3rd largest on Earth (~3,200,000 km^2) and provides an average discharge of 18,400 m^3/s to the apex of its deltaic plain (Mossa, 1996; U.S. Army Corps of Engineers, 2020). The drainage area includes much of the United States between the Rocky Mountains and the Appalachian Mountains, which encompasses semi-arid zones, sub humid forests, large swaths of intensively cultivated lands, and large urban centers. Notably, it is one of the most heavily engineered large river systems on Earth (Hudson et al., 2008) and includes many tributaries that are regulated by dams. The cumulative effects of river engineering, flood control, regulation, and land use in the drainage basin have resulted in myriad deviations from naturally occurring physical processes (Smith and Winkley, 1996; Meade and Moody, 2010) and biogeochemical conditions (Ward and Stanford, 1995; Lohrenz et al., 2008) along the river and its floodplain.

3.1 SAMPLE LOCATIONS

The study areas for this research include the embanked floodplains (i.e., regularly flooded between the valley wall and flood-control levee) of the Lower Mississippi River (LMR) near Natchez, Mississippi (Figure 3.1). The study area is immediately upstream and adjacent to the Old River Control Structure where ~30% of the total LMR discharge is diverted to the Atchafalaya River. Thus, these study areas constitute the channel-floodplain system at the location of maximum discharge before entering the deltaic plain downstream.

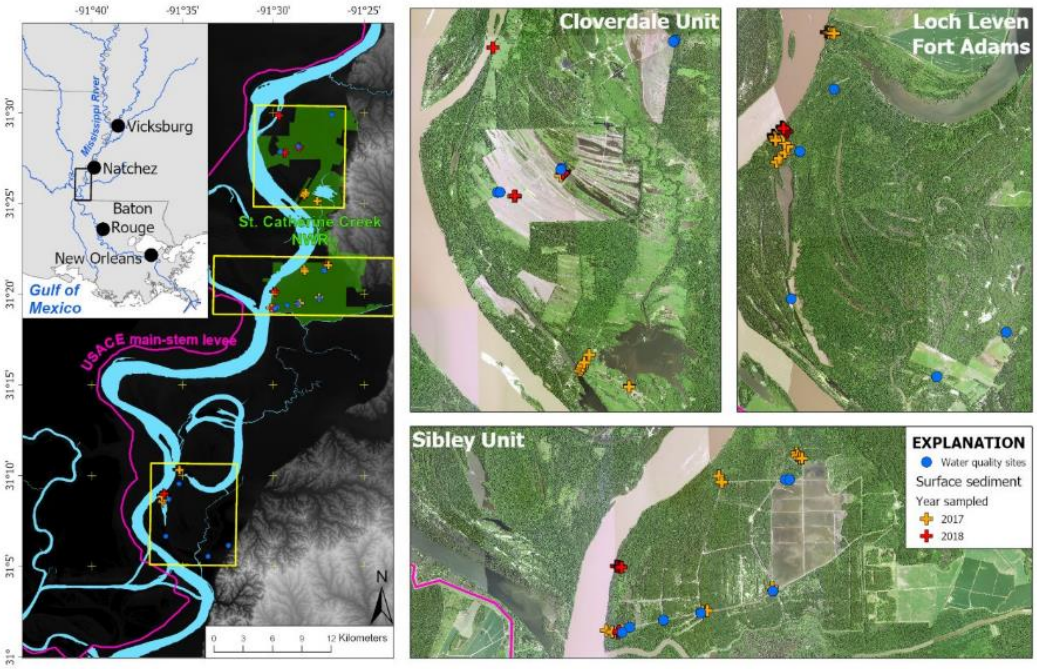

Figure 3.1 *Map of study areas to investigate sedimentary dynamics and water quality in embanked floodplains of the Lower Mississippi River in Adams and Wilkinson counties near Natchez, Mississippi. Symbols indicate the different sample locations: orange (surface sediments, October 2017), red (surface sediments, September 2018), and blue (water samples, March and June 2019). Elevation model and imagery were obtained from the U.S. Geological Survey National Map (2019) for all location maps for this study. The aerial images were acquired in 2014 and 2015).*

3.1.2 ST. CATHERINE CREEK NATIONAL WILDLIFE REFUGE, MISSISSIPPI

Most of the sample sites are located in St. Catherine Creek National Wildlife Refuge (SCCNWR) in Adams County, Mississippi (Figure 3.1). The refuge is intended for wildlife conservation, hunting, fishing, wildlife photography, environmental education, and wildlife interpretation and observation.

This is an ideal study area because natural overbank processes are not inhibited by flood-control levees and the LMR regularly inundates the floodplain between the channel and valley wall. The refuge area includes the bluff line to the east and is bounded by the LMR to the west, Natchez to the north, and the Homochitto River to the south. The Abernathy Channel serves as the southernmost boundary, that functions as the connection

between the Homochitto River and the LMR. The bluffs include the Miocene-aged Hattiesburg Formation and Plio-Pleistocene-aged Citronelle Formation that are capped by Pleistocene loess silt (MDEQ, 2020).

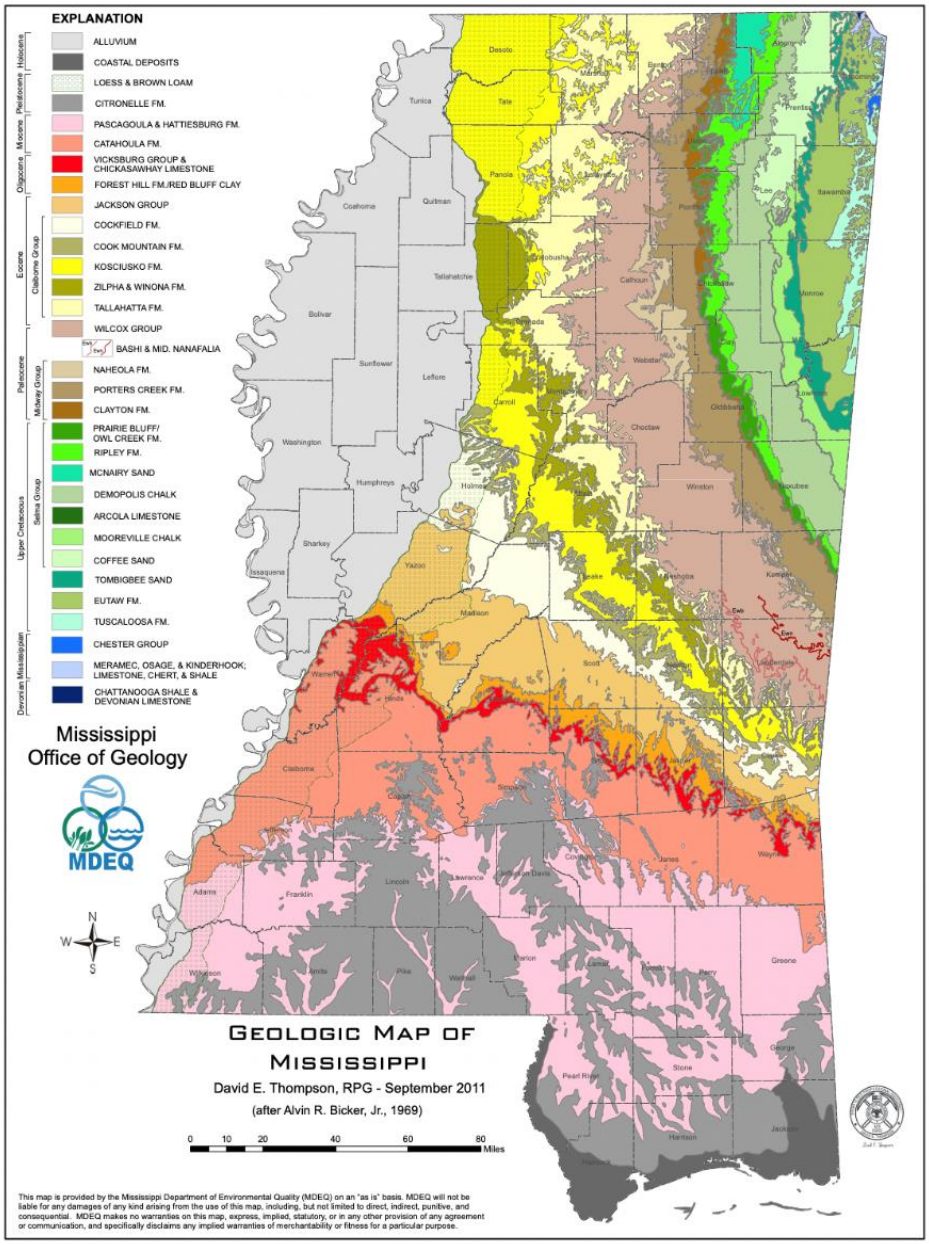

Figure 3.2 *Geologic map of Mississippi (MDEQ, 2020).*

SCCNWR was established in 1990 to return previous row-crop agricultural fields back to the natural riparian ecosystem. Native bottomland hardwood tree species were

planted at the establishment of SCCNWR (U.S Fish and Wildlife Service, 2014). Species of trees include: bald cypress, cottonwood, oak, elm, ash, and gum in the SCCNWR. A percentage of land is open water for aquatic ecosystems and cleared land, which was created due to the migration and meander of the MSR (U.S Fish and Wildlife Service, 2014).

At the refuge, natural levee banks are overtopped almost every water year, sometimes multiple times a year, inundating the floodplain that includes meander scrolls, backswamps, and various lakes, swamps, and yazoo tributaries. Overbank floods are commonly retained in the floodplain for a period of time, up to several months, resulting in sediment deposition and nutrient sequestration. These are important riparian ecosystem services, allowing for plants and other organisms to thrive during emergent periods.

The study areas in SCCNWR include the Cloverdale Unit, Sibley Unit, and Butler Lake Unit (Figure 3.3). Each location is different in its proximity to the LMR channel and other floodplain characteristics. Sibley Unit also includes Salt Lake being which is an extension of the LMR to the north.

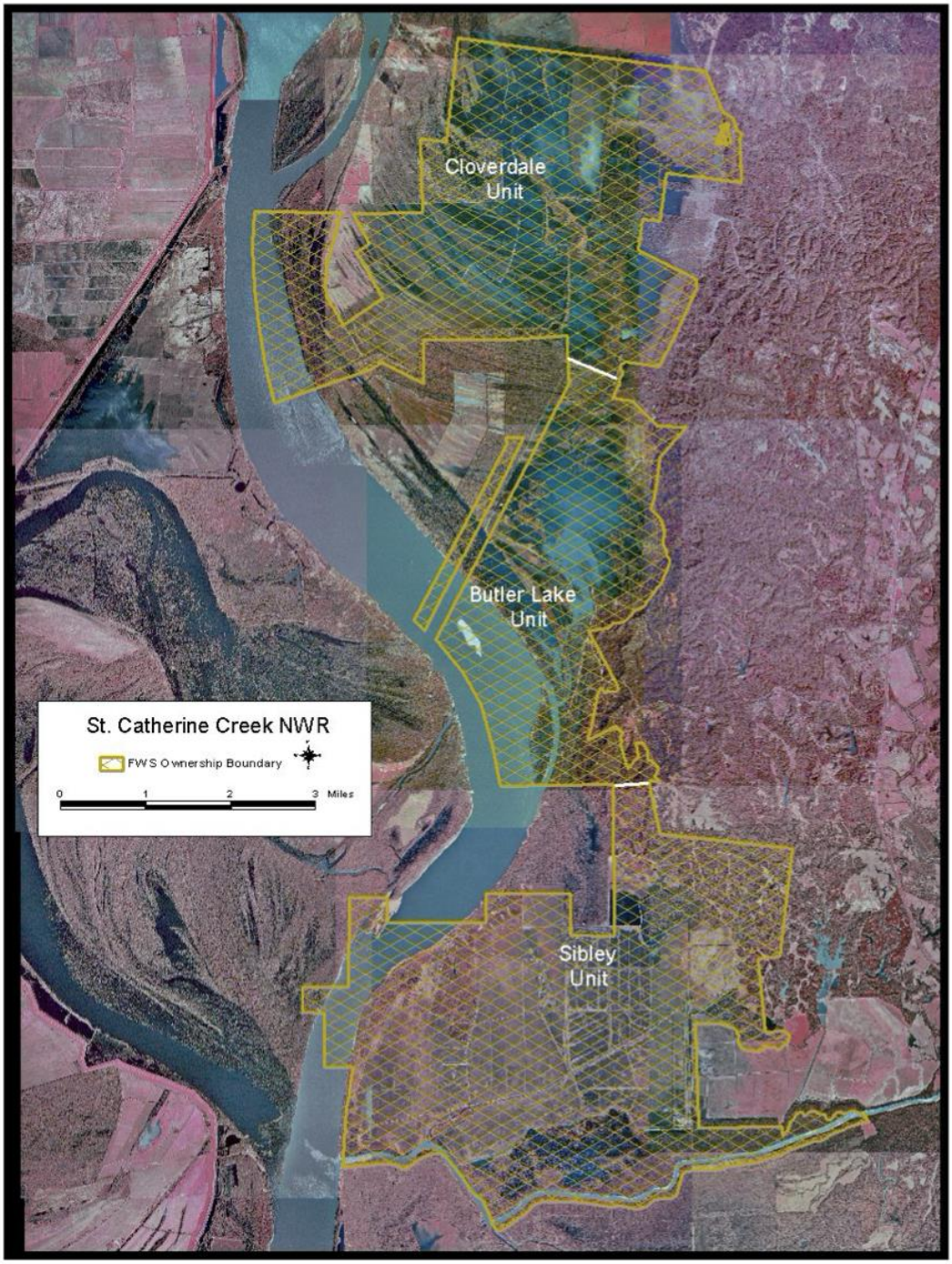

Figure 3.3 *Map of St. Catherine Creek National Wildlife Refuge in Adams County, Mississippi (SCCNWR Comprehensive Conservation Plan, 2006). This map is separated into the three locations of study at SCCNWR: Cloverdale Unit, Butler Lake Unit, and Sibley Unit.*

3.1.2.2 CLOVERDALE UNIT

The Cloverdale Unit includes meander scroll ridges and swales, a yazoo tributary (former St. Catherine Creek channel), and for the purposes of this investigation, is influenced by a natural levee and crevasse located off of the SCCNWR property on Carthage Point Road (Figure 3.4). The floodplain in the Cloverdale Unit is predominantly characterized by gentle undulations of linear ridges and relatively low elevation swales that parallel historical LMR positions as the channel laterally migrated toward the west. During periods of low LMR flow, major swales retain water as shallow lakes (e.g., Long Lake, Willow Lake).

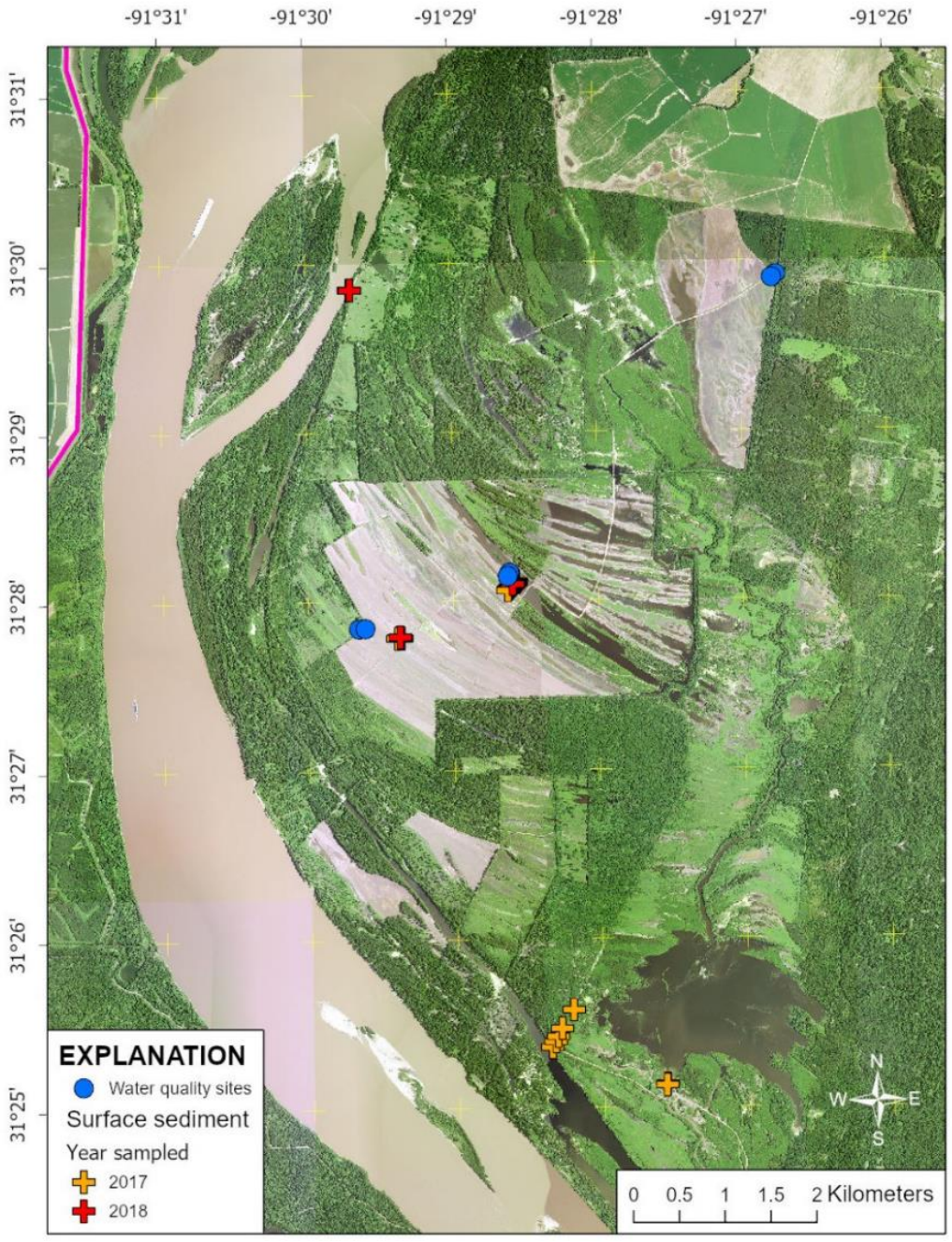

Figure 3.4 *Sample sites in the Cloverdale Unit and Butler Lake Unit of St. Catherine Creek National Wildlife Refuge in Adams County, Mississippi. This Cloverdale Unit is characterized by meander scrolls with lakes occurring in swales. The Butler Lake Unit and Salt Lake are included in this area with an additional series of meander scrolls. Mississippi orthoimages (2014-15) came from the U.S. Geological Survey National Map (downloaded in 2019).*

3.1.2.3 CARTHAGE POINT ROAD

Carthage Point Road is the northernmost site where samples were collected, and the closest site to Natchez, MS. This location is on an active chute of the LMR. Carthage Point Road is located on a natural levee ~4 m (~13 ft) high (height measured in Google Earth).

Figure 3.5 *Carthage Point Road in Adams County, Mississippi (Google Earth, 2019). The sample location is located on the natural levee along a chute of the LMR.*

3.1.2.4 LONG LAKE

Long Lake is a prominent swale lake located in a large meander scroll sub-environment east of the LMR (Figure 3.6). Between each ridge and swale there was an observable difference in the topography. This area includes a dense population of riparian biota.

Figure 3.6 *Cloverdale Unite in St. Catherine Creek National Wildlife Refuge in Adams County, Mississippi (Google Earth, 2019). The sediment and water samples are located in the meander scroll subenvironment along the LMR and just south of a chute of the LMR*

3.1.2.5 BUTLER LAKE UNIT AND SALT LAKE

The Butler Lake Unit includes the oblong Butler Lake and the narrower Salt Lake that is closer to and parallel with the LMR channel. The irregular shape of Butler Lake is highly affected by ridges and swales that are parallel to the LMR. Butler Lake is 464 acres of open water and includes bald cypress trees along its shoreline. Butler Lake is one of two (Old Saint Catherine Creek) bodies of water that is part of the Clean Water Act (Section 303(d)) (SCCNWR Comprehensive Conservation Plan, 2006), which implies that it does not reach the total maximum daily levels that are needed to be at applicable water quality standards. Standards that are not reached include elevated sediment loads, nutrients, pesticides, and low dissolved oxygen (Mississippi Department of Environmental Quality 2004).

Salt Lake's surface is ~70 acres of open water (SCCNWR Comprehensive Conservation Plan, 2006). The origin of the lake is apparently a swale that during a previous time was a chute channel of the LMR during periods of high flow.

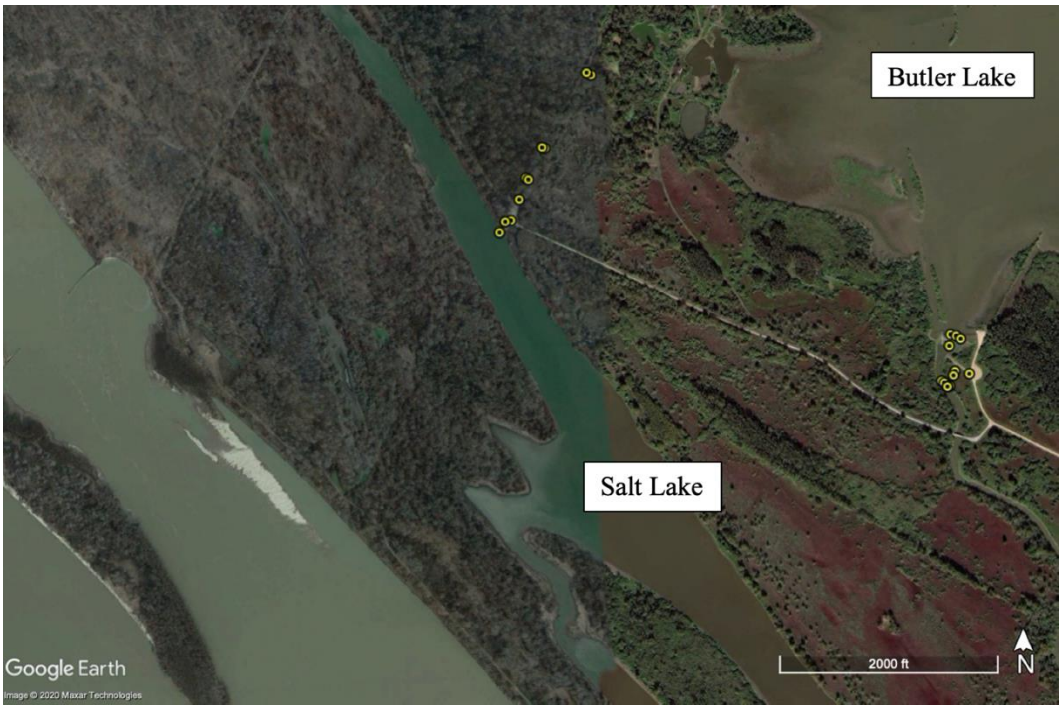

Figure 3.7 *Butler Lake and Salt Lake in Adams County, Mississippi (Google, 2019).*

3.1.2.6 SIBLEY UNIT

The Sibley Unit consists of a natural levee, backswamp, a semi-engineered open flood basin (devoid of tree growth), and access roads and trails. During periods below LMR flood stage, water levels in the open flood basin are partially controlled by a series of inflow and outflow gates maintained by SCCNWR staff. Thus, water-level fluctuations in the open basin occur with local runoff rates.

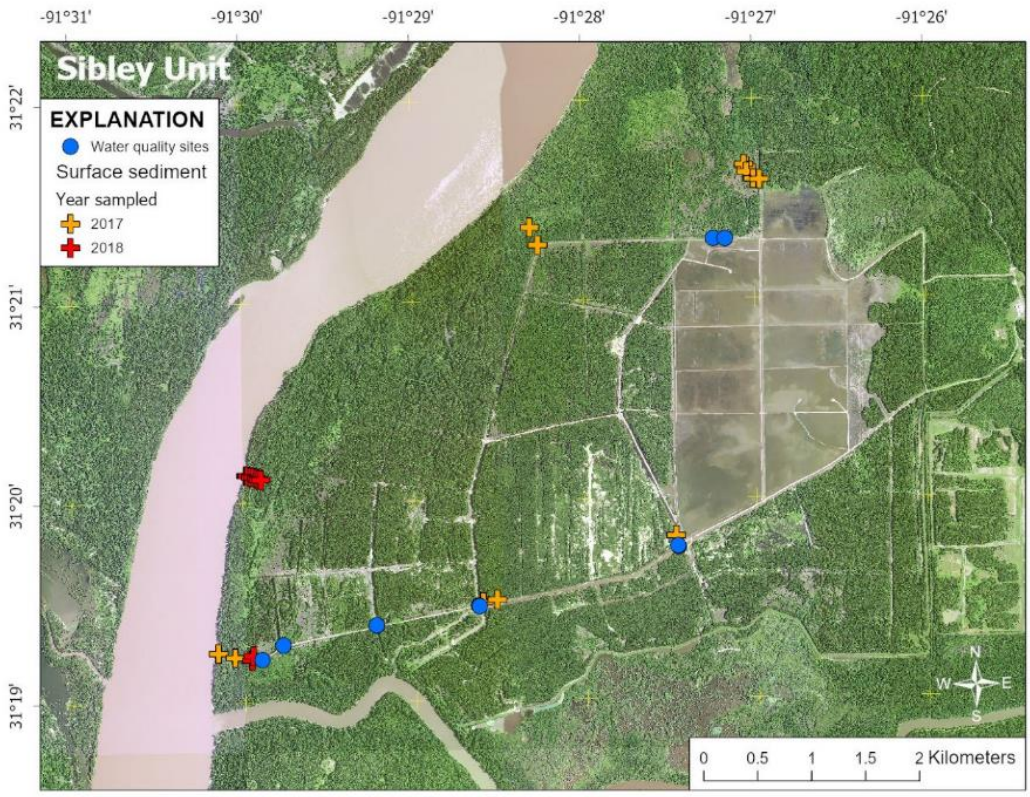

Figure 3.8 *Sibley Unit of St. Catherine Creek National Wildlife Refuge in Adams County, Mississippi orthoimages (2014-15) came from the U.S. Geological Survey National Map (downloaded in 2019).*

3.1.3 WILKINSON COUNTY, MISSISSIPPI

The study area in Wilkinson County, Mississippi, extends from the southern arm of Lake Mary to the Fort Adams community (Figure 3.8). This is the southernmost part of the study region. This area includes Artonish Lake, south of Loch Leven.

3.1.3.1 ARTONISH LAKE / LAKE MARY

Artonish Lake is an abandoned chute cutoff of the LMR that presently occupies a swale of the meander scroll topography. Lake Mary is a large oxbow lake maintained by a control structure at the western end of its northern arm.

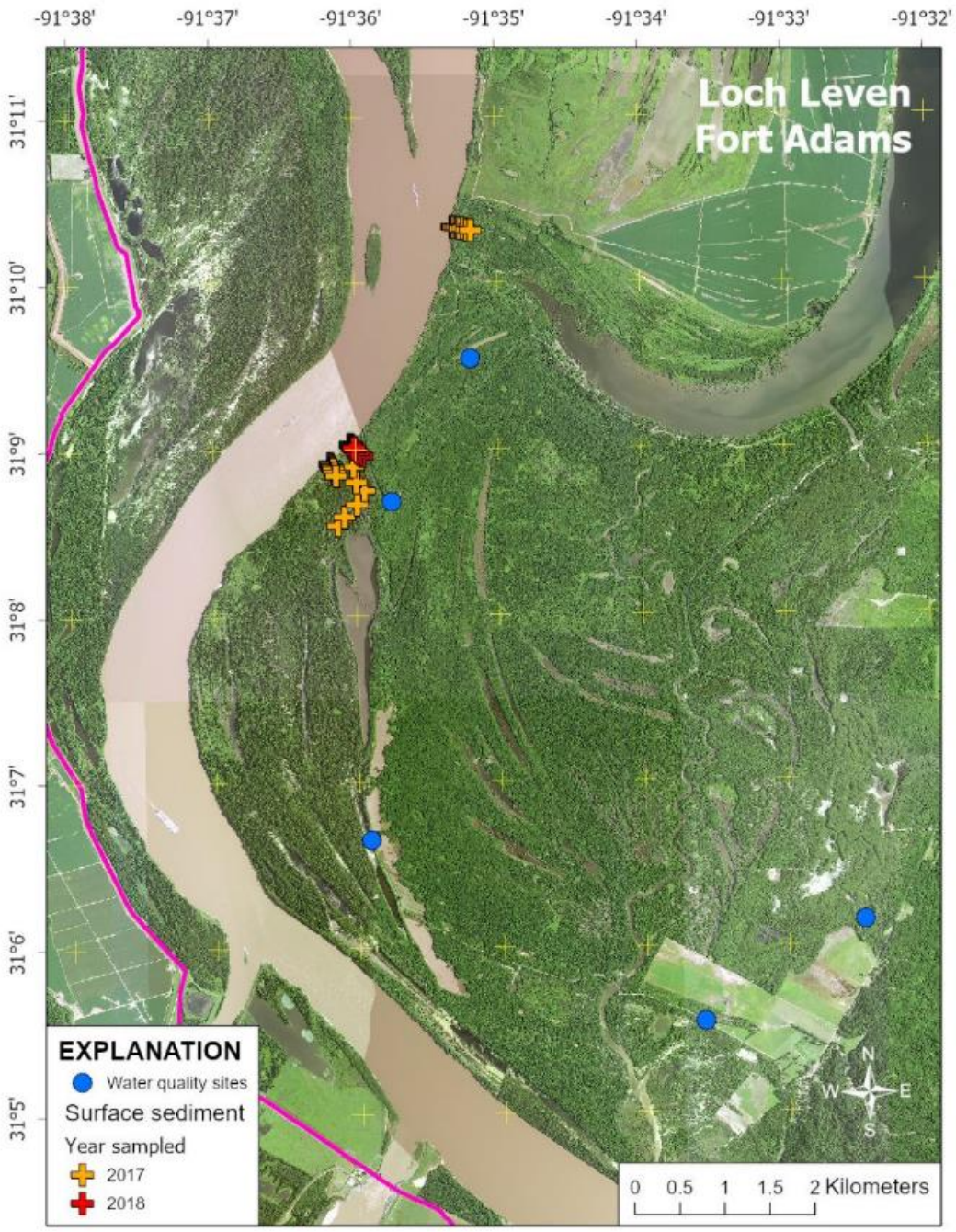

Figure 3.9 *Artonish Lake and Fort Adams areas in Wilkinson County, Mississippi. The Lake Mary oxbow (north) is shown to the east of the LMR and Lake Artonish (south) is also shown to the east of the LMR. Mississippi orthoimages (2014-15) came from the U.S. Geological Survey National Map (downloaded in 2019).*

Two important tributaries to the MSR are the Buffalo River and the Homochitto River. The Buffalo River (at Woodville, MS) is a rather small river with an annual

discharge during 2018 of 18.03 m^3/s (194.1 ft^3/s) and in 2019 an annual discharge of 28.08 m^3/s (302.2 ft^3/s) and a drainage of 3107.99 square kilometers (1,200 square miles) (180 square miles at Woodville, MS) that contributes to the MSR (USGS, 2020).

The Homochitto River at Eddiceton, MS has a larger influence on the MSR with an annual discharge during 2018 of 16.23 m^3/s (174.7 ft^3/s) and in 2019 an annual discharge of 29.99 m^3/s (322.8 ft^3/s) and a drainage basin of 3107.99 square kilometers (1,200 square miles) (181 square miles at Eddiceton, MS) (USGS, 2020). Many channel modifications have been made by the U.S. Army Corps of Engineers in the lower reach of the Homochitto River. One major modification was a reduction of the length of the river by 24 km (14.91 miles), which changed the slope of the river and increased channel movement and vertical degradation (Wilson, 1979). Channelization increased the depth of the river to 5 m (16.40 ft) (Kesel and Yodis, 1992). The Homochitto River's "old course" (before channelization) would drain into Lake Mary (farther upstream).

Lake Mary is an old abandoned channel of the LMR that was cutoff and now is classified as an oxbow lake (Figure 3.9). Residential housing occurs along the eastern and southern sides of the lake (natural levee positions); the western side of Lake Mary includes mostly cleared fields and wooded areas across meander scroll ridges and swale.

Figure 3.10 *Southern portion of Lake Mary (Google, 2019). The study area is located between the Lake Mary limb and the main channel of the LMR.*

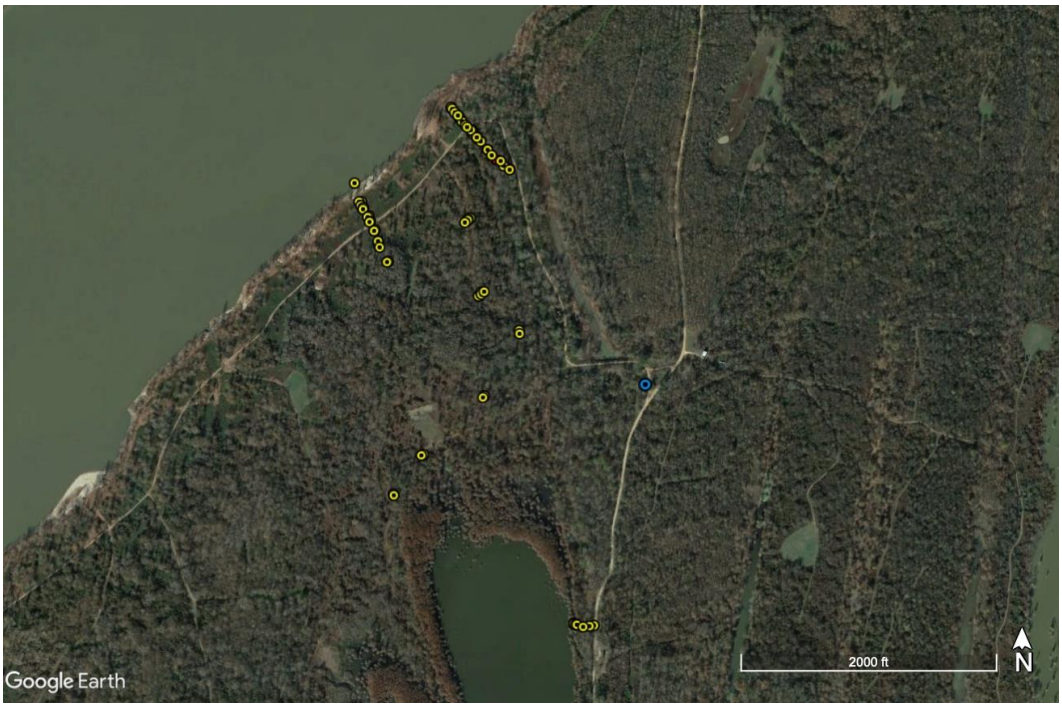

Figure 3.11 *Northernmost portion of Lake Artonish (Google, 2019). Study locations are located in the floodplain in-between Lake Artonish and the main MSR channel.*

3.1.4 FORT ADAMS

The Fort Adams area includes backswamp sub-environments adjacent to the bluff line and meander scroll environments in closer proximity to the LMR channel. The main-stem flood-control levee on the Louisiana side of the LMR and the bluff line on the Mississippi side narrows the embanked floodplain here considerably. The Buffalo River serves as an important overbank conveyance channel during LMR flood events.

3.2 LMR FLOODING PATTERNS

Floods along the LMR exhibit a range of temporal patterns, including seasonal timing, duration, and peak symmetry as evidenced by hydrographs during the last 20 years.

Four flood patterns include: symmetrical, early, late, and irregular short. Some water years include multiple flood peaks, whereas other flood hydrographs are skewed making them early or late (seasonally). In some cases, long duration floods with intermittent peaks (mostly not symmetrical) characterizes the pattern during a water year.

3.2.1 ONE SYMMETRICAL LARGE PEAK

Water years 2016-2017, 2010-2011, and 2007-2008 had flood cycles with one large peak between April and June. The three floods crested above 12.19 m (40 ft) with discharges greater than 28,316 m^3/s (1,000,000 m^3/s) (U.S. Army Corps of Engineers, 2020). The peaks are rather symmetrical with little skewness. The occurrence of symmetrical peaks along the LMR has been 10 out of the last 20 years. The symmetrical peak flood hydrograph is the most frequent of those discussed in this study.

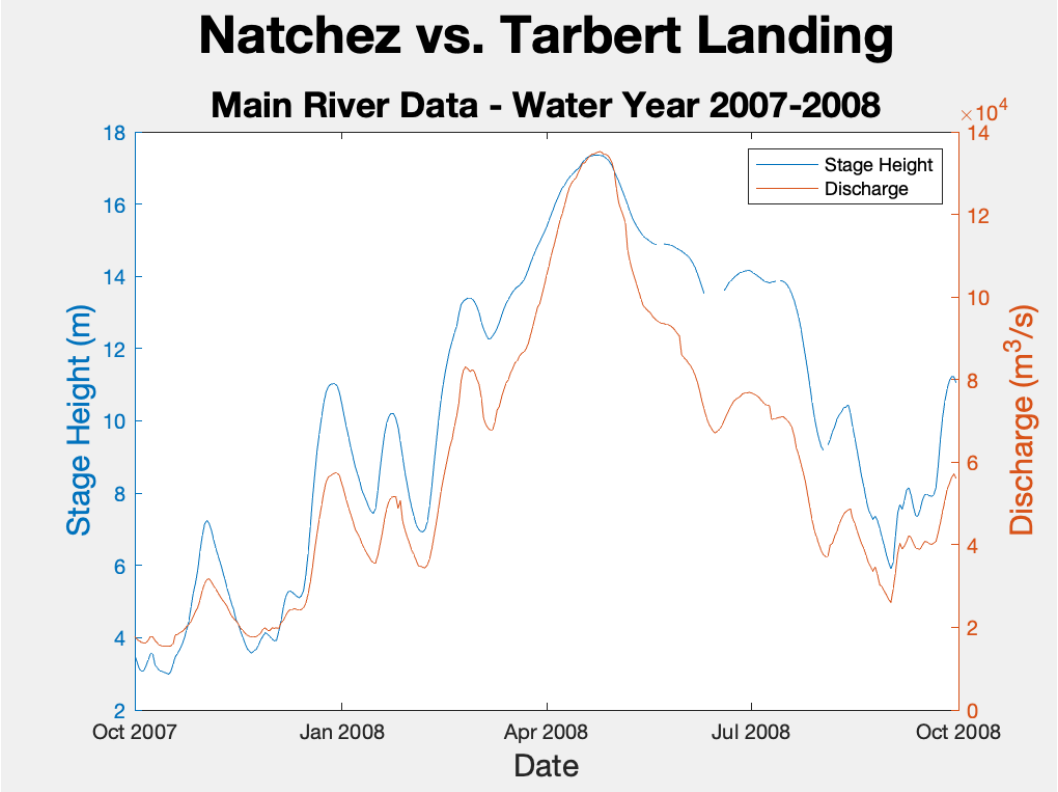

Figure 3.12 *Flood hydrographs along the LMR in 2007-2008 at Natchez and Tarbert Landing. These hydrographs are classified as a large symmetrical peak.*

3.2.2 MULTIPLE PEAKS, SEASONAL PEAKS (EARLY AND LATE), AND IRREGULAR PEAKS

Multiple peak floods that have more than one main crest above 11.58 m (38 ft) are spread throughout the water year.

Early flood peaks along the LMR occur toward the beginning of the water year between November and April. These early flood events tend to recede slowly (right skewed).

Late flood peaks along the LMR occur relatively late in the water year between April and September. These late flood events are commonly left skewed on their hydrographs.

3.2.3 IRREGULARLY SHORT AND UNPREDICTABLE PEAKS

Not all floods along the LMR are consistent, large discharge events. Irregular and short-duration floods have no particular temporal pattern (Figure 3.12). The flood hydrographs during these years consist of rapid rises and recessions, in some cases with a rapid rise followed by an extended plateau of high discharge. The patterns and durations of these hydrographs are unique from flood patterns discussed above. The range of irregular peak floods is from less than action stage (11.58 m (38 ft)) to a major flood. During these flood years, stages above action stage can occur for more cumulative months than months less than action stage.

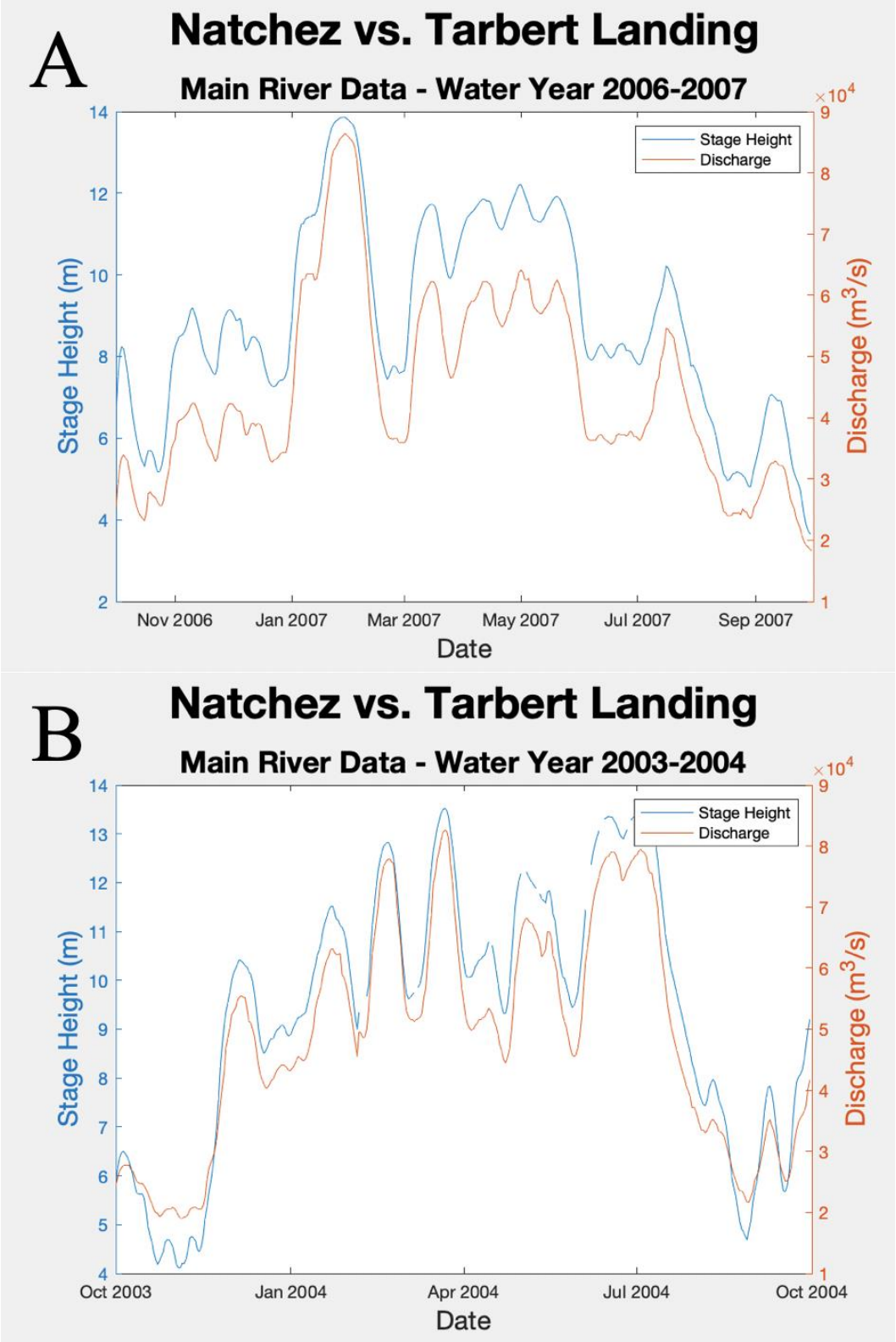

Figure 3.13 *The 2006-2007 and 2003-2004 flood hydrographs along the LMR at Natchez and Tarbert Landing (U.S. Army Corps of Engineers, 2020), which are classified as multiple, irregular short peaks.*

3.3 PRECIPITATION MAPS

Precipitation maps from 2018 and 2019 are essential to understand and interpret where the floods initiated and where the source of suspended sediment and nutrients came from for the flood of 2018 and 2019 in the LMR. The precipitation occurring before the 2018 flood occurred mainly in the Ohio River drainage basin. The precipitation for the 2019 flood event originated in three out of four of the major tributary systems: the Ohio River, the MS River, and the Missouri River drainage basins (Figure 3.14). Additionally, there was a larger average and duration of precipitation after the 2018 flood event and continuing during the 2019 flood, which consequently lead to the 2019 flood being the largest flood on record.

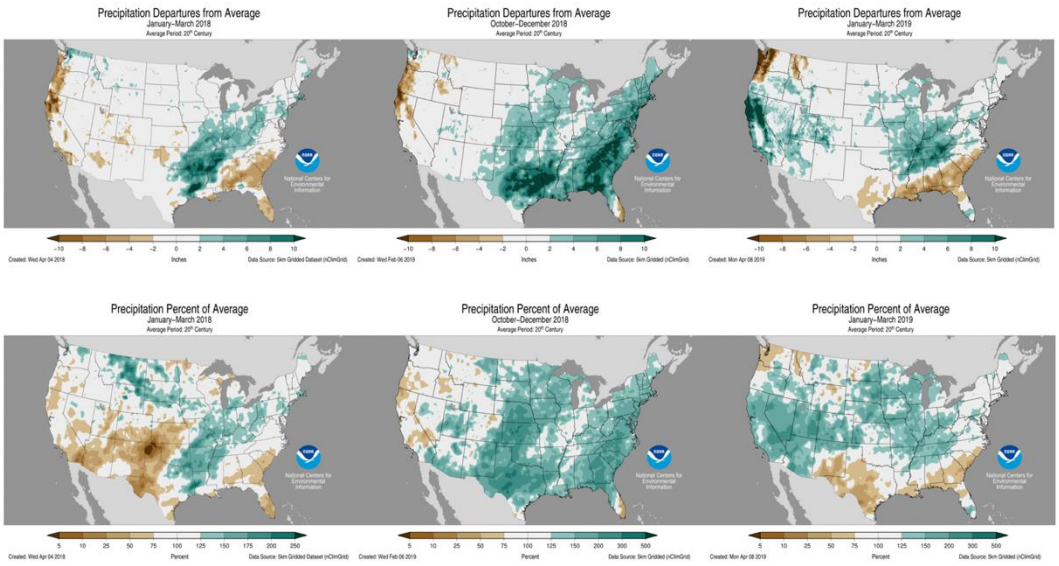

Figure 3.14 *Precipitation maps of the water years (2018 and 2019) that are recorded before the 2019 flood event.*

3.4 RIVER GAUGE LOCATIONS

Four gauging stations are discussed in this study: Vicksburg, Natchez, Tarbert Landing, and St. Francisville; all have different flood stages. The stations are designated for monitoring different parameters, thus they are all included here to enable a full

understanding of flooding patterns and values during the 2018 and 2019 flood events.

3.4.1 VICKSBURG, MISSISSIPPI

The flood stage at Vicksburg, Mississippi is 13.11 m (43.00 ft). The flood of 2018 arrived on 03/03/18 at a stage height of 13.23 m (43.42 ft) and lasted for 25 days. The flood of 2018 was, however, only the 13th highest crest on record at Vicksburg at 15.21m (49.90 ft) on 03/16/18. Discharge peaked at 51,253.49 m^3/s (1,810,000 ft^3/s) for the three days of 3/14/18-3/16/18 (US Army Corps of Engineers, 2020).

The flood of 2019 was the eighth highest crest on record with a maximum stage of 15.69m (51.47 ft) on 03/10/2019, which lasted a total of 162 days (U.S. Army Corps of Engineers, 2020). Discharge peaked for five days at 53235.67 m^3/s (1880000 ft^3/s) during the dates of 3/10/19-3/14/19 (US Army Corps of Engineers, 2020).

Table 3.1 *Action and flood stages for the Mississippi River at Vicksburg, Mississippi (USGS 322023090544500) (USACE, 2020).*

Flood Categories	Feet (Meters)
Major Flood Stage	50.00 (15.24)
Moderate Flood Stage	46.00 (14.02)
Flood Stage	43.00 (13.11)
Action Stage	35.00 (10.67)

3.4.2 NATCHEZ, MISSISSIPPI

Recognizing that the 2018 and 2019 flood events (2017–2019 water years) are the main foci of this study, the imperative characteristics of these floods are peak stage height (meters (ft)), maximum discharge (m^3/s), and total duration of flood event (days/months). These characteristics are compared with previous flooding in the LMV.

Table 3.2 *Action and flood stages along the Lower Mississippi River at Natchez, Mississippi (USGS 07290880) (USACE, 2020).*

Flood Categories	Meters (Ft.)
Major Flood Stage	17.37 (57.00)
Moderate Flood Stage	15.54 (51.00)
Flood Stage	14.63 (48.00)
Action Stage	11.58 (38.00)

The flood of 2018 had overbank conditions occur between March and May of 2018 with at a maximum stage at Natchez of 17.41 m (57.12 ft) on 3/18/18, qualifying as the fifth highest crest on record at that location. The maximum discharge at Tarbert Landing, Mississippi was 40889.53 m^3/s (1,444,000 m^3/s) on 3/18/18 (US Army Corps of Engineers, 2020). The start of the flood event was on 3/1/18 and it ended on 5/8/18, an approximate two-month duration. The river receded but remained above normal stages through September 2018 (U.S. Geological Survey, 2020).

The 2019 flood event on the LMR has remained above flood stage for 212 days resulting in a new flood duration record and a maximum stage of 17.65 m (57.91 ft) in March making this flood of 2019 the third highest crest on record on 03/12/19 (U.S. Geological Survey, 2020).

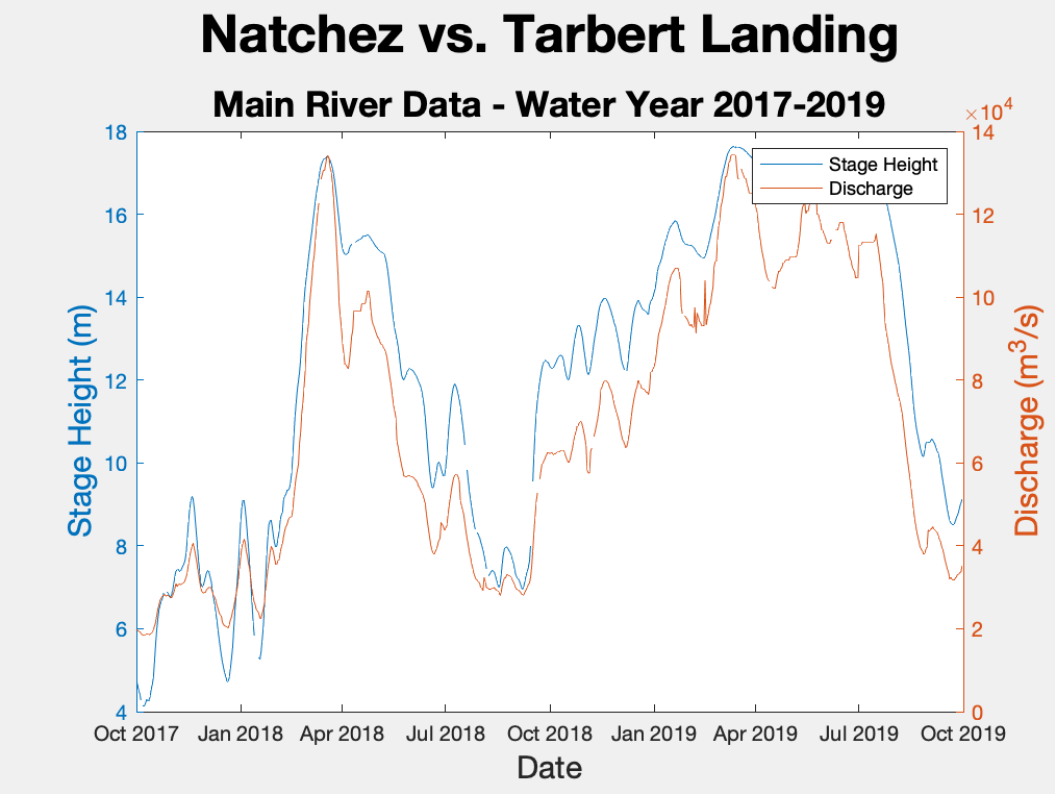

Figure 3.15 *Stage (m) and discharge (m^3/s) of the Mississippi River at Natchez, Mississippi (07290880) between June 2017 and August 2019.*

Note: Stage height (ft)(left) and discharge (cfs)(right).

Table 3.3 *Historic flood crests along the Mississippi River at Natchez, Mississippi (U.S. Geological Survey, 2020). Pertaining to this study, the 2018 and 2019 flood are listed as the third and fifth largest flood event of the area of Natchez, MS.*

Date	Historic Crests **m** (ft.)
05/19/2011	18.88 (61.95)
02/21/1937	17.69 (58.04)
03/21/201**9**	17.65 (57.91)
0X/XX/2020	XX (XX)
03/18/2018	17.41 (57.12)
04/23/2008	17.38 (57.03)
01/17/2016	17.30 (56.75)

3.4.3 TARBERT LANDING

Tarbert Landing, MS being the closest gauge location that actively records discharge, was used to compare to the stage height at Natchez, MS. During the 2018 flood at Tarbert Landing reached a peak discharge of 40,889.53cms (1,444,000 cfs)

during 3/19/18. During the 2019 flood at Tarbert Landing, discharge reached a high of (1,445,000) during a five day span (3/10/19-3/14/19) (US Army Corps of Engineers, 2020).

For the years 2018 and 2019 a visual comparison between stage height and discharge is shown with similar peaks and trends. This pattern of flooding is a symmetrical large peak on a hydrograph. During the classification of a major flood event, high stands and peaks reach a stage height above 14.63m (48.00 ft.).

3.4.4 ST. FRANCISVILLE, LOUISIANA

Flood stages downstream of the study area at St. Francisville, Louisiana, have not been officially established so this study considers a stage height above 46.00 ft (14.02m) to represent overbank conditions. During the flood of 2018, St. Francisville had 23 days where stage height was above 46.00 ft (14.02m), and a maximum stage height reached 51.84 ft. (15.80m) making it the 3rd highest on record. During the flood of 2019, the maximum stage height reached 52.17 ft (15.90m) on 03/19/2019 and stages above 14.02 m (46 ft) lasted for 141 days (U.S. Army Corps of Engineers, 2020). Flood categories for St. Francisville, LA are not provided.

CHAPTER IV - METHODOLOGY

4.1 FIELD RESEARCH

The research questions for this study required field sampling and monitoring coupled with laboratory analyses of sediment and water samples collected during four sampling trips to the study areas (Table 4.1). Floodplain surface sediment samples were collected in October 2017 and September 2018; overbank water quality was measured and water samples were collected in March and June 2019 during flood conditions. Additionally, data from water level and temperature sensors deployed in October 2017 were subsequently retrieved by Dr. Franklin Heitmuller and Dr. Paul Hudson in October 2019.

Table 4.1 *Field research collection periods to study areas in the embanked floodplain of the Lower Mississippi River in Adams and Wilkinson counties, Mississippi.*

Sample Dates	Transects sampled	Water samples	Other
October 2017	12	none	none
September 2018	6	none	1 Trench
March 2019	none	8	none
June 2019	none	13	none

4.1.2 FLOODPLAIN SURFACE SEDIMENTS

Floodplain surface samples were collected along transects in a wide variety of depositional sub-environments, including natural levees, backswamps, and meander scrolls (Figure 1.1). Floodplain surface samples were collected with a clean metal trowel, inserted into Whirl Pack bags, and placed in a cooler with ice packs. Upon return each day, samples were transferred to a freezer and they remained below freezing until analyzed in the laboratory (see below). GPS was used to obtain position and elevation data of sediment samples. The antenna mounted to a prism pole of the Trimble GeoXH was placed directly on the ground adjacent to where the sediment was collected. The

GPS and software used was a Trimble GeoXH GPS with Trimble Zephyr Model 2 antenna mounted to a prism pole (Trimble TerraSync software) (centimeter edition). Data were differentially corrected using Trimble Pathfinder software in the office (not all points obtained accuracy of 1 cm).

4.1.2.1 TRANSECTS

Three transects in Adams County, MS are collected located in-between Lake Artonish and the LMR main channel. The first two transects (T1A and T2) are perpendicular the main channel of the LMR, where the third transect (T1B) is oblique to the LMR (Figure 4.1). The three transects were ~~all~~ sampled in September 2017 and only T1 was sampled again during October 2018. Transect ~~(~~T1A~~)~~ data collection initiated at the MSR shoreline and continued southeast by increasing distance. The October 2017 T1A data set, started with a 0 meters sample close to the LMR shoreline, and continued with increasing distance of 10m, 20m, 40m, 60m, 80m, 120m, 160m, and ending at 190m away (nine samples total). Five samples were collected along the same transect line for the September 2018 collection at Transect 1A, but sample locations were not systematically measured. Transect T2 data were collected in between Lake Artonish and the main LMR channel, with increasing distance from the LMR channel. For October 2017, T2 started with 0 meters from the main LMR channel shoreline and continued with increasing distance of 10m, 20m, 40m, 53m, 80m, 120m, ending at 160m (eight samples total). Transect T1B sample collection started obliquely between T1 and T2 and continued southwest to north of Lake Artonish. Since transect for T1B was more oblique to the LMR channel than other transects, samples were selectively picked instead of using an increasing distance (GPS locations located for each location) (Figure 4.1).

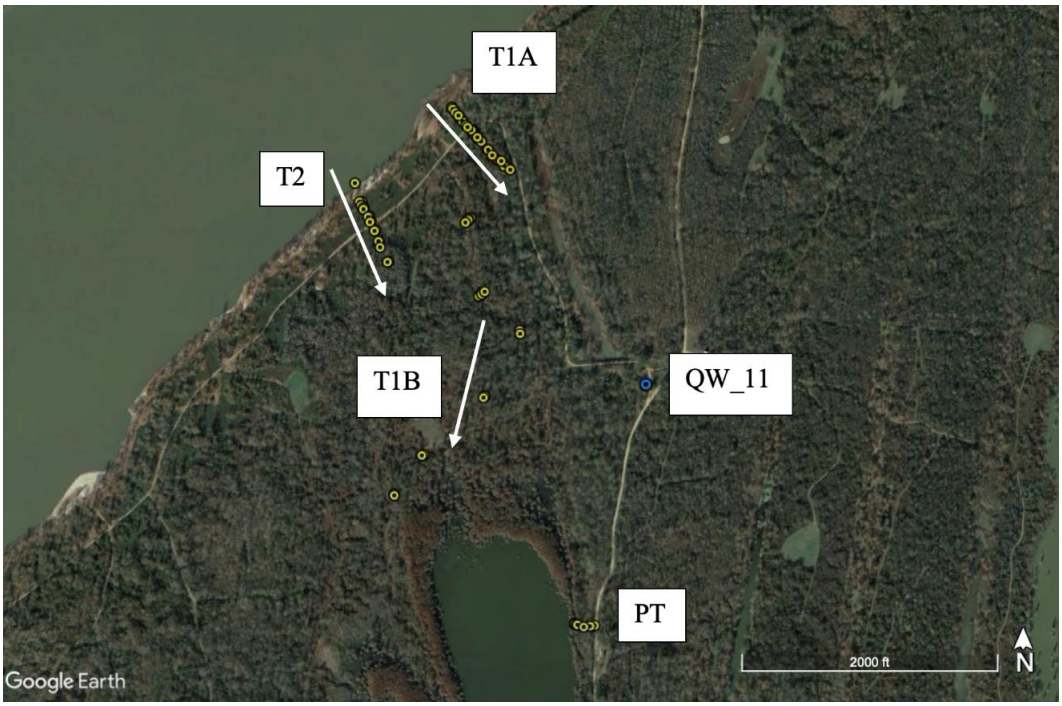

Figure 4.1 *Map of study area at Fort Adams. Transect T1A, T2, and T1B are shown in embanked floodplains of the Lower Mississippi River.*

Note: Symbols indicate sample localities: yellow (surface sediments, October 2017), red (surface sediments, September 2018), and blue (water samples, March and June 2019). Elevation model and imagery were obtained from Google Earth (2020) and the aerial images were acquired in 2019).

Transect three (T3) is an area of land located ~~in~~ between the southern portion of the oxbow lake, Lake Mary and the main LMR channel (Figure 4.2). Only one transect of sediment was collected in October of 2017. T3 data collection started at 0m and increased distances and location of the samples along the transect to 10m, 20m, 40m, 60m, 80m, 120m, 160m, and 190m, for the October 2017 (nine samples total).

Figure 4.2 *Map of study area near Lake Mary. Transect 3 is shown in embanked floodplains of the Lower Mississippi River.*

Note: Symbol indicates sample localities: yellow (surface sediments, October 2017). Elevation model and imagery were obtained from Google Earth (2020) and the aerial images were acquired in 2019).

The Cloverdale Unit is a meander scroll location. Two transects of sediment samples were collected for both the October 2017 and the September 2018 data set. The more distal transect (from LMR) is T4 and the second transect being furthest west (closest to LMR) is named T5. Transect four (T4) data collection started at the Long Lake shoreline and continued east by increasing distance (Figure 4.3). Sediment samples were collected in both October of 2017 and September of 2018 at both T4 and T5. For October, 2017, T4 started with 0 meters from Long Lakes' shoreline, and continued with increasing distance of 10m, 20m, 40m, 50m, 61m, 80m, 90m, 100m, 110m, 120m, ending at 130m away. The second transect (T5) was collected on another series of meander scrolls closer to the LMR main channel than T4 (Figure 4.4). For October 2017, T5's

total distance totaled 20 m; with four sample locations, 0 meters (two samples), 10 m and 20m.

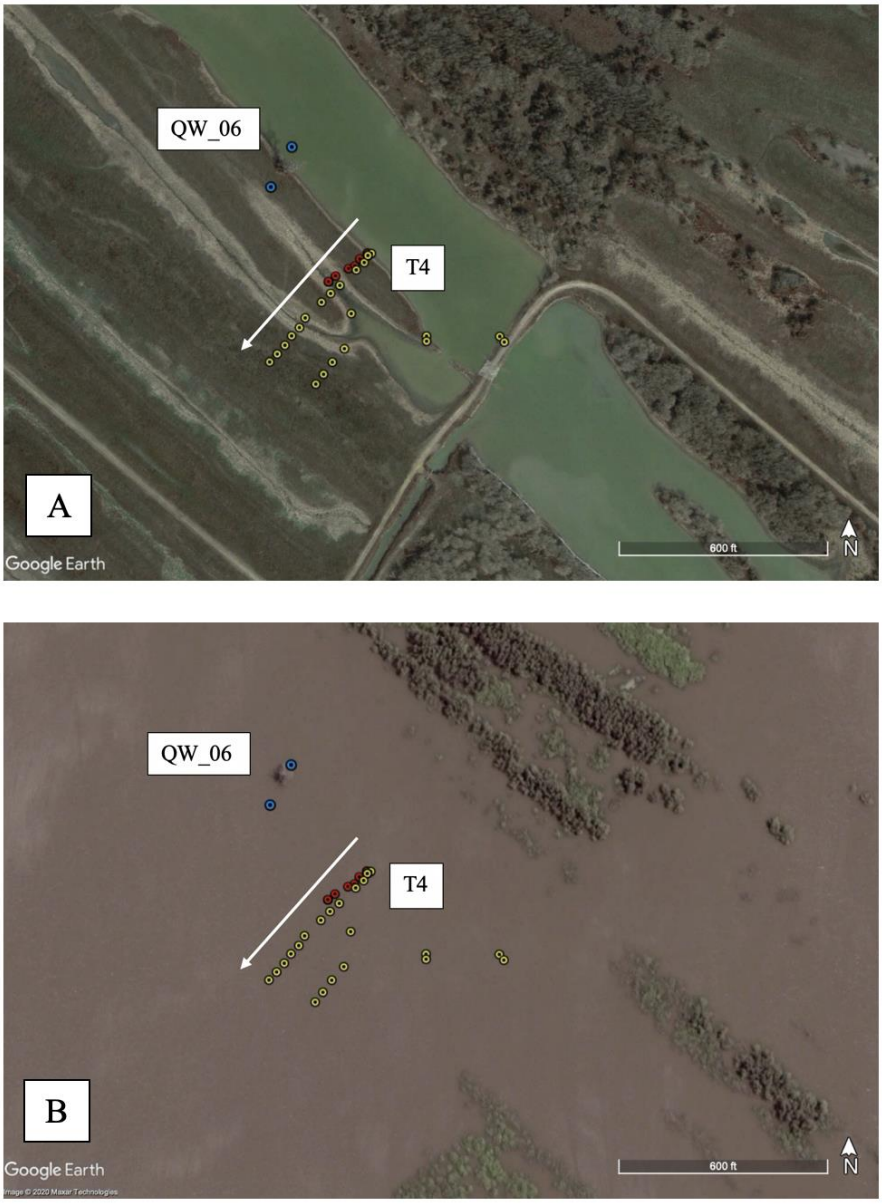

Figure 4.3 *Map of study area at the Cloverdale Unit. A: is a google image before the 2018 flood. B: is a google image during the 2018 flood. Transect T4 and QW_06 is shown in embanked floodplains of the Lower Mississippi River. Symbols indicates sample localities: yellow (surface sediments, October 2017), red (surface sediments, September 2018), and blue (water samples, March and June 2019). Elevation model and imagery were obtained from Google Earth (2020) and the aerial images were acquired on 8/2018 (A) and 4/2019 (B).*

Figure 4.4 *Map of study area at the Cloverdale Unit. Transect T5 is shown in embanked floodplains of the Lower Mississippi River. Symbols indicates sample localities: yellow (surface sediments, October 2017) and red (surface sediments, September 2018). Elevation model and imagery were obtained from Google Earth (2020) and the aerial images were acquired on 8/2018 (A) and 4/2019 (B)).*

Transect seven was collected just south of Lake Butler, where the lakes outlet is. Two sediment samples were taken only in October 2017 of Butler Lake. Sediment was collected for only October 2017 (Figure 4.5). Transect eight of sediment samples started at Salt Lake and collected perpendicular to Salt Lake (and MSR) with increasing distance, extending northeast towards the western side of Lake Butler (Figure 4.5).

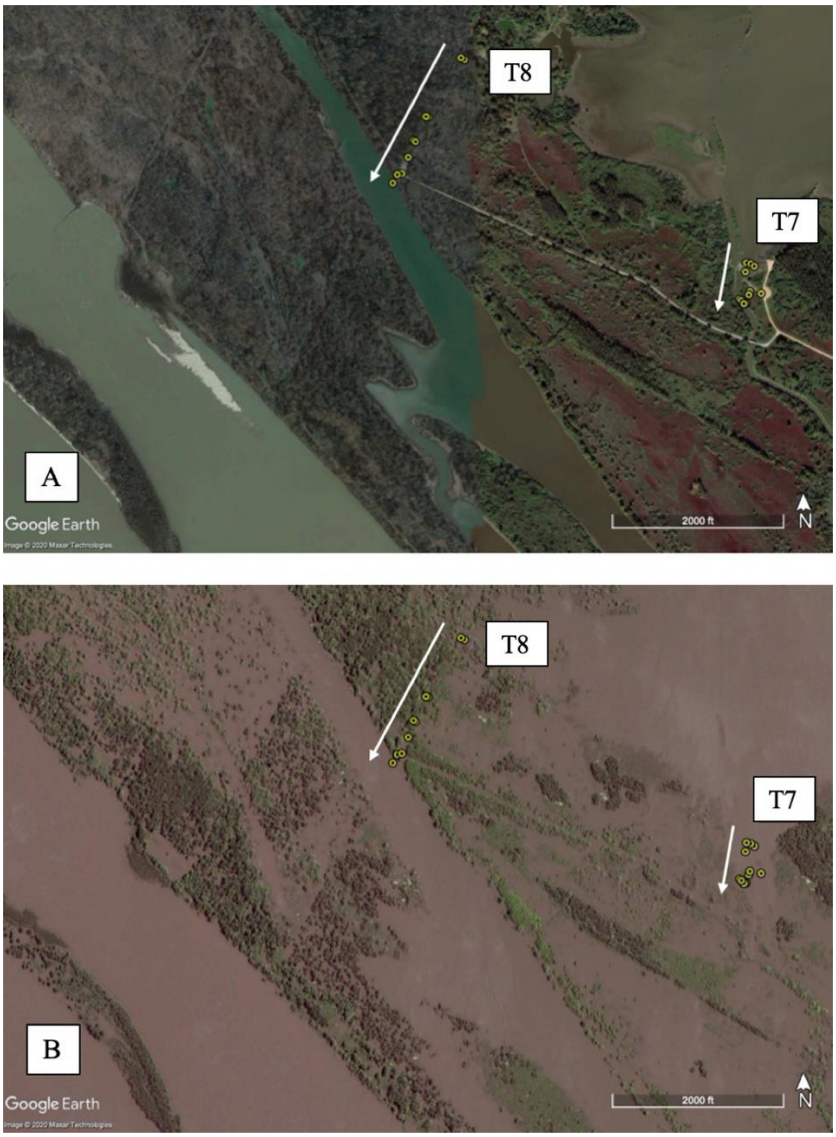

Figure 4.5 *Map of study area at Salt Lake and Butler Lake. Transect T5 is shown in embanked floodplains of the Lower Mississippi River. Symbol indicates sample localities: yellow (surface sediments, October 2017). Elevation model and imagery were obtained from Google Earth (2020) and the aerial images were acquired on 8/2018 (A) and 4/2019 (B).*

T9-T13 are backswamp locations within SCCWNR. T9-12 were collected during October 2017 collection period and T11 and T13 were collected during the September 2018 data set (Figure 4.6). T9 and T12 were collected moving perpendicularly away from the LMR main channel. T10 and T11 were collected perpendicularly away from the LMR as well, but on a meander (northwest to southeast). T13 was collected very close to the LMR with the transect collected perpendicular to the LMR.

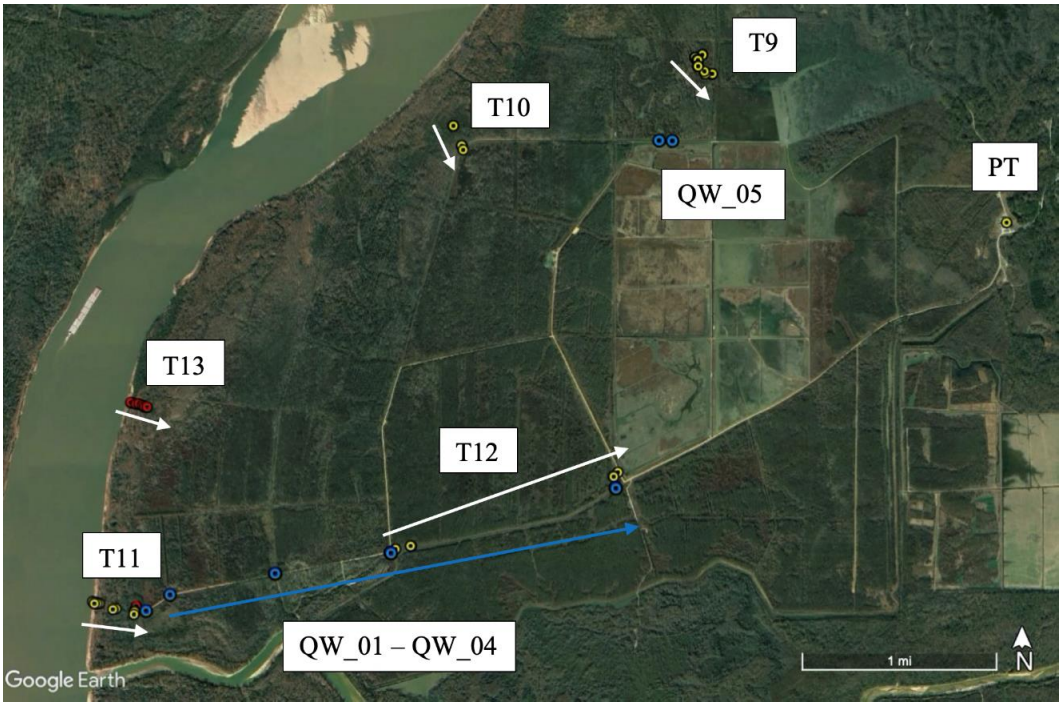

Figure 4.6 *Map of study area at the Sibley Unit. Transect T9-T13, QW_01-QW_05, and the barometric PT is shown in embanked floodplains of the Lower Mississippi River. Symbols indicates sample localities: yellow (surface sediments, October 2017 and PT, October 2017), red (surface sediments, September 2018), and blue (water samples, March and June 2019). Elevation model and imagery were obtained from Google Earth (2020) and the aerial images were acquired in 2019.*

4.1.2.2 DISCRETE SAMPLES

Carthage Point Road sample is at a levee crest located directly off ~~of~~ the main LMR channel (named transect 6 even though it could not be designated a transect due to

only the limitation of one sample). Sediment samples were collected for both October 2017 and the September 2018 (one sample each) (Figure 3.5).

4.1.2.3 TRENCH SAMPLES

In October 2017, sediment was collected within a 24-cm deep trench at the northern side of the Sibley Unit of SCCNWR (Figure 4.6). This trench was collected directly adjacent to the first sample collected along T13 (sample 13.01). The trench was dug until multiple horizons were identified by obvious color and grain size differences. Samples were collected from each horizon and placed in individual sample bags for laboratory analyses. Samples will be listed as following with the thickness in parenthesis: C1 (4.2 cm), S1 (11.1 cm), C2 (1.5 cm), S2 (6.2 cm), C3 (2.9 cm), S3 (20.2), and C4 (undefined) (Figure 4.7).

Figure 4.7 *Trench dug in the Sibley Unit of SCCNWR. Alternating sand and clay layers were observed and samples were collected (uppermost layer being C1, alternating with depth).*

4.1.3 WATER TEMPERATURE/DEPTH SENSORS

Onset HOBO pressure and temperature sensors (PT) were deployed at five sites: Artonish Lake, Lake Mary, Long Lake, Butler Lake, a chute of the LMR at the lower (southern) end of the Butler Lake Unit, and the Sibley Unit. A HOBO barometric pressure sensor was also deployed at the SCCNWR maintenance shed (above historic

flood stages). Each sensor was placed in a protective case made out of PVC pipe that was secured by hose clamps to a metal fence post hammered into the substrate. This allowed for protection and stability during higher energy floods, as well as water exchange through holes drilled throughout the case. A galvanized bolt at the bottom of the PVC case ensured consistent sensor position. The Hobo instrument designated for barometric pressure compensation was placed in a secure non-inundated location. Barometric compensation for each sensor and data analysis were done in ONSET HOBOware software. Time stamps for each observation were corrected from Central Daylight Savings Time to Central Standard Time as needed. GPS was used to obtain position and elevation data of the PT. The antenna mounted to a prism pole of the Trimble GeoXH was placed directly on a bolt drilled into the casing of the PT that was adjacent to where PT was encapsulated in the casing.

4.1.3.1 INSTALLATION

Pressure transducers were placed at differing locations to try to retrieve inundation data at multiple sub environments that represent the study area's floodplain. Data were collected during a two-year span between October, 2017 and October, 2019 at Artonish Lake, Lake Mary, Long Lake, Butler Lake, a chute of the LMR at the lower (southern) end of the Butler Lake Unit, and the Sibley Unit. At Butler Lake the PT was installed on the east side of St. Catherine Creek, directly south of the riprap dam and first riser at Butler Lake's output at St. Catherine Creek. South of Butler Lake, a PT was installed on a chute channel of the MSR~~,~~ directly below the confluence of St. Catherine Creek. The PT was inserted onto the eastern bank of the chute channel (midway down steep channel). At Long Lake, a PT was installed on the southwest side of the lake, along

the shoreline. At Artonish Lake, the PT was installed on the eastern side of the lake parallel with Jackson Point Road. The PT was inserted into the shoreline, along groves cypress trees. At Lake Mary, a PT was installed along the shoreline on the south end of the lake's oxbow. Water sensors located at varying geomorphological settings and proximities to the LMR provided a full range and variability of complex mechanisms of the LMR floodplain regime.

4.1.3.2 DATA RETRIEVAL

Water level and temperature sensors deployed in October 2017 were subsequently retrieved by Dr. Franklin Heitmuller and Dr. Paul Hudson in October 2019. The PT sensors were then returned into the floodplain to collect data for future studies.

4.1.4 OVERBANK FLOOD SAMPLING

Overbank water column samples were collected from a jon boat during March and June, 2019. The March and June 2019 collection periods were made during or close to the peak of the flood events. Large amounts of water were flowing within the floodplain up to ~7.3 m (~24 ft) deep during times of overbank flow. GPS was used to obtain position and elevation data of the jon boat in which all samples were collected directly off the bow. The antenna mounted to the prism pole of the Trimble GeoXH was placed directly on a boat that was adjacent to where the water surface contacted the side of the boat (Figure 4.8). Samples collected in March and June, 2019 were collected as close as possible using the GPS and tree line to correlate collection locations.

Figure 4.8 *Dr. Frank Heitmuller collecting a GPS position in the Sibley Unit at St. Catherine Creek NWR. The jon boat was stabilized by latching onto a nearby tree.*

Three transects of water samples were collected in the floodplain water column. The first transect consisting of QW_01-QW_05 was collected in the Sibley Unit. Starting closest to the LMR and moving distal into the floodplain, the transect is ordered QW_02, QW_03, QW_04, QW_01, and QW_05. QW_05 is oblique to QW_01 - 04. QW_01 - 05 was collected for both March and June, 2019. Samples were collected as close as possible (horizontally) to T9, T11, and T12 (Figure 3.15).

Three water samples were collected for both the March and June, 2019 sample periods. Starting closest to the LMR, QW_07 (from east to west QW_07,QW_06, then QW_08). Sampling locations are collected in a transect, but more importantly along the LMR meander. Samples were collected as close as possible (horizontally) to T4 and T5 (Figure 3.17).

Water samples were taken only in June of 2019 for the Fort Adams area only, (Figure 4.9). QW_9 - QW_12 were collected within a desired proximity of the LMR, rather than a transect. QW_11 was collected as close as possible (horizontally) to T1A, T1B, and T2 (Figure 4.1).

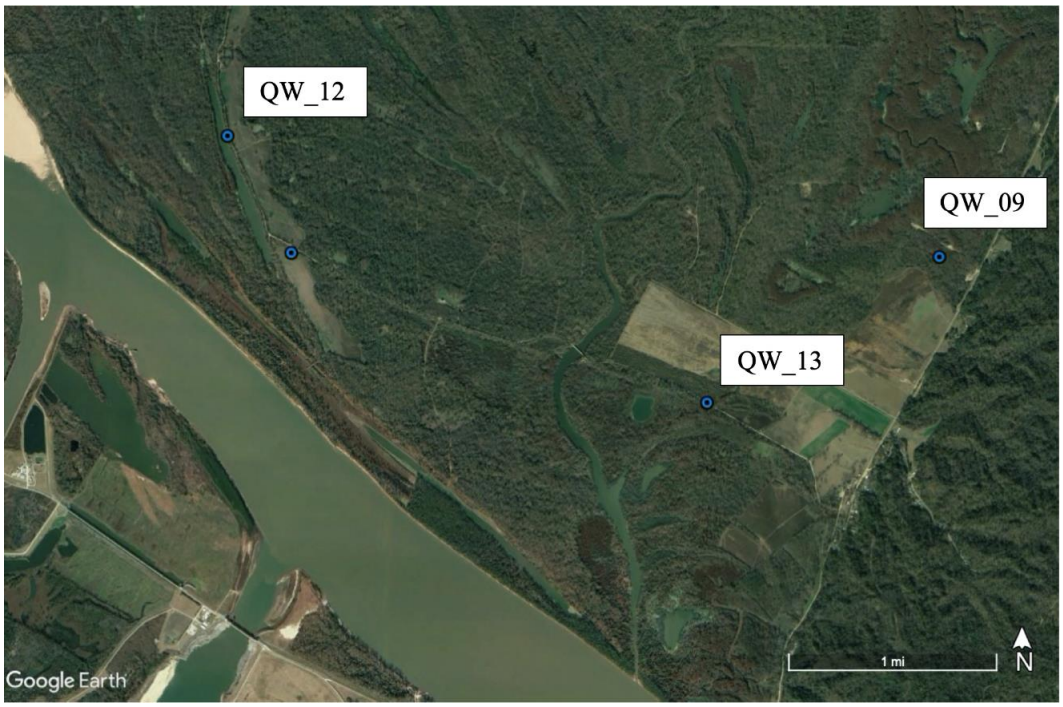

Figure 4.9 *Map of study area at Fort Adams. Transect QW_09, QW_12, and QW_13 is shown in embanked floodplains of the Lower Mississippi River. Symbols indicates sample localities: blue (water samples, March and June 2019). Elevation model and imagery were obtained from Google Earth (2020) and the aerial images were acquired in 01/2019.*

4.1.4.2 IN-SITU WATER QUALITY

Two different Yellow Springs Instrument (YSI) Professional water-quality instruments were used. Each sensor was lowered into the water at two different depths for each sample location. The shallow depth was measured at 0.25 m for each sample. For the deeper measurements, a depth near the bottom was selected based on the measured depth at that site.

The first YSI instrument measured temperature (°C), pressure (mm Hg), dissolved oxygen (DO) percent, DO (mg/L), conductivity (mS/cm), total dissolved solids (TDS) (mg/L), salinity (ppt), pH, and ORP (mV). The second YSI probe measured temperature (°C), atmospheric pressure (mm Hg), dissolved oxygen (DO) percent, and DO (mg/L). All instruments were calibrated before entering the field.

Figure 4.10 *Typical overbank flood conditions along the LMR in the study area while accessing sample sites using a jon boat.*

4.1.4.3 FLWO DEPTH AND VELOCITY

Depth was measured using a handheld Sontek depth sounder off the side of the jon boat. The Sontek was used by holding the tip of the instrument in the water to the recommended line and taking a reading. Three measurements were taken to get an average depth of the water column.

Flow velocity at a depth of 1.22 m (4 ft) was also measured off the side of the

boat using a Marsh-McBirney Flowmate 2000. The Flowmate 2000 was attached to a measured rod holder in which the instrument was lowered to 4ft and pointed to the direction of flow. Three to five measurements were taken to get an average flow rate.

4.1.4.4 DEPTH-INTEGRATED SAMPLING

A Type A-55 reel mounted to a custom portable plate attached to the jon boat was used to lower and raise a DH-59 sampler at a pre-determined transit rate to a maximum depth of 4.57 m (15 ft) (Figure 4.11). A 3/16th-inch nozzle was selected for the DH-59 sampler to fill a clean, acid-washed, and deionized water rinsed, pint-sized sample bottle. The transit rate was determined by dividing the total filling time determined from a chart (using measured flow velocity) (Figure 4.12) by the depth sampled and dividing by two to account for the two-way travel time. Note that even if the water column reached a depth of more than 15 ft. (max depth of ~24 ft.), only the top 15 ft. of the water column was collected due to the depth restrictions of the USGS DH-59 sampler. For three water quality sample sites near Artonish Lake and Fort Adams, a manual hand rope (with marked length increments) and D-59 sampler was used because the Type A-55 reel line slipped off of the spool and could not be repaired in the field. The two-way transit rate was determined by the same procedures outlined above and samples were successfully collected.

Two samples were collected at each sample site, one for nutrient analyses and one for suspended sediment analyses. Further, duplicate samples were collected for both nutrients and suspended sediments at some sites.

Figure 4.11 *A water sample collected using a USGS DH-59 sampler. The reel was used to maintain a consistent transit rate.*

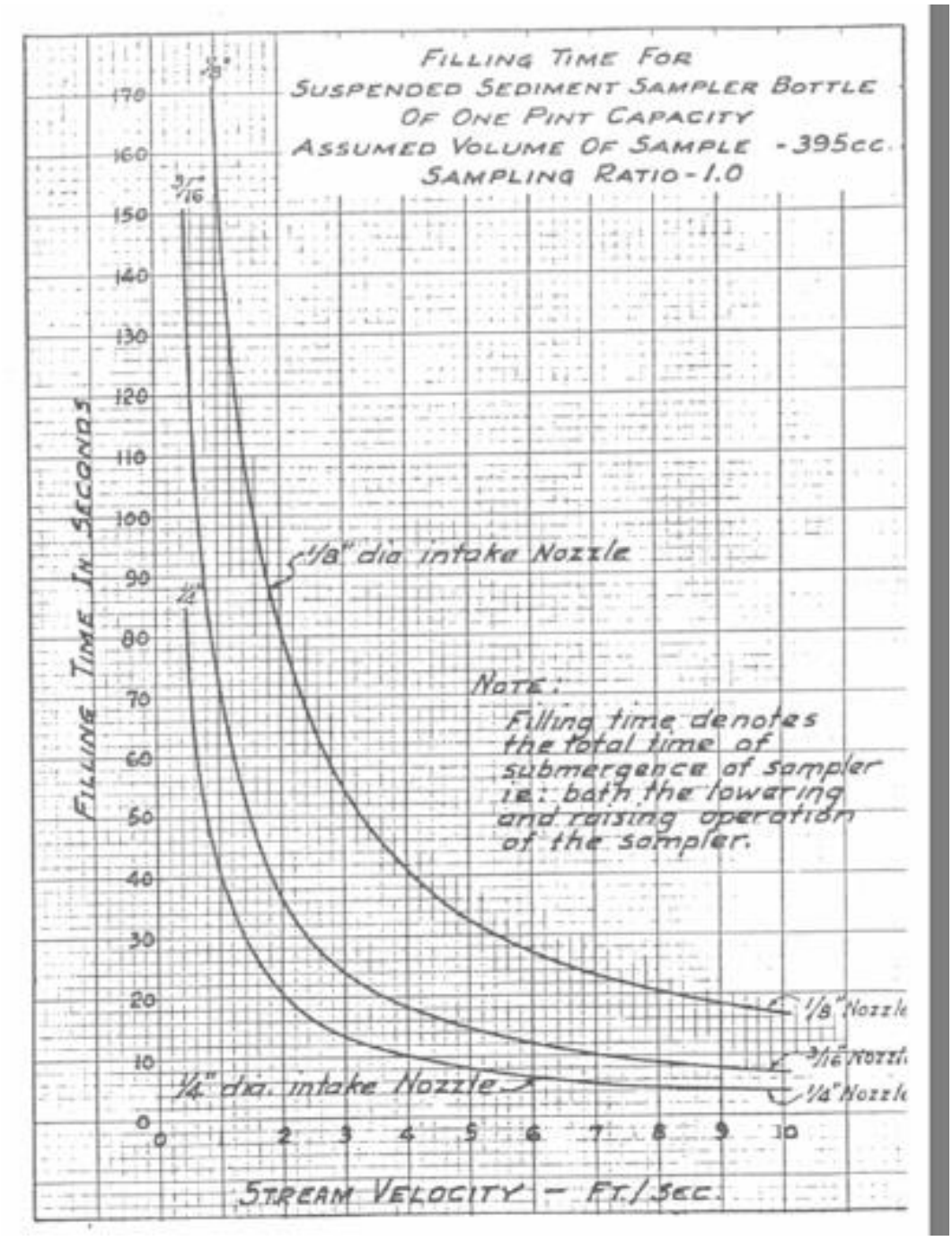

Figure 4.12 *Transit rate calculation sheet with axis of stream velocity, filling time in seconds, and a nozzle diameter in inches. This chart was used for every USGS DH-59 water sample site to collect samples for nutrient and suspended sediment analysis (Davis, 2005).*

4.2 LABORATORY ANALYSIS

Laboratory analysis were conducted for all ~~of~~ the sediment and water samples collected in the field to measure textural and/or compositional variables. Three laboratories were used at The University of Southern Mississippi: (i) the Sedimentology Laboratory with Dr. Franklin Heitmuller from the School of Biological, Environmental, and Earth Sciences, (ii) the Microbiology Laboratory supervised by Dr. Kevin Kuehn from the School of Biological, Environmental, and Earth Sciences, and (iii) the Coastal Hazards Laboratory at Stennis Space Center with Dr. Davin Wallace from the School of Ocean Science and Engineering.

A portion of sediment was taken from the entire floodplain sediment sample after homogenizing the entirety of the bag before sampling. Munsell color was conducted as a single test, and discarded after. In order, using the same sediment sample, OM then physical size was conducted. Lastly, carbon and nitrogen were conducted together with the same sample, where phosphorous was conducted separately as its own sediment sample.

A portion of water was used after homogenizing the entirety of the water sample collect in the field. Two different samples were used; a strictly physical water sample and an acid washed bottle was used for all nutrient analysis. The physical water sample was used for suspended sediment, physical size, and turbidity. The nutrient sample was used for C/N (suspended sediment), P (suspended sediment), P (filtered water), and nitrite/nitrate (filtered water).

4.2.1 FLOODPLAIN SURFACE SEDIMENTS

4.2.1.1 MUNSELL COLOR

Lab samples were dampened and rolled into a ball/ribbon to determine color using a Munsell soil color chart. Color was selected for each sample based on the closest match to the chart. Hue, value, chroma, and common name were recorded.

4.2.1.2 ORGANIC MATTER CONTENT

Organic matter content was found using the loss-on-ignition (LOI) method used by Heiri et al. (2001). Sediment samples were dried overnight in a convection oven at 105°C in glass beakers, crushed using a mortar and pestle, weighed using an Ohaus digital scale (hundredths of a gram precision), and subsequently placed in a muffle furnace at 550°C for 6 hours. Pre-weighed ceramic crucibles (~5 mL) were tared and the sample was reweighed and the difference in weight before and after combustion were recorded to determine the amount of organic matter by weight (%) or loss of mass percentage.

4.2.1.3 GRAIN (PARTICLE) SIZE

Sediment samples were analyzed for grain size at the Coastal Hazards Laboratory at Stennis Space Center, Mississippi. A Malvern Matersizer 3000 apparatus paired with a Hydro LV wet dispersion unit was used, engaging a wet sieve technique, to calculate grain size. Each sediment sample was dried, OM burned off, crushed, deflocculated (5% sodium hexametaphosphate was utilized) and bottled before the wet sieve was run.

For water sample analysis, raw water samples were untreated, centrifuged, and aspirated which condensed the sediment of ~500 ml of raw water into ~50 ml.

Afterword, samples were deflocculated using 5% sodium hexametaphosphate and bottled before being run on the Malvern Mastersizer 3000.

Results of particle size were calculated within the Mastersizer program. The main form of sediment representation used was D(10), D(50), and D(90). However other percentiles were found as well; D(16), D(25), D(75), D(84), and particle size by size (mm).

4.2.1.4 MAGNETIC SUSCEPTIBILITY

Sediment samples were measured for magnetic susceptibility (MS) in order to widely interpret the environmental geochemisty, provenance, and mineralogy of each sample. Using a volume-specific program and the appropriate container (10 cm^3), two methods of measurement were used: 5 grams of measured sediment and sediment filled to the appropriate line on the sample container. This study will use the filled container measurements. MS was measured using a Bartington MS2B dual-frequency sensor and MS3 meter. Before field samples were run, the machine was calibrated using the known calibration sample ($3062*10^{-5}$ SI at 22°C) included with the instrument. Each sample was first dried, OM was burned off, and then crushed and measured into 10cm^3 sample vials. Samples were run on low frequency (0.46 kHz).

In the literature there are known values for MS with differing geologic material. High MS values are ferrimagnetic, low MS values are paramagnetic, and negative values are diamagnetic. Ferrimagnetic (high MS values) sediment samples are found to contain iron-bearing minerals (i.e., magnetite) that are magnetized (with no magnetic field). For minerals with low susceptibility (i.e., iron irons and manganese), a MS value is shown when a magnetic field is present. When negative MS values are shown, this means an

absence of minerals that contain iron (i.e., quartz and $CaCO_3$), even with a magnetic field. Sedimentary rocks have a scope of $0.001 – 0.01*10^{-6}$ m3-1kg

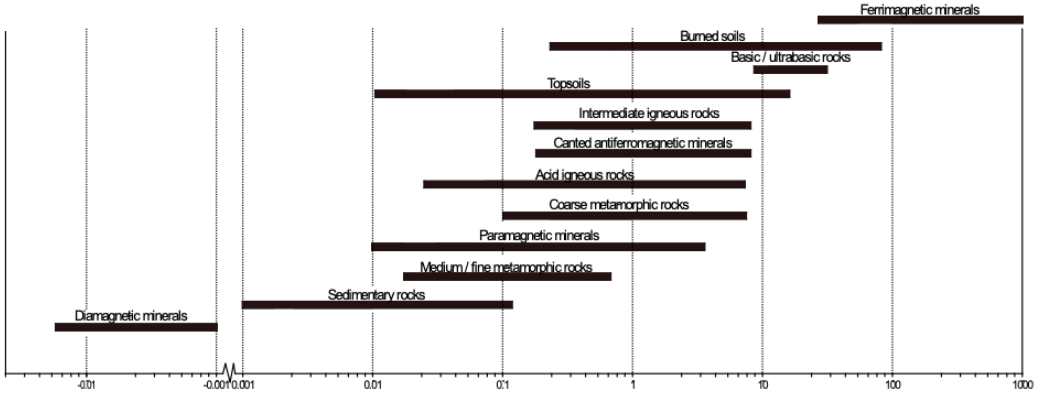

Figure 4.13 *Chart of environmental materials and minerals of typical scopes of magnetic susceptibility values (room temperature) (Dearing, 1999).*

4.2.1.5 CARBON/NITROGEN (C/N)

Samples were dried at 55°C, homogenized, weighed to the nearest 0.01 mg while wrapped in tin foil capsules, and stored dry. Total carbon and nitrogen were measured through total loss of mass (combustion) in a Costech Elemenal CN Analyzer (Costech Analytical Technologies, Valencia, CA) CN 802 Carbon / Nitrogen Analyzer. C/N in this report is expressed in percentage by weight.

4.2.1.6 PHOSPHORUS (P), NITRATE (NO^{3-}) + NITRITE (NO^{2-})

Nutrient analysis was conducted using the molybdate-ascorbic acid method. Samples were dried at 55°C, homogenized, combusted (500°C), and weighed to the nearest 0.01 mg. Sequentially, samples were digested (extracted) in 1N HCL at 90°C and diluted to 25% of the original concentration in preparation to run the nutrient analysis. Two sets of dilutions were utilized (one for P and one for NO^{3-} and NO^{2-}), centrifuged and measured out into sterile containers for measurement. PO_4, NO^{3-}, and NO^{2-} were calculated using a SEAL AutoAnalyzer3 (AA3) (SEAL Analytical, Milwaukee, WI).

4.2.2 WATER SAMPLES

4.2.2.1 SUSPENDED SEDIMENT ANALYSIS

Raw water samples were filtered and weighed on glass filter paper. The amount of fluid filtered was measured and divided by the weight of the amount of sediment on the filter. The amount of suspended sediment was measured with the following formula: mg OF SEDIMENT/ml OF WATER = SUSPENDED SEDIMENT

4.2.2.2 PARTICLE SIZE

For particle size, raw water samples were centrifuged in order to condense all sediment to the bottom of the water sample. The sample was then aspirated using a vacuum to dispose of access water. This process was done until enough sediment was accumulated to run the Malvern Matersizer 3000 (using the same technique as above).

4.2.2.3 TURBIDITY

Turbidity of water samples was measured using a Lamotte turbidity meter. Standards of both 1 and 10 Nephelometric Turbidity Units (NTU) were used to calibrate the meter. Raw untreated water samples were poured into the affiliated container after being homogenized.

4.2.2.4 CARBON AND NITROGEN

Suspended sediment on filter papers were used for nutrient analysis. Samples were dried at 55°C, homogenized, weighed to the nearest 0.01 mg while wrapped in tin foil, and stored dry. Total carbon and nitrogen were measured through total loss of mass (combustion) in a Costech Elemental CN Analyzer (Costech Analytical Technologies, Valencia, CA) CN 802 Carbon / Nitrogen Analyzer. C/N in this report is expressed in percentage by suspended sediment weight.

4.2.2.5 PHOSPHORUS AND NITRATE + NITRITE

Suspended sediment on filter papers were used for nutrient analysis. Nutrient analysis was conducted using the molybdate-ascorbic acid method. Samples were dried at 55°C, homogenized, combusted (500°C), and weighed to the nearest 0.01 mg. Sequentially, samples were digested (extracted) in 1N HCL at 90°C and diluted to one/eighth of the original concentration in preparation to run the nutrient analysis. Two sets of dilutions were utilized (one for P and one for NO^{3-} and NO^{2-}), centrifuged and measured out into sterile containers for measurement. $P\text{-}PO_4$, NO^{3-}, and NO^{2-} was calculated using a SEAL AutoAnalyzer3 (AA3) (SEAL Analytical, Milwaukee, WI).

4.3 ONLINE DATA

4.3.1 LMR MAIN RIVER CHANNEL DATA

The Vicksburg, MS LMR data was found using downloaded archives from the U.S. Army Corps of Engineer's database. Vicksburg, MS is the northernmost location used for flood data, located at mile marker 438 (U.S. Army Corps of Engineers). The St. Francisville LA LMR data was downloaded from the U.S. Army Corps of Engineers database. All data from the army Engineer Corps were organized and used for comparison to actual field data.

CHAPTER V – RESULTS

5.1 OVERBANK SEDIMENT CHARACTERISTICS BEFORE AND AFTER THE 2018 FLOOD (OCTOBER 2017 AND SEPTEMBER 2018)

Results reported in this chapter include physical and chemical characteristics of sediment samples collected from the floodplain surface in October 2017 and September 2018, suspended sediment samples collected from the overbank water column in March and June 2019, and overbank water samples (in situ and collected).

Sediment sample data are ordered by location from north to south: Cloverdale Unit (T4 and T5), Butler Lake (T7), Salt Lake (T8), Sibley Unit (T9 to T13), Lake Mary (T3), and Artonish Lake (T1 and T2).

5.1.1 TRANSECT SAMPLES

5.1.1.1 CLOVERDALE UNIT (LONG LAKE) (TRANSECTS 4 AND 5)

The Cloverdale Unit is a meander scroll location. Two transects of sediment samples were collected in both October 2017 and September 2018. The more distal transect (from LMR) is T4 and one furthest west is T5 (Figure 4.3 and 4.4).

Transect four (T4) data collection initiated at the southwestern Long Lake shoreline and continued west with increasing distance. For October 2017, T4 started at the shoreline and continued at distances of 10m, 20m, 40m, 50m, 61m, 80m, 90m, 100m, 110m, 120m, and 130m. Sediment grain size values are reported in micrometers (microns) below for the 10^{th} (D10), 50^{th} (D50), and 90^{th} (D90) percentiles. The median grain size (D50) ranges from 25.1 to 116.0 microns (Figures 5.1 and 5.2). Munsell color is 10YR for all samples. Organic matter ranges from 7.64% to 16.34%. Magnetic susceptibility ranges from 1.84×10^{-04} SI to 2.41×10^{-04} SI. For carbon and nutrient

analysis, carbon ranges from 1.72% to 3.64%, nitrogen ranges from 0.18% to 0.40%, and phosphorus ranges from 0.02% to 0.19% (Figure 5.1) (Appendix A.1; 04.01.00 to 04.12.130).

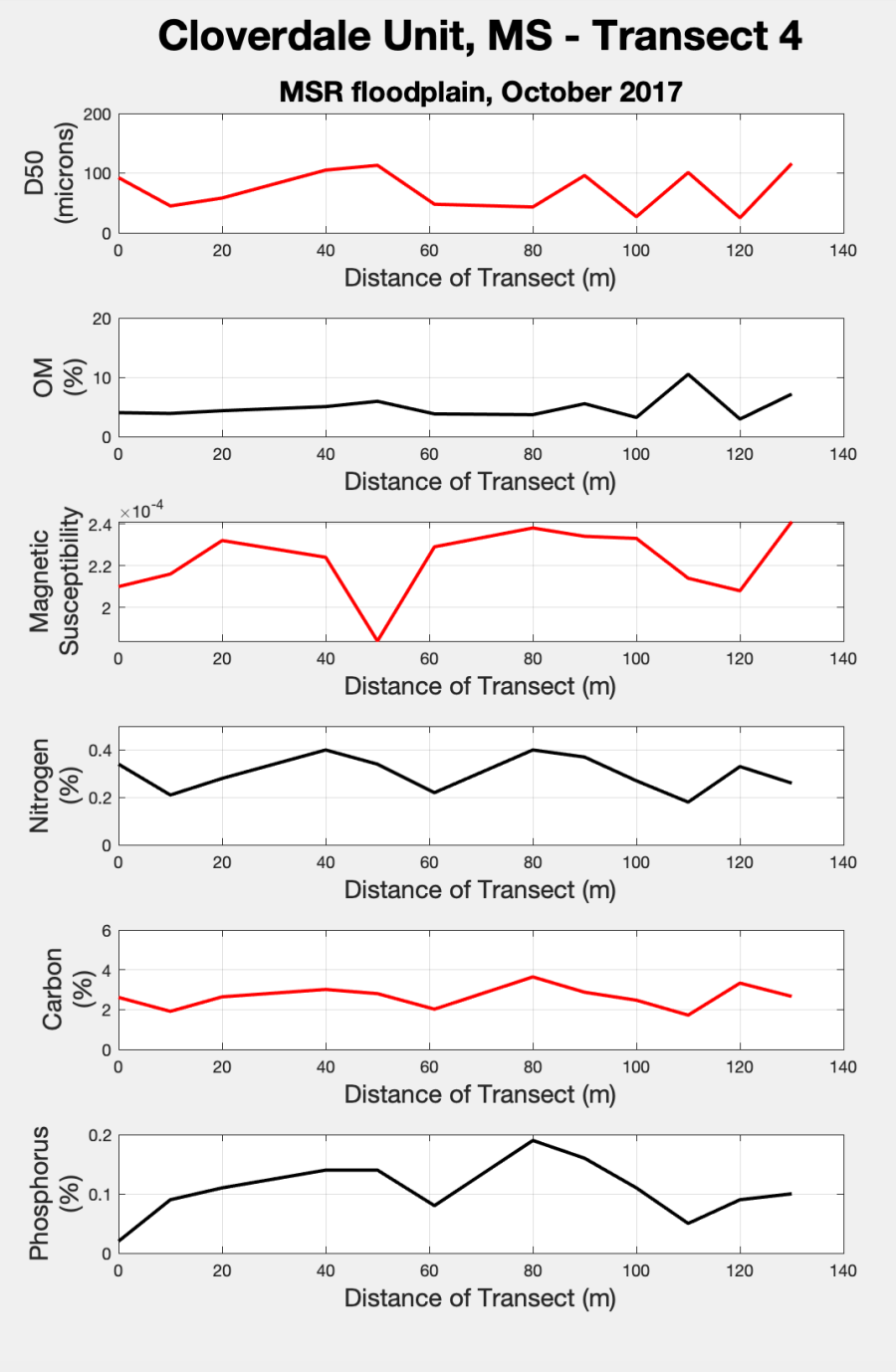

Figure 5.1 *Laboratory analysis results for T4 at the Cloverdale Unit, MS, for October 2017.*

Note: Transect length = 130m. All percentages are by weight.

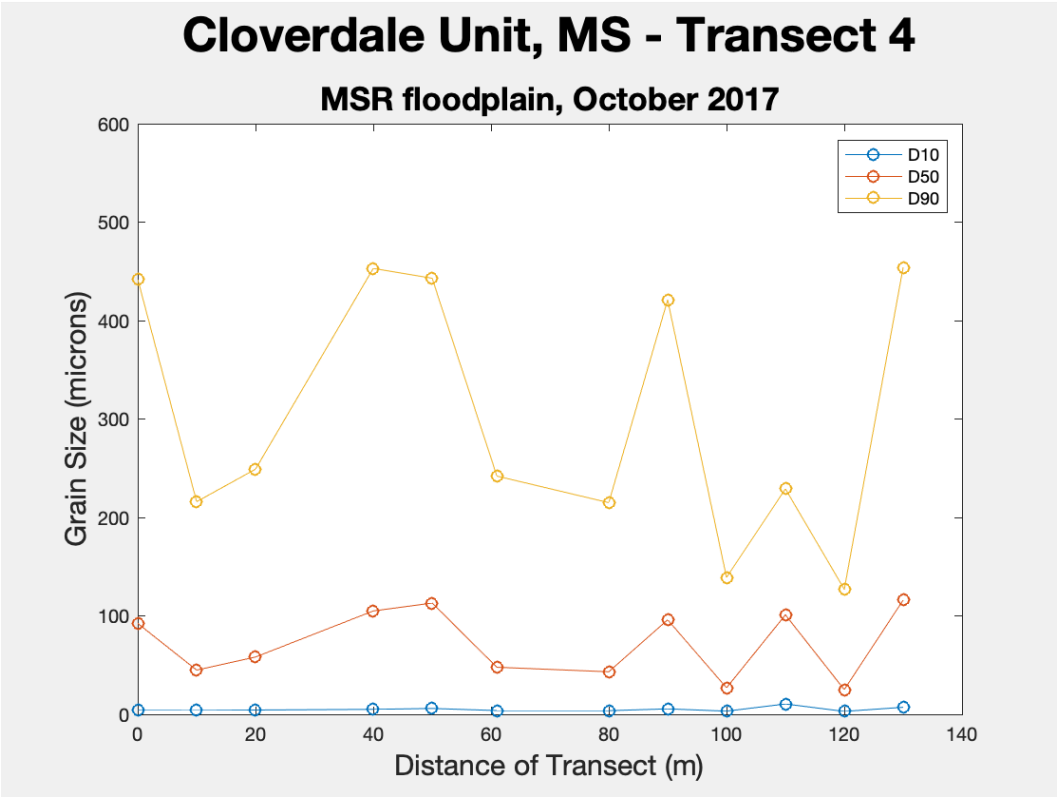

Figure 5.2 *Laboratory analysis of grain size (D10, D50, and D90) for T4 at the Cloverdale Unit, MS, for October 2017.*

Note: Transect length = 130m.

The same sedimentary parameters were analyzed for samples collected along T4 in September 2018. In September 2018, T4 started at the shoreline and continued at distances of 9m, 25m, 38m, 58m, and79m. D50 ranges from 45.5 to 67.5 microns (Figures 5.3 and 5.4). Munsell color is 10YR for all samples. Organic matter ranges from 12.8% to 16.5%. Magnetic susceptibility ranges from 2.04×10^{-04} SI to 2.65×10^{-04} SI. For carbon and nutrient analysis, carbon ranges from 3.01% to 4.30%, nitrogen ranges from 0.35% to 0.48%, and phosphorus ranges from 0.12% to 0.16% (Figure 5.13) (Appendix A.2; 24B to 29B).

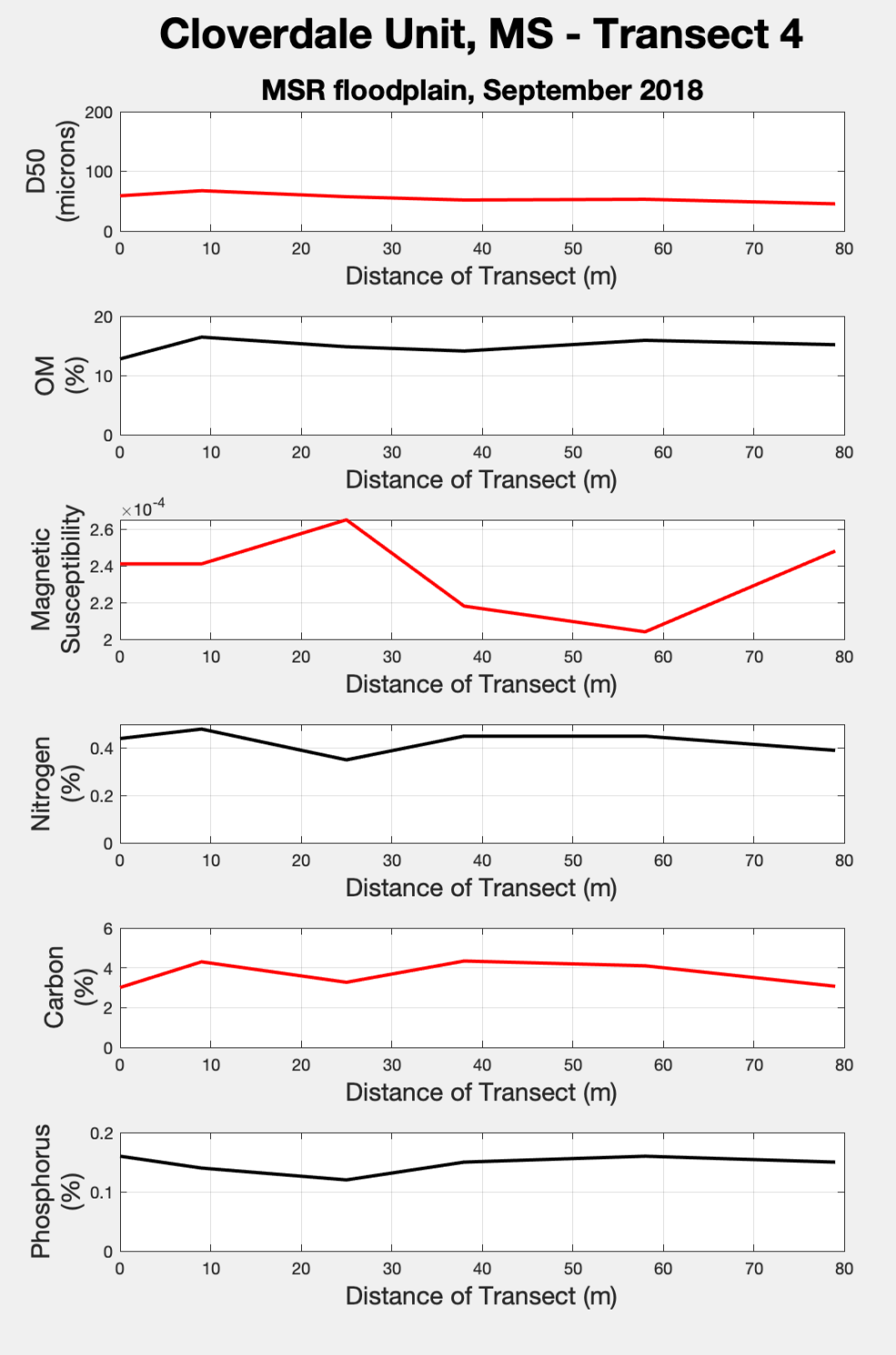

Figure 5.3 *Laboratory analysis results for T4 at the Cloverdale Unit, MS, for September 2018.*

Note: Transect length = 79. All percentages are by weight.

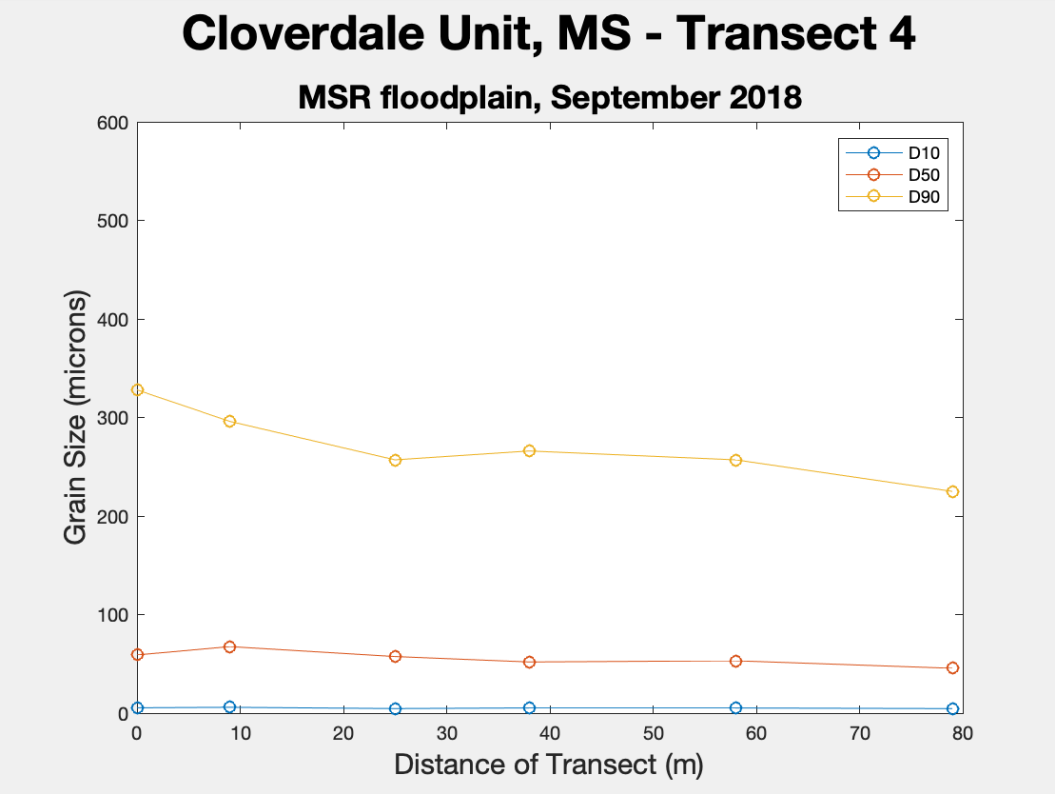

Figure 5.4 *Laboratory analysis of grain size (D10, D50, and D90) for T4 at the Cloverdale Unit, MS, for September 2018.*

Note: Transect length = 79m.

T5 is a meander scroll location west of T4 between the LMR main channel and T4. For October 2017, a distance of 20 m was sampled beginning at 0m (two samples collected adjacent to each other), 10m, and 20m. D50 ranges from 24.1 to 112 microns (Figures 5.5 and 5.6). Munsell color is 10YR for all samples. Organic matter ranges from 10.11% to 12.70%. Magnetic susceptibility ranges from 2.12×10^{-04} SI to 3.27×10^{-04} SI. For carbon and nutrient analysis, carbon ranges from 1.30% to 2.18%, nitrogen ranges from 0.14% to 0.26%, and phosphorus ranges from 0.08% to 0.13%. (Figure 5.5) (Appendix A.3; 05.01.00A to 05.03.20).

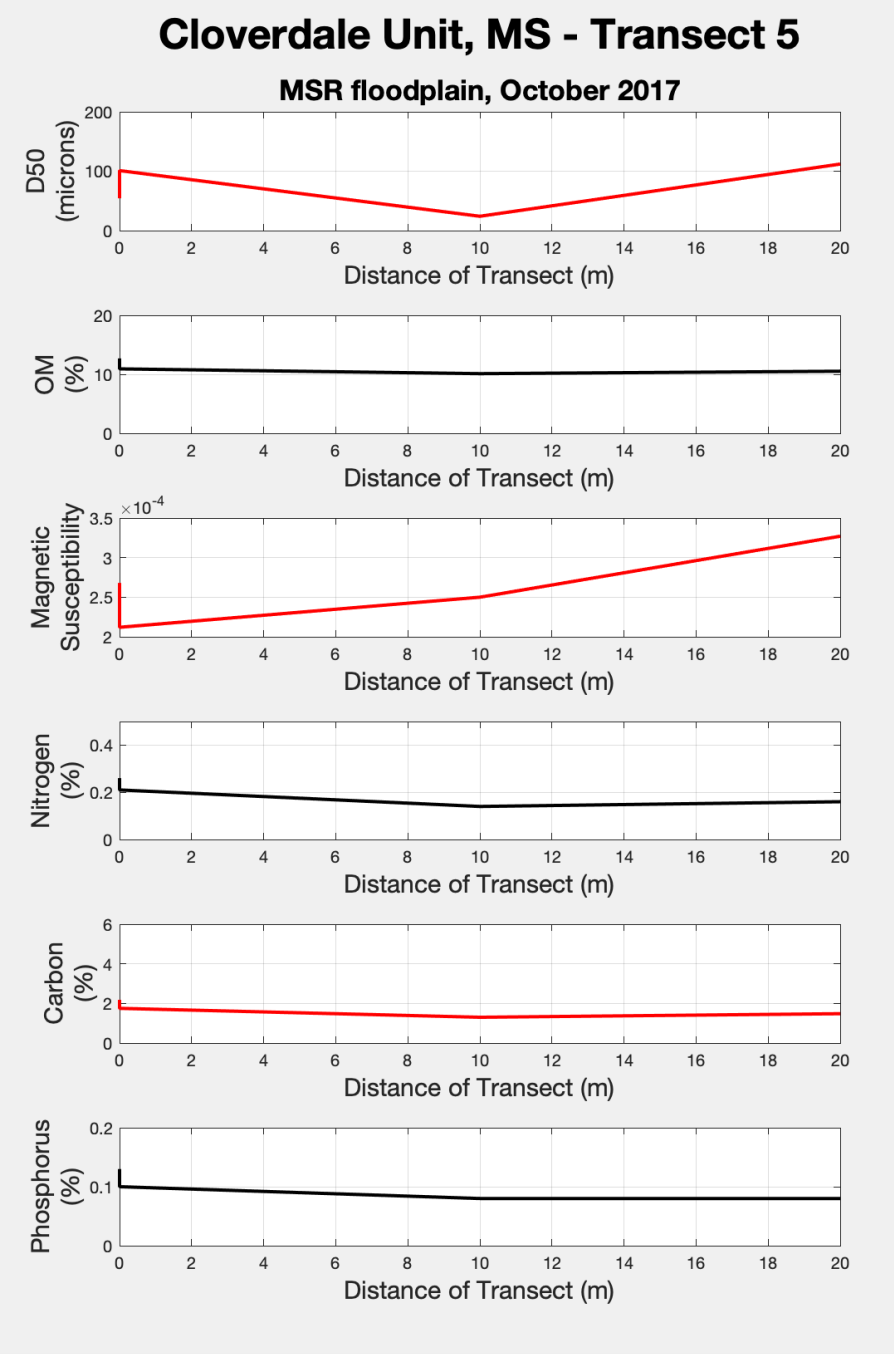

Figure 5.5 *Laboratory analysis results for T5 at the Cloverdale Unit, MS, for October, 2017.*

Note: Transect length = 20m. Samples 05.01.00A, 05.01.00B, 05.02.10, 05.03.20 analyzed. All percentages are by weight.

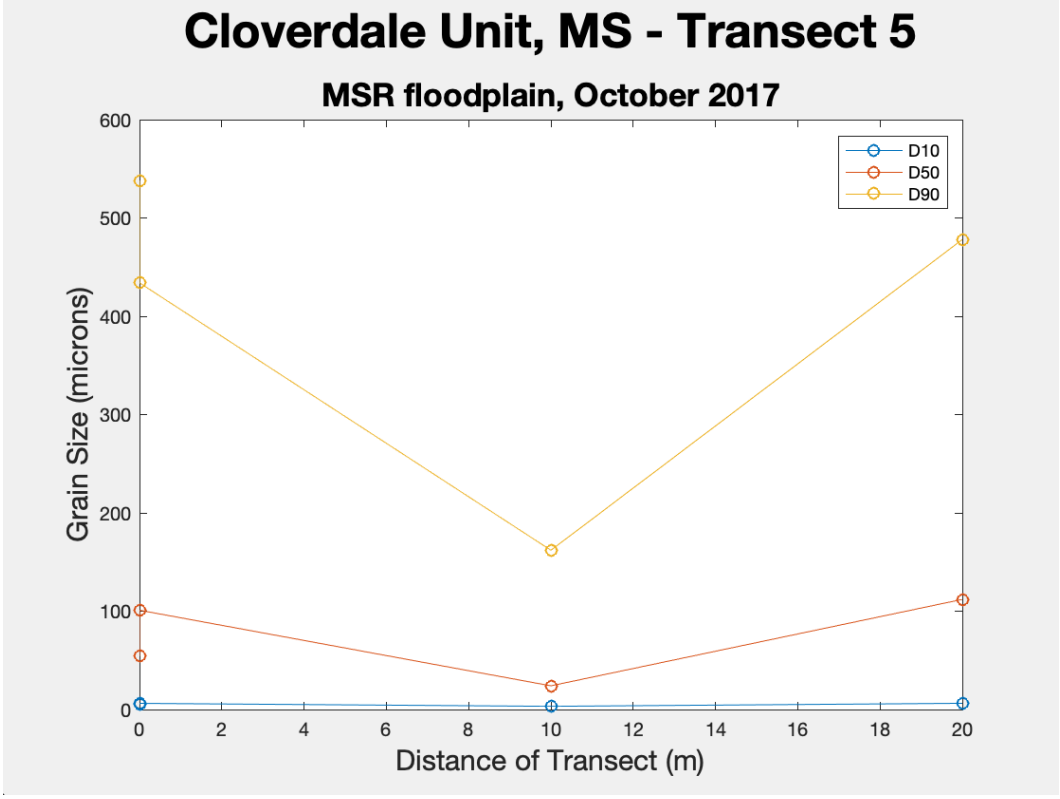

Figure 5.6 *Laboratory analysis of grain size (D10, D50, and D90) for T5 at the Cloverdale Unit, MS, for October 2017.*

Note: Transect length = 20m. Samples 05.01.00A, 05.01.00B, 05.02.10, 05.03.20 analyzed. All percentiles in microns.

The same sedimentary parameters were analyzed for samples collected along T5 in September 2018. In September 2018, T5 started at 0m (two samples adjacent to each other), 1m (two samples adjacent to each other), and 21m. D50 ranges from 37.70 to 74.40 microns (Figures 5.7 and 5.8). Munsell color is 10YR for all samples. Organic matter ranges from 8.8% to 11.9%. Magnetic susceptibility ranges from 2.4×10^{-04} SI to 4.5×10^{-04} SI. For carbon and nutrient analysis, carbon ranges from 1.67% to 2.51%, nitrogen ranges from 0.17% to 0.26%, and phosphorus ranges from 0.09% to 0.13% (Figure 5.7) (Appendix A.4; 36B to 38BB).

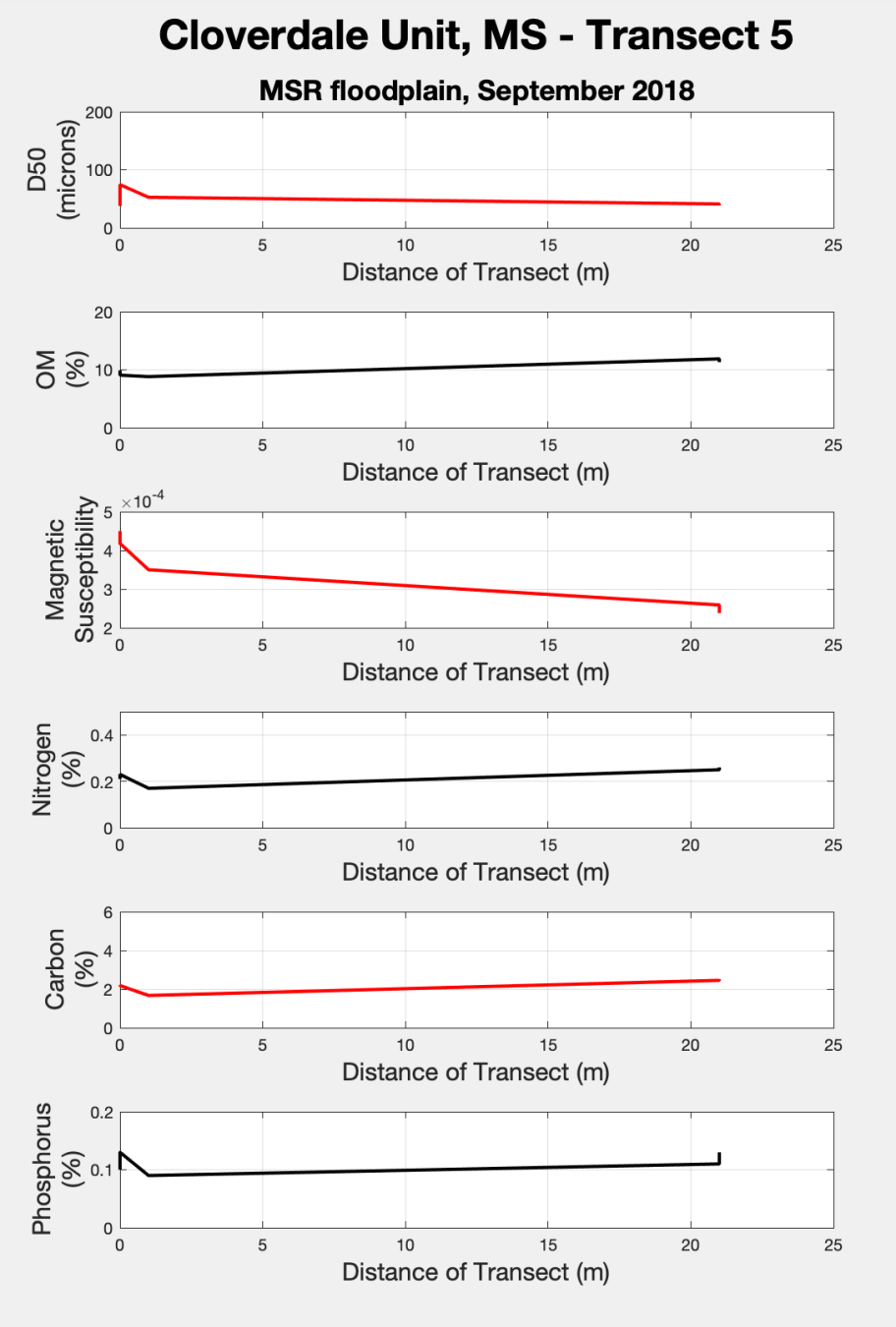

Figure 5.7 *Laboratory analysis results for T5 at the Cloverdale Unit, MS, for September, 2018.*

Note: Transect length = 21m. Samples 36B.00, 36BB.00, 37B.01, 38B.21, and 38BB.21 analyzed. All percentages are by weight.

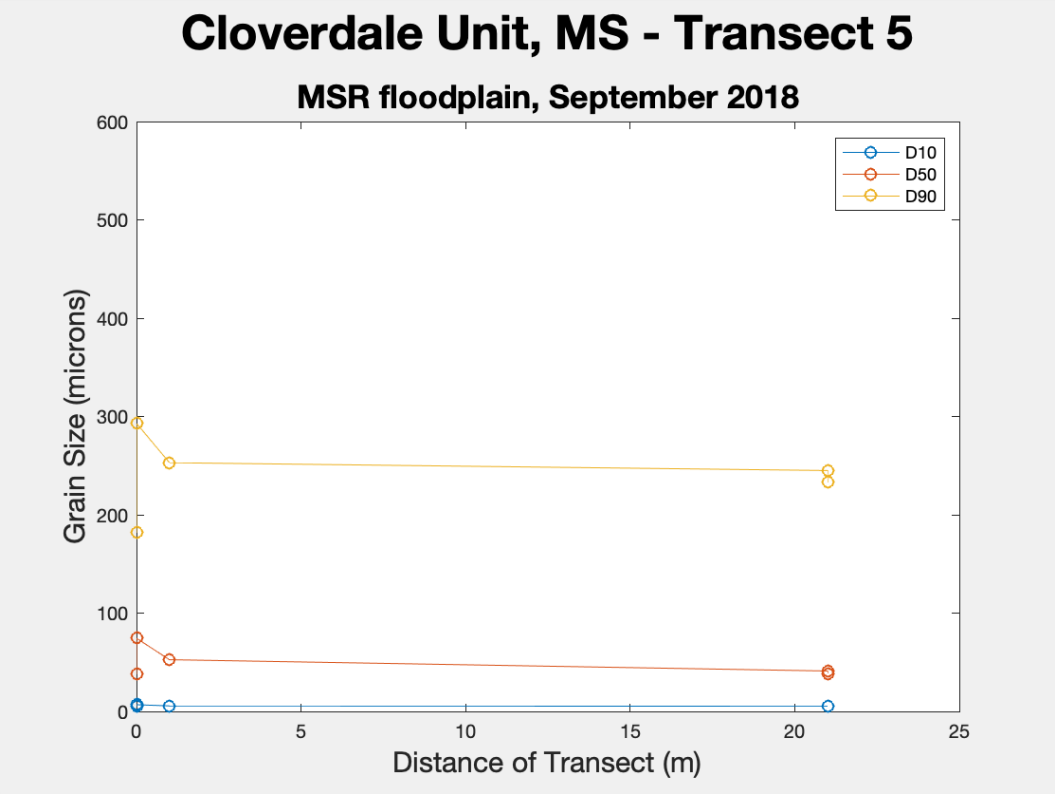

Figure 5.8 *Laboratory analysis of grain size (D10, D50, and D90) for T5 at the Cloverdale Unit, MS, for October 2017.*

Note: Transect length = 21m. Samples 36B.00, 36BB.00, 37B.01, 38B.21, and 38BB.21 analyzed. All percentiles in microns.

5.1.1.2 BUTLER LAKE (TRANSECT 7)

The transect 7 (T7) location is a meander scroll. Two sediment samples were collected in October 2017, just south of Butler Lake. D50 grain size for T7 is 30.7 microns (Sample 07.01) and 17.6 microns (Sample 07.02). Munsell color is 10YR for both samples. Organic matter is 13.2% (07.01) and 12.4% (07.02). Magnetic susceptibility is 3.82×10^{-04} SI (07.01) and 3.73×10^{-04} SI (07.02). For carbon and nutrient analysis, carbon is 2.61% (07.01) and 2.65% (07.02), nitrogen is 0.27% (07.01) and 0.25% (07.02), and phosphorus is 0.10% for both samples (Appendix A.5; 07.01 and 07.02).

5.1.1.3 SALT LAKE (TRANSECT 8)

Transect 8 (T8) is a meander scroll sub-environment. The transect started at the east bank of Salt Lake and continued northeast towards Butler Lake. Sediment samples were collected in both October 2017 and September 2018 (Figure 5.9).

For October, 2017, T8 started with 0 meters from Salt Lakes' shoreline, and continued with increasing distance of 73m, 135m, 234m; ending at 475m away. The median grain size (D50) for T8 ranges from 22.4 to 83.3 microns (Figures 5.9 and 5.10). Munsell color is 10YR for all samples. Organic matter ranges from of 13.4% to 17.5%. Magnetic susceptibility ranges from 2.67×10^{-04} SI to $x10^{-04}$ SI. For carbon and nutrient analysis, carbon ranges from 4.05% to 5.71%, nitrogen ranges from 0.34% to 0.45%, and phosphorus ranges from 0.10% to 0.12 (Figure 5.17) (Appendix A.6; 08.01 to 08.05).

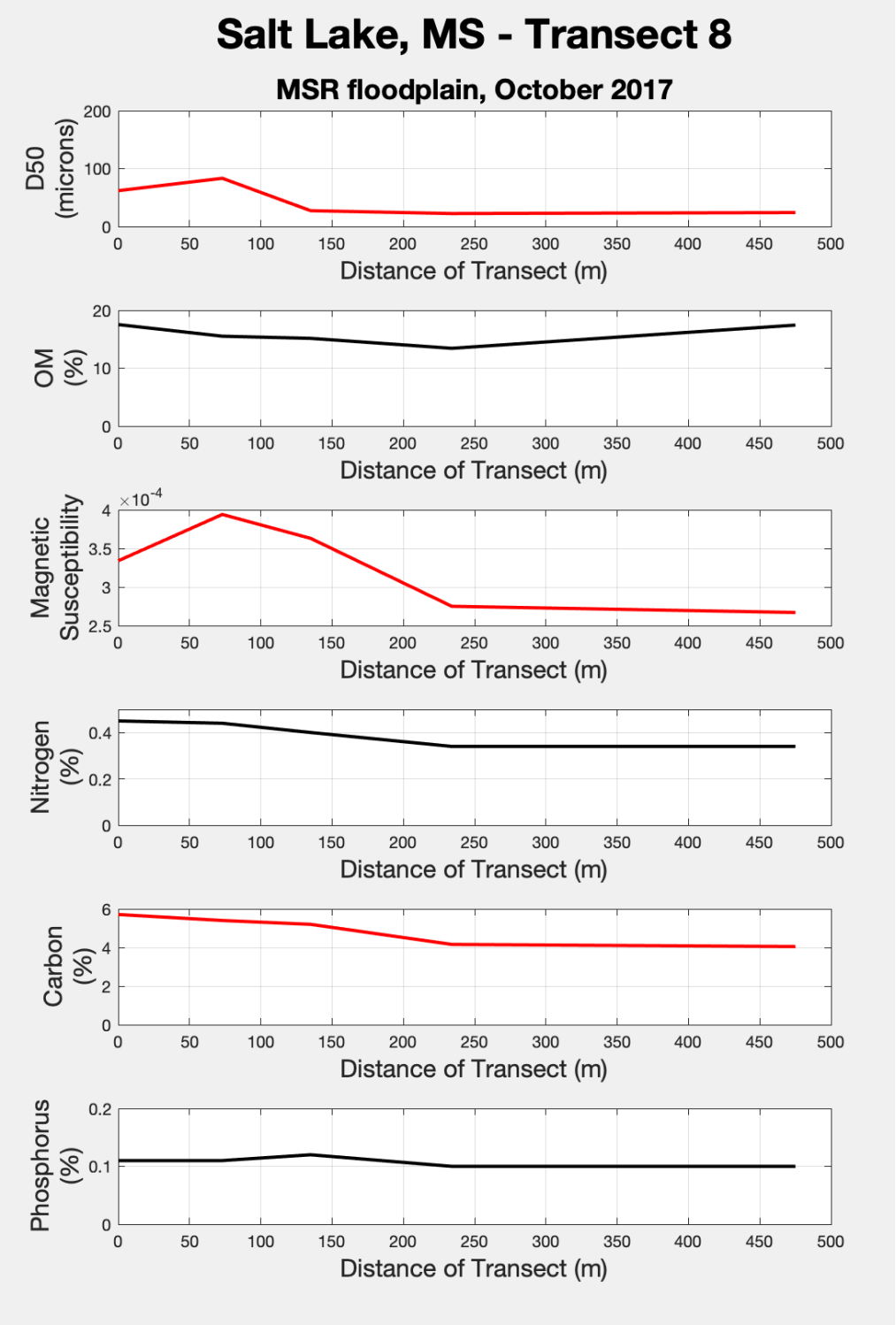

Figure 5.9 *Laboratory analysis results for T8 at Salt Lake, MS, for October, 2017.*

Note: Transect length = 475m. Samples 08.01.00, 08.02.73, 08.03.135, 08.04.234, and 08.05.475 analyzed. All percentages are by weight.

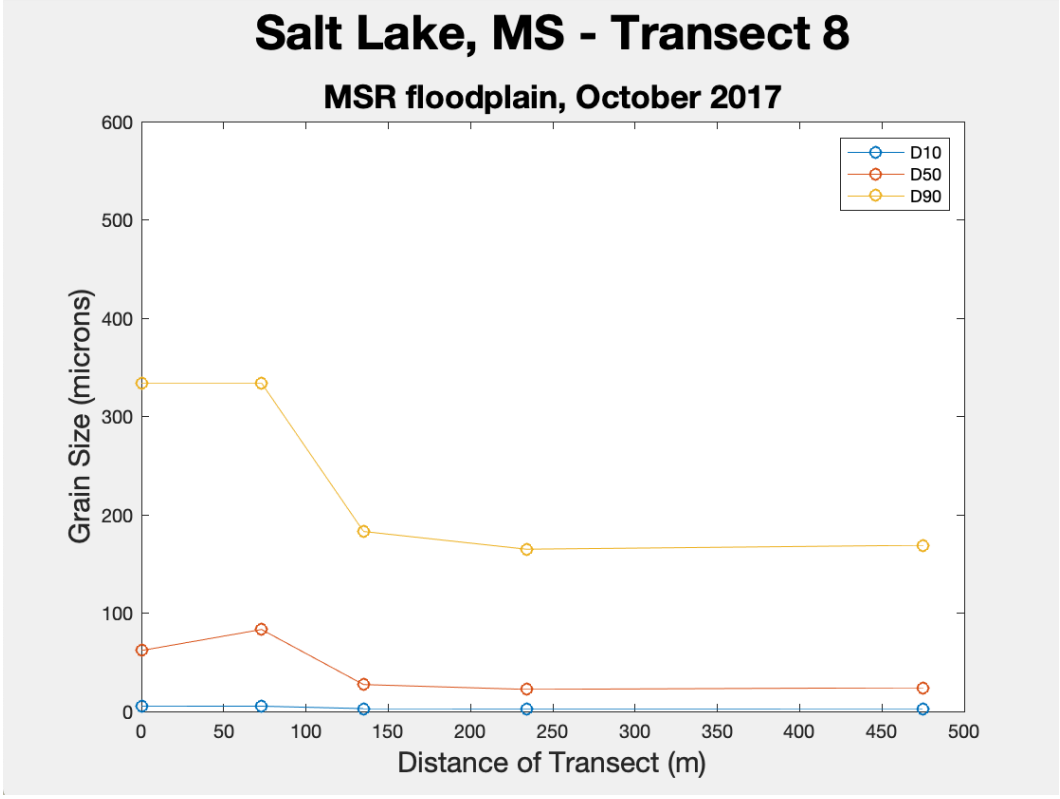

Figure 5.10 *Laboratory analysis of grain size (D10, D50, and D90) for T8 at Salt Lake, MS, for October 2017.*

Note: Transect length = 475m. Samples 08.01.00, 08.02.73, 08.03.135, 08.04.234, and 08.05.475 analyzed. All percentiles in microns.

5.1.1.4 SIBLEY UNIT (TRANSECTS 9, 10, 11, 12, and 13)

Transect 9 (T9) is ~~only~~ a backswamp subenvironment. Sample locations are aligned northwest to southeast perpendicular from the LMR main channel. Sediment samples along T9 were collected only in October 2017, and from the LMR into the floodplain they are: Samples 09.02.00, 09.01.27, 09.03.77, 09.04.168, and 09.05.223 (Figure 5.11).

The median grain size (D50) for T9 ranges from 24.5 to 44.6 microns (Figures 5.11 and 5.12). Munsell color is 10YR for all samples. Organic matter ranges from 9.0% to 14.7%. Magnetic susceptibility ranges from 3.79×10^{-04} SI to 4.80×10^{-04} SI. For carbon and nutrient analysis, carbon ranges from 1.71% to 2.02%, nitrogen ranges from 0.16% to

0.20%, and phosphorus ranges from 0.07% to 0.16% (Figure 5.11) (Appendix A.7; 09.02.00 to 09.05.223).

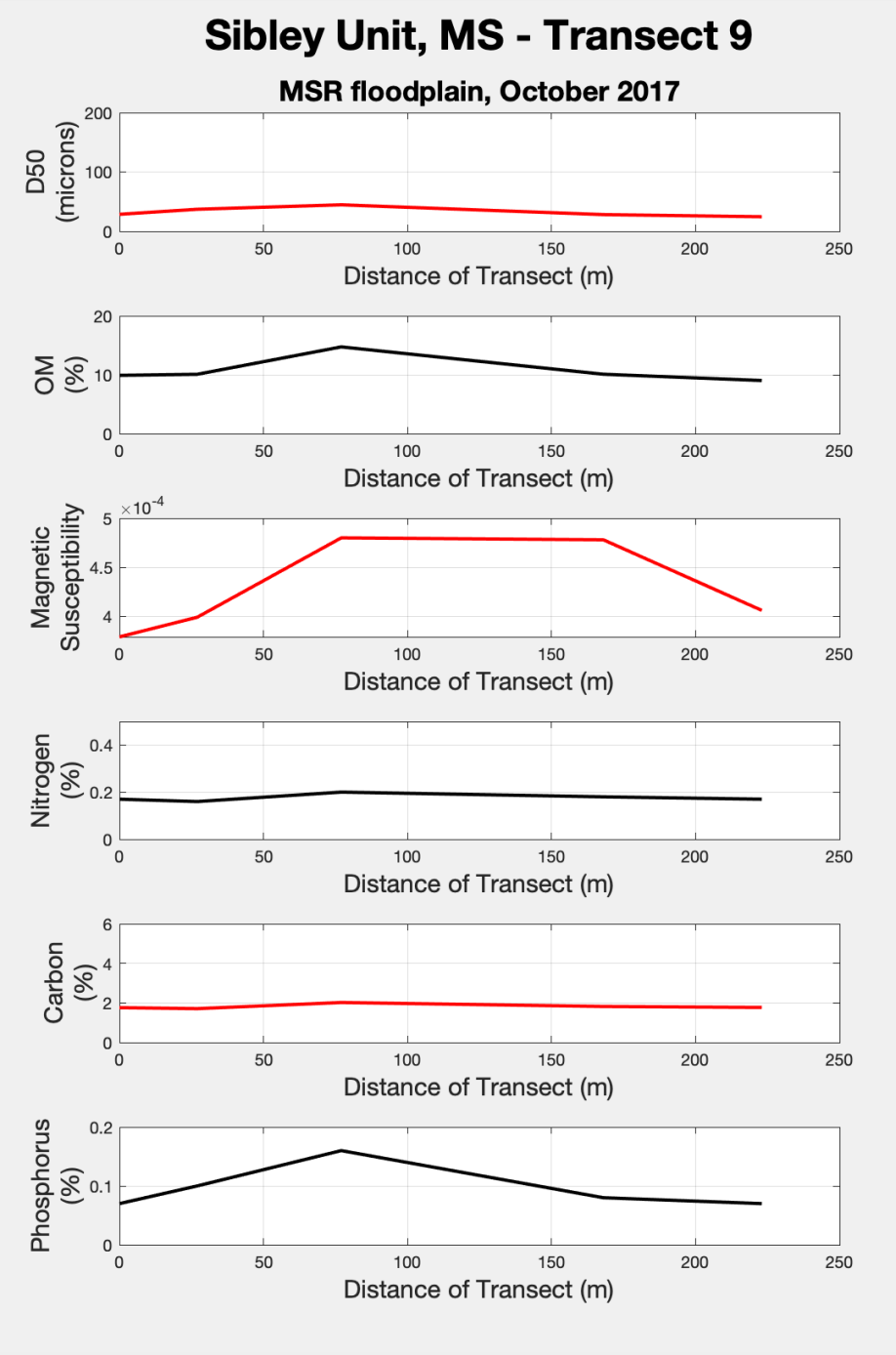

Figure 5.11 *Laboratory analysis results for T9 at the Sibley Unit, MS, for October, 2017.*

Note: Transect length = 223 m. Samples 09.02.00, 09.01.27, 09.03.77, 09.04.168, and 09.05.223 analyzed. All percentages are by weight.

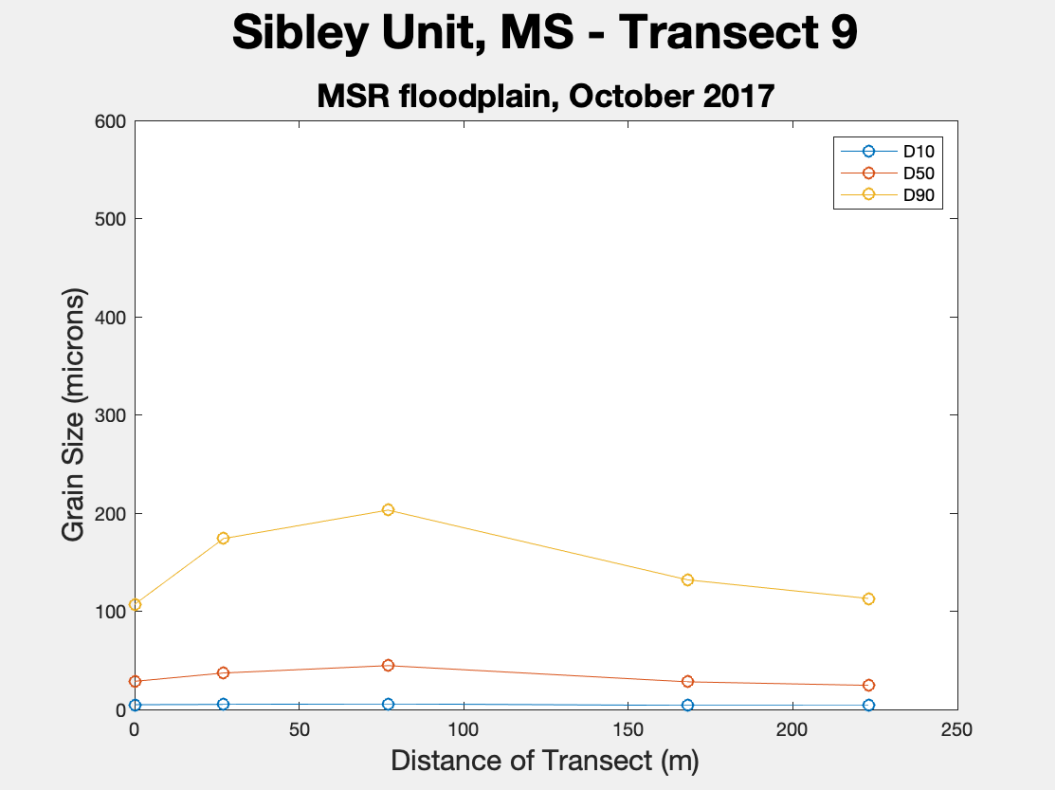

Figure 5.12 *Laboratory analysis of grain size (D10, D50, and D90) for T9 at the Sibley Unit, MS, for October 2017.*

Note: Transect length = 223 m. Samples 09.02.00, 09.01.27, 09.03.77, 09.04.168, and 09.05.223 analyzed.

Transect 10 (T10) is a natural levee crest and extends into a backswamp subenvirnment. Sediment samples along T10 were collected in October 2017 and September 2018 at two locations; both extending perpendicular from the LMR channel. Samples 10.01.00 and 10.02.180 were located 180m apart. For October 2017, Munsell color is 10YR for all samples. The median grain size (D50) at T10 for the two sediment samples, D50 is 49.1 microns (10.01) and 45.0 microns (10.02). Organic matter is 4.95% (10.01) and 6.84% (10.02). Magnetic susceptibility is 4.82×10^{-04} SI (10.01) and 3.63×10^{-04} SI (10.02). For carbon and nutrient analysis, carbon is 1.06% (10.01) and 1.82% (10.01), nitrogen is 0.08% (10.01) to 0.16% (10.02), and phosphorus is 0.05% (10.01) and 0.05% (10.02). (Appendix A.8; 10.01 and 10.02).

Transect 11 (T11) is a natural levee crest and extends into a backswamp subenvironment. Sediment samples along T11 were collected in October 2017 and September 2018. The transect includes three sediment samples extending perpendicular from the main LMR channel; 0m (11.01.00), 160m (11.02.160), and 316m (11.03.316) away. The median grain size (D50) for T11 ranges from 26.9 to 186 microns (Figures 5.13 and 5.14). Munsell color was found to be 10YR at all locations. Organic matter ranges from 0.58 to 7.55%. Magnetic susceptibility ranges from 3.66×10^{-04} SI to 1.44×10^{-03} SI. For carbon and nutrient analysis, carbon ranges from 0.16% to 1.84%, nitrogen ranges from 0.01% to 0.18%, and phosphorus ranges from 0.02% to 0.09% (Appendix A.9; 11.01A to 11.03).

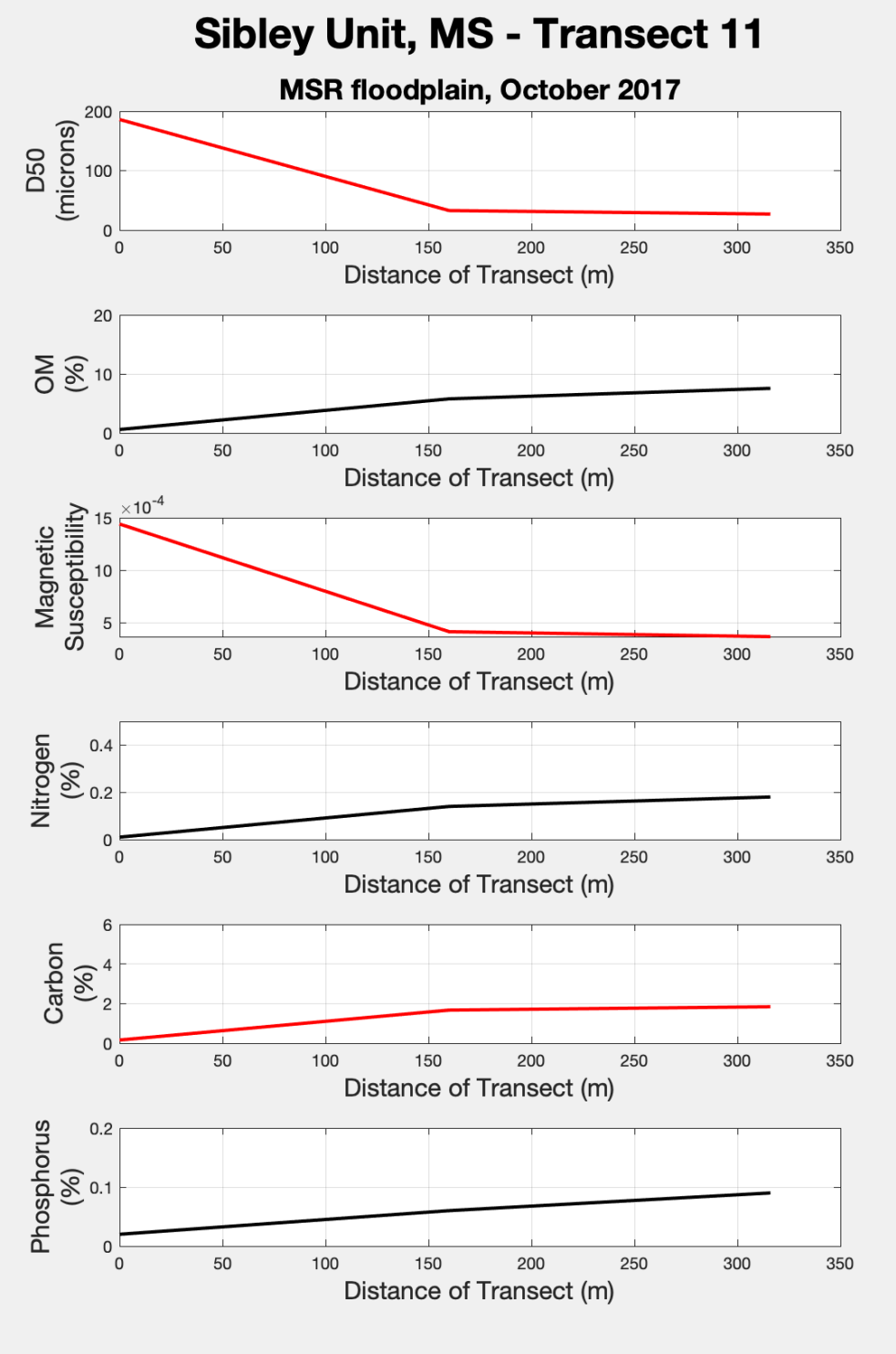

Figure 5.13 *Laboratory analysis results for T11 at the Sibley Unit, MS, for October, 2017.*

Note: Transect length = 316 m. Samples 011.01.00, 11.02.160, and 11.03.316 analyzed. All percentages are by weight.

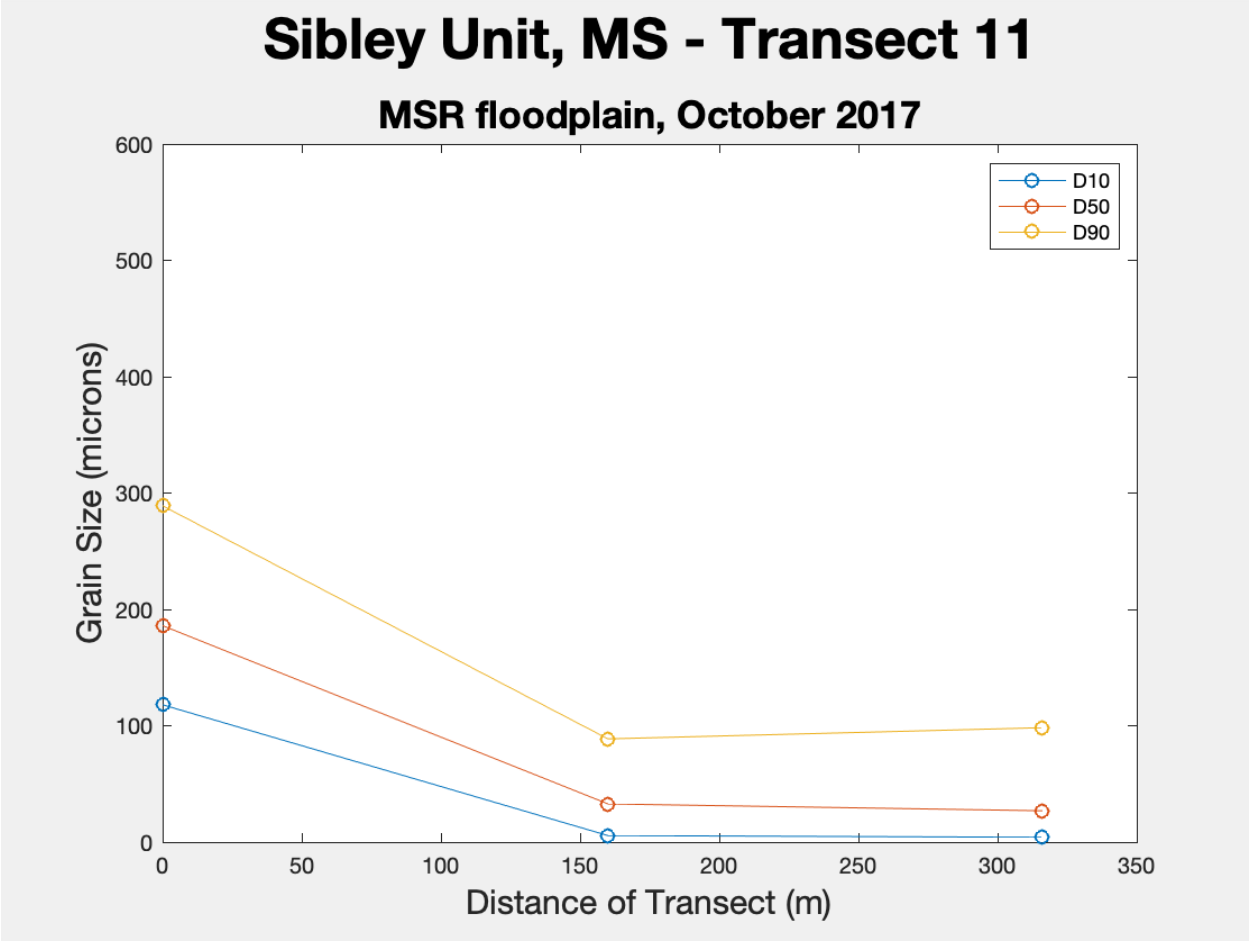

Figure 5.14 *Laboratory analysis of grain size (D10, D50, and D90) for T11 at the Sibley Unit, MS, for October 2017.*

Note: Transect length = 316 m. Samples 011.01.00, 11.02.160, and 11.03.316 analyzed.

The same sedimentary parameters were analyzed for samples collected along T11 in September 2018. The median grain size (D50) is 33.2 (56B) and 34.5 microns (57B). Munsell color is 10YR for all samples. Organic matter is 8.7% (56B) and 8.3% (57B). Magnetic susceptibility is 3.95×10^{-04} SI (56B) and 3.94×10^{-04} SI (57B). For carbon and nutrient analysis, carbon is 2.00% (56B) and 1.76% (57B), nitrogen is 0.17% (56B) and 0.15% (57B), and phosphorus is 0.09% (56B) and 0.08% (57B) (Appendix A.10; 56B and 57B).

Transect 12 (T12) is directly west of T11, further from the main LMR channel and a backswamp subenvironment. Sediment samples were collected in October 2017 and September 2018. For October, 2017, T12 started at 0m, and continued with increasing distance of 134m, and ending at 1808m away. The median grain size (D50) for T12 ranges from 26.3 to 41.1 microns (Figures 5.15 and 5.16). Munsell color is 10YR for all samples. Organic matter ranges from 9.3% to 11.8%. Magnetic susceptibility ranges from 3.2×10^{-04} SI to 3.7×10^{-04} SI. For carbon and nutrient analysis, carbon ranges from 2.73% to 3.22%, nitrogen ranges from 0.26% to 0.27%, and phosphorus ranges from 0.07% to 0.10% (Figure 5.15) (Appendix A.11; 12.01 to 12.03).

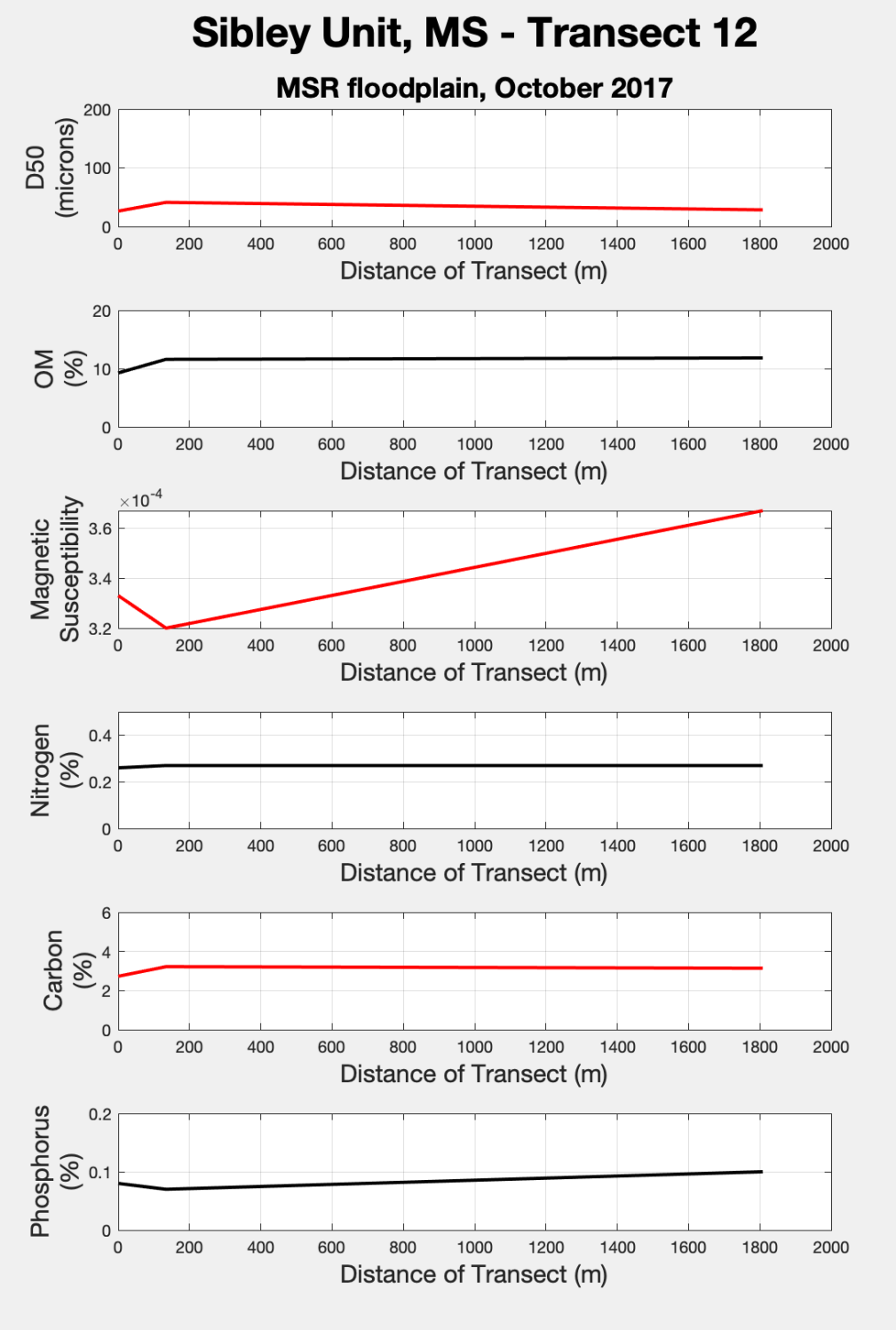

Figure 5.15 *Laboratory analysis results for T12 at the Sibley Unit, MS, for October, 2017.*

Note: Transect length = 1808 m. Samples 12.01.00, 12.02.134, and 12.03.1808 analyzed. All percentages are by weight.

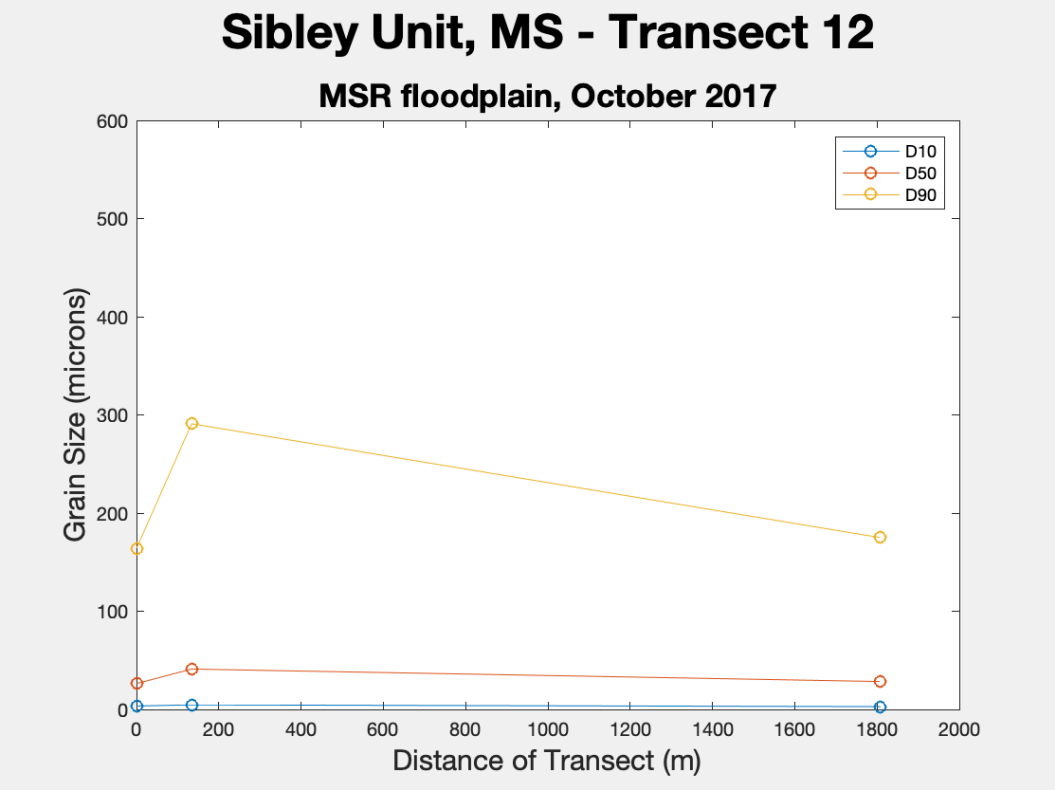

Figure 5.16 *Laboratory analysis of grain size (D10, D50, and D90) for T12 at the Sibley Unit, MS, for October 2017.*

Note: Transect length = 1808 m. Samples 12.01.00, 12.02.134, and 12.03.1808 analyzed.

In September 2018, a new transect (T13) was established that was not sampled in October 2017. T13 is a natural levee crest and extends into a backswamp subenvironment, perpendicular from the main LMR channel. For September, 2018, T13 started with 0 meters near the LMR, and continued with increasing distance of 11m, 26m, 44m, 69m, 97m, 119m; ending at 142m away. The median grain size (D50) for T13 ranges from 43.5 microns to 148.0 microns (Figure 5.17 and 5.18). Munsell color is 10YR for all samples. Organic matter ranges from 1.26% to 6.53%. Magnetic susceptibility ranges from 3.47×10^{-04} SI to 5.56×10^{-04} SI. For carbon and nutrient analysis, carbon ranges from 0.50% to 1.64%, nitrogen ranges from 0.02% to 0.12%, and phosphorus ranges from 0.03% to 0.06% (Figure 5.17) (Appendix A.12; 12B to 19B).

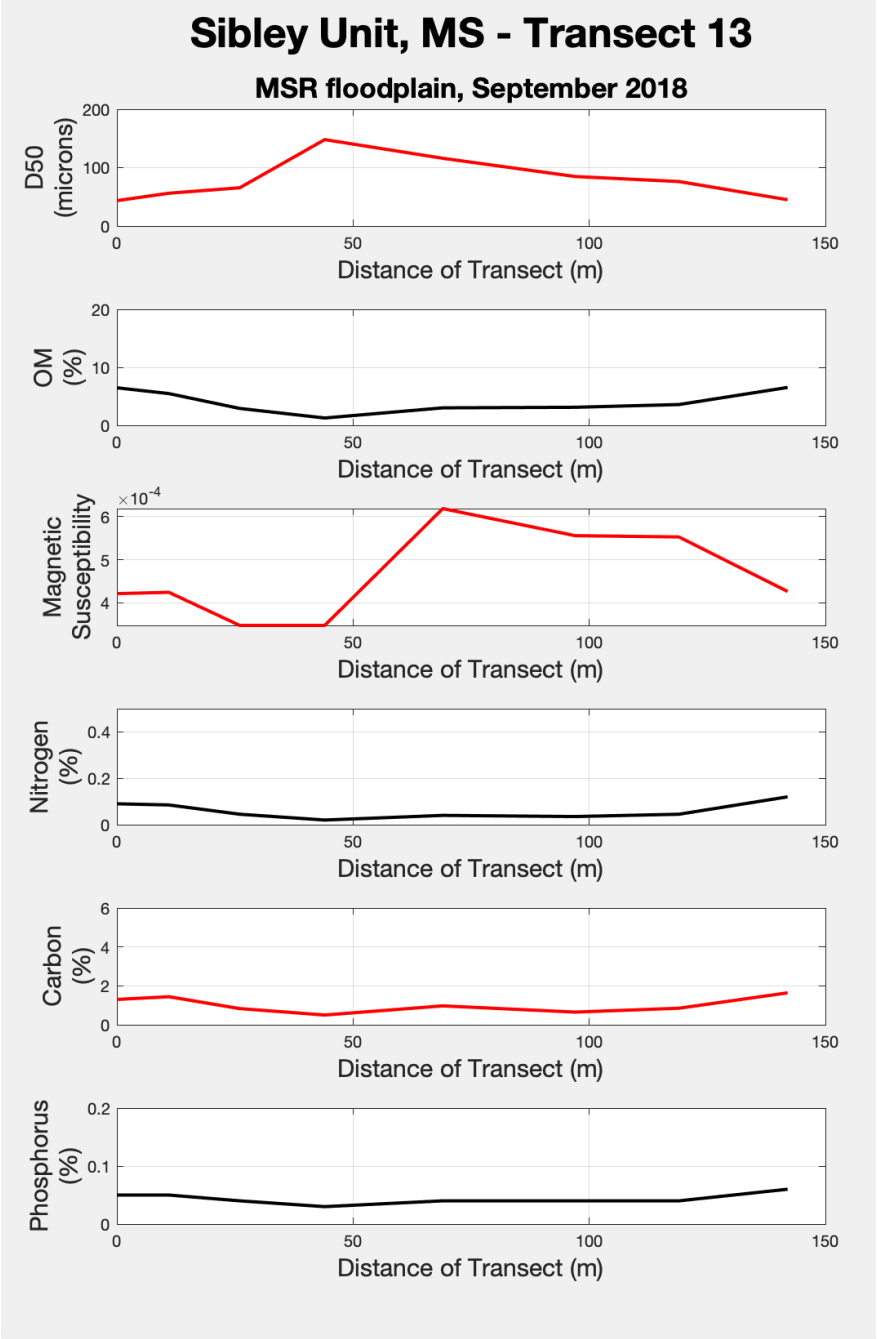

Figure 5.17 *Laboratory analysis results for T13 at the Sibley Unit, MS, for September, 2018.*

Note: Transect length = 142m. Samples 12B.00, 13B.11, 14B.26, 15B.44, 16B.69, 17B.97, 18B.119, and 19B.142 analyzed. All percentages are by weight.

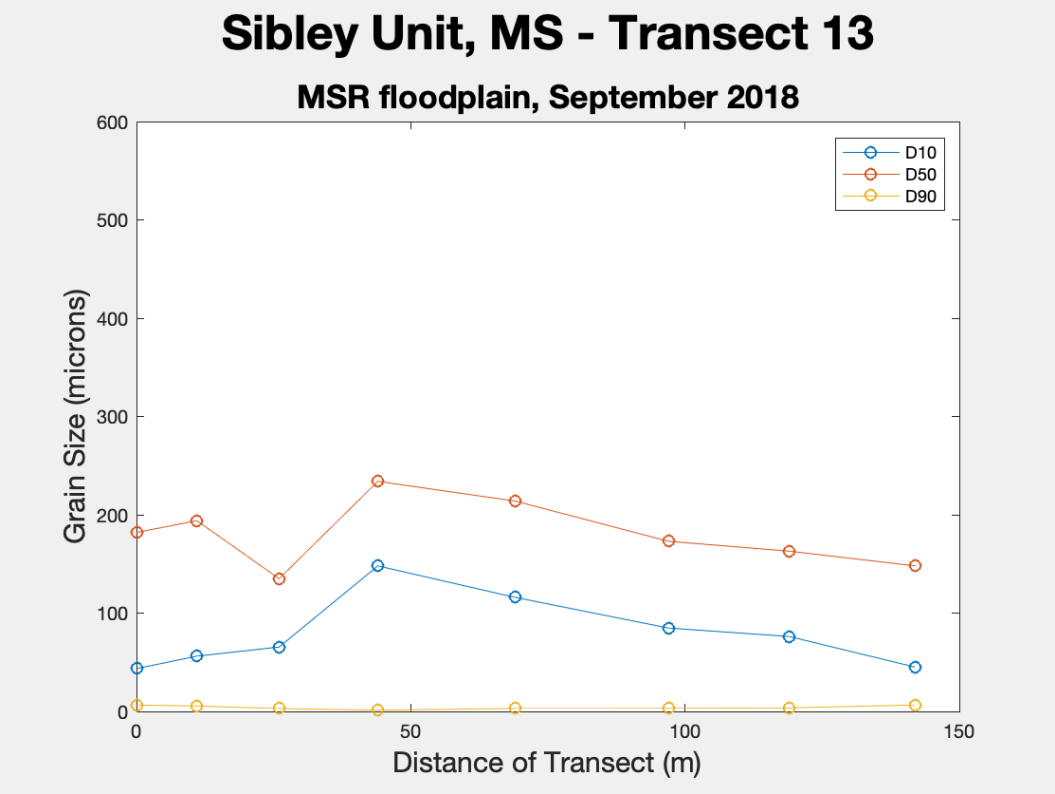

Figure 5.18 *Laboratory analysis of grain size (D10, D50, and D90) for T13 at the Sibley Unit, MS, for October 2018.*

Note: Transect length = 142m. Samples 12B.00, 13B.11, 14B.26, 15B.44, 16B.69, 17B.97, 18B.119, and 19B.142 analyzed. All percentiles in microns.

5.1.1.5 LAKE MARY (TRANSECT 3)

Transect three (T3) is located between the southern arm of the oxbow lake, Lake Mary, and the main LMR channel, effectively in the area of oxbow infill (Figure 5.19). T3 was collected in October 2017. For T3 data collection, the distances and location of the samples along the transect were 0m (start), 10m, 20m, 40m, 60m, 80m, 120m, 160m, and 190m, for the October 2017. The median grain size (D50) for T3 ranges from 27.9 to 163 microns (Figures 5.19 and 5.20). Munsell color is 10YR for all samples. Organic matter ranges from 1.39% to 9.84%. Magnetic susceptibility ranges from 3.14×10^{-04} SI to 7.56×10^{-04} SI. For carbon and nutrient analysis: carbon ranges from 0.47% to 2.78%,

nitrogen ranges from 0.02% to 0.25%, and phosphorus ranges from 0.02% to 0.08% (Figure 5.19) (Appendix A.13; 03.01.00 to 03.09.190).

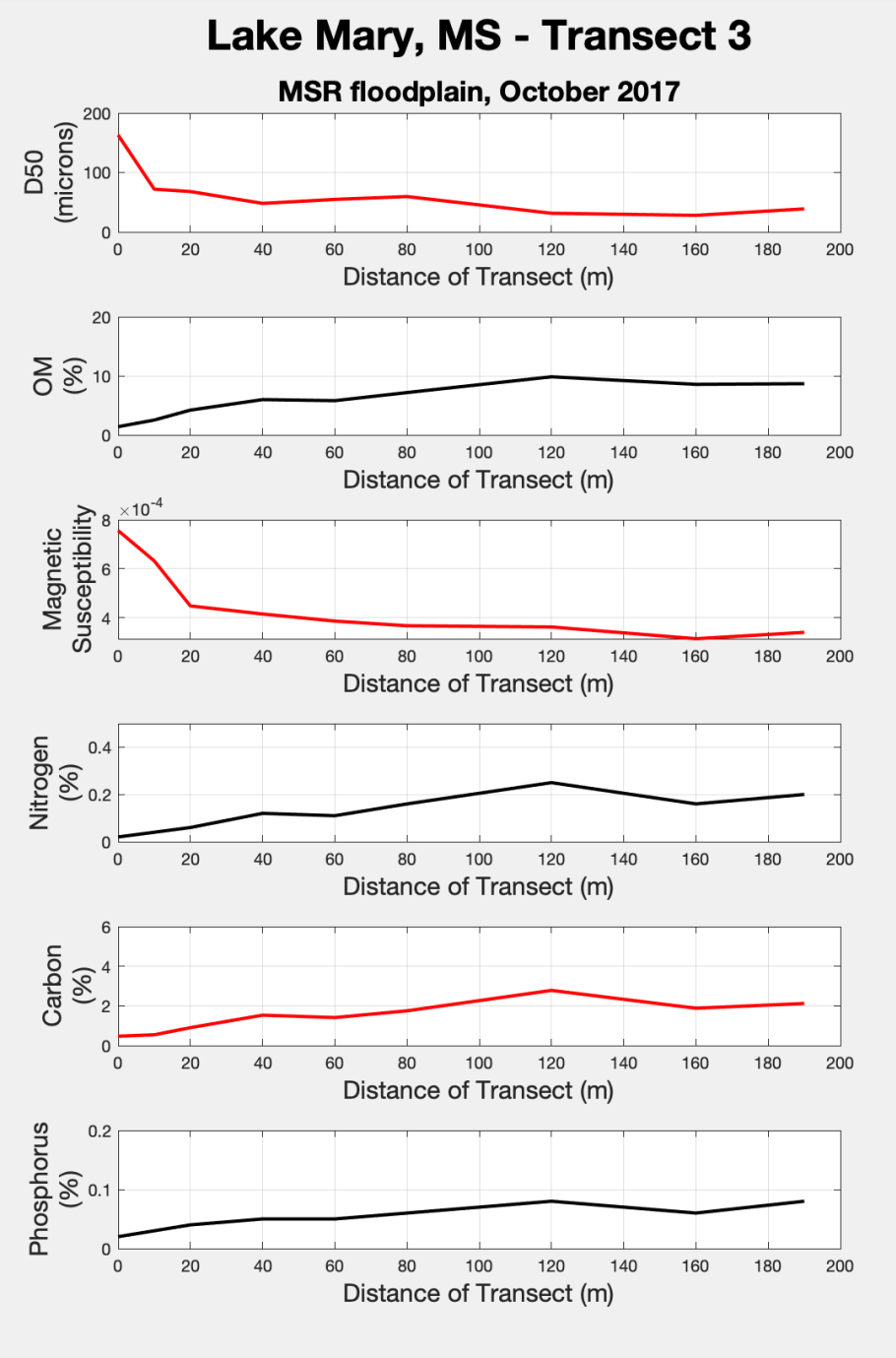

Figure 5.19 *Laboratory analysis results for T3 at Lake Mary, MS, for October, 2017.*

Note: Samples 03.01.00, 03.02.10, 03.03.20, 03.04.40, 03.05.60, 03.06.80, 03.07.120, 03.08.160 and 03.09.190 analyzed. Transect length = 190m. All percentages are by weight.

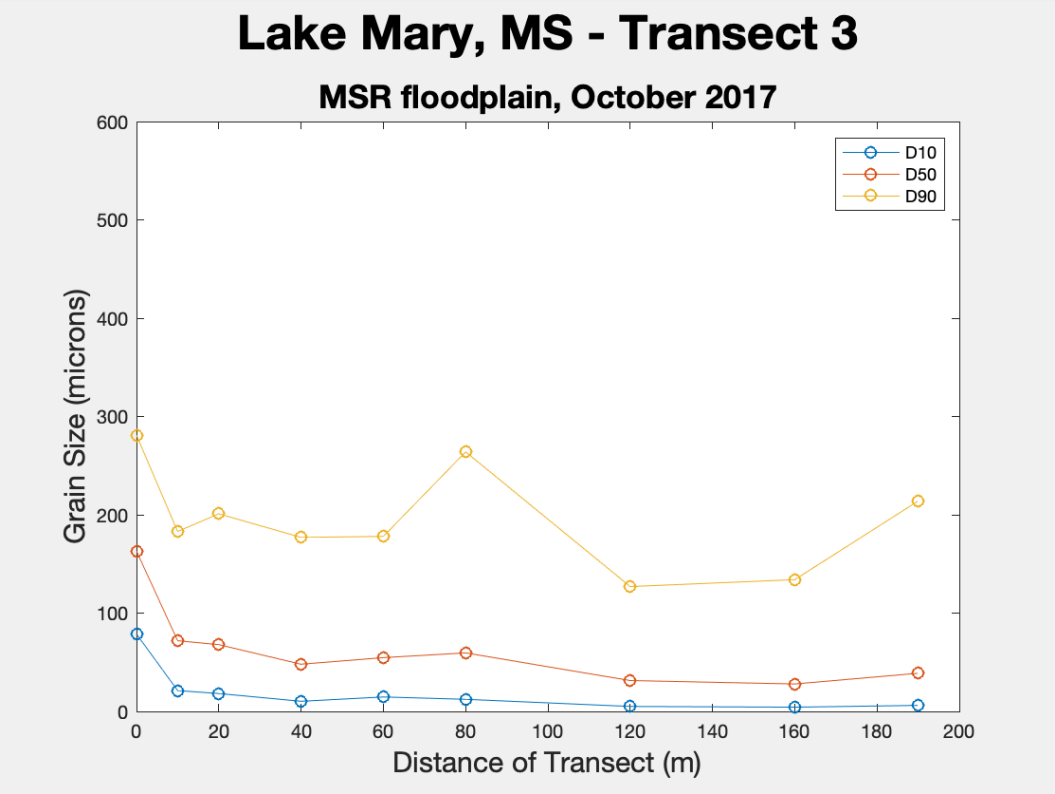

Figure 5.20 *Laboratory analysis of grain size (D10, D50, and D90) for T3 at Lake Mary, MS, for October 2017.*

Note: Samples 03.01.00, 03.02.10, 03.03.20, 03.04.40, 03.05.60, 03.06.80, 03.07.120, 03.08.160 and 03.09.190 analyzed. Transect length = 190m.

5.1.1.6 ARTONISH (TRANSECTS 1 AND 2)

Transect one (T1) extends from the natural levee crest of the LMR and continues southeast toward a meander scroll environment (Figure 5.21). For the October 2017 data set, T1 started from 0 meters (levee crest) and continued to 10m, 20m, 40m, 60m, 80m, 120m, 160m, 190m, 347m, 524m, 652m, 830m, 1032m, and 1151m. The median grain size (D50) at T1 ranges from 45.7 to 189.0 microns (Figures 5.21 and 5.22). Munsell color for most samples is in the 10YR range, except for Sample 01.01.00 being 2.5Y. Organic matter ranges from 0.98% to 10.28%. Magnetic susceptibility ranges from 3.06×10^{-04} to 5.22×10^{-04} SI. For carbon and nutrient analysis, carbon ranges from 0.13%

to 3.27%, nitrogen ranges from 0.01% to 0.31%, and phosphorus ranges from 0.01% to 0.08% (Figure 5.21) (Appendix A.14; 01.01.00 to 01.15.1151).

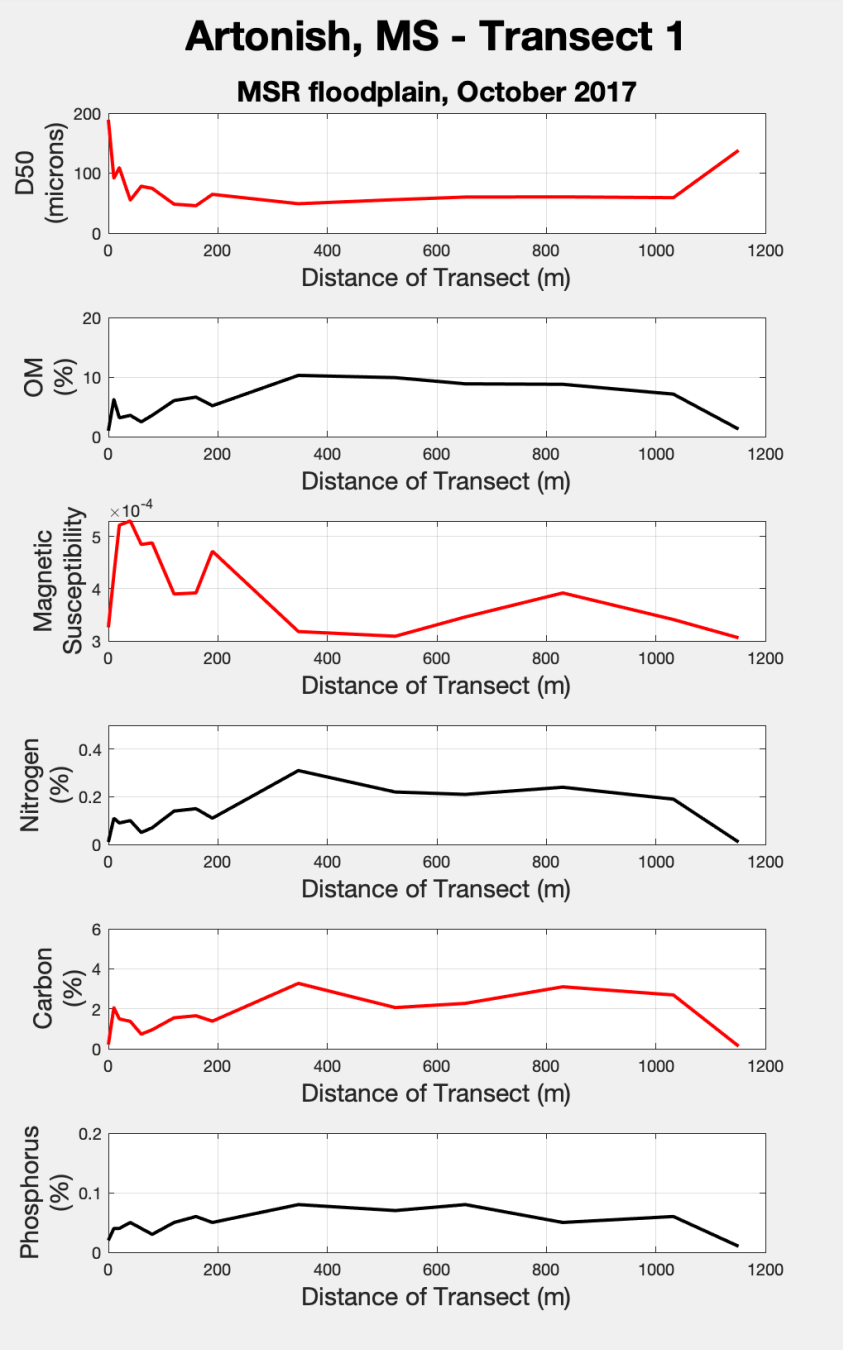

Figure 5.21 *Laboratory analysis results for sediment samples along Transect 1 the Artonish Lake area, for October 2017.*

Note: Samples 0m, 10m, 20m, 40m, 60m, 80m, 120m, 160m, 190m, 347m, 524m, 652m, 830m, 1032m, and 1151m analyzed.

Transect length = 1151 m. All percentages are by weight.

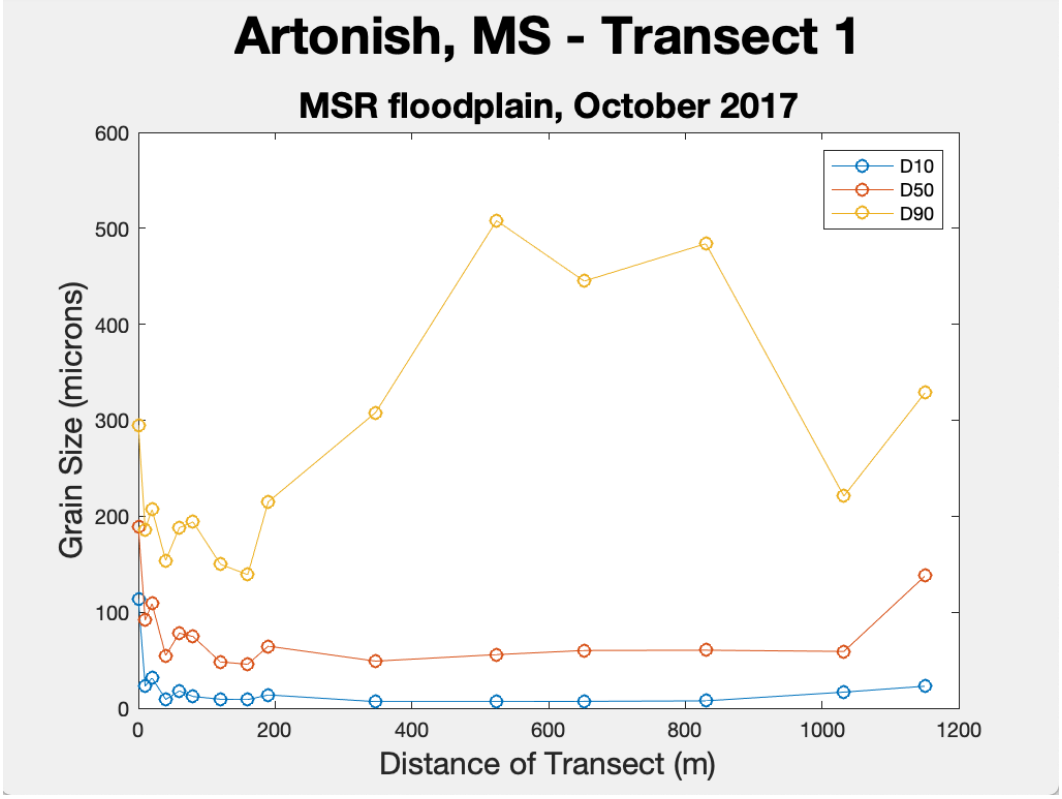

Figure 5.22 *Laboratory analysis for grain size (D10, D50, and D90) of sediment samples along Transect 1 at the Artonish Lake area, for October 2017.*

Note: Samples 0m, 10m, 20m, 40m, 60m, 80m, 120m, 160m, 190m, 347m, 524m, 652m, 830m, 1032m, and 1151m analyzed.

Transect length = 1151 m.

The same sedimentary parameters were analyzed for samples collected along T1 in September 2018. In September 2018, Transect 1 was sampled beginning at 0 meters (the LMR levee crest) and continued with at distances of 21m, 59m, 91m; ending at 129m away. The median grain size (D50) ranges from 36.5 to 69.4 microns (Figures 5.23 and 5.24). All Munsell colors are within the 10YR range. Organic matter ranges from 4.46% to 7.83%. Magnetic susceptibility ranges from 3.91×10^{-04} SI to 5.05×10^{-04} SI. For carbon and nutrient analysis: carbon ranges from 1.08% to 2.01%, nitrogen ranges from 0.07% to 0.17%, and phosphorus ranges from 0.06% to 0.10% (Figure 5.23) (Appendix A.15; 5B to 9B).

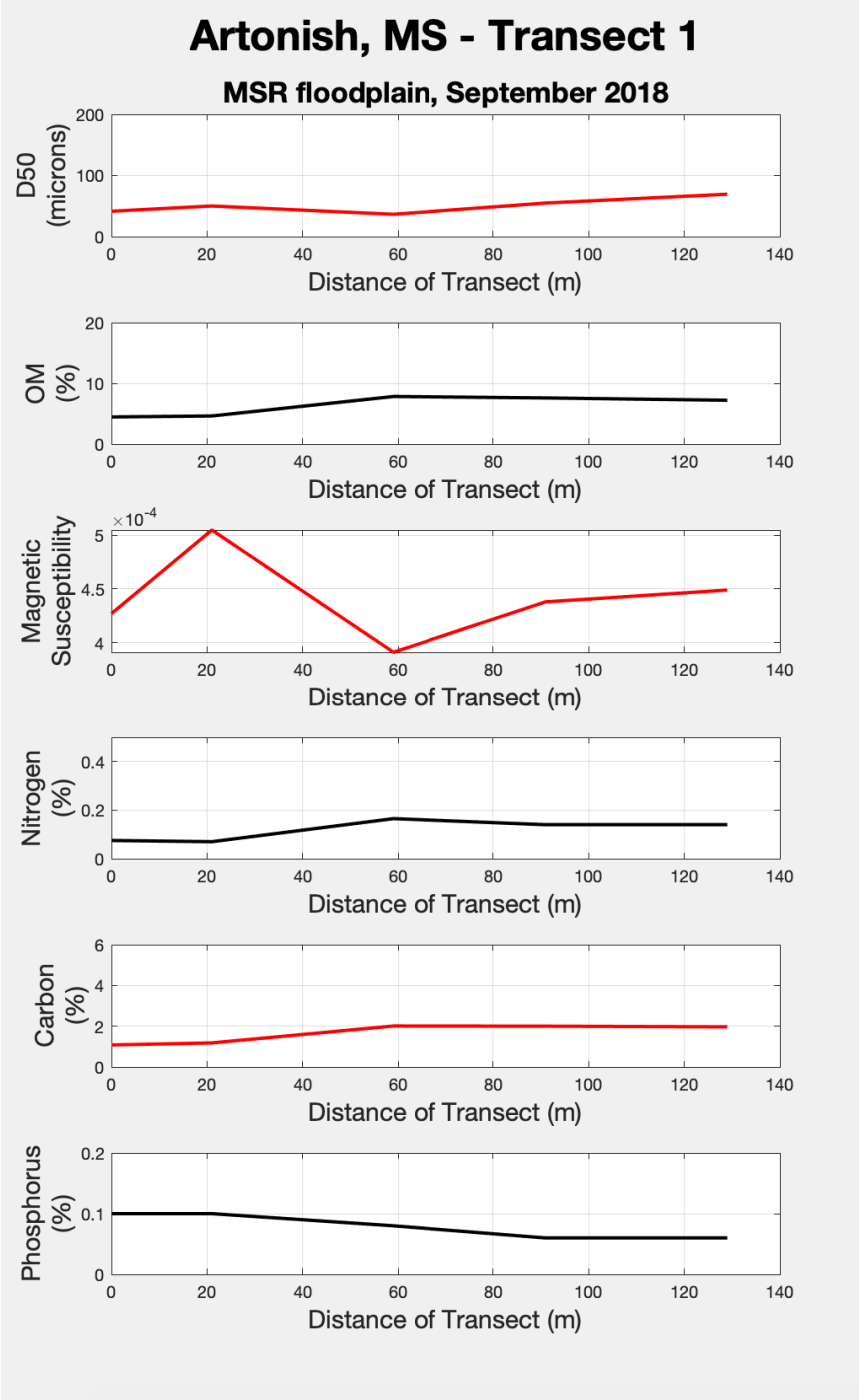

Figure 5.23 *Laboratory analysis results for Transect 1 at the Artonish Lake area, MS, September 2018.*

Note: Transect length = 129m. Samples 5B.00, 6B.21, 7B.59, 8B.91, and 9B.129 analyzed. All percentages are by weight.

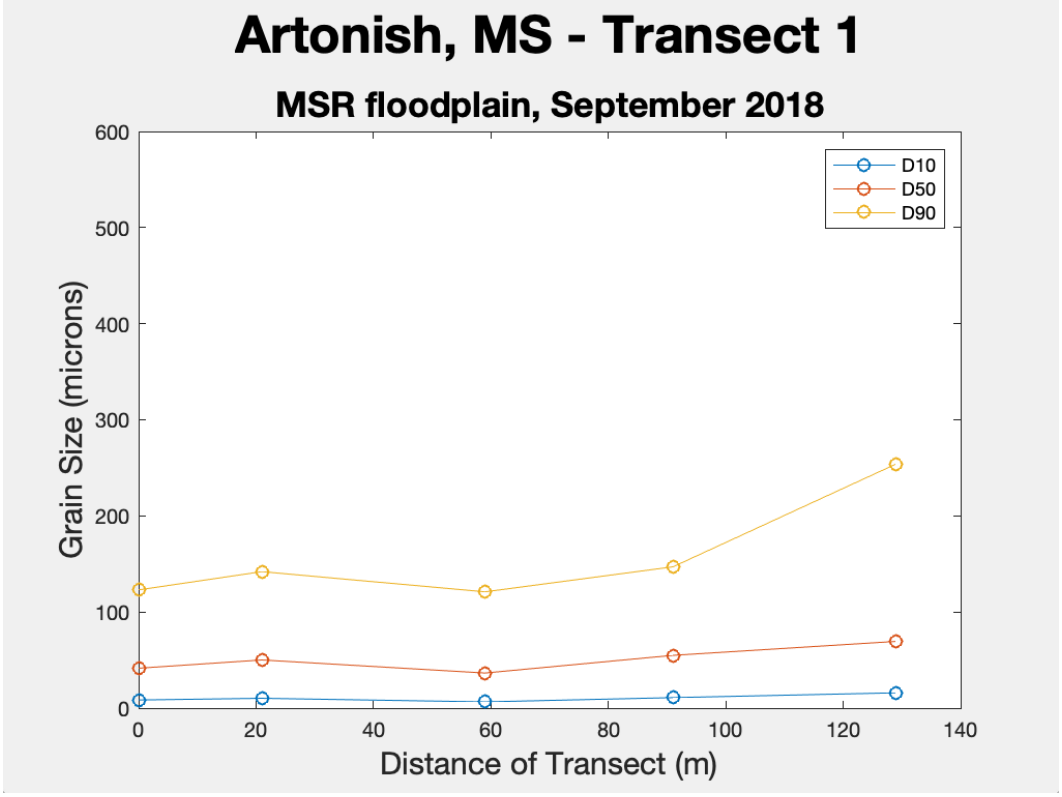

Figure 5.24 *Laboratory analysis of grain size (D10, D50, and D90) for Transect 1 at the Artonish Lake area, MS, for September 2018.*

Note: Transect length = 129 m. Samples 5B.00, 6B.21, 7B.59, 8B.91, and 9B.129 analyzed. All percentiles in microns.

Transect 2 (T2) data collection initiated between Lake Artonish and the levee crest of the LMR, with increasing distance from the main LMR channel. T2 was only collected in October 2017. In October 2017, T2 initiated at 0 meters from the main LMR levee crest and continued to 10m, 20m, 40m, 53m, 80m, 120m, and 160m. The median grain size (D50) for T2 ranges from 37.8 to 151.0 microns (Figures 5.25 and 5.26). Munsell color is 10YR for all samples. Organic matter ranges from 1.03% to 8.27%. Magnetic susceptibility ranges from 3.39×10^{-04} SI to 6.27×10^{-04} SI. For carbon and nutrient analysis: carbon ranges from 0.26% to 2.73%, nitrogen ranges from 0.01 to 0.22%, and phosphorus ranges from 0.03% to 0.07% (Figure 5.25) (Appendix A.16; 02.16.00 to 02.23.160).

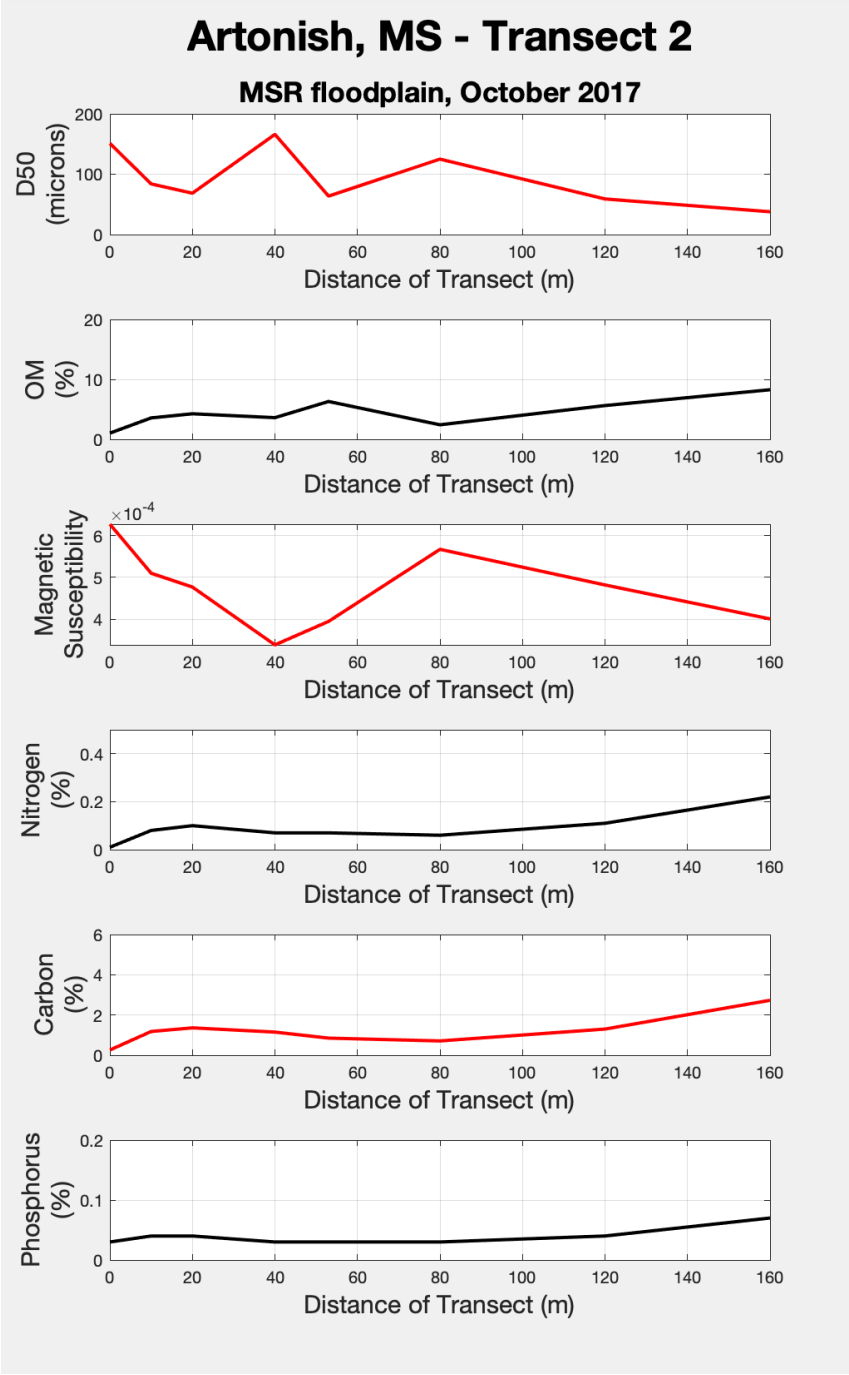

Figure 5.25 *Laboratory analysis results for T2 at the Artonish Lake area, MS, for October 2017.*

Note: Samples 02.16.00, 02.17.10, 02.18.20, 02.19.40, 02.20.53, 02.21.80, 02.22.120, and 02.23.160 analyzed. Transect length = 160m. All percentages are by weight.

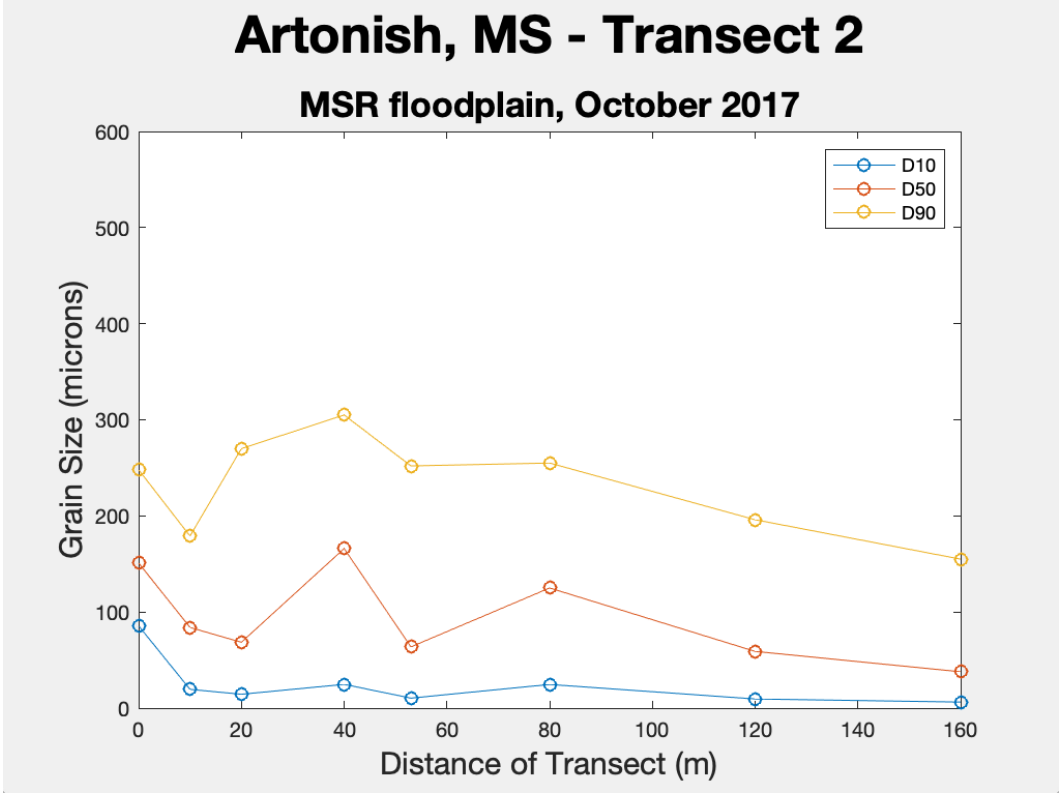

Figure 5.26 *Laboratory analysis of grain size (D10, D50, and D90) for T2 at the Artonish Lake area, MS, for October 2017.*

Note: Samples 02.16.00, 02.17.10, 02.18.20, 02.19.40, 02.20.53, 02.21.80, 02.22.120, and 02.23.160 analyzed. Transect length = 160m.

5.1.2 DISCRETE SAMPLES

5.1.2.1 CARTHAGE POINT ROAD (TRANSECT 6)

The Carthage Point Road sample (T6) is a natural levee crest along the main LMR channel (named Transect 6 even though it is limited to one sample). Sediment samples were collected in both October 2017 and September 2018 (one sample each).

For October 2017, the median grain size (D50) for T6 is 114.00 micrograms for D10, 194.00 micrograms for D50, and 308.00 micrograms for D90. Munsell color was found to be 10YR(4/3). Organic matter is 0.89%. Magnetic susceptibility is 5.17×10^{-04}

SI. For carbon and nutrient analysis, carbon is 0.19%, nitrogen is 0.01%, and phosphorus is 0.02% (Appendix A.17; 06.01).

The same sedimentary parameters were analyzed for samples collected along T6 in September 2018. For physical size, D10 is 66.3 microns, D50 is 173.0 microns, and D90 is 296 microns. Munsell color was found to be 10YR(3/4). Organic matter is 1.60%. Magnetic susceptibility is 1.12×10^{-04} SI. For carbon and nutrient analysis, carbon range is 0.34%, nitrogen is 0.02%, and phosphorus is 0.03% (Appendix A.18; 40B).

5.1.3 PIT SAMPLES

5.1.3.1 SIBLEY UNIT (PIT)

The pit sample was collected at the SSCWR within a transitioning period between a natural levee crest and into a backswamp sub environment. The pit site in the Sibley Unit includes samples collected at different depths. This pit was sampled directly adjacent to the first sample collected along T13 (13.01) in September 2018. The median grain size (D50) ranged from 54.1 microns to 184.0 microns. Organic matter ranges from 0.82% to 5.6%. Munsell color is 10YR for all samples except, S2B.230 is 2.5YR(4/4). Magnetic susceptibility ranges from 4.7×10^{-04} SI to 1.2×10^{-03} SI. For carbon and nutrient analysis, carbon ranges from 0.50% to 1.64%, nitrogen ranges from 0.02% to 0.09%, and phosphorus ranges from 0.03% to 0.06% (Appendix A.19; C1, S1, C2, S2, C3, S3, and C4).

5.2 FLOODPLAIN WATER LEVELS AND TEMPERATURES DURING THE 2018 AND 2019 FLOODS

The results below include water levels (stage) and water temperatures in the study area during the 2018 and 2019 floods. The Natchez stage and temperature data were

downloaded from the USACE RiverGages.com website (USACE, 2020) and the remaining data are from sensors that were originally installed during the research trip in October 2017, and were subsequently downloaded in October 2019 (Figure 5.27). Note that stage heights at Natchez are arbitrary and specific to that river gauge, whereas stage heights for the remaining sensors are derived from differentially-corrected GPS elevations at the bolt position where the sensor head rests.

5.2.1 NATCHEZ

The Natchez river stage gauge is operated by the U.S. Army Corps of Engineers. During the 2018 flood, the maximum stage height at Natchez was 17.41 m (57.12 ft) on March 18th. Water temperature is not available for this site location. The total duration above flood stage in 2018 was 71 days.

During the 2019 flood, the maximum stage height at Natchez was 17.65 m (57.91 ft) on March 12th. The total duration above flood stage in 2019 was 214 days.

5.2.2 LONG LAKE

During the 2018 flood, the maximum stage height at Long Lake was 21.50 m (70.54 ft) on March 19th. The range of water temperatures recorded during overbank conditions were 11.69°C on 03/14-15/2018 and 15.44°C on 04/07/2018. The average daily water temperature at the flood stage crest on 03/19/1018 was 12.09°C. The duration that the sensor was inundated by the flood in 2018 was 119 days.

During the 2019 flood, the maximum stage height at Long Lake was 21.78 m (71.49 ft) on March 12th. The range of water temperatures recorded during overbank conditions were 6.52°C on 01/31//2019 and 28.70°C on 07/21//2019. The average daily

water temperature at the flood stage crest on 03/12/2018 was 7.98°C. The duration that the sensor was inundated by the flood in 2019 was 341 days.

5.2.3 SIBLEY

During the 2018 flood, the maximum stage height was 20.84 m (68.37 ft) on March 19th. The range of water temperatures recorded during overbank conditions were 11.38°C on 03/01/2018 and 20.35°C on 05/10/2018. The average daily water temperature at the flood stage crest on 03/19/2018 was 12.29°C. The duration that the sensor was inundated by the flood in 2019 was 196 days.

During the 2019 flood, the maximum stage height was 21.10 m (69.23 ft) on March 12th. The range of water temperatures recorded during overbank conditions were 6.96°C on 02/01/2019 and 29.37°C on 08/05/2019. The average daily water temperature at the flood stage crest on 03/12/2019 was 8.20°C. The duration that the sensor was inundated by the flood in 2019 was 396 days.

5.2.4 LAKE MARY

During the 2019 flood, the maximum stage height was 19.84 m (65.09 ft) on March 19th. The range of water temperatures recorded during overbank conditions were 11.85°C on 03/14-15/2018 and 19.92°C on 05/10/2018. The average daily water temperature at the flood stage crest on 03/19/2018 was 12.29°C. The duration that the sensor was inundated by the flood in 2019 is 199 days.

During the 2019 flood, the maximum stage height was 20.03 (65.72 ft) on March 18th. The range of water temperatures recorded during overbank conditions were 9.57°C on 03/18/2019 and 29.35°C on 08/05/2019. The average daily water temperature at the

flood stage crest on 03/18/2019 was 9.57°C. The duration that the sensor was inundated by the flood in 2019 is 367 days.

5.2.5 ARTONISH LAKE

During the 2018 flood, the maximum stage height at Artonish Lake was 19.04 m (62.47 ft) on March 19th. The range of water temperatures recorded during overbank conditions were 11.79°C on 03/14-15/2018 and 19.63°C on 05/10/2018. The average daily water temperature at the flood stage crest on 03/19/2018 was 12.19°C. The duration that the sensor was inundated was for the entire 2018 year.

During the 2019 flood, the maximum stage height at Artonish Lake was 19.22 m (63.06 ft) on March 18th. The range of water temperatures recorded during overbank conditions were 6.08°C on 02/05/2019 and 29.29°C on 08/04/2019. The average daily water temperature at the flood stage crest on 03/18/2019 was 9.69°C. The duration that the sensor was inundated by the flood of 2018 and 2019 was 733 days.

5.2.6 MAXIMUM FLOOD STAGE TIMING

During the 2018 flood, all stage and water level locations had a maximum stage on March 19th. During the 2019 flood, Long Lake and the Sibley Unit had maximum stage heights on March 12th, whereas Lake Mary and Artonish Lake had maximum stage heights on March 18th.

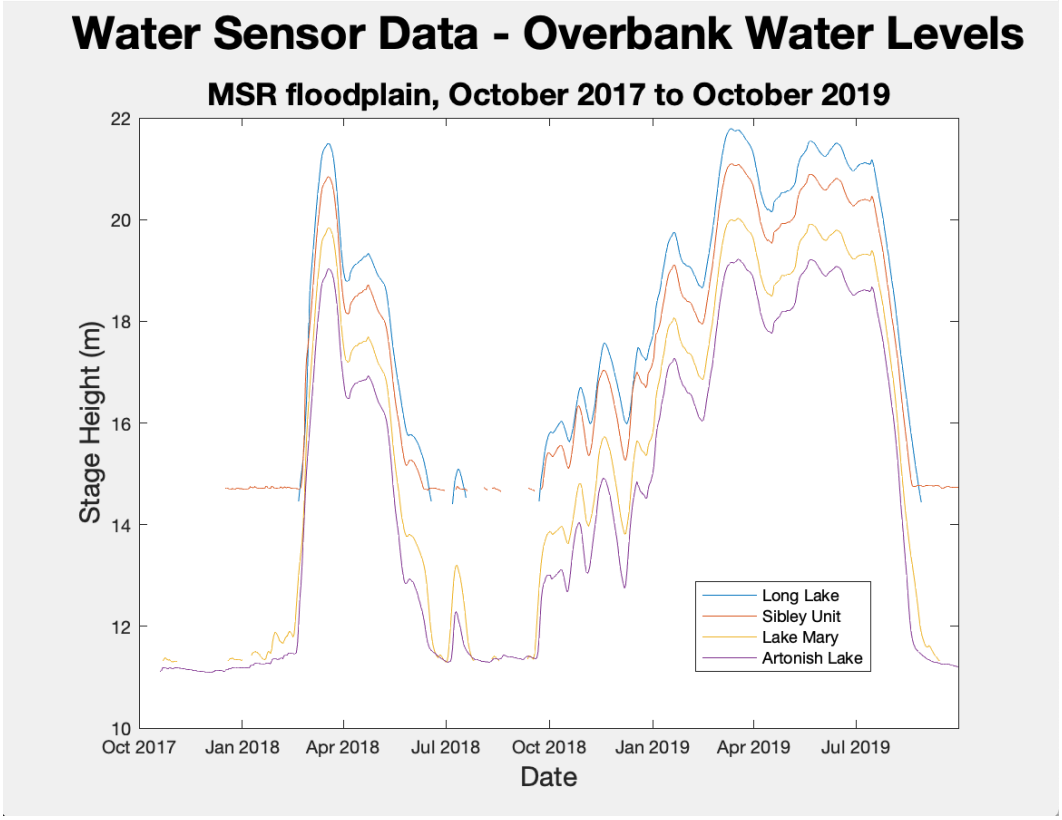

Figure 5.27 *Lower Mississippi River stage heights (m) at Long Lake, MS, Sibley Unit, MS, Lake Mary, MS, and Artonish Lake, MS, between October 2017 and October 2019.*

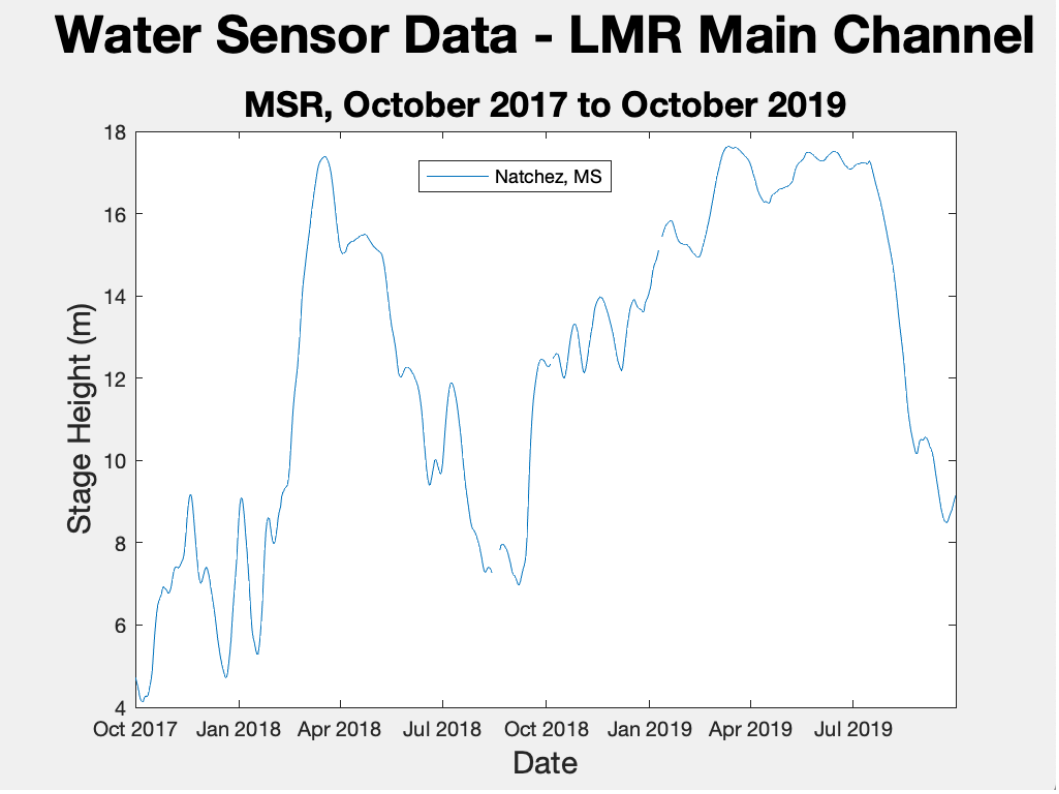

Figure 5.28 *Lower Mississippi River stage heights (m) at Natchez, MS, between October 2017 and October 2019.*

5.3 OVERBANK WATER QUALITY DURING THE 2019 FLOOD

The results below include in situ measurements of overbank water quality and laboratory analyses of suspended sediment and water samples collected across inundated floodplains in the study areas in March and June 2019. In-situ water-quality measurements are provided for both shallow and deep sensor positions. The data below are presented by location in order of north to south. The Cloverdale Unit is the most northern location with samples QW06 to QW08.

5.3.1 CLOVERDALE UNIT (QW06 TO QW08)

5.3.1.1 MARCH 2019

On March 11th, 2019, in situ water-quality at QW06, QW07, and QW08 was measured at a depth of 0.25m (0.82 ft). In order of overbank flow distance from the LMR

channel, samples are organized as: QW08 (4.0 km), QW07 (4.5 km), and QW06 (4.6 km). Temperature ranges from 8.1°C to 8.2°C (with an average of 8.1°C). Dissolved oxygen ranges from 89.9% to 91.1% (with an average of 90.57% or 10.59 mg/L). Conductivity ranges from 174.2 to 175.3 μS/cm (with an average of 174.8 μS/cm). Total dissolved solids range from 167.05 to 168.35 mg/L (with an average of 167.70 mg/L for all samples). Salinity remained the same for all samples at 0.12 ppt (±0.01 ppt). pH ranges from 6.85 to 6.98 (with an average of 6.90). Oxidation-reduction potential ranges between -62.9 to 40.4 mV (with an average of -49.4 mV) (Figure 5.28).

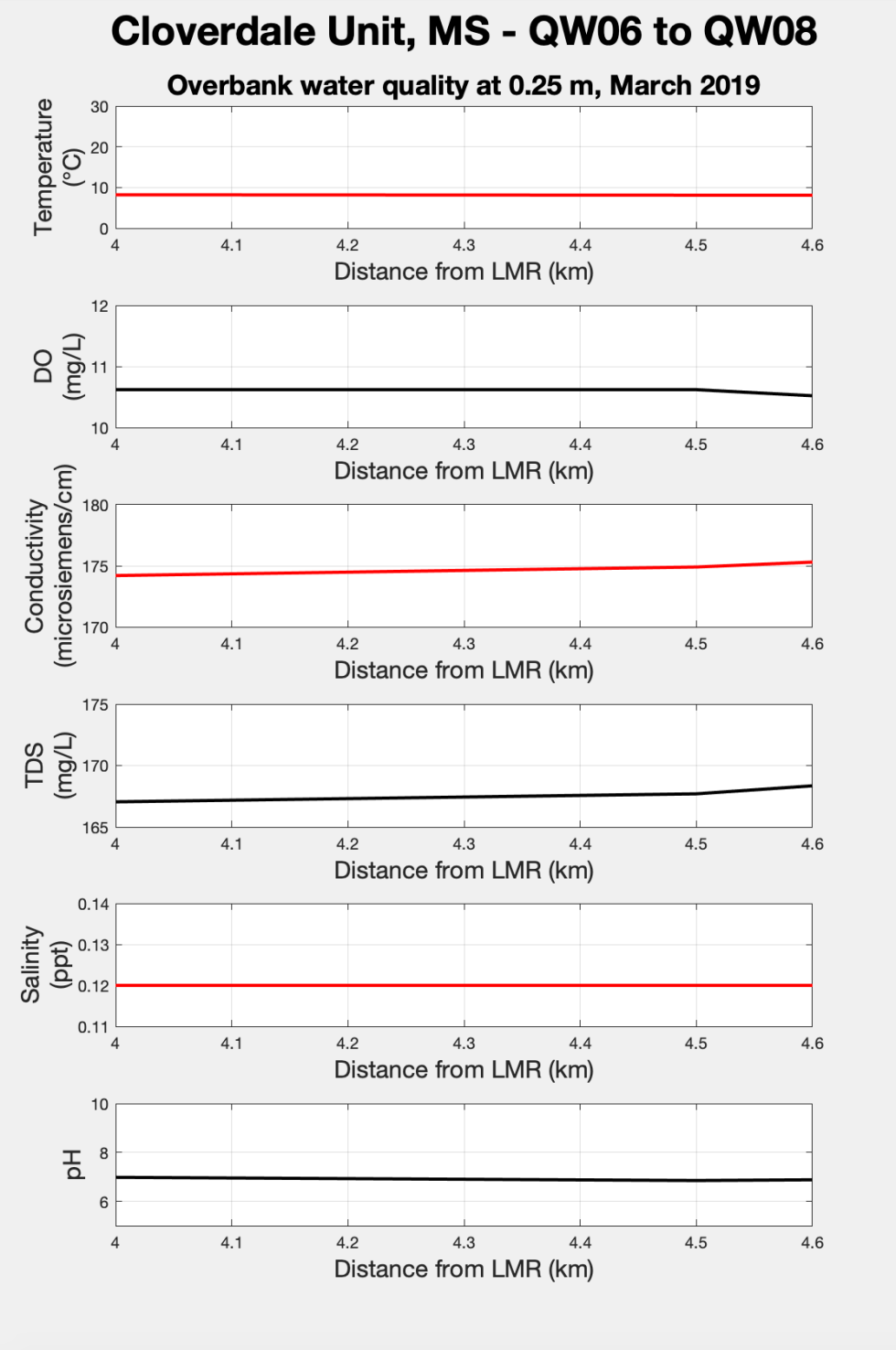

Figure 5.29 *In-situ water quality measurements at a 0.25 m depth in the overbank water column at the SCCNWR Cloverdale Unit, MS, on March 11th, 2019.*

Note: Graphs are plotted by overbank flow distance from the LMR channel. Samples QW08 (4.0 km), QW07 (4.5 km), and QW06 (4.6 km) are included.

In March 2019, for samples QW06 and QW08 measurements were taken with a YSI at a depth of 5.0m (16.4 ft) and for sample QW07 water quality measurements were taken at 4.0m (13.1 ft) due to lack of overbank depth. Temperature ranges from 8.0°C to 8.1°C (with an average of 8.03°C for all samples). Dissolved oxygen ranges from 89.2% to 90.0% (with an average of 89.73% or 10.51 mg/L). Conductivity ranges from 173.6 to 175.0 μS/cm (with an average of 174.33 μS/cm). Total dissolved solids range from 167.05 to 168.35 mg/L (with an average of 167.70 mg/L for all samples). Salinity remained the same for all samples at 0.12 ppt (±0.01 ppt). PH ranges from 6.51 to 6.68 (with an average pH of 6.58). Oxidation reduction potential ranges between -36.9 to 22.0 mV (with an average of 27.47 mV) (Figure 5.29).

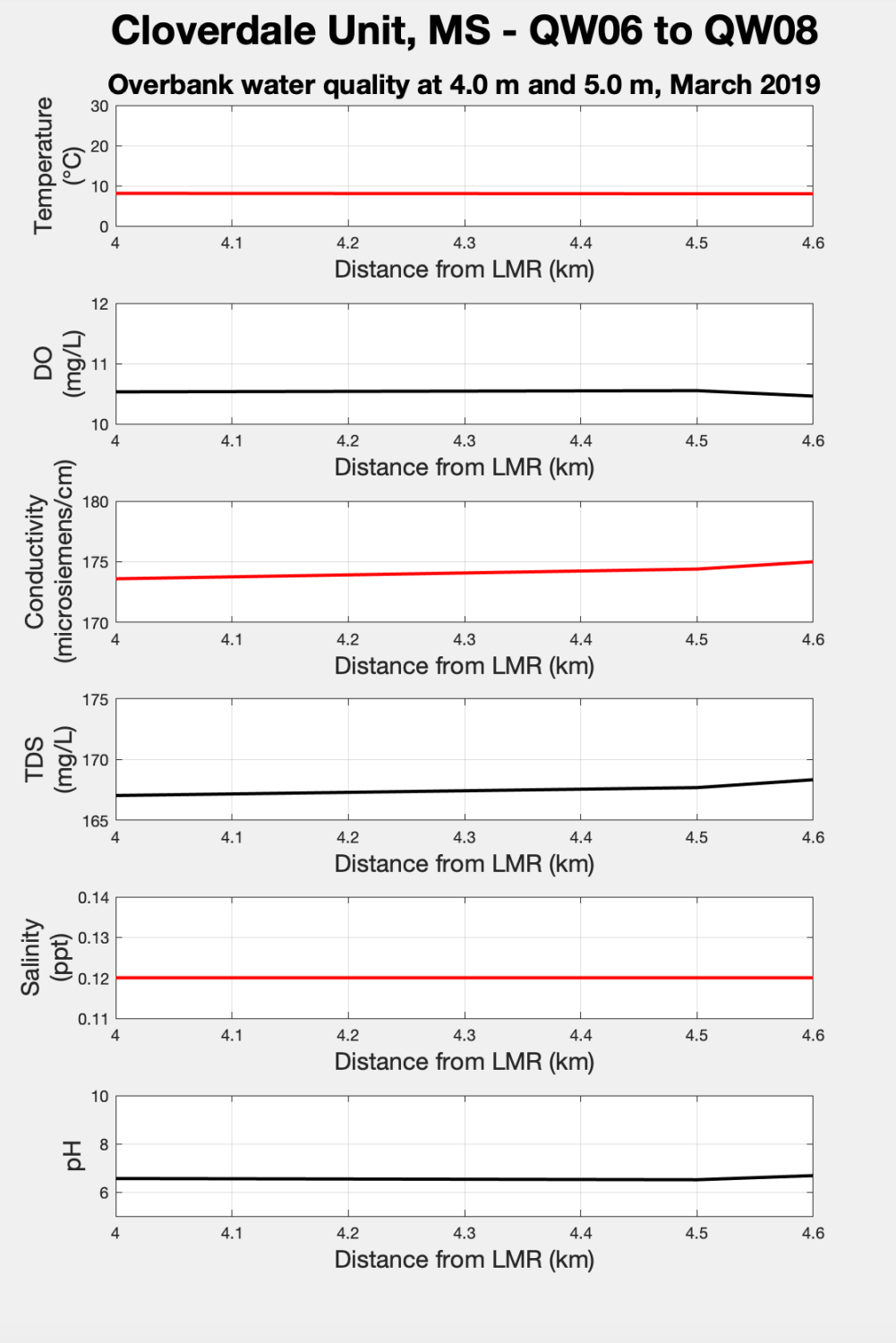

Figure 5.30 *In-situ water quality measurements at a 5.0 m depth in the overbank water column at the SCCNWR Cloverdale Unit, MS, on March 11th, 2019.*

Note: = Graphs are plotted by overbank flow distance from the LMR channel. Samples QW08 (4.0 km), QW07 (4.5 km), and QW06 (4.6 km) are included.

The overbank flow depth range for QW 06-08 in March 2019 was 4.83 to 7.19 m (15.83 to 23.60 ft) (with an average of 6.04 m (19.80 ft)). Flow velocity at a 1.2 m (4.0) depth ranged from 0.08 to 0.15 m/s (with an average of 0.12 m/s). Water samples collected for laboratory analyses of suspended sediment, turbidity, carbon, and nutrients were collected from a depth-integrated range of 0 to 4.57 m (15.0 ft) for QW06 and QW08 and 0 to 3.4m (11 ft.) for QW07. Suspended sediment collected on filter papers from depth-integrated water samples ranges from 39.5 to 53.0 mg/L (with an average of 47.97 mg/L). Median grain size (D50) for the suspended sediment ranges from 12.3 to 30.6 microns (with an average of 21.2 microns). Total phosphorus of suspended sediment ranges from 0.12% to 0.13% (with an average of 0.12%); total nitrogen ranges from 0.36% to 0.39% (with an average of 0.38%); and total carbon ranges from 3.33% to 4.24% (with an average of 3.68%). For filtered water samples, dissolved phosphorus ranges from 0.05 to 0.06 m/L (average of 0.05 mg/L) and dissolved nitrite/nitrate ranges from 0.50 to 0.61 mg/L (average of 0.55 mg/L) (Figure 5.30).

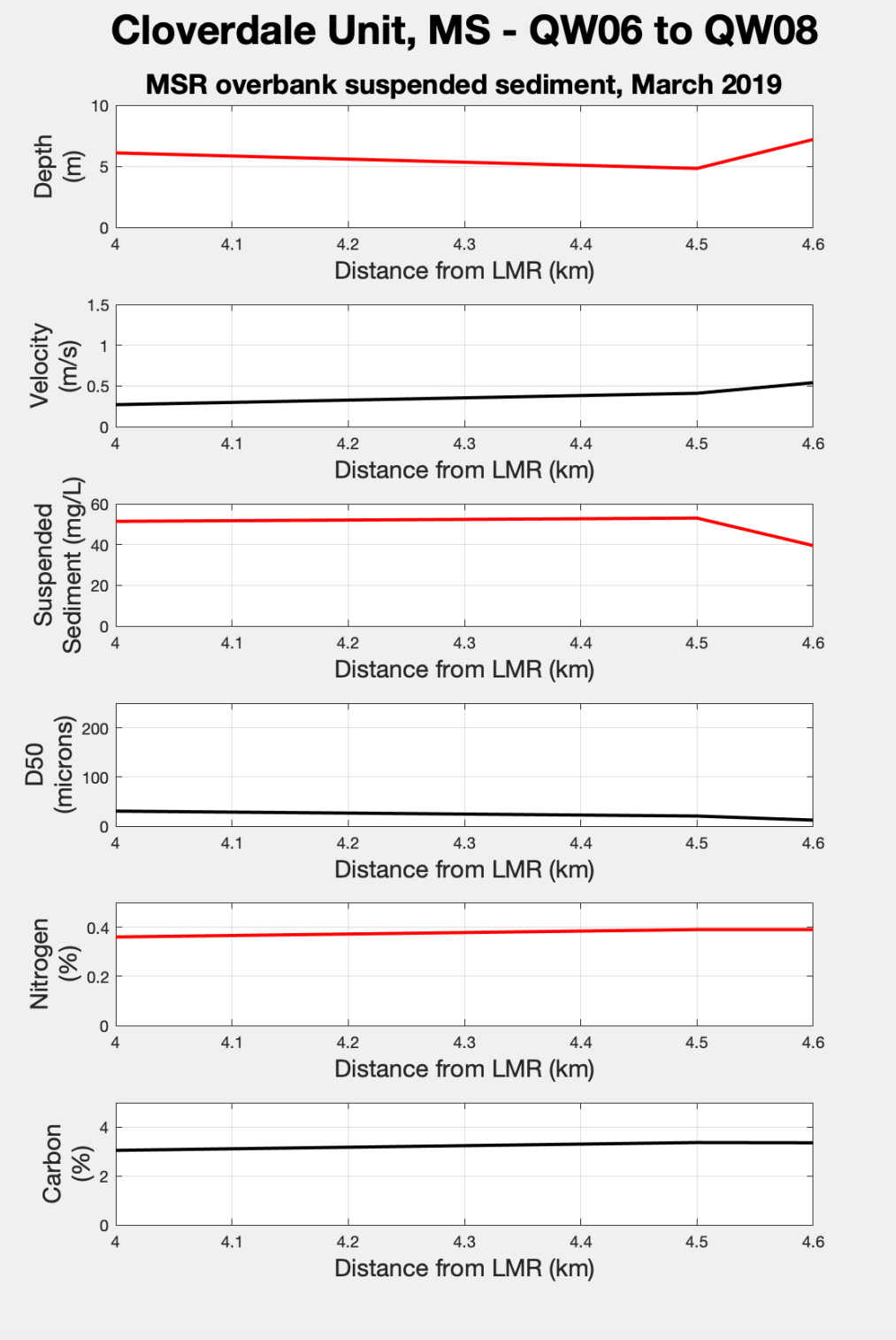

Figure 5.31 *Laboratory analysis results for overbank water and suspended sediment collected at the SCCNWR Cloverdale Unit, MS, on March 11th, 2019.*

Note: Graphs are plotted by overbank flow distance from the LMR channel. Samples QW08 (4.0 km), QW07 (4.5 km), and QW06 (4.6 km) are included. All percentages are by weight.

5.3.1.2 JUNE 2019

On June 23rd, 2019, in situ water-quality at QW06, QW07, and QW08 was measured at a depth of 0.25m (0.82 ft). In order of overbank flow distance from the LMR channel, samples are organized as: QW08 (4.0 km), QW07 (4.5 km), and QW06 (4.6 km). Temperature ranges from 26.3°C to 26.5°C (with an average of 26.43°C for all samples). Dissolved oxygen ranges from 79.0% to 82.7% (with an average of 81.20% or 6.53 mg/L). Conductivity ranges from 385.4 to 399.9 µS/cm (with an average of 393.10 µS/cm). Total dissolved solids range from 244.4 to 252.2 mg/L (with an average of 248.7 mg/L for all samples). Salinity remained the same for all samples at 0.12 ppt (±0.01 ppt). pH ranges from 6.15 to 6.35 (with an average pH of 6.24). Oxidation-reduction potential ranges between -32.4 to 14.6 mV (with an average of -9.40 mV) (Figure 5.31).

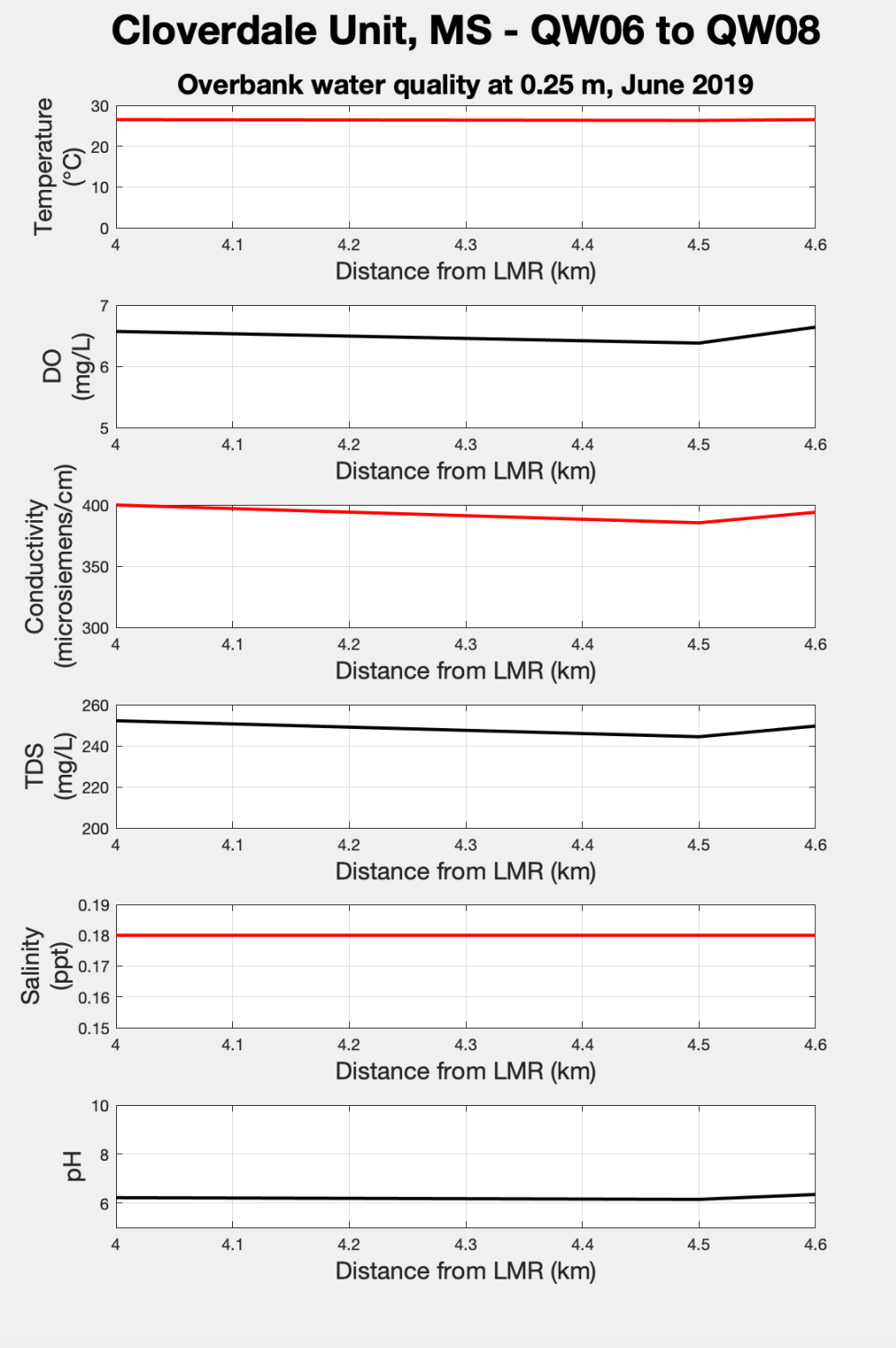

Figure 5.32 *In-situ water quality measurements at a 0.25 m depth in the overbank water column at the SCCNWR Cloverdale Unit, MS, on June 23rd, 2019.*

Note: Graphs are plotted by overbank flow distance from the LMR channel. Samples QW08 (4.0 km), QW07 (4.5 km), and QW06 (4.6 km) are included.

On June 23rd, 2019, in situ water-quality at QW06 and QW08 was measured at a depth of 5.0m (16.4 ft) and QW07 was measured at a depth of 3m (9.8 ft.). Temperature ranges from 26.0°C to 26.4°C (with an average of 26.2°C for all samples). Dissolved oxygen ranges from 75.1% to 81.0% (with an average of 78.2% or 6.29 mg/L). Conductivity ranges from 390.7 to 399.2 µS/cm (with an average of 393.87 µS/cm). Total dissolved solids range from 248.95 to 252.85 mg/L (with an average of 250.25 mg/L for all samples). Salinity remained the same for all samples at 0.12 ppt (±0.01 ppt). pH ranges from 6.25 to 6.95 (with an average pH of 6.54). Oxidation-reduction potential ranges between -17.4 to 39.7 mV (with an average of 10.73 mV) (Figure 5.32).

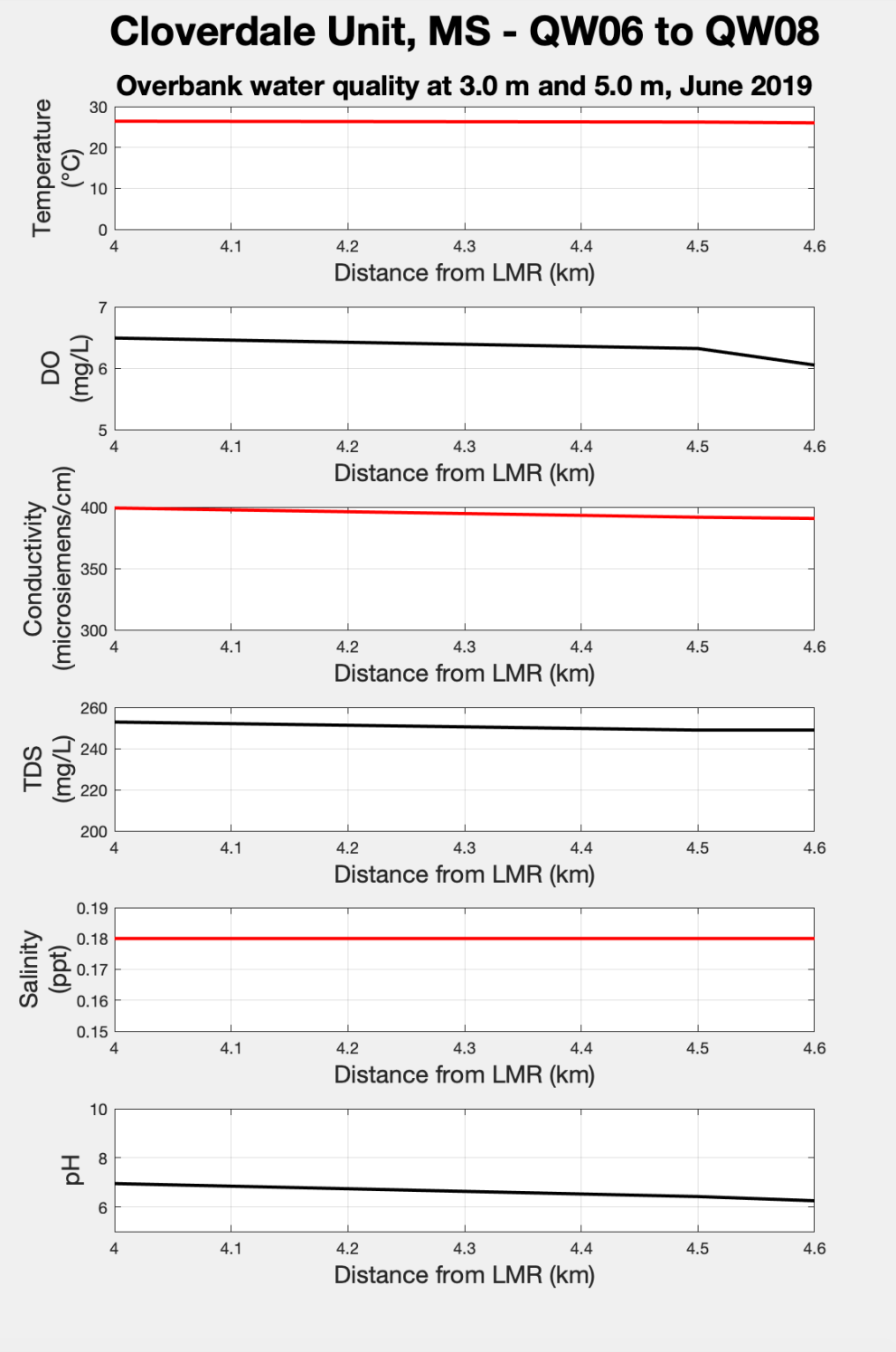

Figure 5.33 *In-situ water quality measurements at a 5.0 m depth in the overbank water column at the SCCNWR Cloverdale Unit, MS, on June 23rd, 2019.*

Note: Graphs are plotted by overbank flow distance from the LMR channel. Samples QW08 (4.0 km), QW07 (4.5 km), and QW06 (4.6 km) are included.

The overbank flow depth range for QW06 to QW08 on June 23rd, 2019 was 3.14 to 7.32 m (10.30 to 24.00 m) (with an average of 5.53 m (18.14 ft) for all samples). Flow velocity at a 1.2 m (4.0 ft) depth ranged from 0.07 to 0.21 m/s (with an average of 0.14 m/s). Water samples collected for laboratory analyses of suspended sediment, turbidity, carbon, and nutrients were collected from a depth-integrated range of 0 to 4.6m (15 ft.) for QW06 and 08 and 0 to 2.7 m (9 ft) for QW07. Suspended sediment collected on filter papers from depth-integrated water samples ranges from 24.30 to 41.10 mg/L (with an average of 34.70 mg/L for all samples). Median grain size (D50) for the suspended sediment ranges from 10.5 to 247.0 microns (with an average of 89.5 microns). Total phosphorus of suspended sediment ranges from 0.13% to 0.14% (with an average of 0.13% for all samples); total nitrogen ranges from 0.38% to 0.45% (with an average of 0.41% for all samples); and total carbon ranges from 3.70% to 4.68% (with an average of 4.04% for all samples). For filtered water samples, dissolved phosphorus ranges from 0.05 to 0.08 m/L (average of 0.07 mg/L for all samples) and dissolved nitrite/nitrate ranges from 0.90 to 1.29 mg/L (average of 1.14 mg/L for all samples) (Figure 5.33).

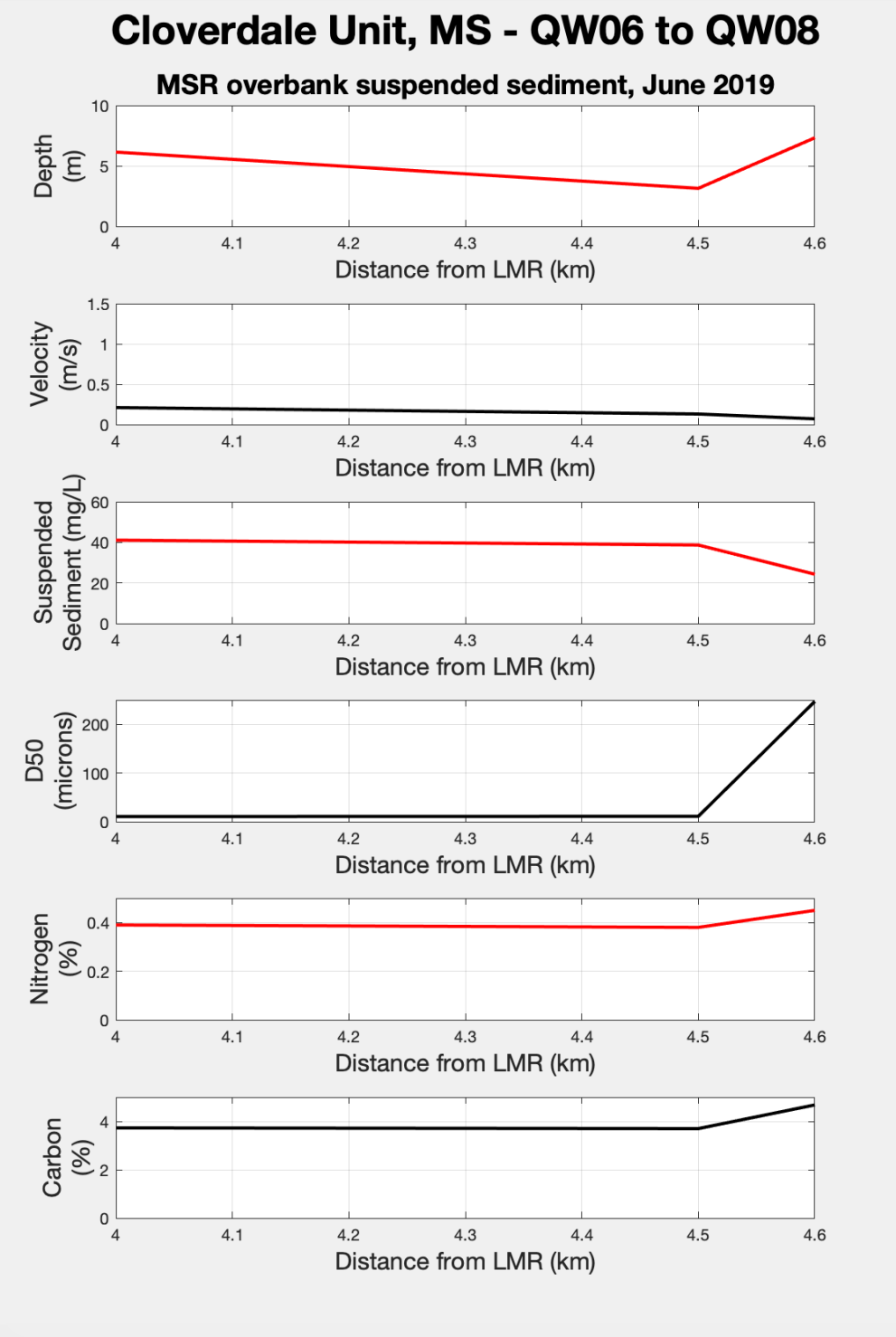

Figure 5.34 *Laboratory analysis results for overbank water and suspended sediment collection at the SCCBWR Cloverdale Unit, MS, on June 23rd, 2019.*

Note: Graphs are plotted by overbank flow distance from the LMR channel. Samples QW08 (4.0 km), QW07 (4.5 km), and QW06 (4.6 km) analyzed. All percentages are by weight.

5.3.2 SIBLEY UNIT (QW01 TO QW05)

5.3.2.1 MARCH 2019

Overbank water-quality measurements and samples in the Sibley Unit were collected in proximity to sediment samples along T12 and T13. In order of distance from the LMR (smallest to largest) samples are organized as: QW02 (2.3), QW05 (2.5), QW03 (3.1), QW01 (3.9), and QW04 (4.0).

On March 10th, 2019, in situ water-quality at QW 01, QW02, QW03, QW04, and QW05 was measured at a depth of 0.25m (0.82 ft). Temperature ranges from 7.9°C to 8.2°C (with an average of 8.0°C for all samples). Dissolved oxygen ranges from 90.3% to 90.6% (with an average of 90.42% or 10.59 mg/L). Conductivity ranges from 174.2 to 177.2 µS/cm (with an average of 176.14 µS/cm). Total dissolved solids range from 168.35 to 170.30 mg/L (with an average of 169.39 mg/L for all samples). Salinity remained the same for all samples at 0.12 ppt (±0.01 ppt). pH ranges from 6.42 to 8.02 (with an average pH of 7.18). Oxidation-reduction potential ranges between -27.4 to 127.80 mV (with an average of 49.08 mV) (Figure 5.34).

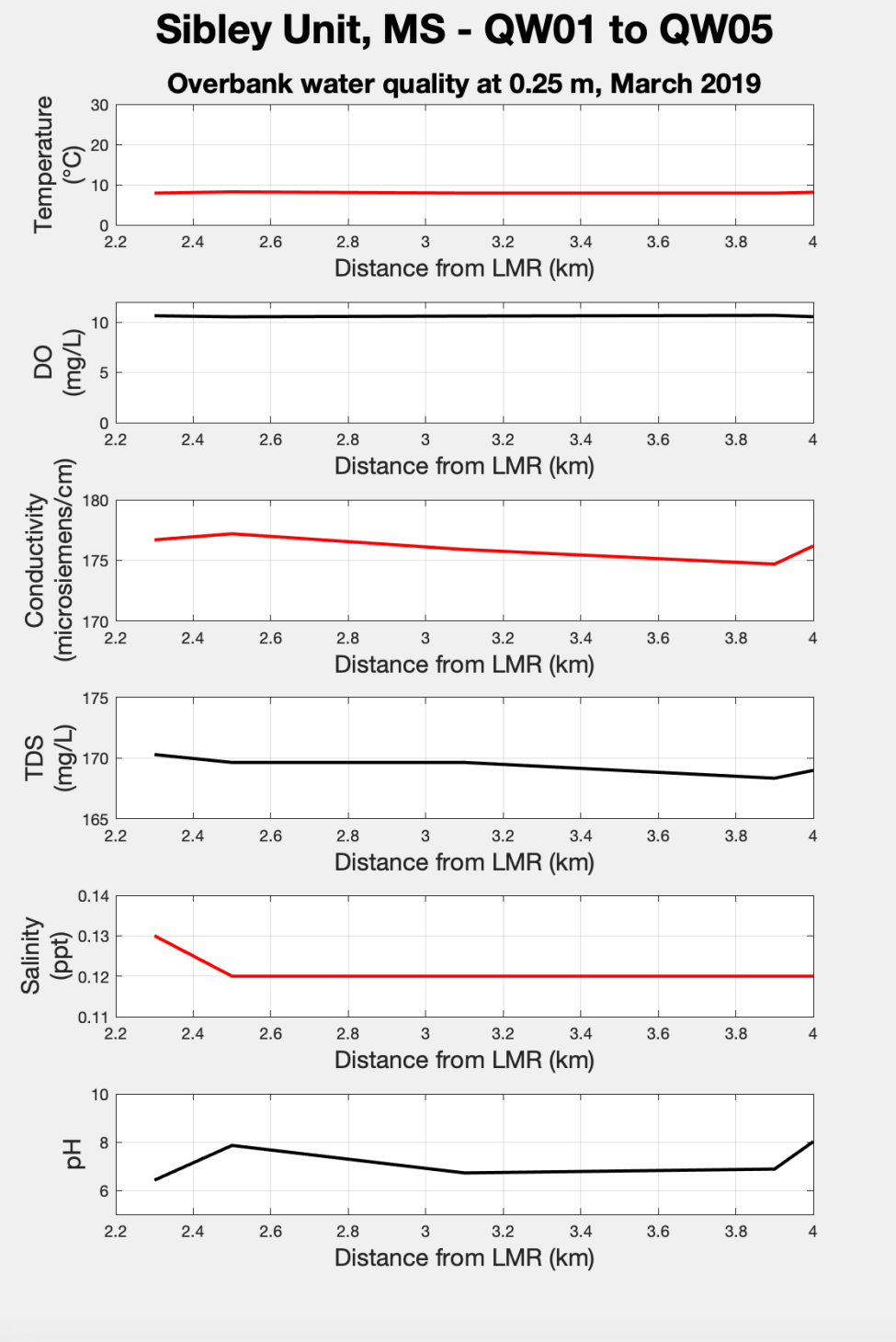

Figure 5.35 *In-situ water quality measurements at a 0.25 m depth in the overbank water column at the SCCNWR Sibley Unit, MS, on March 10th, 2019.*

Note: Graphs are plotted by overbank flow distance from the LMR channel. Samples QW02 (2.3 km), QW05 (2.5 km), QW03 (3.1 km), QW01 (3.9 km), and QW04 (4.0 km) are included.

On March 10th, 2019, in situ water-quality at QW 01, QW02, QW03, QW04, and QW05 was measured at a depth of 5.00 m (16.4 ft). Temperature ranges from 7.9°C to 8.2°C (with an average of 7.96°C for all samples). Dissolved oxygen ranges from 89.6% to 90.0% (with an average of 89.84% or 10.56 mg/L). Conductivity ranges from 175.6 to 176.8 μS/cm (with an average of 176.00 μS/cm). Total dissolved solids 169.65 mg/L for all samples. Salinity remained the same for all samples at 0.12 ppt (±0.01 ppt). pH ranges from 5.30 to 8.02 (with an average pH of 6.95). Oxidation-reduction potential ranges between -21.6 to 92.1 mV (with an average of 32.82 mV) (Figure 5.35).

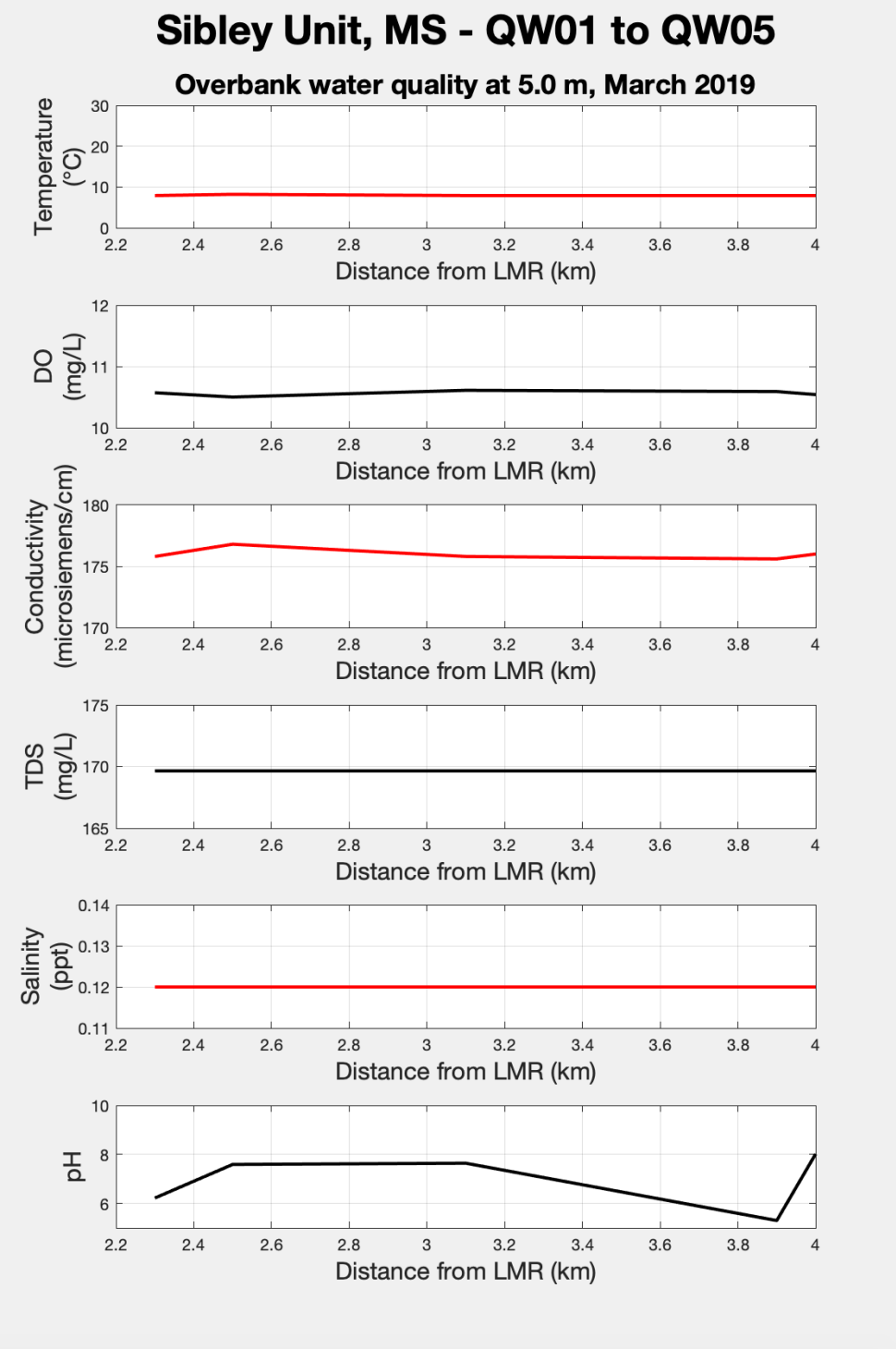

Figure 5.36 *In-situ water quality measurements at a 5.0 m depth in the overbank water column at the SCCNWR Sibley Unit, MS, on March 10th, 2019.*

Note: Graphs are plotted by overbank flow distance from the LMR channel. Samples QW02 (2.3 km), QW05 (2.5 km), QW03 (3.1 km), QW01 (3.9 km), and QW04 (4.0 km) are included.

The overbank flow depth range for QW 01, QW02, QW03, QW04, and QW05 on March 10th, 2019 was 5.34 to 7.75 m (17.53 to 25.43 ft) (with an average of 6.42 m for all samples). Flow velocity at a 1.2 m (4.0 ft.) depth ranged from 0.12 to 0.41 m/s (with an average of 0.27 m/s). Water samples collected for laboratory analyses of suspended sediment, turbidity, carbon, and nutrients were collected from a depth-integrated range of 0 to 4.57 m (15.00 ft.). Suspended sediment collected on filter papers ranges from 34.6 to 48.7 mg/L (with an average of 42.4 mg/L for all samples). Median grain size (D50) for the suspended sediment ranges from 14.3 to 184.0 microns (with an average of 79.70 microns). Total phosphorus to suspended sediment ranges from 0.12% to 0.14% (with an average of 0.13% for all samples); total nitrogen ranges from 0.37% to 0.44% (with an average of 0.41% for all samples); and total carbon ranges from 3.33% to 4.24% (with an average of 3.68% for all samples). For filtered water samples, dissolved phosphorus ranges from 0.03 to 0.04 mg/L (average of 0.04 mg/L for all samples) and dissolved nitrite/nitrate ranges from 0.33 to 0.49 mg/L (average of 0.41 mg/L for all samples) (Figure 5.36).

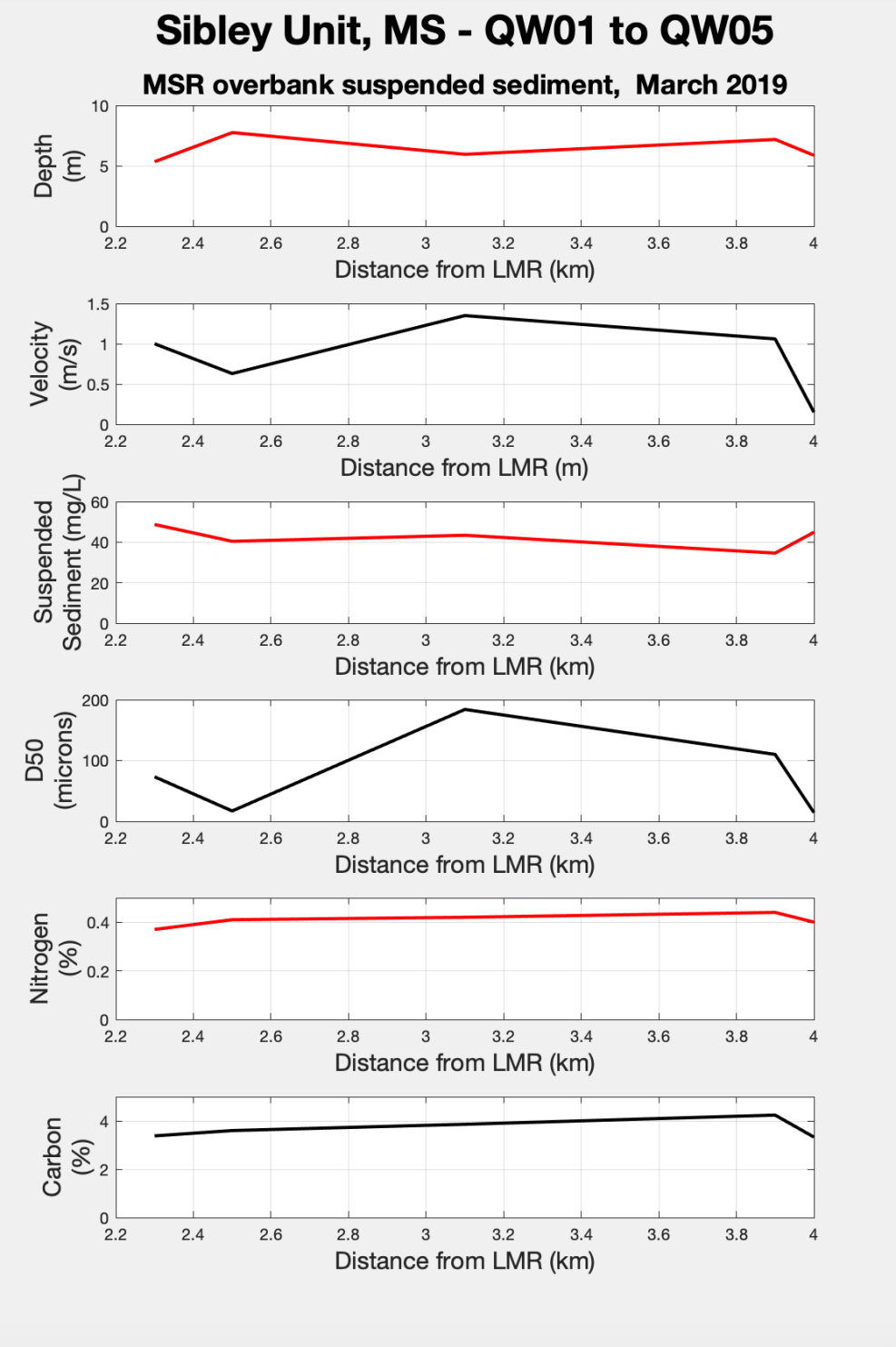

Figure 5.37 *Laboratory analysis results for overbank water and suspended sediment collection at the SCCBWR Sibley Unit, MS, on March 10th, 2019.*

Note: Graphs are plotted by overbank flow distance from the LMR channel. Samples QW02 (2.3 km), QW05 (2.5 km), QW03 (3.1 km), QW01 (3.9 km), and QW04 (4.0 km) are included. All percentages are by weight.

5.3.2.2 JUNE 2019

Sample locations in June 2019 are in the same locations as March 2019 with an error of less than 10 meters, except for Sample QW02, which is 235m east of the March 2019 sampling location. In order of overbank flow distance from the LMR samples are organized as: QW02 (2.3), QW05 (2.5), QW03 (3.1), QW01 (3.9), and QW04 (4.0).

On June 21st, 2019, in situ water-quality at QW01, QW02, QW03, QW04, and QW05 was measured at a depth of 0.25m (0.82 ft). Temperature ranges from 25.8°C to 26.9°C (with an average of 26.26°C for all samples). Dissolved oxygen ranges from 75.3% to 80.2% (with an average of 77.22% or 6.24 mg/L). Conductivity ranges from 373.5 to 396.1 μS/cm (with an average of 374.3 μS/cm). Total dissolved solids range from 238.55 to 250.25 mg/L (with an average of 241.54 mg/L for all samples). Salinity remained the same for all samples at 0.12 ppt (±0.01 ppt). pH ranges from 5.95 to 7.70 (with an average pH of 6.8). Oxidation-reduction potential ranges between -11.5 to 309.8 mV (with an average of 81.78 mV) (Figure 5.37).

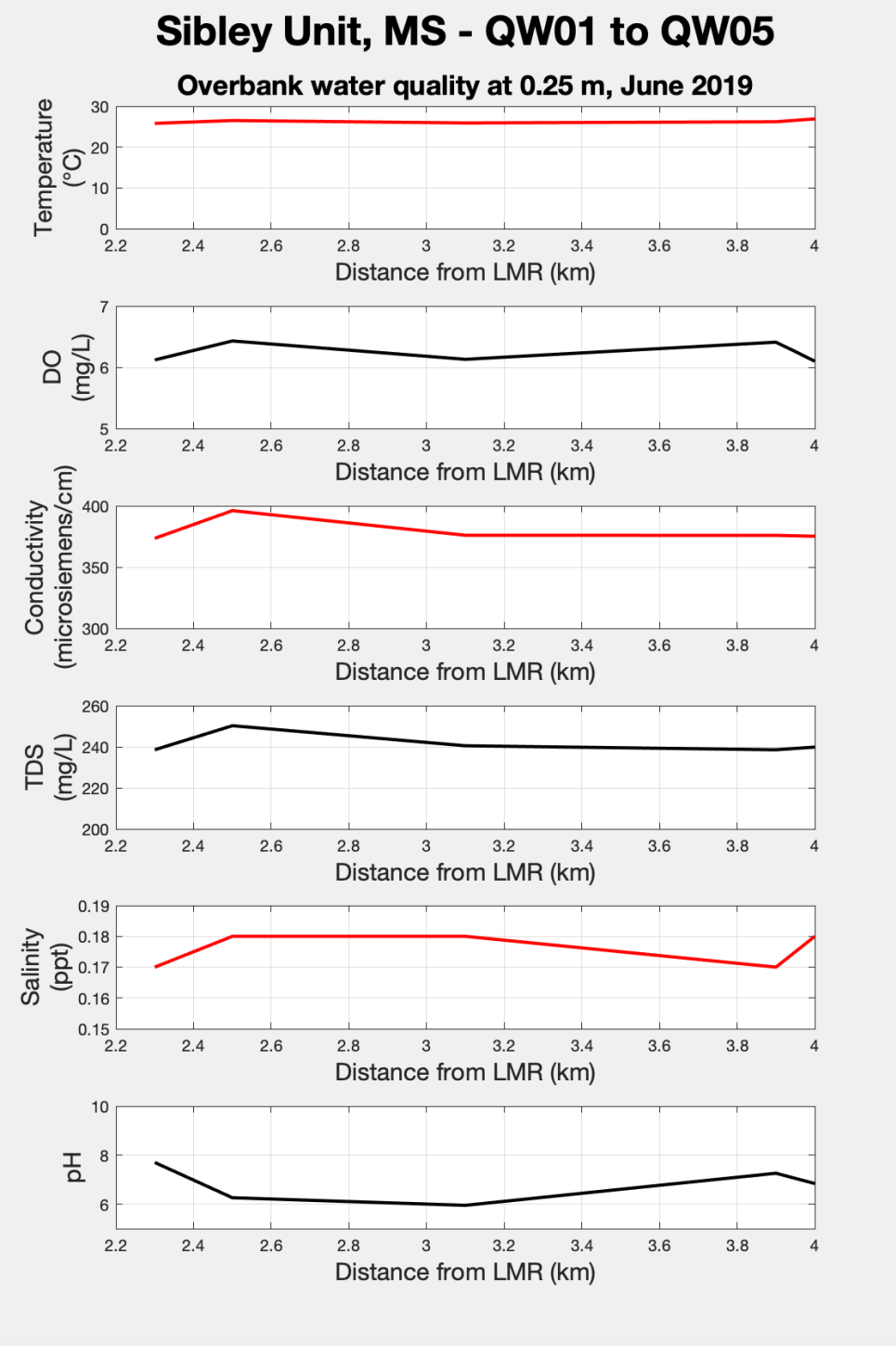

Figure 5.38 *In-situ water quality measurements at a 0.25 m depth in the overbank water column at the SCCNWR Sibley Unit, MS, on June 21st, 2019.*

Note: = Graphs are plotted by overbank flow distance from the LMR channel. Samples QW02 (2.3 km), QW05 (2.5 km), QW03 (3.1 km), QW01 (3.9 km), and QW04 (4.0 km) are included.

On June 21st, 2019, in situ water-quality at QW01, QW03, QW04, and QW05 was measured at a depth of 5.0m (16.4 ft) and QW02 was measured at 4m (13.1 ft.). Temperature ranges from 25.8°C to 26.7°C (with an average of 26.1°C for all samples). Dissolved oxygen ranges from 74.3% to 79.5% (with an average of 75.74% or 6.13 mg/L). Conductivity ranges from 373.2 to 395.2 μS/cm (with an average of 378.66 μS/cm). Total dissolved solids range from 238.55 to 250.25 mg/L (with an average of 241.80 mg/L for all samples). Salinity remained the same for all samples at 0.12 ppt (±0.01 ppt). pH ranges from 5.90 to 9.73 (with an average pH of 7.20). Oxidation-reduction potential ranges between 7.8 to 61.2 mV (with an average of 37.26 mV) (Figure 5.38).

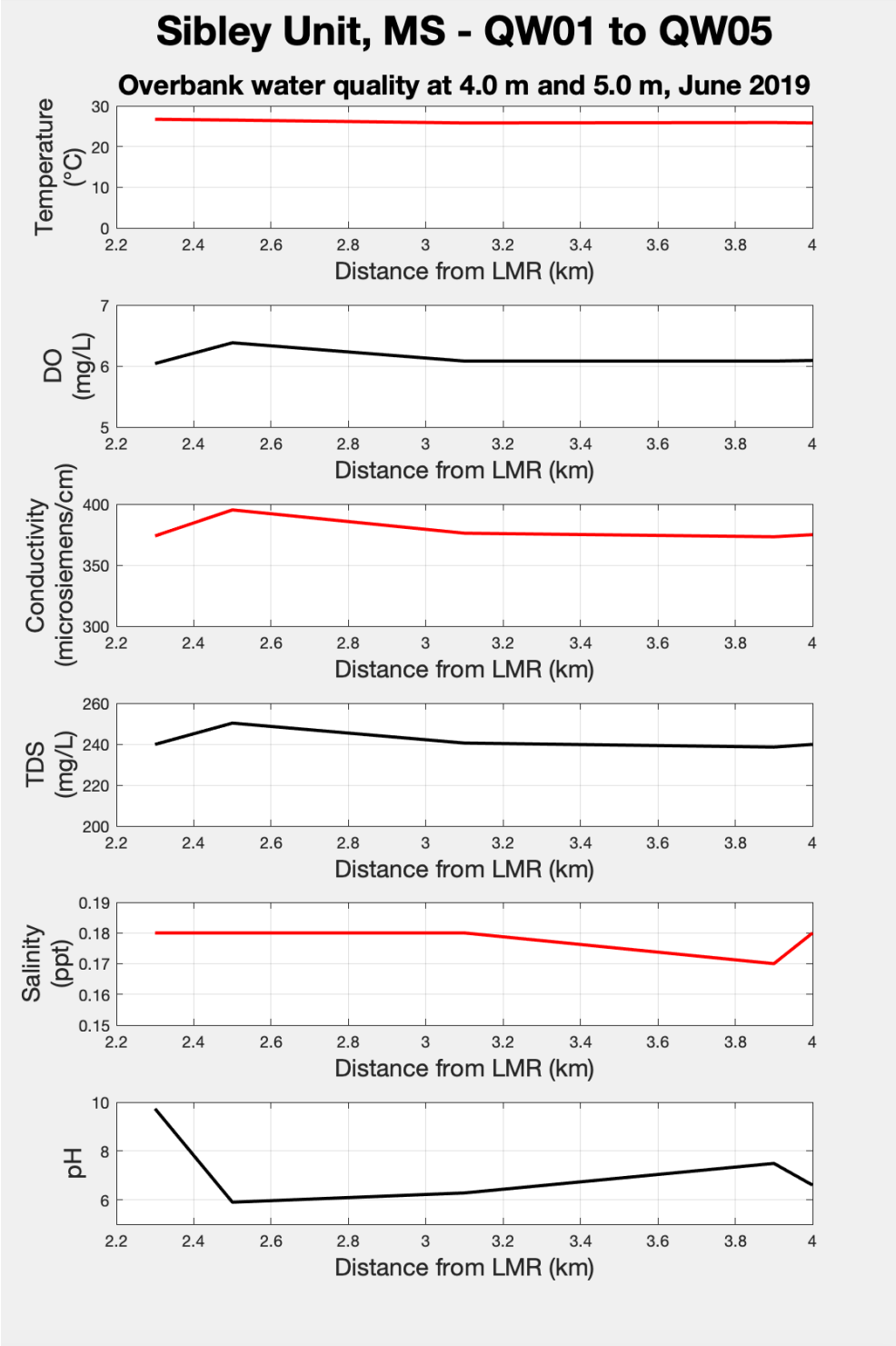

Figure 5.39 *In-situ water quality measurements at a 5.0 m depth in the overbank water column at the SCCNWR Sibley Unit, MS, on June 21st, 2019.*

Note: = Graphs are plotted by overbank flow distance from the LMR channel. Samples QW02 (2.3 km), QW05 (2.5 km), QW03 (3.1 km), QW01 (3.9 km), and QW04 (4.0 km) are included.

The overbank flow depth range for QW 01, QW02, QW03, QW04, and QW05 on June 21st, 2019 was 4.59 to 6.54 m (15.07 to 21.47 ft) (with an average of 5.60 m (18.37 ft). Flow velocity at a 1.2 m (4.0 ft,) depth ranged from 0.12 to 0.44 m/s (0.25 to 1.25 ft/s) (with an average of 0.23 m/s (0.62 ft/s)). Water samples collected for laboratory analyses of suspended sediment, turbidity, carbon, and nutrients were collected from a depth-integrated range of 0 to 4.57 m (15.00 ft), except QW02 that was collected at 3m (9.8 ft.). Suspended sediment collected on filter papers from depth-integrated water samples ranges from 36.20 to 56.80 mg/L (with an average of 42.48 mg/L for all samples). Median grain size (D50) for the suspended sediment ranges from 7.5 to 19.7 microns (with an average of 15.1 microns). Total phosphorus of suspended sediment ranges from 0.10% to 0.13% (with an average of 0.11% for all samples); total nitrogen ranges from 0.26% to 0.39% (with an average of 0.33% for all samples); and total carbon ranges from 2.65% to 3.87% (with an average of 3.42% for all samples). For filtered water samples, dissolved phosphorus ranges from 0.06 to 0.07 m/L (average of 0.06 mg/L for all samples) and dissolved nitrite/nitrate ranges from 0.71 to 1.32 mg/L (average of 1.00 mg/L for all samples) (Figure 5.39).

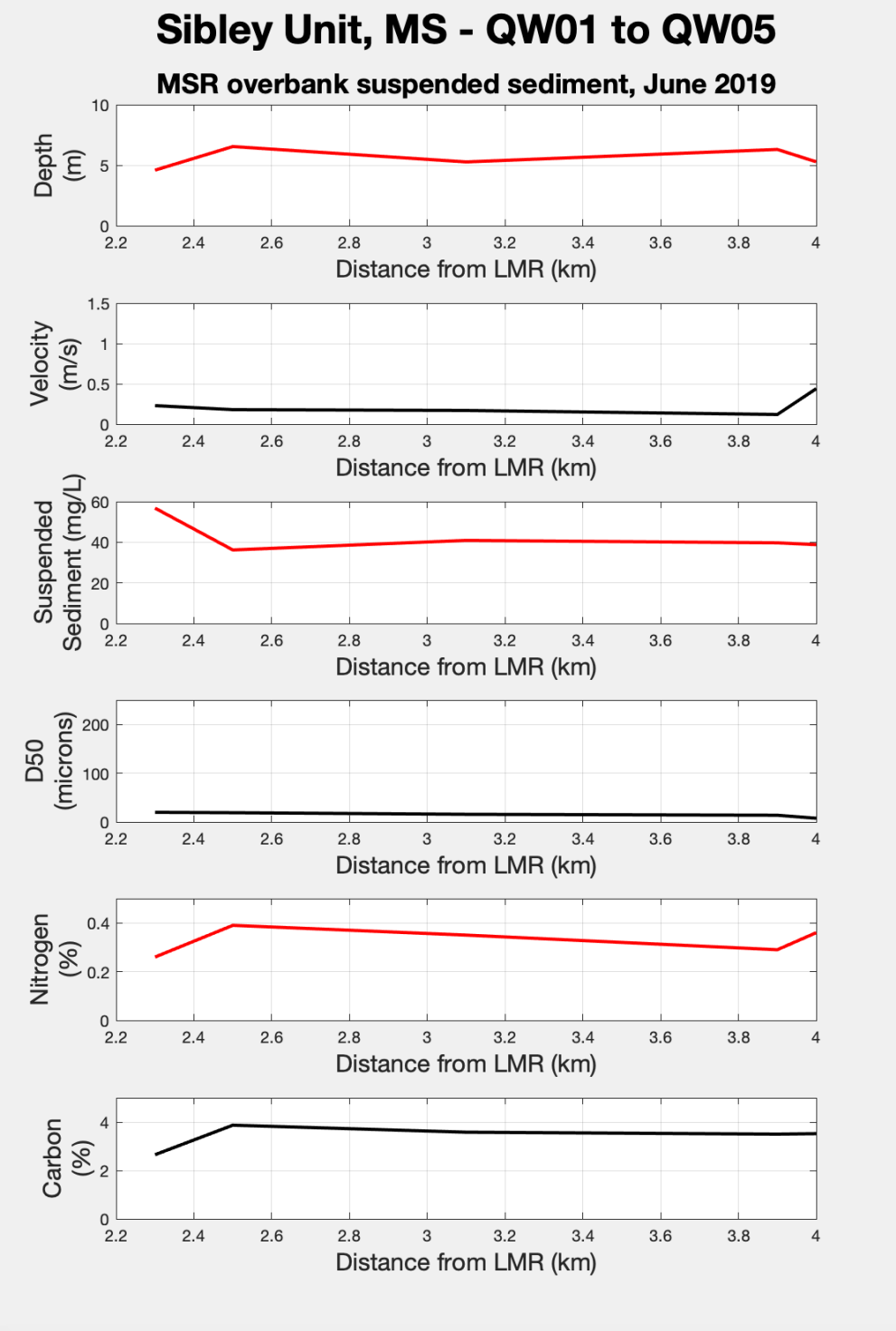

Figure 5.40 *Laboratory analysis results for overbank water and suspended sediment collection at the SCCNWR Sibley Unit, MS, on June 21st, 2019.*

Note: Graphs are plotted by overbank flow distance from the LMR channel. Samples QW02 (2.3 km), QW05 (2.5 km), QW03 (3.1 km), QW01 (3.9 km), and QW04 (4.0 km) are included. All percentages are by weight.

5.3.3 FORT ADAMS AND ARTONISH (QW09 TO QW13)

5.3.3.1 JUNE 2019

Overbank water quality measurements and water samples in Wilkinson County, MS (QW 09-13) were only collected on June 22nd, 2019. In order of overbank flow distance from the LMR, samples are organized as: QW10 (1.2 km), QW11 (1.3 km), QW12 (4.4 km), QW09 (17.3 km), and QW13 (18.5 km).

In-situ water-quality at QW09, QW10, QW11, QW12, and QW13 was measured at a depth of 0.25m (0.82 ft). Temperature ranges from 25.9°C to 26.7°C (with an average of 26.18°C for all samples). Dissolved oxygen ranges from 70.1% to 79.1% (with an average of 76.38% or 6.16 mg/L). Conductivity ranges from 340.8 to 390.5 µS/cm (with an average of 364.48 µS/cm). Total dissolved solids range from 214.5 to 247.0 mg/L (with an average of 235.7 mg/L for all samples). Salinity remained the same for all samples at 0.12 ppt (±0.01 ppt). pH ranges from 6.24 to 6.91 (with an average pH of 6.54). Oxidation-reduction potential ranges between -43.2 to 92.6 mV (with an average of 7.60 mV) (Figure 5.40).

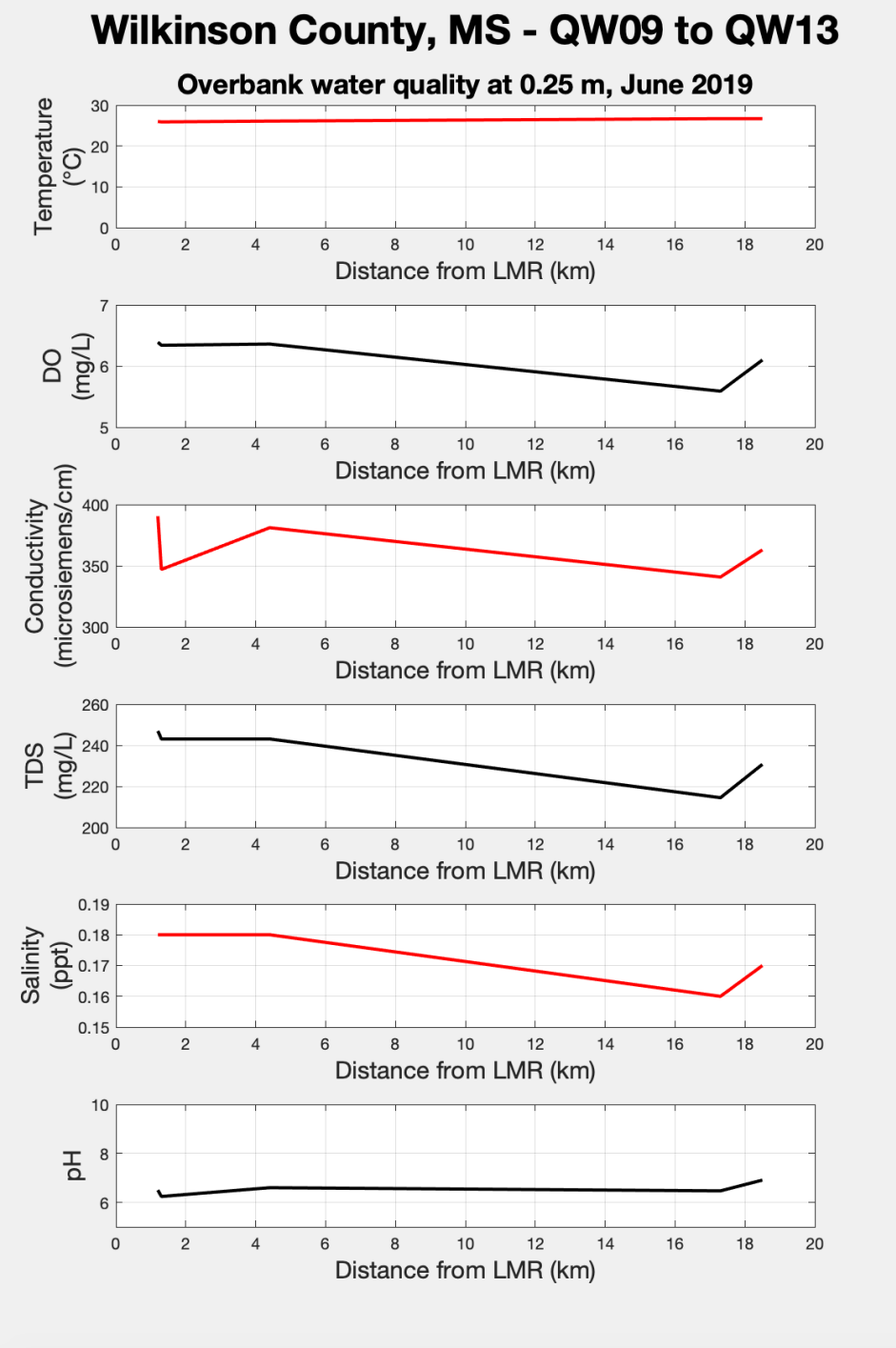

Figure 5.41 *In-situ water quality measurements at a 0.25 m depth in the overbank water column at the Wilkinson County, MS, on June 22nd, 2019.*

Note: = Graphs are plotted by overbank flow distance from the LMR channel. Samples QW10 (1.2 km), QW11 (1.3 km), QW12 (4.4 km), QW09 (17.3 km), and QW13 (18.5 km) are included.

In situ water-quality was measured at depths of 5.0 m for QW09, 3m for QW10, 2.5m for QW11, 4m for QW12, and 4m for QW13. Temperature ranges from 25.9°C to 26.6°C (with an average of 26.12°C for all samples). Dissolved oxygen ranges from 68.3% to 78.6% (with an average of 75.6% or 6.10 mg/L). Conductivity ranges from 344.3 to 381.3 μS/cm (with an average of 369.24 μS/cm). Total dissolved solids range from 217.1 to 245.7 mg/L (with an average of 236.8 mg/L for all samples). Salinity remained the same for all samples at 0.12 ppt (±0.01 ppt). pH ranges from 6.18 to 7.21 (with an average pH of 6.70). Oxidation-reduction potential ranges between -46.6 to 87.0 mV (with an average of -1.22 mV) (Figure 5.41).

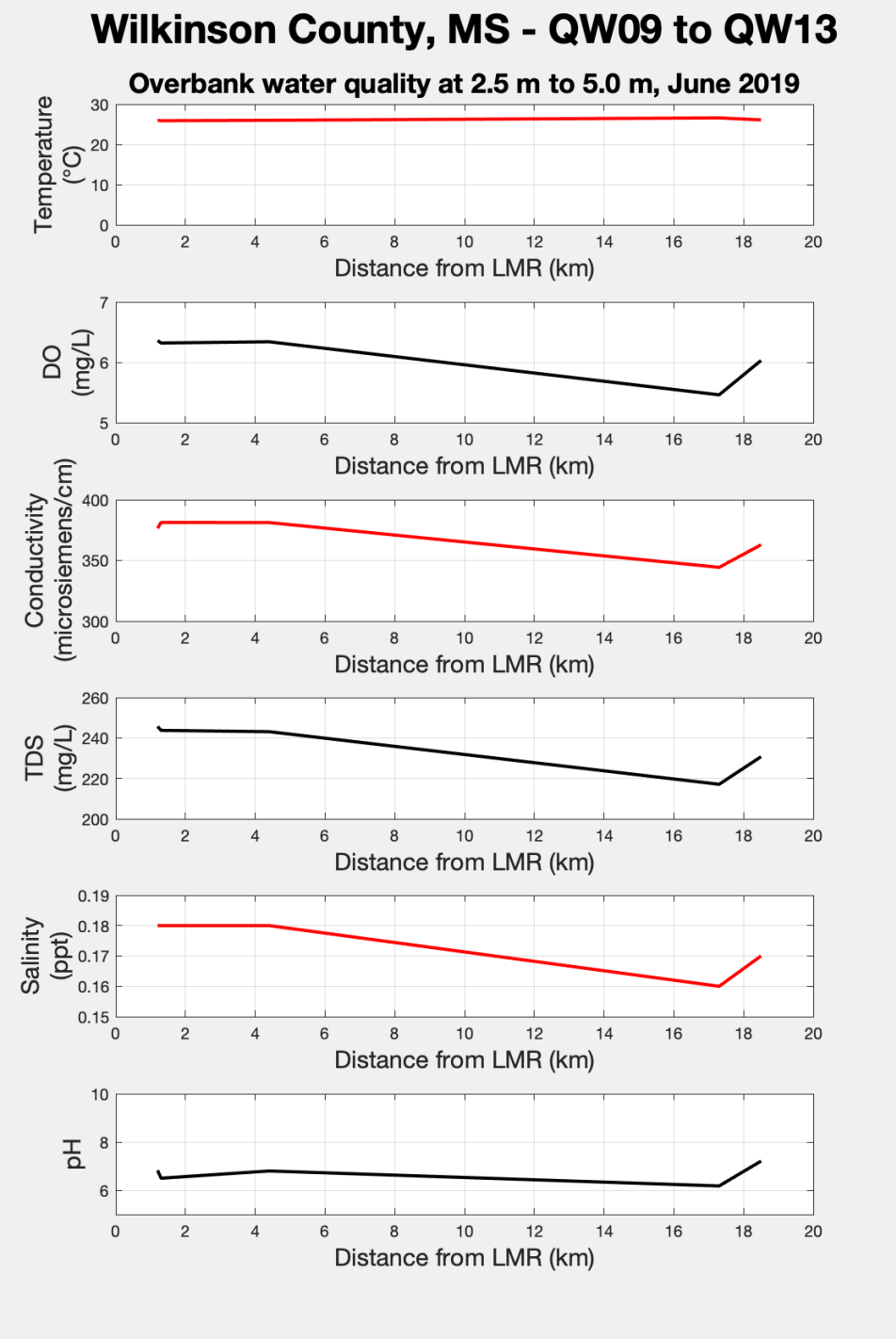

Figure 5.42 *In-situ water quality measurements at a 5.0 m depth in the overbank water column at Wilkinson County, MS, on June 22nd, 2019.*

Note: = Graphs are plotted by overbank flow distance from the LMR channel. Samples QW10 (1.2 km), QW11 (1.3 km), QW12 (4.4 km), QW09 (17.3 km), and QW13 (18.5 km) are included.

The overbank flow depth range for QW09, QW10, QW11, QW12, and QW13 on June 22nd, 2019 was 2.60 to 7.58 m (8.53 to 24.87 ft) (with an average of 4.60 m (15.08 ft)). Flow velocity at a 1.22 m (4.0 ft) depth ranged from 0.23 to 0.62 m/s (0.67 to 1.65 ft) (with an average of 0.40 m/s (1.13 ft)). Water samples collected for laboratory analyses of suspended sediment, turbidity, carbon, and nutrients were collected from a depth-integrated range of 0 to 4.57 m (15.0 ft). Suspended sediment collected on filter papers from depth-integrated water samples ranges from 35.30 to 51.00 mg/L (with an average of 44.46 mg/L for all samples). Median grain size (D50) for the suspended sediment ranges from 5.7 to 15.1 microns (with an average of 8.9 microns). Total phosphorus of suspended sediment ranges from 0.10% to 0.13% (with an average of 0.12% for all samples); total nitrogen ranges from 0.15% to 0.37% (with an average of 0.31% for all samples); and total carbon ranges from 1.47% to 3.82% (with an average of 3.12% for all samples). For filtered water samples, dissolved phosphorus ranges from 0.05 to 0.06 m/L (average of 0.06 mg/L for all samples) and dissolved nitrite/nitrate ranges from 0.61 to 1.38 mg/L (average of 1.09 mg/L for all samples) (Figure 5.42).

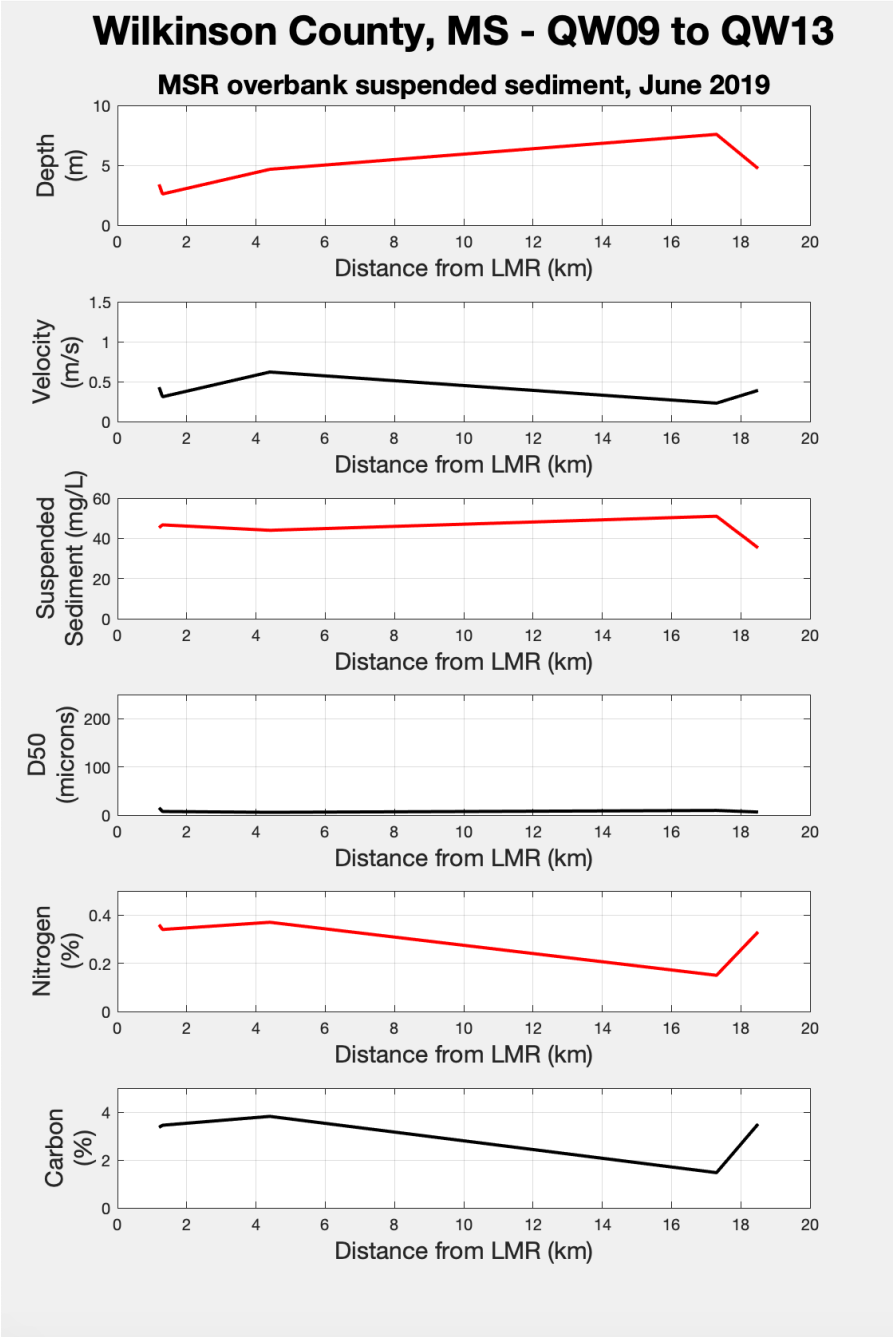

Figure 5.43 *Laboratory analysis results for overbank water and suspended sediment collection at Wilkinson County, MS, on June 22nd, 2019.*

Note: Graphs are plotted by overbank flow distance from the LMR channel. Samples QW10 (1.2 km), QW11 (1.3 km), QW12 (4.4 km), QW09 (17.3 km), and QW13 (18.5 km) are included. All percentages are by weight.

5.4 WATER QUALITY IN THE LMR CHANNEL DURING THE 2019 FLOOD

Water quality and suspended sediment samples were periodically collected in the main LMR channel at Vicksburg, MS, and at St. Francisville, LA, by the U.S. Army Corps of Engineers (Flood Stage Data) (USACE, 2020) and the U.S. Geological Survey (Water-Quality Data) (USGS, 2020) during the 2019 flood event.

5.4.1 VICKSBURG, MS

During the 2019 flood at Vicksburg, MS, all samples were collected at a water depth of 0.91 m (3 ft). Values selected to associate with overbank sampling in this study are for samples overlapping the flood duration at Natchez, MS (01/04/19 – 08/05/19 with crest on 03/12/19). Water temperature (°C) ranged from 6.3°C to 28.4°C during the flood duration. Water temperature values closest to the author's sampling dates were 7.4°C on 3/12/2019, 11.7°C on 3/29/19, 24.4°C on 06/11/19, and 25.9°C on 06/27/19. Instantaneous discharge (m^3/s) ranged from 32,200 m^3/s to 54,900 m^3/s (1,140,000 ft^3/s to 1,940,000 ft^3/s) during the flood duration. Instantaneous discharge values closest to the author's sampling dates were 54,900 m^3/s on 3/12/2019, 49,800 m^3/s on 3/29/19, 39,600 m^3/s on 06/11/19, and 42,500 m^3/s on 06/27/19. pH ranged from 7.5 to 8.0 during the flood duration. pH values closest to the author's sampling dates were 7.6 on 3/12/2019, 7.7 on 3/29/19, 7.5 on 06/11/19, and 8.0 on 06/27/19. Nitrite-nitrate (mg/L) ranged from 0.997 mg/L to 1.64 mg/L during the flood duration. Nitrite-nitrate (mg/L) values closest to the author's sampling dates were 0.997 mg/L on 3/12/2019, 1.25 mg/L on 3/29/19, 1.56 mg/L on 06/11/19, and 1.63 mg/L on 06/27/19. Phosphorus (mg/L) (filtered) ranged from 0.06 mg/L to 0.09 mg/L during the flood duration. Phosphorus (mg/L) (filtered) values closest to the author's sampling dates were 0.06 mg/L on 3/12/2019, 0.07 mg/L on

3/29/19, 0.08 mg/L on 06/11/19, and 0.09 mg/L on 06/27/19. Total carbon (mg/L) ranged from 1.40 mg/L to 3.14 mg/L during the flood duration. Total carbon (mg/L) values closest to the author's sampling dates were 1.47 mg/L on 3/12/2019, 3.14 mg/L on 3/29/19, 2.31 mg/L on 06/11/19, and 1.77 mg/L on 06/27/19. Suspended sediment (mg/L) values ranged from 76 mg/L to 164 mg/L. Suspended sediment (mg/L) values closest to the author's sampling dates were 146 mg/L on 3/12/2019, 164 mg/L on 3/29/19, 162 mg/L on 06/11/19, and 76 mg/L on 06/27/19.

5.4.2 ST. FRANCISVILLE, LA

During the 2019 flood at St. Francisville, LA, all samples were collected at a water depth of 0.91 m (3 ft). Values selected to associate with overbank sampling in this study are for samples overlapping the flood duration at Natchez, MS water gauge (01/04/19 to 08/05/19 with crest on 03/12/19). Water temperature (°C) ranged from 7.1°C to 28.6°C during the flood duration. Water temperature values closest to the author's sampling dates were 8.3 °C on 3/11/2019, 25.1 °C on 06/17/19, and 26.2 °C on 06/24/19. Instantaneous discharge (m^3/s) ranges from 26800 m^3/s to 38800 m^3/s (946,000 ft^3/s to 1,370,000 ft^3/s) during the flood duration. Instantaneous discharge values closest to the author's sampling dates were 38,500 m^3/s on 3/11/2019 and no data was recorded for 06/17/19 and 06/24/19. pH ranged from 7.0 to 8.0 during the flood duration. pH values closest to the author's sampling dates were 7.2 on 3/11/2019, 7.1 on 06/17/19, and 7.7 on 06/24/19. Nitrite-nitrate (mg/L) ranged from 1.05 mg/L to 1.65 mg/L during the flood duration. Nitrite-nitrate (mg/L) values closest to the author's sampling dates were 1.05 mg/L on 3/11/2019, 1.51 mg/L on 06/17/19, and 1.65 mg/L on 06/24/19. Phosphorus (mg/L) (filtered) ranged from 0.057 mg/L to 0.168 mg/L during

the flood duration. Phosphorus (mg/L) (filtered) values closest to the author's sampling dates were 0.057 mg/L on 3/11/2019, 0.168 mg/L on 06/17/19, and 0.096 mg/L on 06/24/19. Total carbon (mg/L) ranged from 1.06 mg/L to 2.07 mg/L during the flood duration. Total carbon (mg/L) values closest to the author's sampling dates were 1.48 mg/L on 3/11/2019, 2.07 mg/L on 06/17/19, and 1.36 mg/L on 06/24/19. Suspended sediment (mg/L) values ranged from 44mg/L to 130mg/L during the flood duration. Suspended sediment (mg/L) values closest to the author's sampling dates were 92 mg/L on 3/11/2019, 78 mg/L on 06/17/19, and 65 mg/L on 06/24/19.

5.5 SEDIMENT DEPOSITON FROM THE 2019 FLOOD

At the Sibley Unit (SCCNWR), sediment thicknesses deposited by the 2019 flood were measured at selected locations by Kent Ozment (USFWS). Depositional thicknesses ranged from 15 – 114 mm (0.59 – 4.49 in), with an average of 55.5 mm (2.19 in).

Table 5.1 *Flood deposit thicknesses in the Sibley Unit (SCCNWR) floodplain, measured by Kent Ozment in September 16th, 2019.*

GPS Location	mm	GPS Location	mm
Thickness 1	29.0	Thickness 10	54.0
Thickness 2	15.0	Thickness 11	33.0
Thickness 3	27.0	Thickness 12	38.0
Thickness 4	34.0	Thickness 13	52.5
Thickness 5	67.0	Thickness 14	99.0
Thickness 6	50.0	Thickness 15	122.5
Thickness 7	99.0	Thickness 16	36.5
Thickness 8	27.5	Thickness 17	114.0

Thickness 9	37.0	Thickness 18	63.5

Table 5.2 *Eighteen thicknesses of sediment measured in the Sibley Unit after the flood of 2019.*

Figure 5.44 *Eighteen sediment thicknesses collected at the Sibley Unit on September 16th, 2019.*

CHAPTER VI – DISCUSSION

Interpretation of the results in context with data collected by the USGS and USACE answers the following research questions: (1) Are overbank sediment deposit characteristics (i.e., grain size, composition) similar before and after the 2018 flood in different floodplain sub-environments (i.e., natural levees, meander scrolls, backswamps)? (2) Does floodplain topography result in spatially unequal flood durations and stages and do these patterns differ between the LMR channel and the embanked floodplain? (3) Are suspended sediment concentrations, grain sizes, and selected water-quality parameter values (including carbon, nitrogen, and phosphorus) across embanked floodplains different during the 2019 flood event (March and June)? Are the overbank data comparable to those in the main river channel and do they vary across embanked floodplains during large overbank floods?

For each research question, comparisons are drawn between different sampling timeframes, sample locations, and origins of data. An overall discussion of the specific sample locations and collection periods considers sedimentation and biogeochemical cycling in the LMRV.

6.1 OVERBANK DEPOSIT CHARACTERISTICS BEFORE AND AFTER THE 2018 FLOOD

This section considers overbank sediment deposits collected in October 2017 and September 2018, which are used to compare 2018 flood deposits to those previously deposited in different depositional sub-environments. The Cloverdale Unit, Salt Lake, and Butler Lake, and Artonish Lake are all classified as either a levee crest transitioning into a meander scroll location or meander scroll only. Salt Lake is characterized by an

abandoned natural levee (along the Salt Lake chute channel) of the LMR. The Sibley Unit and Lake Mary locations are classified as natural levee deposits that abruptly transition into backswamp or infilled channel deposits, respectively. The Homochitto River on the southern border of the Sibley Unit has negligible influence on sedimentation along the transects in this study. Carthage Point Road is the only location that is individually sampled from a levee crest. Three groupings of study areas are discussed individually; after which, data from all sediment samples (October 2017 and September 2018) are considered to understand differences between pre- and post-2018 flood deposits and their characteristics in sub-environments.

6.1.1 CLOVERDALE UNIT

Grain size distributions of overbank sediment deposits in a meander scroll environment are exemplified along two transects, T4 and T5. Samples collected along T4 in October 2017 display a pronounced difference in grain size between ridges and swales. Relatively coarse D50 values ranging between 92.3 and 116 microns represent ridges, whereas D50 values ranging between 25.1 and 47.8 microns represent swales. However, samples collected at the same locations in September 2018 reveal only slight differences across the meander scroll, with all sediment samples having D50 values between 45.5 and 67.5 microns (Figure 6.1). During average seasonal flood events, alternating patterns of ridge and swale deposition occur within the meander scroll environment; however during a large flood event the sediment deposits are more evenly distributed and homogenous.

T5 is the shorter transect west of T4. D50 values of sediment samples collected in October 2017 had a large separation as well, ranging between 101 and 122 microns for

ridges and between 24.1 and 54.4 microns for swales (Figure 6.1). For samples collected in September 2018, there is no clear differentiation among D50 values (37.7 to 74.4 microns), similar to T4.

Prior to the 2018 flood (October 2017 samples), sediments in the meander scroll environment were deposited by overbank processes that sorted them by grain size along ridges and swales, indicating that ridges are deposited when overbank flow velocities are sufficient to maintain suspension of the relatively fine sediments that eventually settle in swales as flood stage recedes and velocities abruptly decrease. However, the lack of contrast in grain size between ridges and swales for sediments deposited by the large 2018 flood indicates that sorting processes are minimal. Further, the size range occurs in between those for ridges and swales, indicating that most sedimentation uniformly occurs during major flood events, and is not differentiated between periods of overbank flow and post-flood settling in stagnant water bodies.

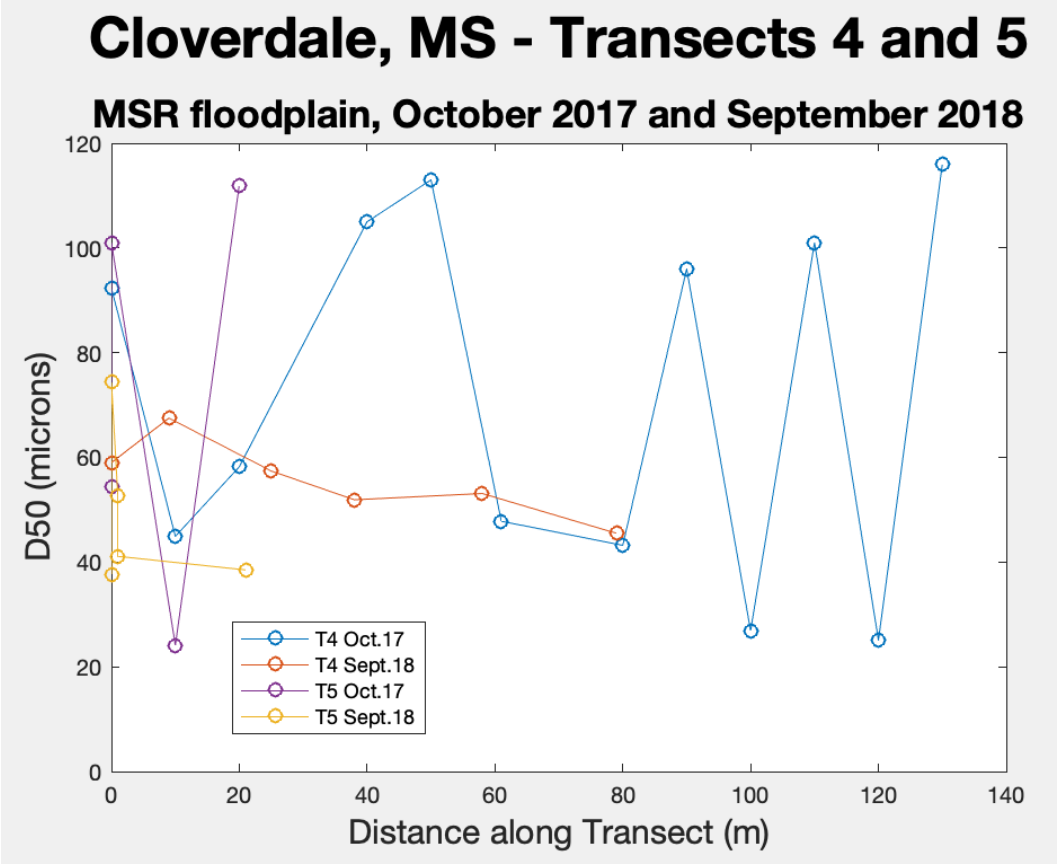

Figure 6.1 *Grain sizes for T4 and T5 plotted for both the October 2017 and September 2018 sediment samples.*

Organic matter trends are shown in Figure 6.2 for T4. In the area where ridges and swales are more prominent with distance from the Long Lake shoreline, OM has a negative trend with grain size. Closer to Long Lake, however, ponding occurs at Long Lake for a longer duration, resulting in less differentiation and higher overall values because of additions by aquatic microorganisms and reduced decomposition rates in these saturated areas.

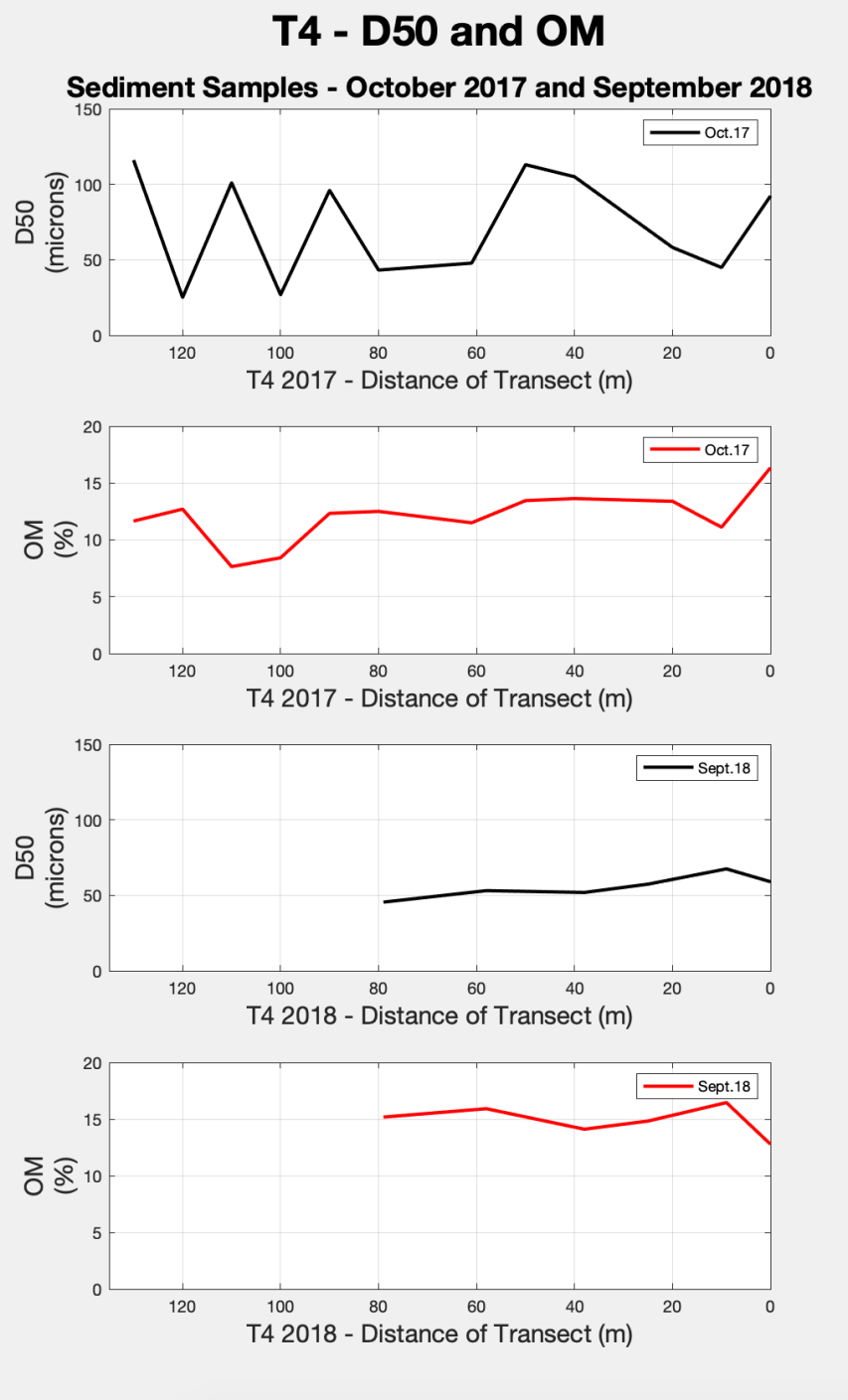

Figure 6.2 *Figure of T4 during both sampling periods, September 2017 and October 2018.*

Note: Transect starts at Long Lake and extends west, therefore, the x-axis is inverted to represent orientation from the LMR.

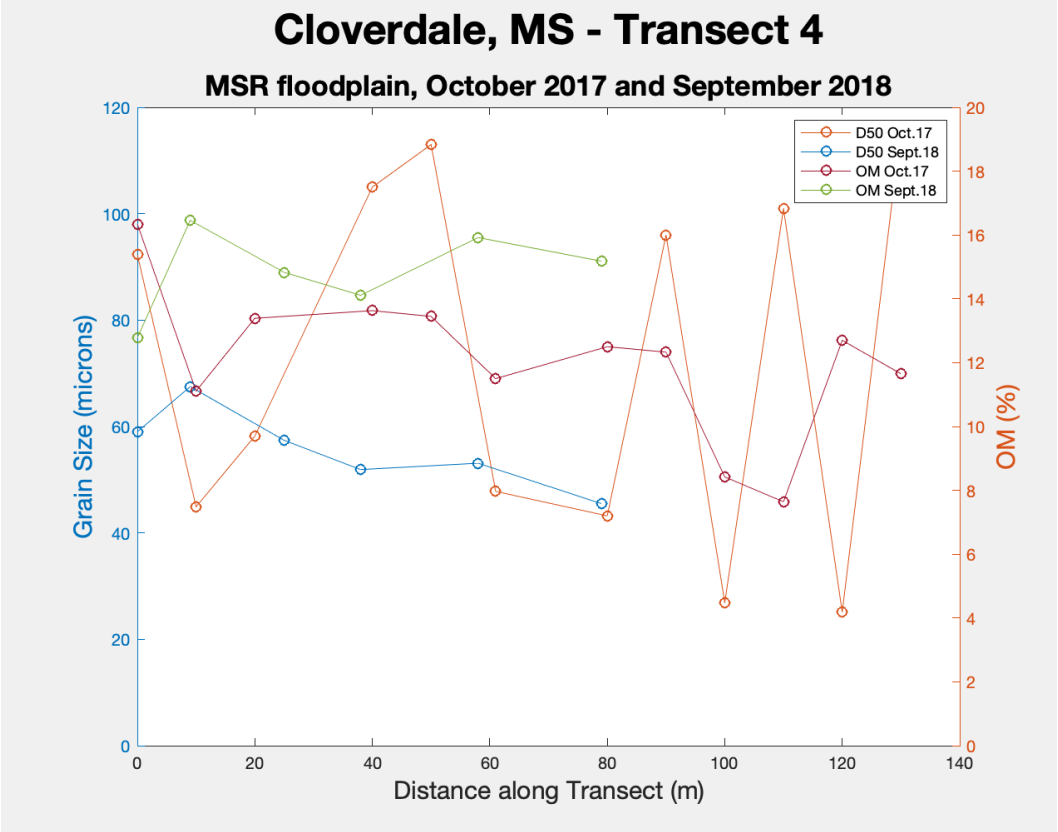

Figure 6.3 *Grain size and organic matter is presented for both October 2017 and September 2018 sediment data.*

Note: D50 is plotted on the left y-axis in microns. OM is plotted on the right side in percent by weight.

Sediment size and carbon and nutrient analysis are compared in order to see correlations with change in sediment size. Figure 6.4 is separated into two sections based on sediment sizes. D50, between 0 and ~34 microns, is the ponded area near Long Lake. The D50 range from ~35.0 to 62.5 microns are swale locations, and >62.5 microns are the ridge locations. This is segregated based off of the soil classification of sand at 62.5 microns. The 2018 data only falls within the 35 to 62.5 microns for D50. This indicates that the 2018 flood sediment blanketed over the area with an overall smaller sediment size than that of the 2017 flood (all deposited by fluvial action).

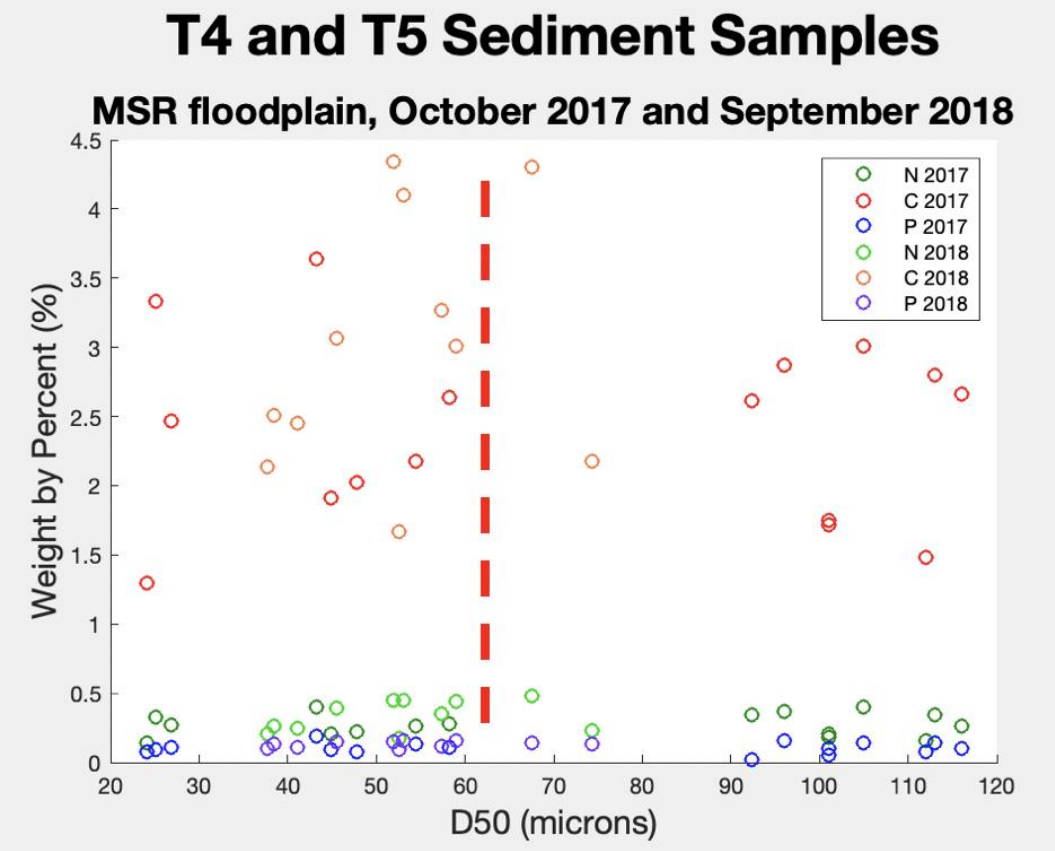

Figure 6.4 *T4 and T5 sediment data for the October 2017 and September 2018 carbon and nutrient data.*

Note: N = nitrogen, C = carbon, and P = phosphorus. The red dashed line indicates the D50 line between sand and silt (sand >62.5 microns).

Other characteristics that were assessed include Munsell color and magnetic susceptibility. For both T4 and T5, color and magnetic susceptibility remained the same for both ridges and swales.

6.1.2 SIBLEY UNIT

Transects T9 to T12 are located within SCCNWR and are lumped together for the discussion section because each transect includes only two to five samples and all transects are oriented perpendicular to the LMR. Samples collected along T9 to T12 in October 2017 display a pronounced difference transitioning from a natural levee into a

backswamp. A relatively coarse D50 value of 186 microns occurs on the levee at the beginning of T11, whereas D50 values ranging between 24.5 and 49.1 microns represent samples collected in the backswamp, with a maximum of 62.5 microns (using 62.5 microns for sand). The 2017 data all falls below the silt/sand boundary (62.5 microns) with a maximum 49.1 microns (except for sample 11.01), whereas the 2018 data had a larger spread of D50 including samples above and below 62.5 microns with D50 particle sizes closer to sand.

Samples collected (56B and 57B) at the same location at T11 and along T12 were collected in September 2018 to compare with samples collected in October 2017. The two samples (56B and 57B) collected in 2018 at T11 have a D50 of 33.2 and 34.5 microns, respectively. These samples fall within the same range of D50 as the backswamp samples collected in 2017. One possible explanation for the similarity is that this area of floodplain has dense vegetation coverage and clayey sediments, which are common for backswamp locations. Between average seasonal flood events, exposure and alternating periods of wetting and drying facilitate the development and subsequent closure of mudcracks that tend to homogenize the sediment composition. Generally, the 2018 data were more evenly distributed (for D50) than 2017, again indicating that the large flood event resulted in more homogenous and evenly distributed sediment deposits.

Trends in OM, carbon, and nutrients are observed with increasing grain size (Figure 6.5). Naturally, coarse sediments occur closer to the main channel (T13 excluded). Clays have a greater capacity to complex with OM and adsorb carbon and nutrients. OM, carbon, and nutrient percentages by weight all decrease with an increase

in grain size. This is expected because coarse sands have less adsorption capacity then finer sediments (i.e., silts and clays).

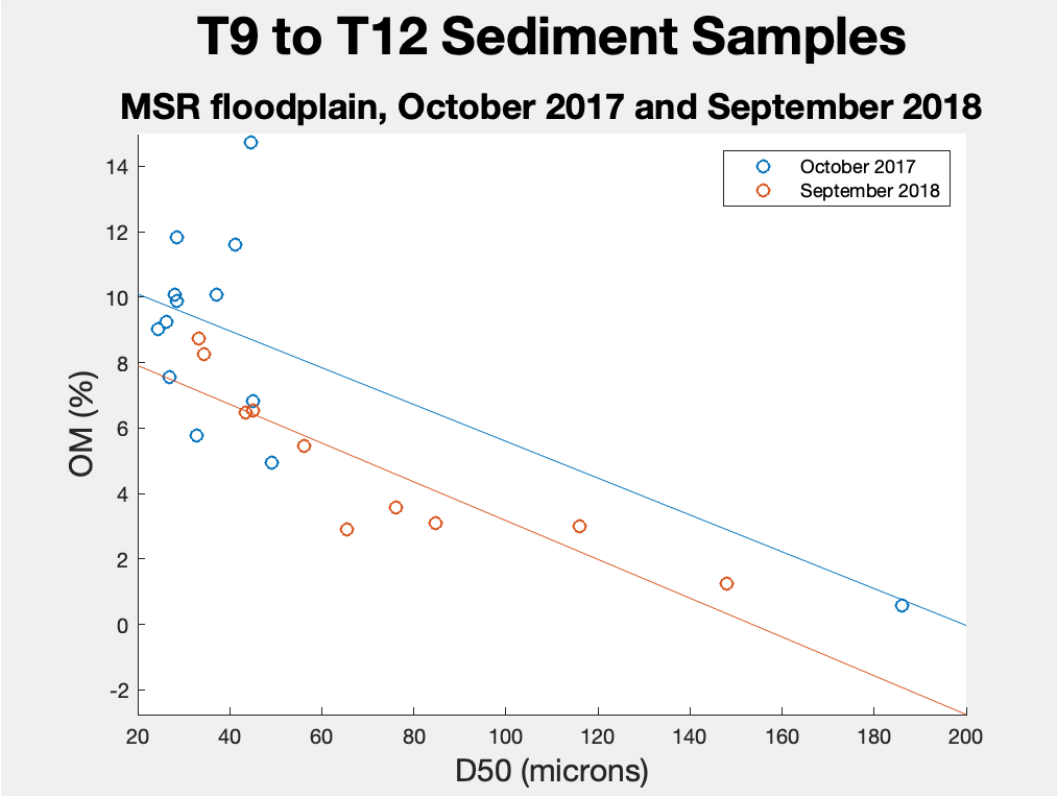

Figure 6.5 *Scatter plots of percent organic matter by weight for sediment samples along T9 to T12.*

Note: blue is October 2017 data and orange is September 2018.

A comparison between 2017 and 2018 samples indicates that the 2017 as a whole had higher OM percentages. This is particularly apparent for grain sizes 50 microns and smaller (Figure 6.5). The OM% for 2017 are higher because they included a longer duration of OM contributions after they were originally deposited, especially for the finer fraction where decomposition is slower.

Carbon and nutrient samples follow similar trends when plotted against sediment size. Nitrogen, carbon, and phosphorus decrease as sediment becomes coarser (Figures 6.6 to 6.9). Comparing the 2017 and 2018 data, the 2017 data was found to have higher

percentages of carbon and nutrients and more similar in weight by percent. The 2018 data on the other hand had a larger range of D50, resulting in a more distributed pattern of carbon and nutrients.

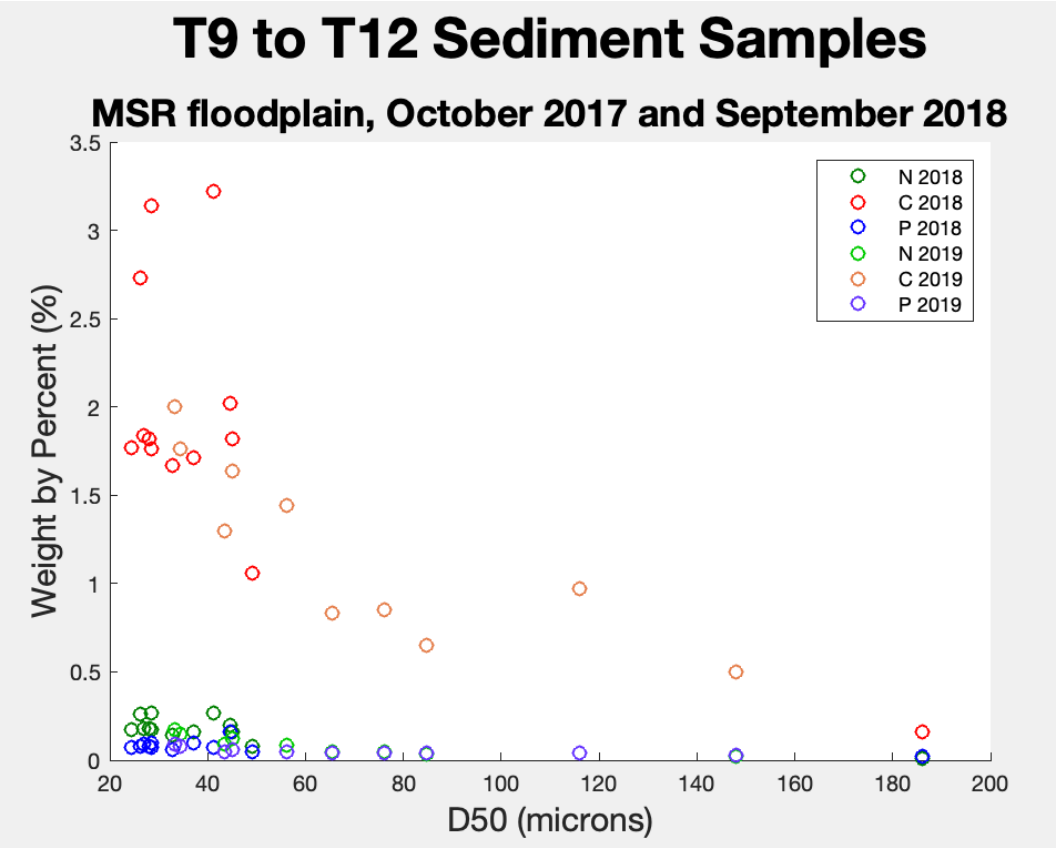

Figure 6.6 *Scatter plot of T9 to T12 sediment data for both the 2018 and 2019 sediment data for all carbon and nutrients weight by percent.*

Note: N is nitrogen (dark green and light green), C is carbon (red and orange), P is phosphorus (blue and purple).

A

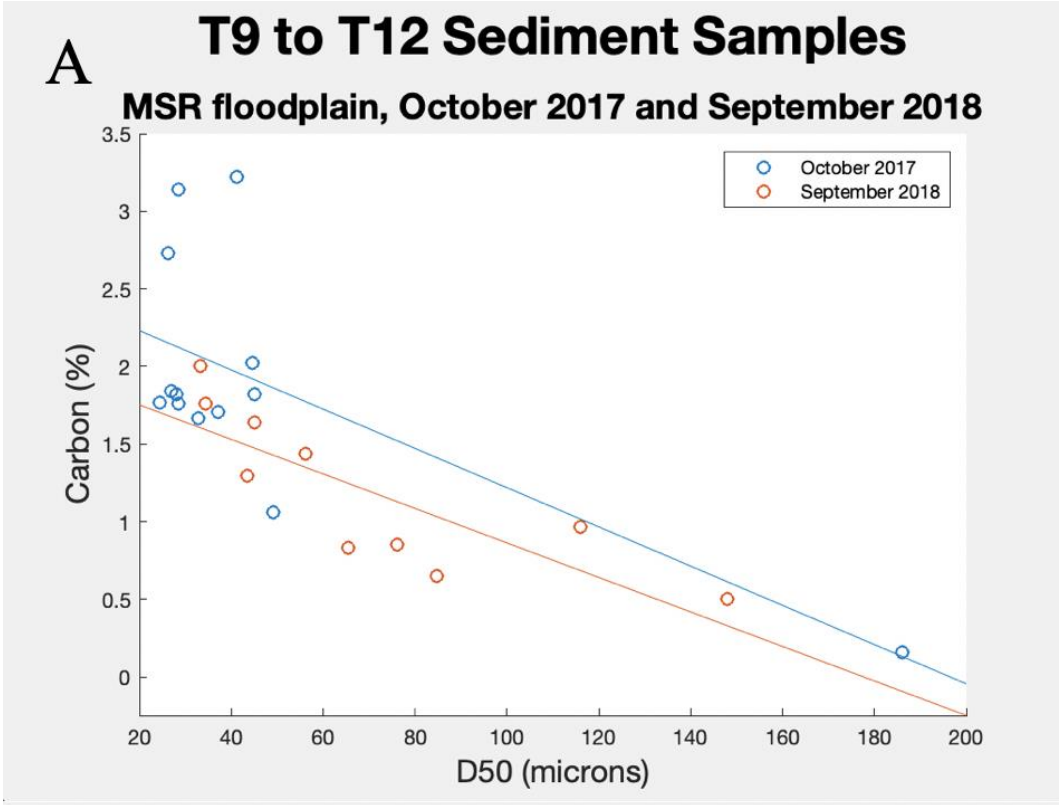
T9 to T12 Sediment Samples
MSR floodplain, October 2017 and September 2018
October 2017
September 2018
Carbon (%)
D50 (microns)
3.5
3
2.5
2
1.5
1
0.5
0
20
40
60
80
100
120
140
160
180
200

B

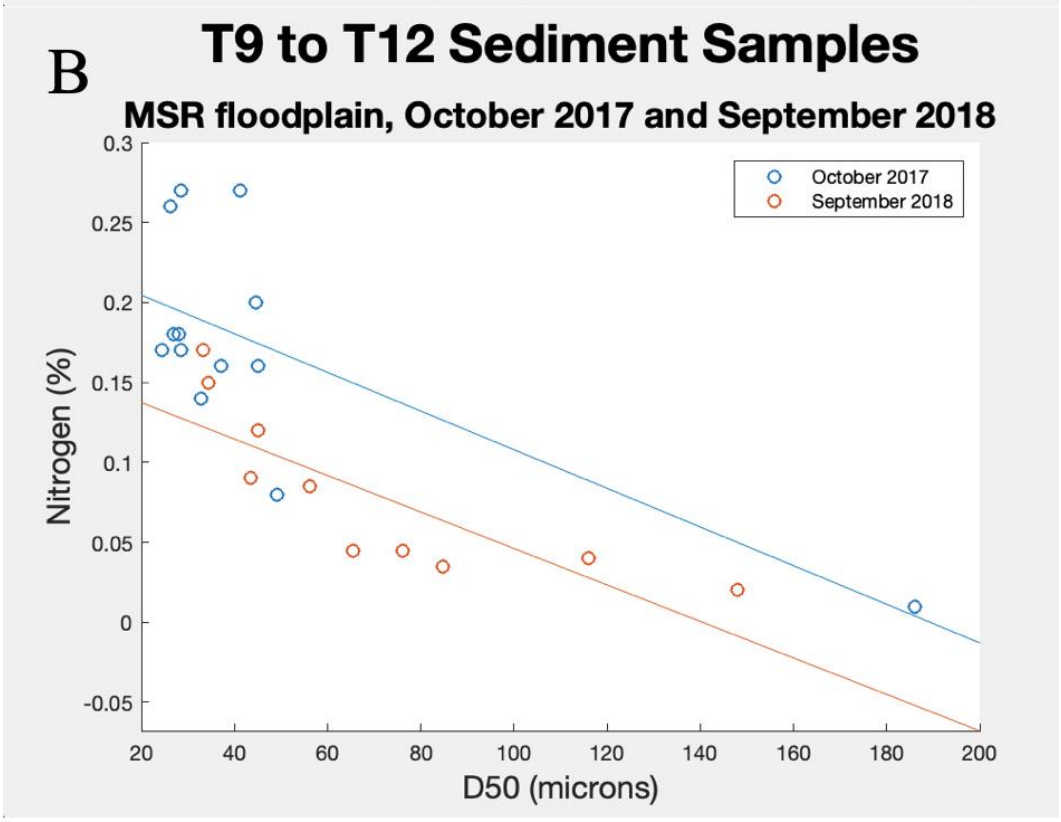
T9 to T12 Sediment Samples
MSR floodplain, October 2017 and September 2018
October 2017
September 2018
Nitrogen (%)
D50 (microns)
0.3
0.25
0.2
0.15
0.1
0.05
0
-0.05
20
40
60
80
100
120
140
160
180
200

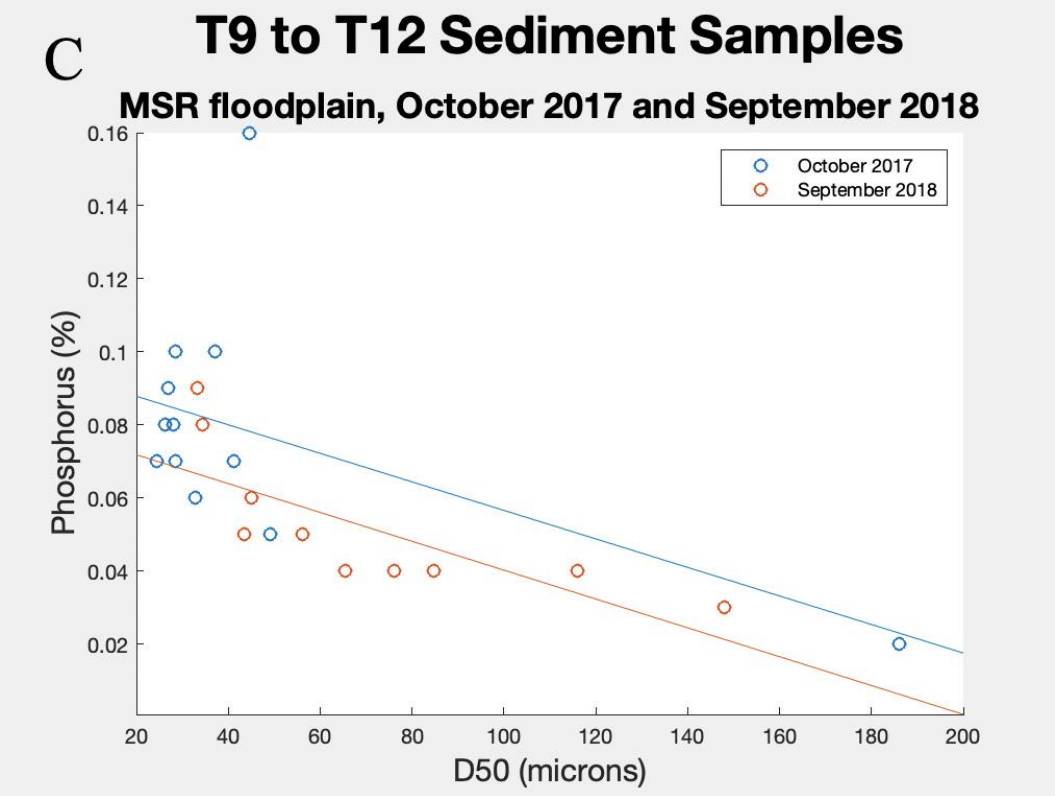

Figure 6.7 *Scatter plots of percent carbon, nitrogen, and phosphorus by weight for sediment samples along T9 to T12.*

Note: blue is October 2017 data and orange is September 2018. Plot A is carbon, plot B is nitrogen, and plot C is phosphorus.

T13 was sampled in September 2018 and includes a natural levee with mainly sandy samples in the first ~50m that transitions into a backswamp. This transect is different from others because grain size peaks (D50 of 148 microns) at 44 meters (Figure 6.8). OM, carbon, and nutrients are have greater values for both the beginning and end of the transect, rather than a transition into the floodplain (Figure 6.8). The transition to the backswamp is represented by the most distal sample along the transect, which has the highest amount of OM (6.35%), carbon (1.64%), and nutrients (0.12% for N and 0.06% for P) of the T13 samples (Figure 5.18). One reasoning behind the varying trend of grain size and other parameters may be due to a large amount of swirling currents in this area. This movement of flood water is likely to result in more heterogeneous depositional

patterns, unlike the more uniform depositional patterns more distal from the channel (sediments collected in 2017). These seemingly inexplicable variations in sand size aren't uncommon along channel margins because of the hydraulic variations during a flood. Coarse channel bed sands can be transported into the floodplain and then, during the receding limb, slumping of the immediate bank can occur that exposes previously buried (slightly finer) sediments. Overall, all values of OM, carbon and phosphorus are lower than other locations for this study. This may be due to the lack of adsorption by sand grains and the oxygen-rich setting.

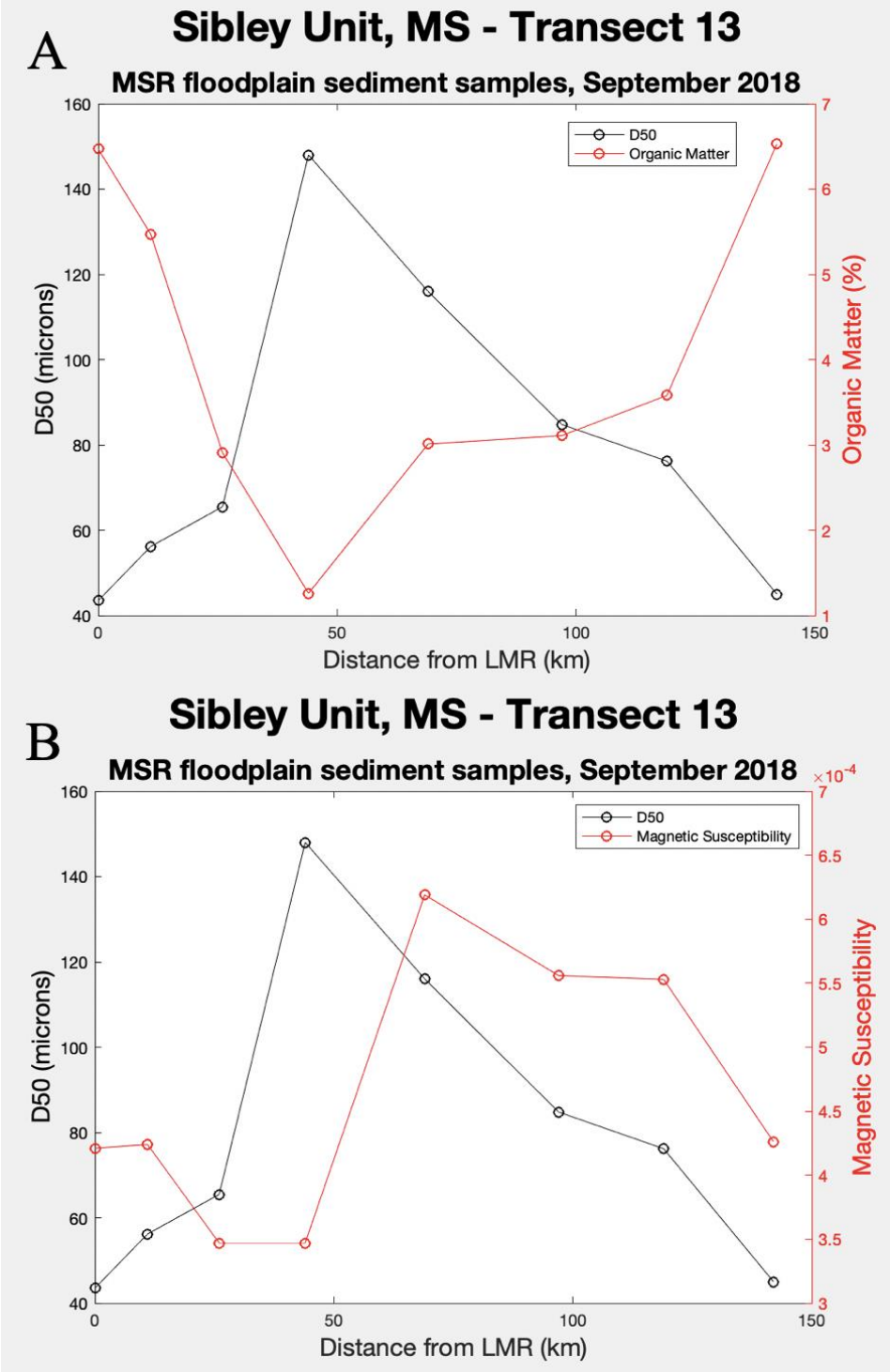

Figure 6.8 *Two plots of sediment samples of Transect 13 at the Cloverdale Unit. for weight by percent during both March and June 2019. Plot A is D50 plotted against organic matter and plot B is D50 plotted against magnetic susceptibility.*

Note: The left y-axis is black and the right y-axis is red.

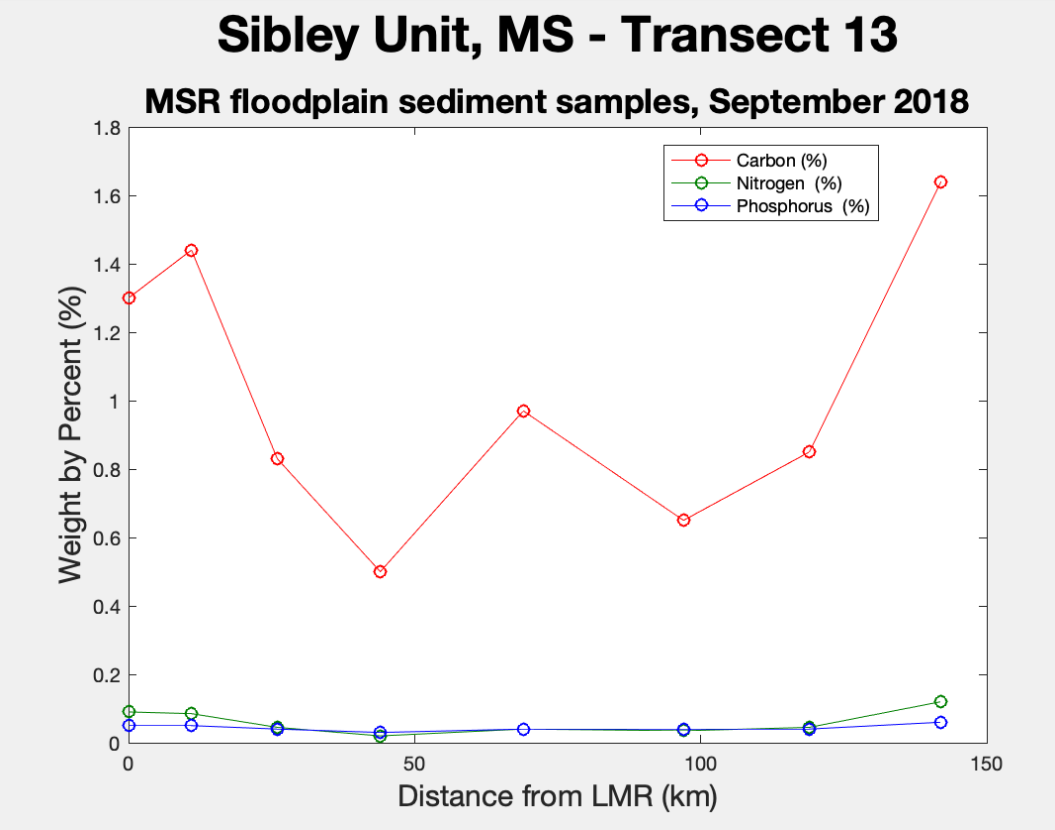

Figure 6.9 *A plot of sediment samples along Transect 13 at the Sibley Unit of percent by weight.*

Note: C is carbon (red), N is nitrogen (green), and P is phosphorus (blue)

6.1.3 SALT LAKE AND BUTLER LAKE UNIT

Transect 8 (T8) at Salt Lake, depicts a slight overall decrease in OM, nitrogen, carbon, and phosphorus with increasing distances from Salt Lake and the LMR (Figure 6.10). However, D50 and magnetic susceptibility both increase for the first 100 m from Salt Lake, and abruptly decrease into the floodplain for the rest of the transect (340 m) (Figure 6.10). These data trends show that the overall water flow is following the floodplain boundaries, instead of the LMR main channel meander, as well as an abrupt change in elevation. This abrupt decline in elevation (at least a couple of meters) where the values change, is at the terminus of the previous natural levee and the beginning of

the meander scroll environment approaching Salt Lake. For all of the data for T8 this overall decreasing trend shows that the Salt Lake reservoir may have more influence on the deposition of the sediment than previously expected, especially when ponding continues even after the flood event.

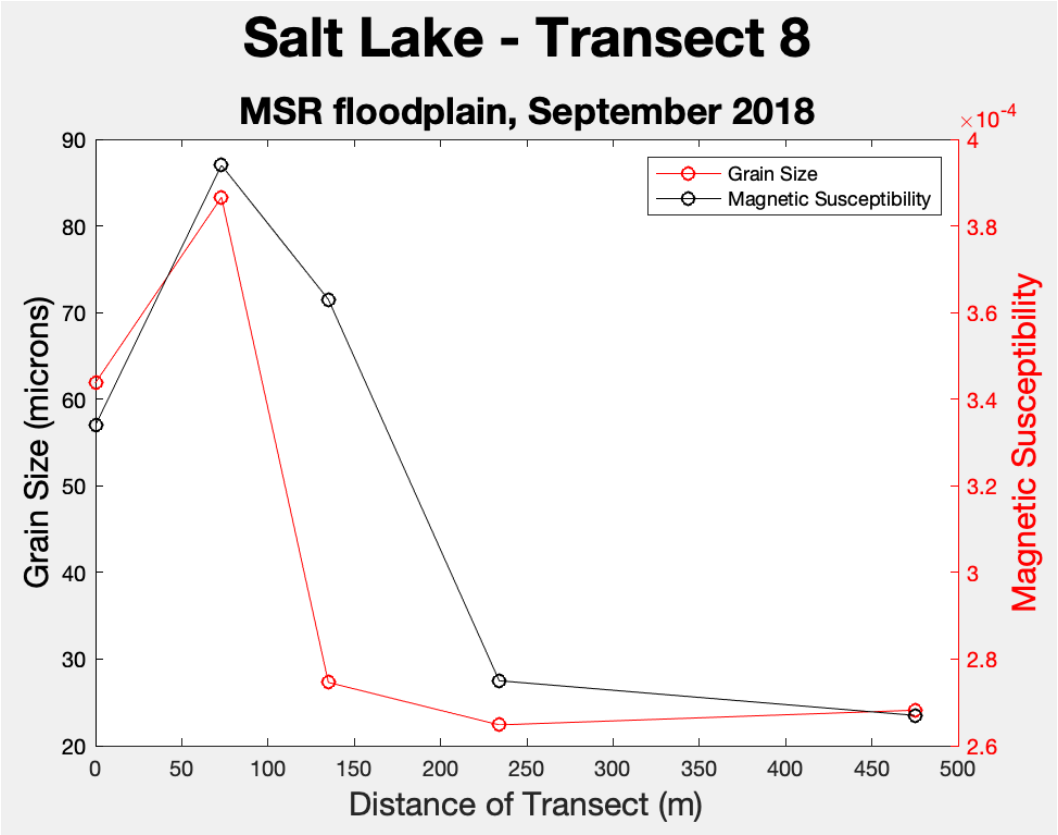

Figure 6.10 *A plot of D50 and magnetic susceptibility of Salt Lake (T8).*

Note: The left y-axis is D50 (microns) in black and the right y-axis is MS in red.

Butler Lake (T7) and Salt Lake (T8) were only collected in 2017 so there is not a comparison of data for before and after the 2018 flood. However, these two transects will be included for the overall data comparison below (by year and sub environment).

6.1.4 ARTONISH / FORT ADAMS

Along T1 near Artonish Lake, a difference in grain size is apparent between sediment sampled before and after the 2018 flood event. Pre-flood median grain size

gradually declines from 189 microns at the natural levee crest to 45.7 microns at the distal end of the transect Along the same transect after the 2018 flood, the median grain size remains relatively similar throughout, ranging from 36.5 to 69.4 microns, with an increase in sediment size at the distal end. However, no sample was collected on the natural levee in 2018 due to artificial sediment mixing (i.e., land smoothing) by the property owner. The first sample for T1 in 2018 was adjacent to sample 01.05.60 (in 2017). Samples were only collected beyond the natural levee crest, thus the levee backslope and meander scroll is depicted (Figure 6.11). In order to compare T1 before and after the 2018 flood, the sediment collected in 2018 was overlapped using the distance of transect of T1 in 2017. A color change from olive brown / brown at the levee crest to dark brown / dark grayish brown with distance into the floodplain is observed. The color change is associated with decreasing sediment size and increasing OM. Color, OM, and grain size all have similar properties within the floodplain, with a substantial change beyond the natural levee (Figure 6.11). When looking at nutrient and carbon concentrations within the sediment samples, a comparable trend is observed. Increases in both total carbon and total nitrogen with distance into the floodplain.

For OM, carbon, and nutrients in both pre- and post-flood samples, higher amounts of sediment are sequestered in the relatively fine-grained silty and clayey sediments similar to other transects (Cloverdale and Sibley Units) (Figure 6.12). Along T1 in 2017, an increase in OM with distance from the LMR channel mimics the decrease in grain size (Figure 6.11). However, sediment collected after the 2018 flood is characterized by an increase in both grain size and OM across the first 100 meters from the LMR channel (Figure 6.11).

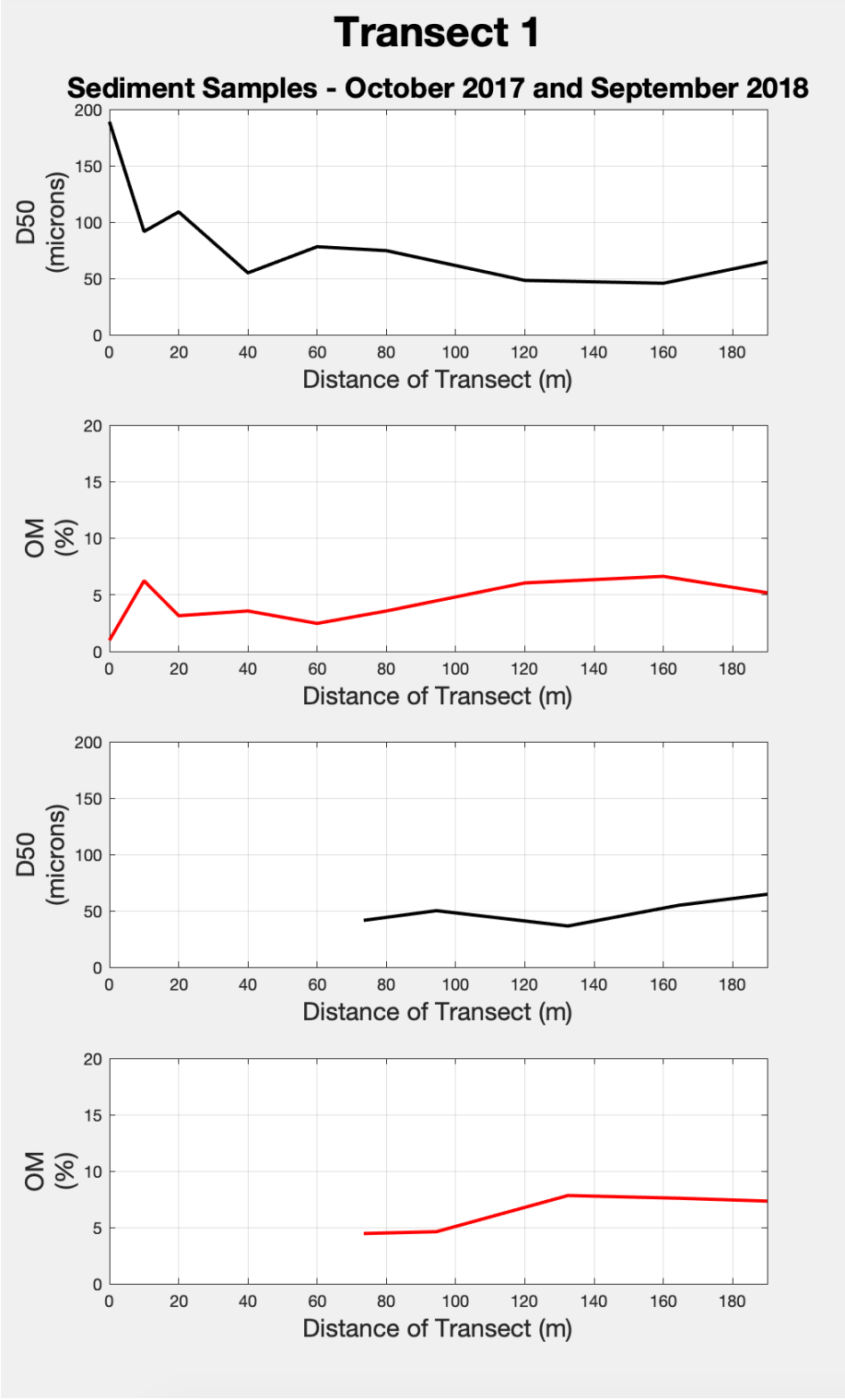

Figure 6.11 *Plot of D50 and organic matter by weight percent for T1.*

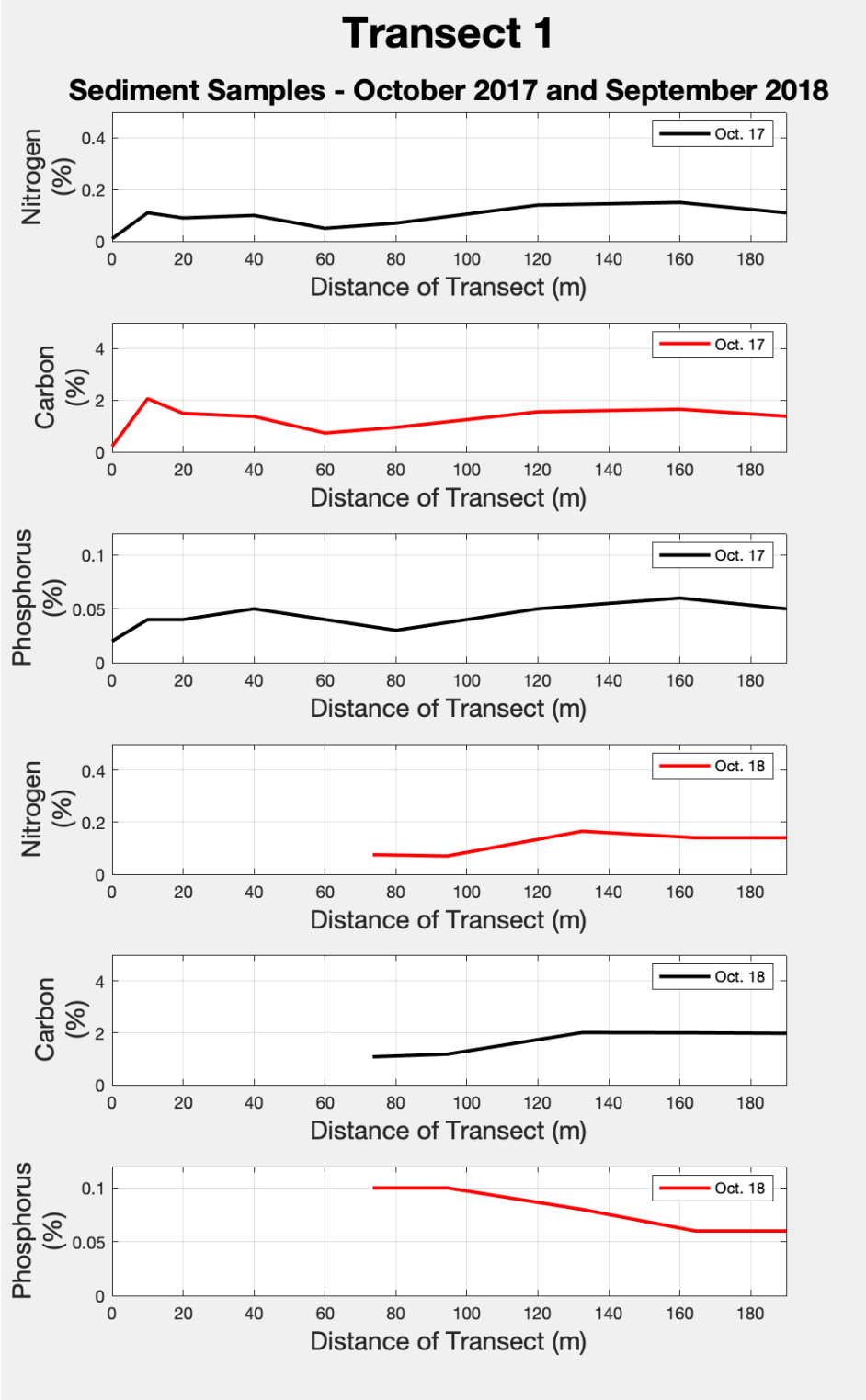

Figure 6.12 *Plot of nitrogen, carbon, and phosphorus by weight percent for T1.*

Transect 2 near Artonish is generally parallel to T1, and displays a somewhat irregular grain size trend with distance from the channel. The overall trend is that grain size decreases into the floodplain as OM, carbon, and nutrient concentrations increase (Figure 6.13). Along both T2 for 2017 and T1 for 2018, OM, carbon, and nitrogen increase (larger increase for T2) toward the end of the transects near Artonish Lake. This indicates that overbank ponding of water and associated sedimentation in the vicinity of Artonish Lake and the meander scrolls influence sedimentary properties. Essentially, the water remains ponded for a longer period and results in a greater amount of relatively fine grains that sequester more OM and adsorbed nutrients.

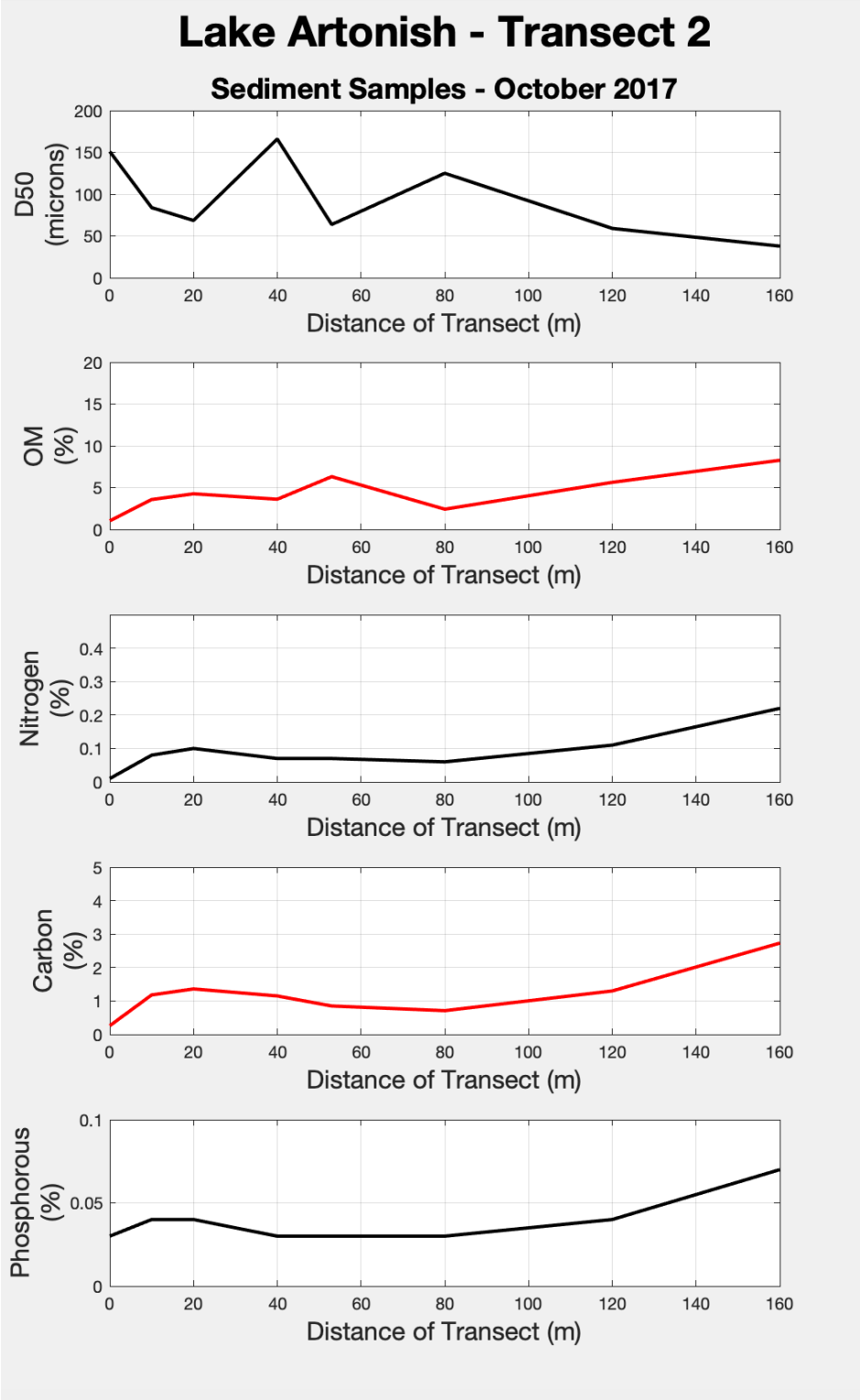

Figure 6.13 *Plot of D50, OM, nitrogen, carbon, and phosphorus by weight percent for T2.*

6.1.5 SEDIMENT IN DEPOSITIONAL SUB-ENVIRONMENTS

A lumped compilation of all floodplain deposit samples collected in both 2017 and 2018 depict typical trends with distance from the LMR channel into the floodplain (with minor exceptions). Natural levees have the largest grain sizes and lowest OM, carbon, and nutrient levels in the floodplain. Meander scroll ridges have relatively larger grain sizes with lower percentages of OM, carbon, and nutrients than swales. Backswamp locations have the smallest grain size and relatively lower concentrations of OM, carbon, and nutrients compared to meander scroll environments. The organic matter from the natural levee locations ranged from 0.89 to 1.03%, whereas the backswamps ranged from 2.42 to 10.3% OM (Figures 6.14 and 6.15). Organic matter for meander scroll ridges ranged from 1.26 to 16.34%, whereas swales ranged from 2.47 to 17.53% (Figures 6.14 and 6.15). Both color and OM are associated with grain size.

A visual comparison of the data (Figures 6.14, 6.16, 6.17, 6.19, and 6.21) does not clearly indicate if the pre- and post-2018 flood deposits have any similarities or differences. However, a clearer picture is revealed when categorizing the data by depositional sub-environment. Natural levees with larger grains have lower amounts of OM, carbon, and nutrients in comparison to backswamps. The two meander scroll environments, ridges and swales, are have a difference in sediment sample parameters (OM, carbon, and nutrients), however less distinguished in comparison to the transition between natural levee and backswamp samples (Figure 6.15).

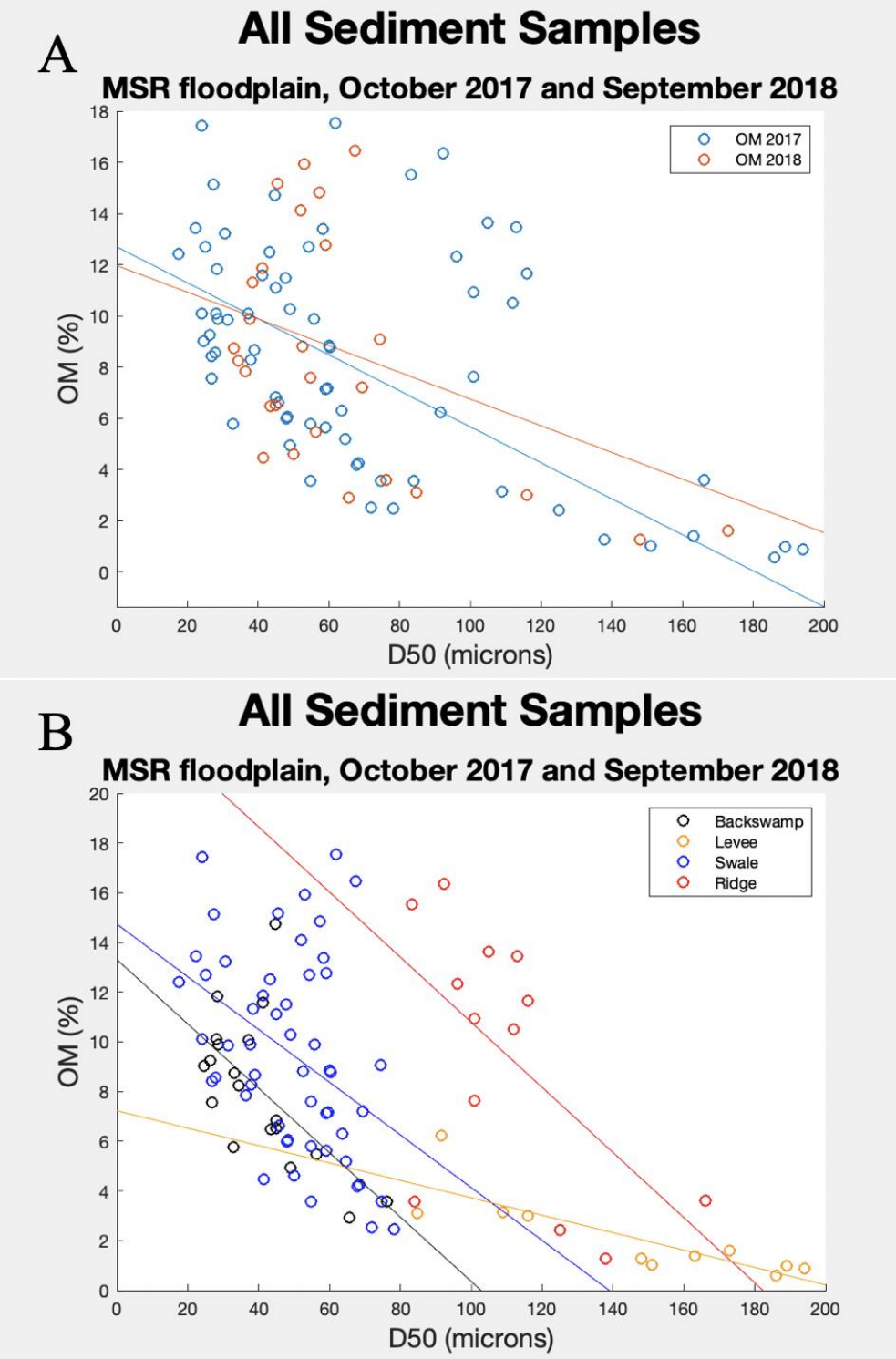

Figure 6.14 *Scatter plots of percent organic matter by weight for all sediment samples.*

Note: for plot A blue is October 2017 data and orange is September 2018. For plot B backswamp data is black, levee data is yellow, swale data is blue, and ridge data is red.

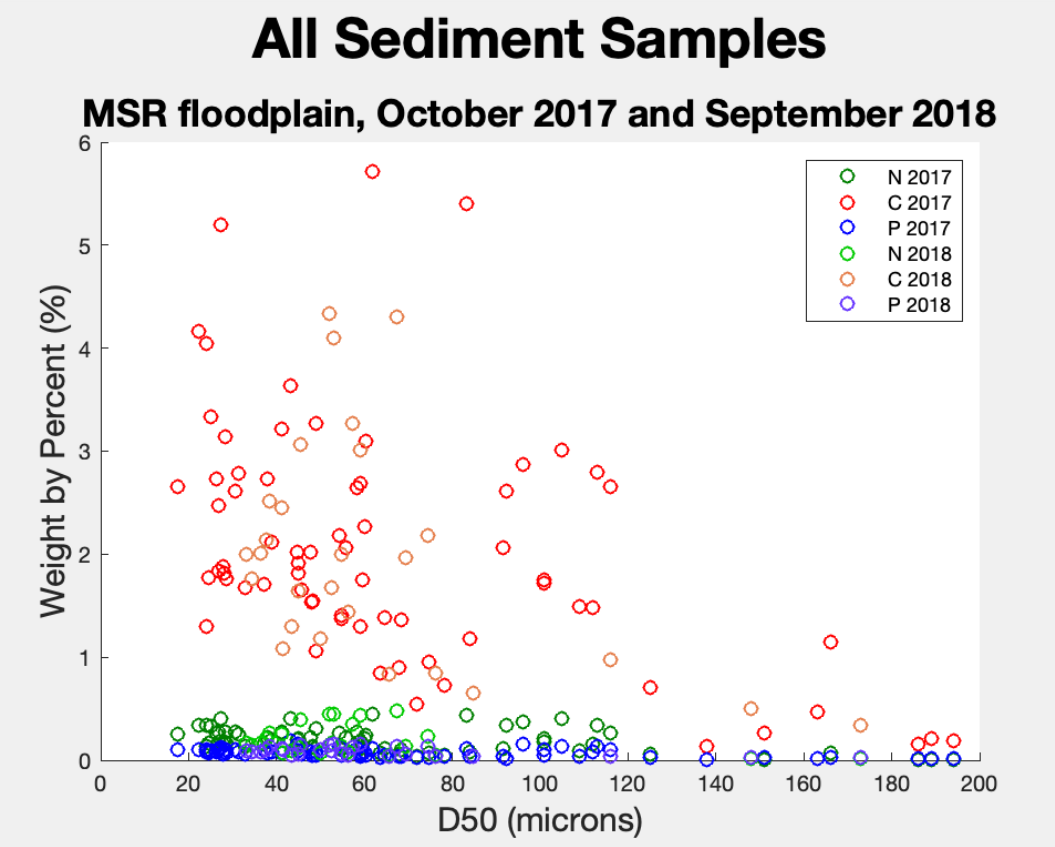

Figure 6.15 *Scatter plot of all sediment data collected in both 2017 and 2018 for weight by percent.*

Note: N is nitrogen (dark green and light green), C is carbon (red and orange), P is phosphorus (blue and purple).

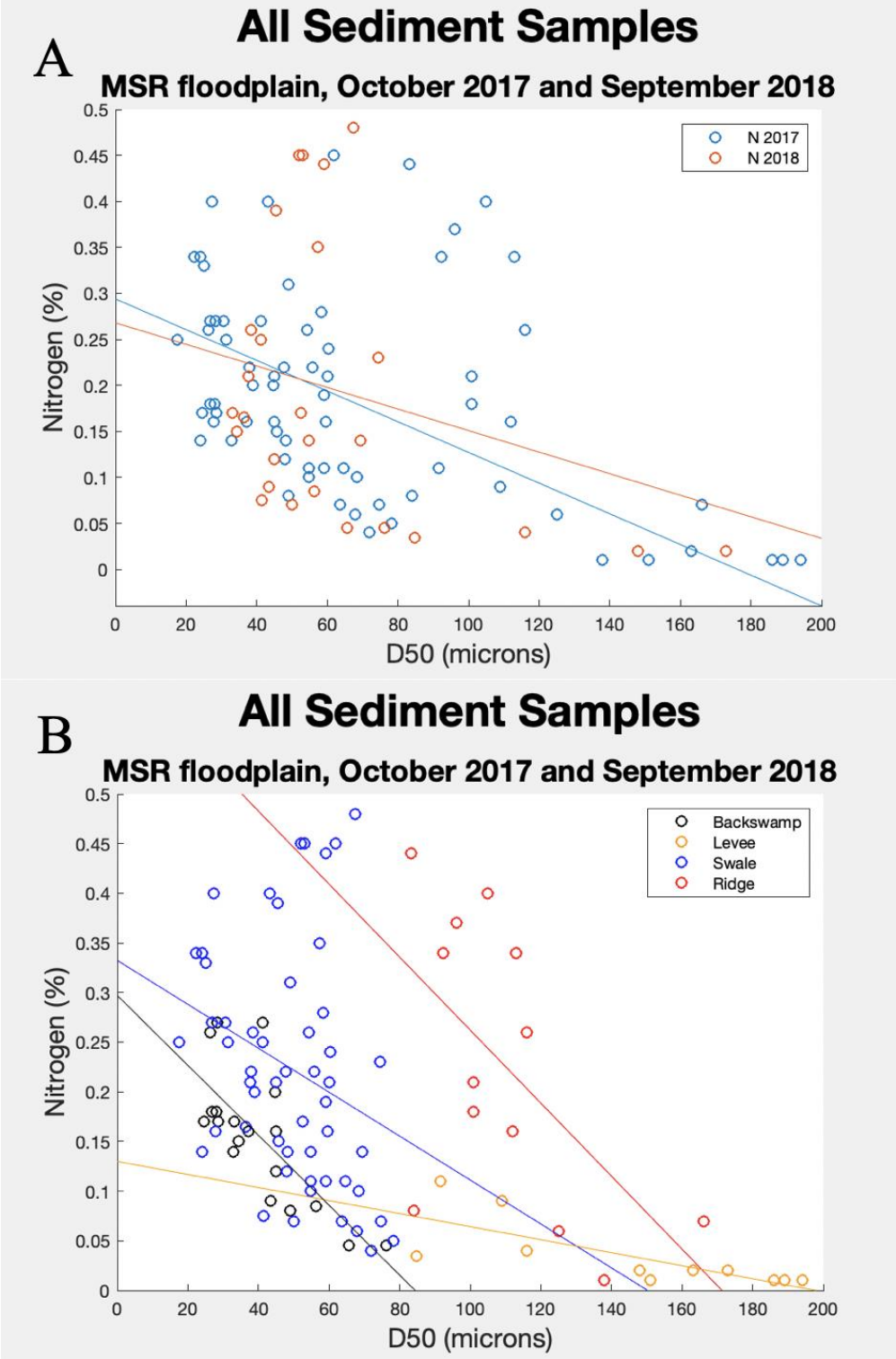

Figure 6.16 *Scatter plots of percent nitrogen by weight for all sediment samples.*

Note: for plot A blue is October 2017 data and orange is September 2018. For plot B backswamp data is black, levee data is yellow, swale data is blue, and ridge data is red.

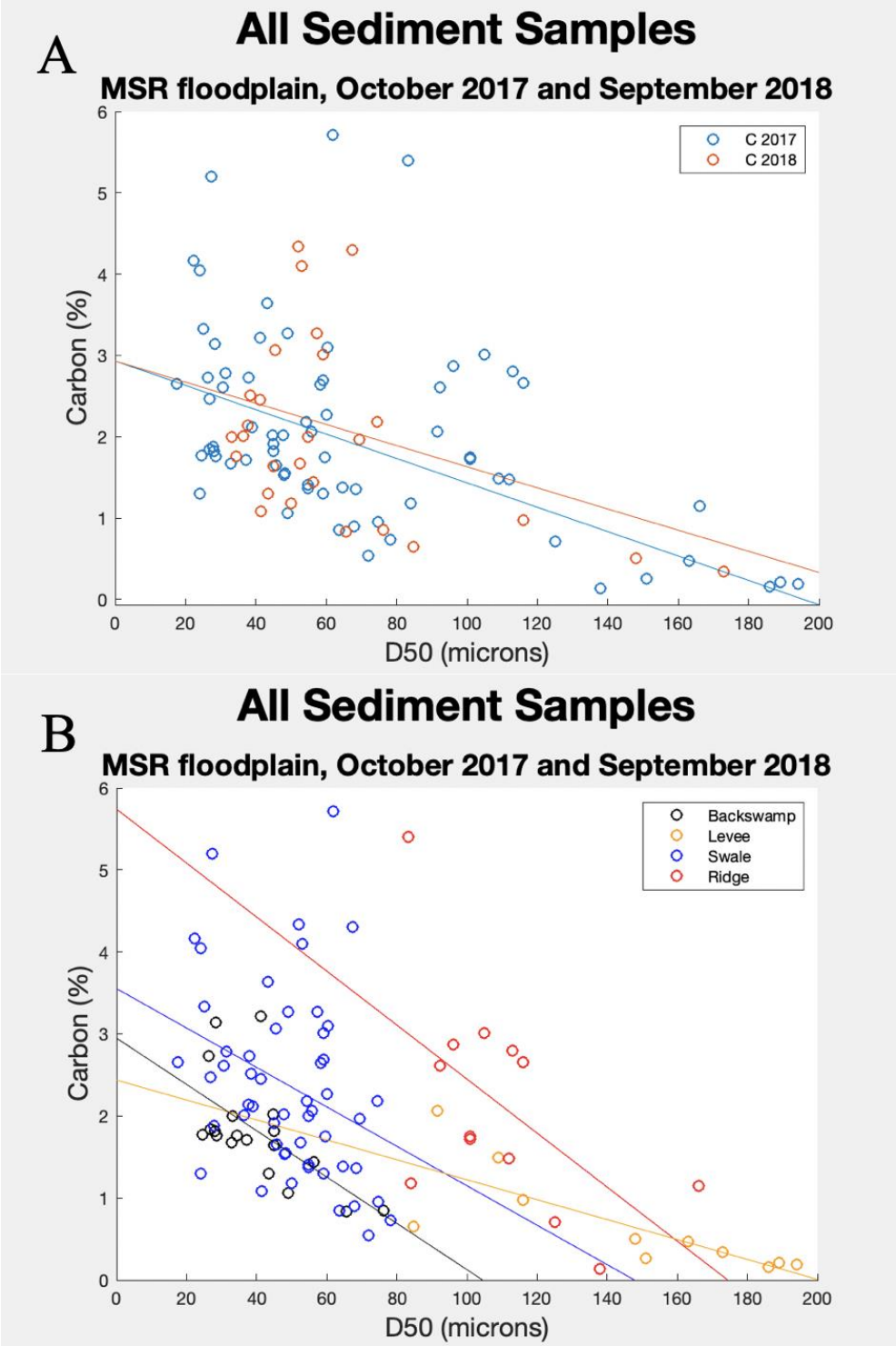

Figure 6.17 *Scatter plots of percent carbon by weight for all sediment samples.*

Note: for plot A blue is October 2017 data and orange is September 2018. For plot B backswamp data is black, levee data is yellow, swale data is blue, and ridge data is red.

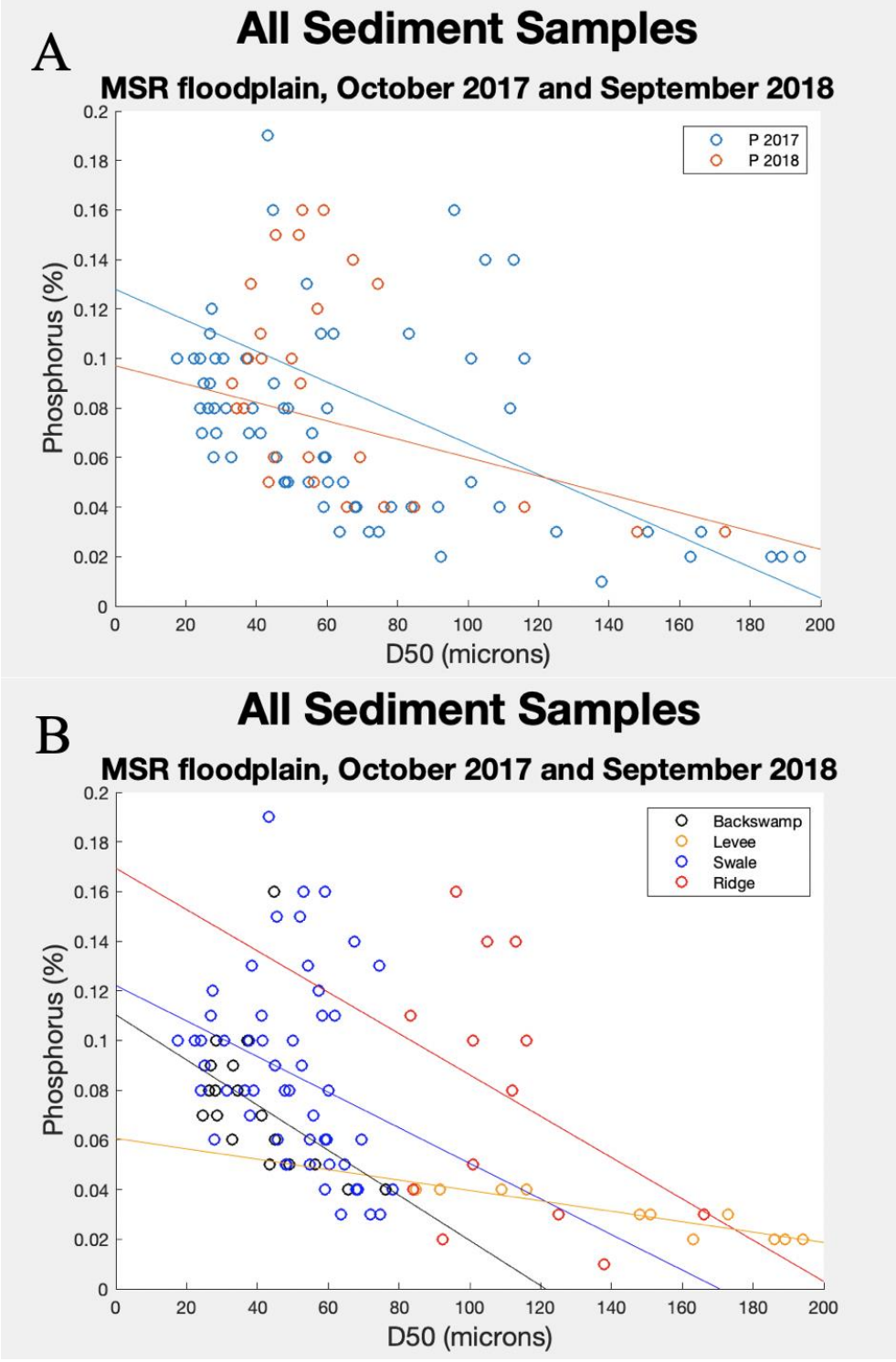

Figure 6.18 *Scatter plots of percent phosphorus by weight for all sediment samples.*

Note: for plot A blue is October 2017 data and orange is September 2018. For plot B backswamp data is black, levee data is yellow, swale data is blue, and ridge data is red.

In order to more accurately discern differences in sedimentary parameters between pre- and post-2018 flood deposits as well as differences among the depositional sub-environments, data were analyzed using ANCOVA (Analysis of Covariance) in the MATLAB software to control for grain size (D50 as a covariate). The reason for assigning D50 as a covariate is because of its strong correspondence with other sedimentary parameters, which precludes discerning if pre-2018 variables are statistically different from 2018 flood samples unless D50 is controlled for. A product of the ANCOVA statistical test is Prob>|T| or *p-value*. If the *p-value* is smaller than the significance level, the group being tested within the ANACOVA test is significantly different that the rest of the group. *P-values* of common significance levels are between 0.05 or 0.01. If you have a p-value less than 0.05, then is a less than 5% chance that the datasets are statistically similar to one another (i.e., over 95% of the variability is explained). For this research the ANCOVA test was done using all sediment samples (n = 97) for different sub-environments (levee, backswamp, ridge, and swales) and by year (2017 and 2018). All tests were done with the covariate as median grain size (D50 in microns).

For each grouping of ANCOVA analysis below, graphs for the lowest and highest p-values will be shown. These are chosen to represent the range of significant differences amount all of the parameters tested (OM, carbon, nutrients, and magnetic susceptibility). All p-values tested will be shown within the tables below.

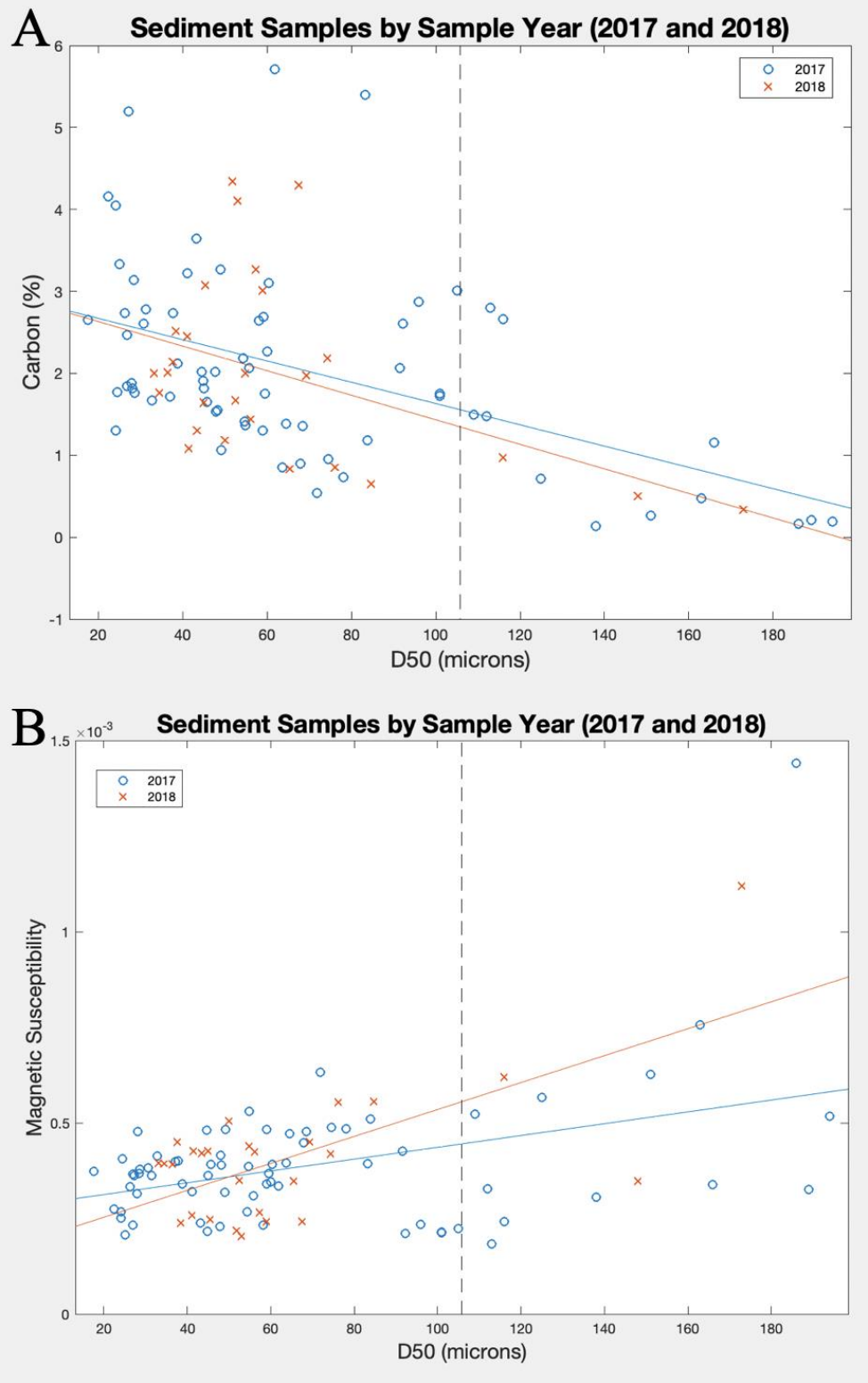

Figure 6.19 *ANACOVA analysis of all sediment samples by year (2017 and 2018) for magnetic susceptibility.*

Note: blue is October 2017 data and orange is September 2018.

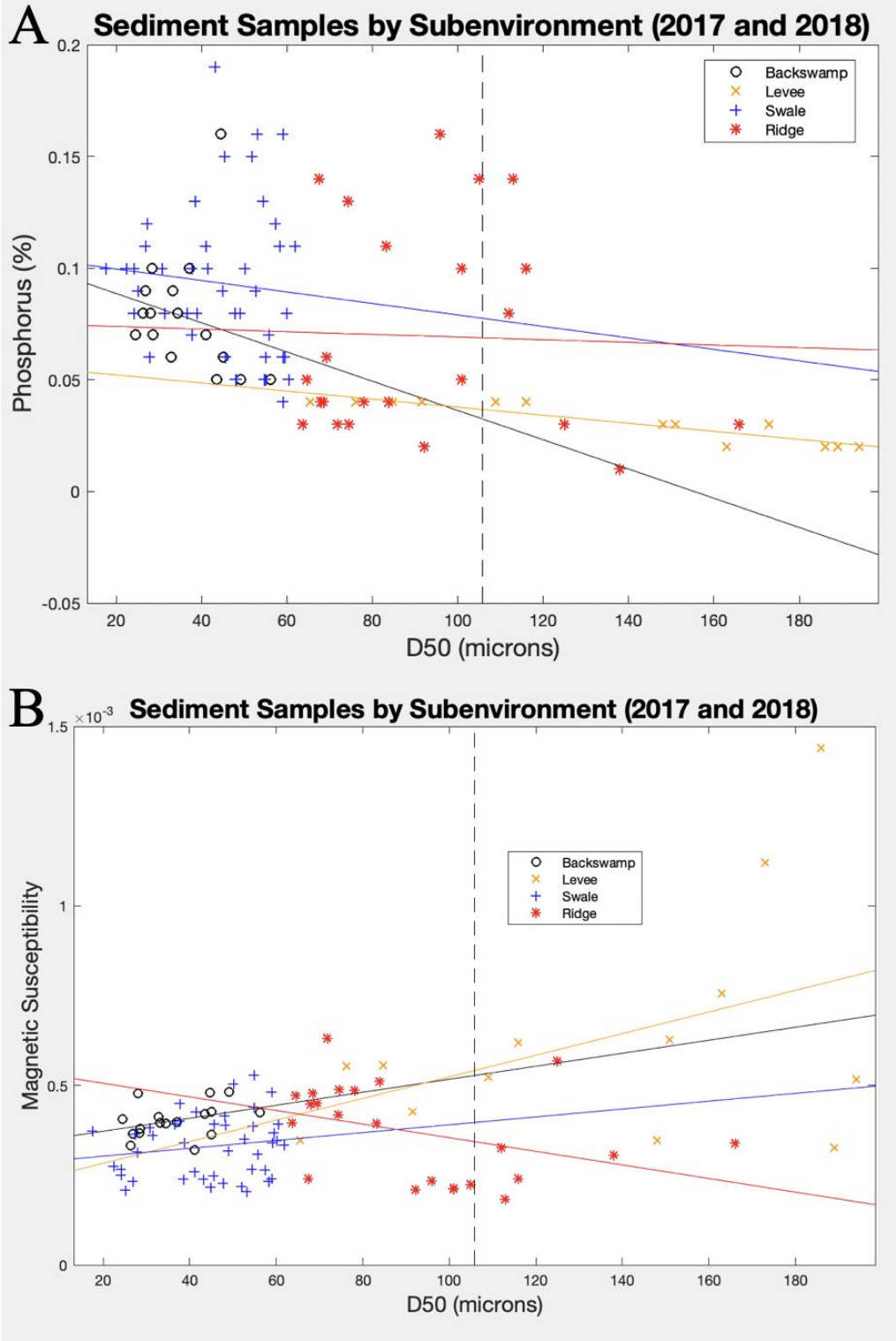

Figure 6.20 *ANACOVA analysis of all sediment samples by year (2017 and 2018) for percent organic matter by weight.*

Note: backswamp data is black, levee data is yellow, swale data is blue, and ridge data is red.

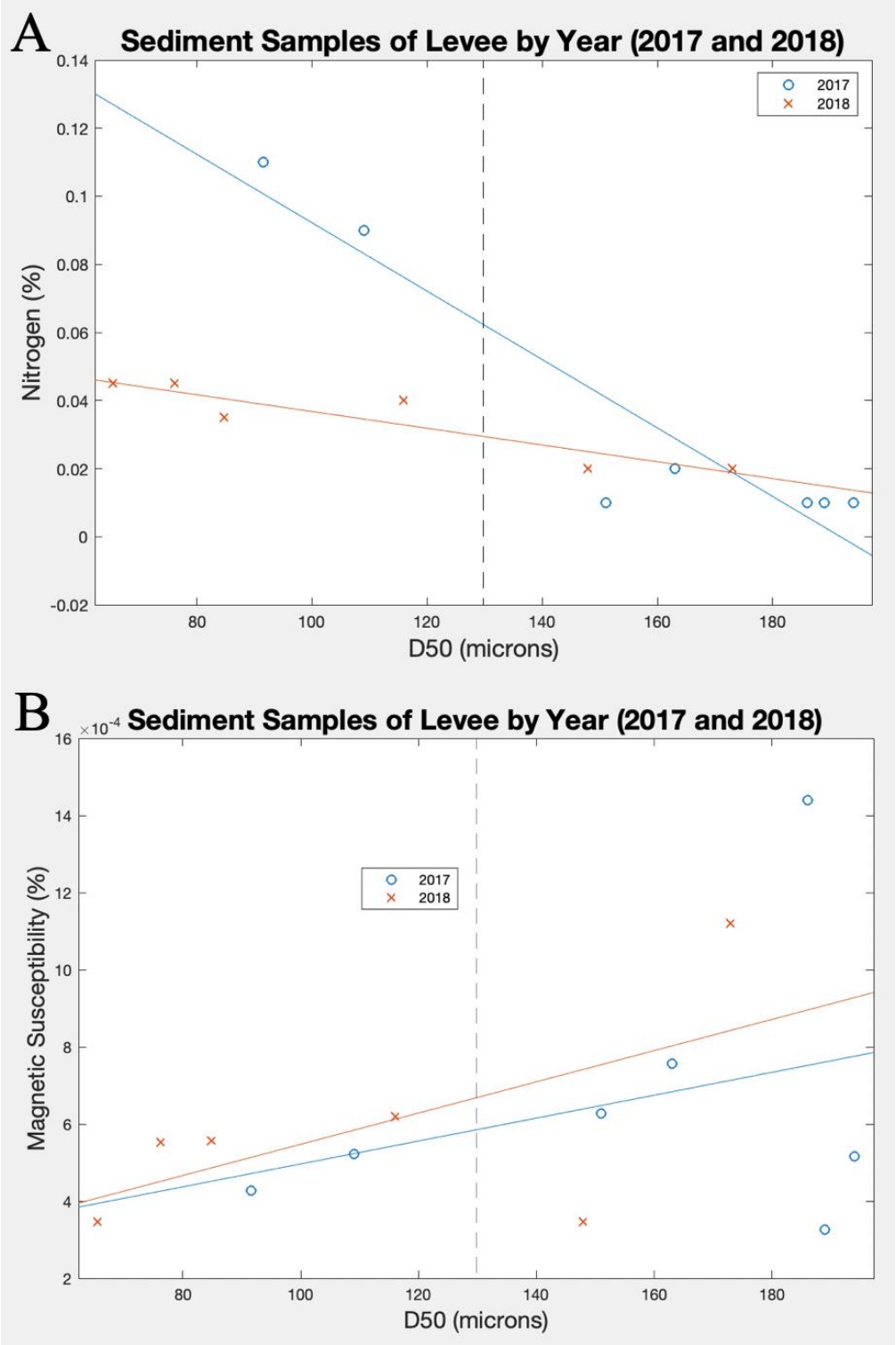

Figure 6.21 *ANACOVA analysis of ridge samples by year (2017 and 2018) for nitrogen (A) and magnetic susceptibility (B). Plot A is the lowest p-value (.0029) of ridge samples and plot B (.8277) is the highest p-value.*

Note: blue is October 2017 data and orange is September 2018.

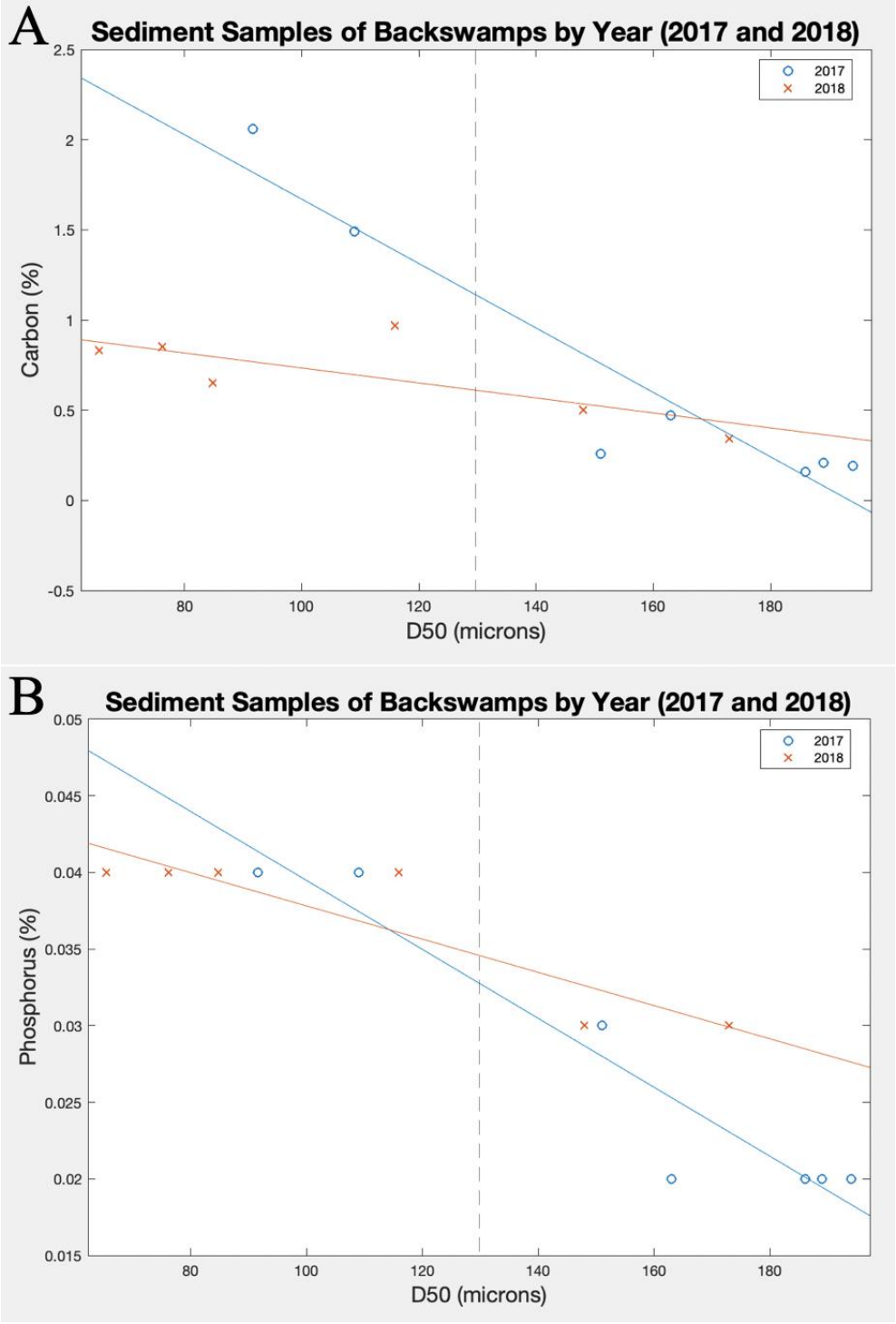

Figure 6.22 *ANACOVA analysis of ridge samples by year (2017 and 2018) for carbon (A) and phosphorus (B). Plot A is the lowest p-value (.3009) of ridge samples and plot B (.9205) is the highest p-value.*

Note: blue is October 2017 data and orange is September 2018.

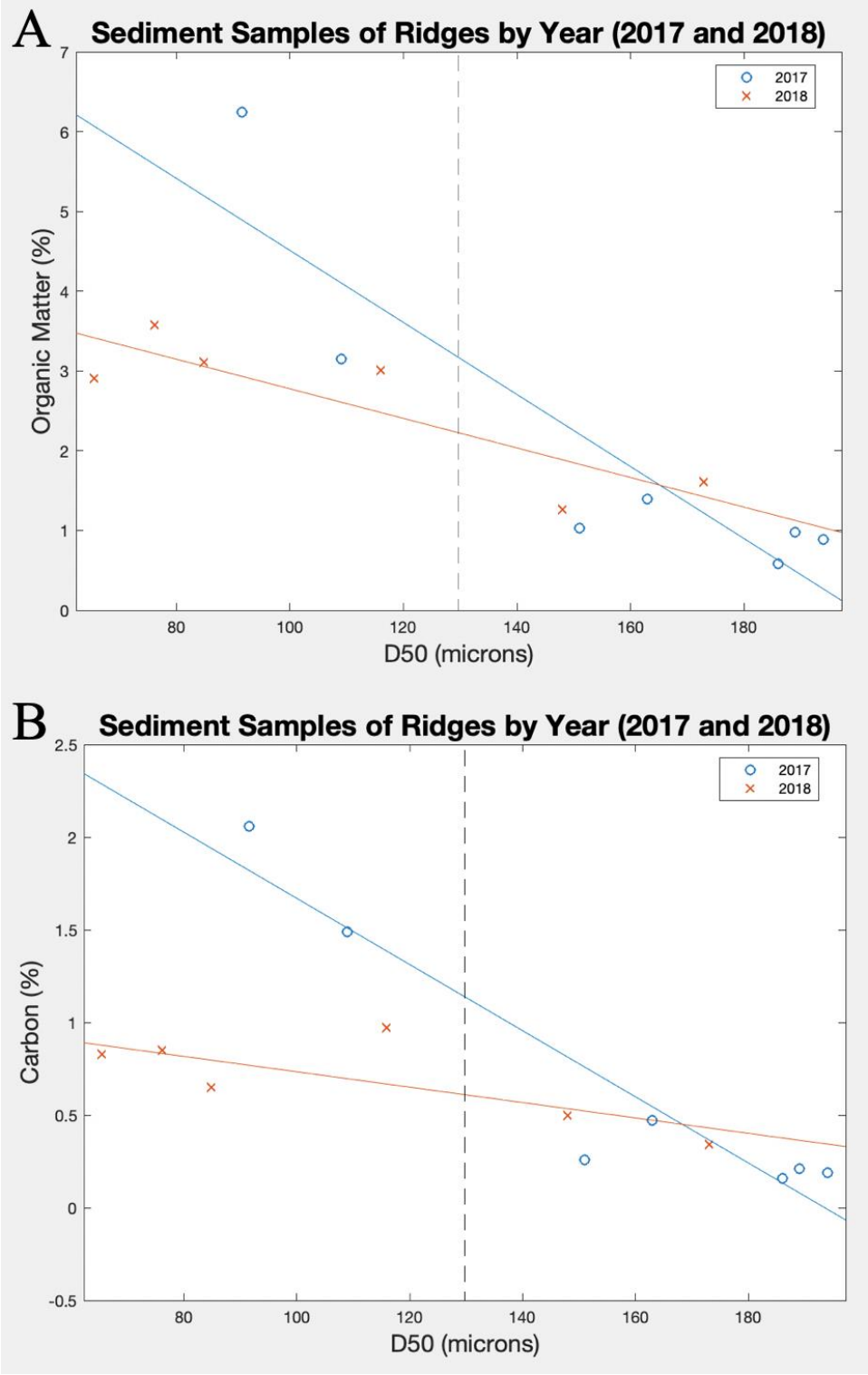

Figure 6.23 *ANACOVA analysis of ridge samples by year (2017 and 2018) for organic matter (A) and carbon (B). Plot A is the lowest p-value (.4003) of ridge samples and plot B (.8609) is the highest p-value.*

Note: blue is October 2017 data and orange is September 2018.

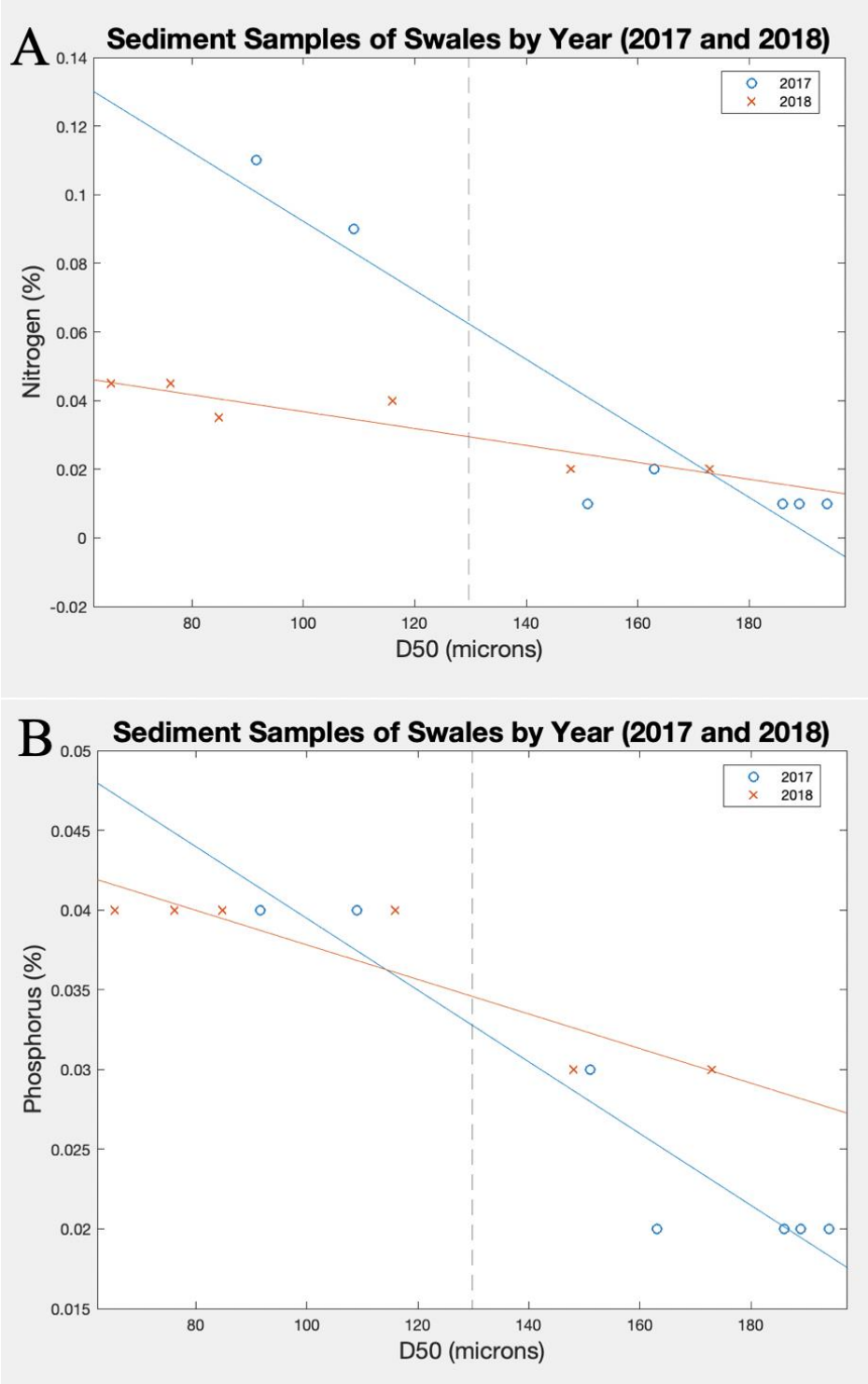

Figure 6.24 *ANACOVA analysis of swale samples by year (2017 and 2018) for nitrogen (A) and phosphorus (B). Plot A is the lowest p-value (.0307) of ridge samples and plot B (.1411) is the highest p-value.*

Note: blue is October 2017 data and orange is September 2018.

Table 6.1 *A table of p values computed by ANACOVA in MATLAB for all sediment samples by the six variables tested (year and subenvironment).*

Variable Tested	By Year	By SE	Levee By Year	Backswamp By Year	Ridge By Year	Swale By Year
OM (%)	0.4673	0.7123	0.0500	0.4800	0.8609	0.0766
N (%)	0.5018	0.7413	0.0029	0.7130	0.5411	0.0307
C (%)	0.7680	0.9125	0.0030	0.9205	0.4003	0.1234
P (%)	0.2749	0.9273	0.0172	0.3009	0.8247	0.1411
MS	0.0507	0.0092	0.8277	0.8700	0.6522	0.1374

Note: Carbon and nutrients are all percentages by weight. OM is organic matter, N is nitrogen, C is carbon, P is phosphorus, and MS is magnetic susceptibility.

Table 6.2 *A table of p values computed by ANACOVA in MATLAB for all sediment samples by the four variables tested (year and subenvironment).*

Variable Tested	Levee - Backswamp	Ridge - Swale	Levee - Ridge	Backswamp - Swale
OM (%)	0.2425	0.4150	0.6461	0.7047
N (%)	0.0116	0.8601	0.8525	0.2986
C (%)	0.2685	0.7644	0.7638	0.6226
P (%)	0.4105	0.7343	0.7620	0.6832
MS	0.8295	0.0463	0.0247	0.7543

Note: Carbon and nutrients are all percentages by weight. OM is organic matter, N is nitrogen, C is carbon, P is phosphorus, and MS is magnetic susceptibility.

Sediment samples collected during 2017 and 2018 for OM, nitrogen, phosphorus and carbon have p-values between 0.2749 and 0.7680, having no p-values below 0.05. However, magnetic susceptibility has p-values at 0.0507 showing a significant difference between the 2017 and 2018 samples (Table 6.1). Sediment samples were also organized by subenvironment (levee, backswamp, meander scroll ridge, and meander scroll swale). The ANACOVA test ran on all four subenvironments, levee, backswamp, meander scroll ridge and meander scroll swale have high p-values all between 0.7413 and 0.9273 for OM, N, C, and P having no significance difference. Again, the only parameter having a significant difference is magnetic susceptibility with a p-value of 0.0092 (Table 6.1).

A more refined ANACOVA analysis was ran splitting samples by both year and subenvironment. During the 2018 and 2019 flood events the natural levee crests tested

had the most significant differences. The p-values of all parameters, except magnetic susceptibility all fell below a p-value of 0.05 (ranging from 0.0029 to 0.05) (Table 6.1). There are no p-values that fall below 0.05 for both backswamp and ridge by year. For swale by year nitrogen (%) is the only parameter to have a p-value of significant difference of 0.0307(Table 6.1).

ANACOVA analysis was conducted for differing subenvironments. Levee-backswamp, ridge-swale, levee-ridge, and backswamp-swale were all compared using ANACOVA. Between all of the four subenvironments compared, there were no p-values that fell below 0.05 (Table 6.2).

6.2 FLOODPLAIN WATER LEVELS AND TEMPERATURES DURING THE 2018 AND 2019 FLOODS

6.2.1 HYDROGRAPHS

Individual flood events are uniquely characterized by different flood periods and patterns associated with timing and duration of overbank conditions in different floodplain environments. Time-series data from sensors in floodplains across the study areas indicate that the timing for the peak stage height of the 2018 flood was the same at all locations (March 19th). However, for the 2019 flood, the inundation peaks were six days apart. During the 2019 flood, Long Lake and the Sibley Unit had maximum stage heights on March 12th, whereas Lake Mary and Artonish Lake had maximum stage heights on March 18th. During this six day period that all locations reached peak stage height, the water column differed by only ~0.1m. Effectively, the entire floodplain basin was evenly flooded at the same time. There was no lag time in the flooding between

different floodplain environments; (i.e., backswamps, meander scrolls, large oxbow lakes).

Within the floodplain and more specifically in the sub-environments, the timing of peak stage in regards to how quickly or slowly water levels increased (during the rising limb of the flood) and receded (during the falling limb) are compared. The 2018 flood had one large symmetrical peak with a skewed recessional limb (Figure 6.27). Water sensors located within three sub-environments flooded evenly throughout the floodplain. When the 2018 flood event was rising, stage increased at a similar rate at all locations. Although at a reduced rate, the overbank stage decline was similar among the different locations.

The 2019 flood hydrograph, although of longer duration, revealed an opposite trend with multiple peaks and a skewed rising limb (Figure 6.27). There was only a small gap in time between the two floods in which the LMR fell below action stage (September 2018 when surface sediment samples were collected). During the rising limb there was a slight lag time between flooding in meander scroll locations versus backswamp locations. This slightly uneven pattern of flooding occurred between October 2018 and January 2019. The receding limb of the 2019 flood had an even, rapid decline. Basically, all sub-environments were equally responsive (Figure 6.27). Both the 2018 and 2019 flood events were considered major floods, allowing for a better understanding of the distribution of inundation throughout the floodplain.

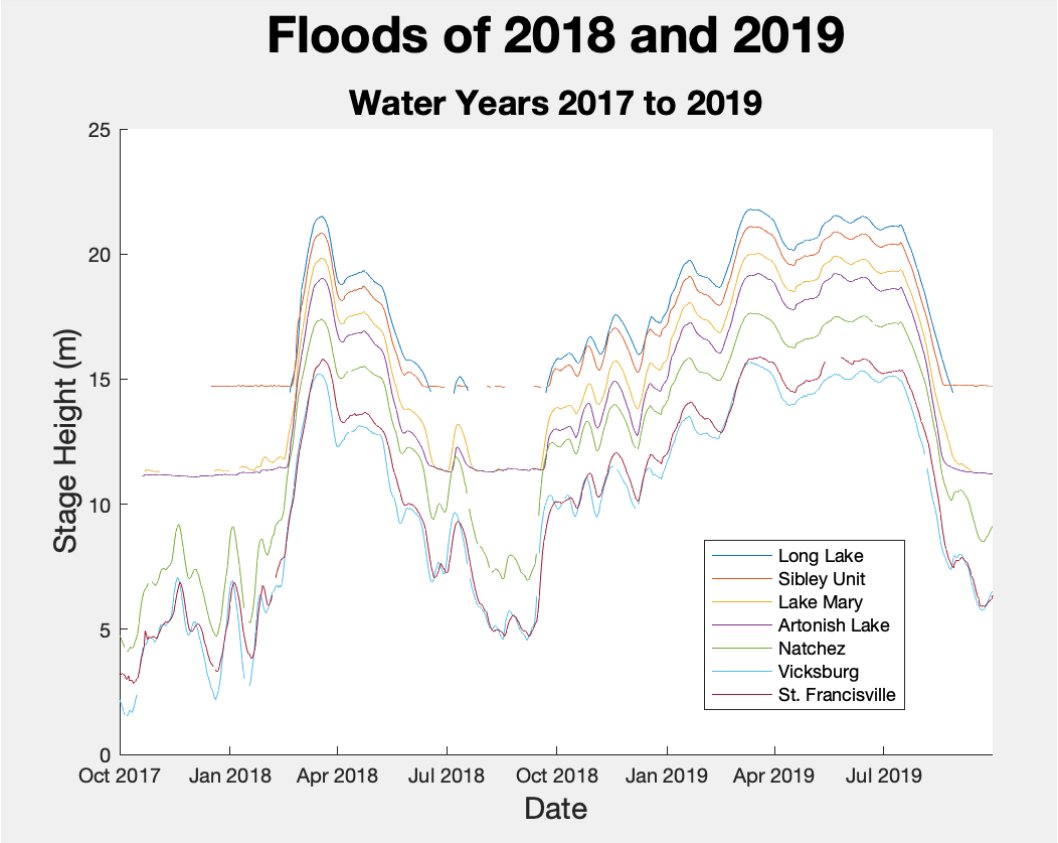

Figure 6.25 *A plot of all stage data (m) including overbank sensor data and river-gauge installations.*

Note: Long Lake is dark blue, Sibley Unit is orange, Lake Mary is yellow, Artonish Lake is purple, Natchez is green, Vicksburg is light blue, and St. Francisville is pink. Natchez, Vicksburg, and St. Francisville have arbitrary stage heights, not surveyed elevations like the authors' sensors.

Findings from Hudson et al. (2012) along the Guadalupe River in Texas reveal flooding patterns in two oxbow lakes, Cuero Oxbow and Horseshoe Oxbow. Flooding patterns and durations are uneven between the two oxbow lakes. A lower amount of days of river connectivity was found for Horseshoe Lake than Cuero Lake. The uneven flooding durations and connectivity to the main river can lead to differences in sedimentation, frequency and magnitude of flooding, and discharge pulses. Comparing all of these parameters can lead to a better understanding of "connectivity signatures" (Hudson et al., 2012).

In comparison to a study by Rosenqvist et al. (2002) along the Jaú River in Brazil, there are similarities in flooding durations being unevenly spaced throughout the floodplain. Flood durations for the 1995 and 1996 floods on the Jaú River show an unevenly distributed duration of flooding from the main channel. Figure 6.26 indicates areas of red through blue to be of different flood durations, with red being the most prominent. The main occurrence of uneven flood durations was found along meanders, limiting the amount of inundation due to the angle of flow from the main channel.

The overbank water sensors along the LMR in this study were placed in the vicinity of three meanders along the LMR. When comparing to the floods of 2018 and 2019 along the LMR and the Jaú, the LMR's floodplain had even distributions of inundation (using peak and duration values), where the Jaú River had an oppositely uneven spacing of flood duration.

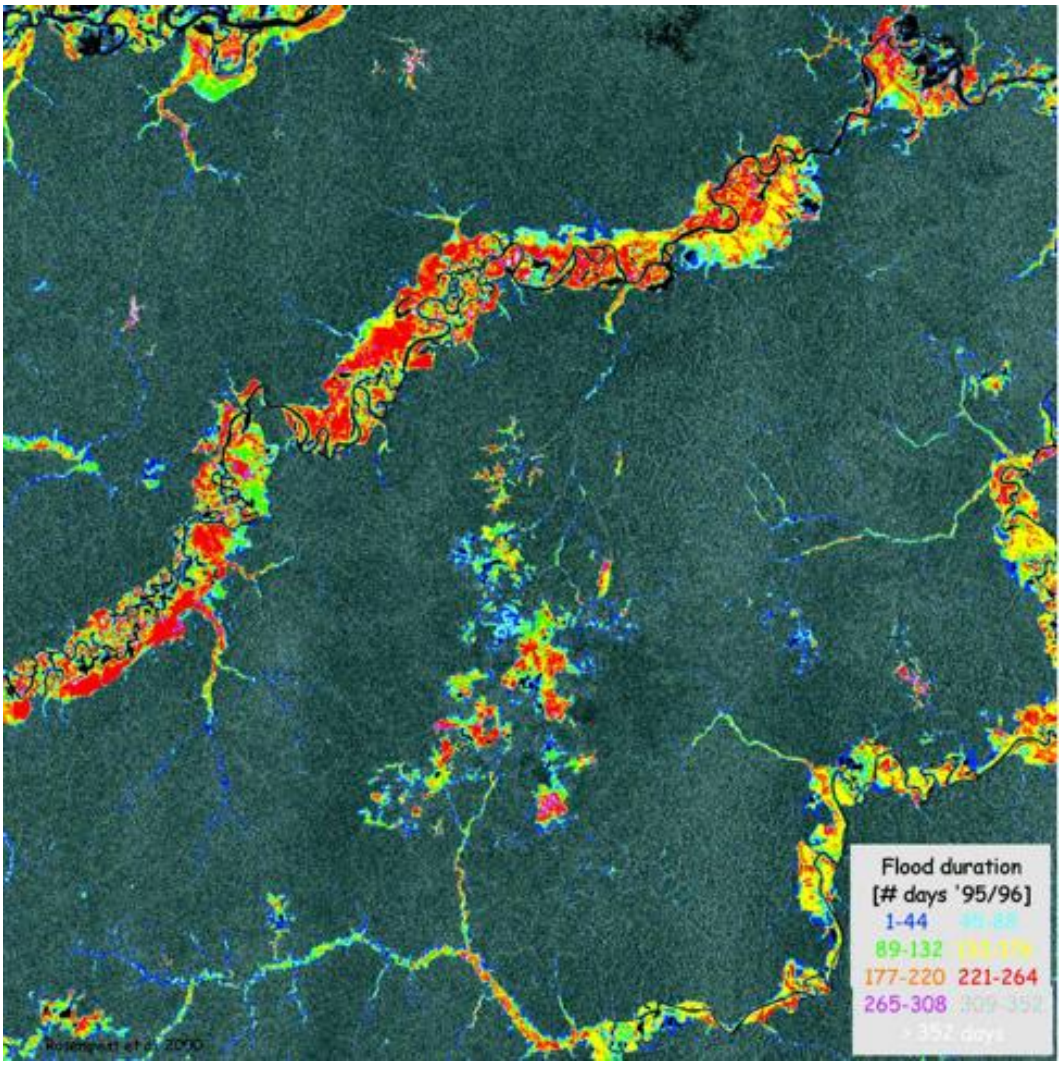

Figure 6.26 *A portion of the Jaú River and its floodplain. The density map indicates the number of days flooded in 1995 and 1996 (Rosenqvist et al., 2002).*

6.2.2 WATER TEMPERATURE

Water temperature was measured by the sensors during both floods and indicate seasonal controls. During the 2018 and 2019 winter months, the water temperature was expectedly the lowest for the two years of data, as opposed to the summer months which had the highest water temperatures. During the transition from spring into summer, water temperature had the sharpest gradient, with little variation between locations. In addition to the increase in temperature because of seasonal change, slight increases in overbank

water temperature are observed during times of inundation. During March (into June) the peak stage heights for both the 2018 and 2019 floods occurred. Water temperature slightly increased by 3° - 5°C during these times of inundation as depicted in the red boxes of Figure 6.29. This slight increase in temperature may be due to upstream water inputs (i.e., cold Upper Mississippi River water replaced for a few days by slightly warmer Arkansas River water). Aside from minor changes in overbank water temperatures, a flood with a stage height peak in March will have a lower temperature than a flood later in the season (August). Therefore, an early season flood will sequester fewer nutrients (N and P) than a mid/late season flood (Schramm et al., 2009). Relatively warm water temperatures promote greater rates of nutrient sequestration in addition to longer flood durations. Therefore, the 2019 flood should have sequestered more nutrients than the 2018 flood.

A second observation is that there are some intervals when overbank water temperatures at all sensors are basically the same and follow similar slopes of change. This occurred during the receding limb of the flood events. When the water levels are more stable (not flooding periods) the water temperatures diverge among the different sensors (blue arrows) (Figure 6.29). This may be caused by the environments becoming "disconnected" from the main channel and therefore become a closed system. This occurs in areas like Long Lake, Lake Artonish, and Lake Mary when the area remains ponded even after the flood has receded. This increase in temperature may be due to a lack of velocity within the lakes and warmer temperatures during the summer months.

Water sensors throughout the water year were not submerged by overbank flow for the entirety of the year. The water sensors become disconnected from overbank flood

waters during dry periods where there is no flood influence. For this study water sensors during the 2018 flood were submerged on 2/20/18 and disconnected on 6/18/18. During the 2019 flood event, water sensors were submerged on 9/28/19 and disconnected on 8/28/19 (Figure 6.27).

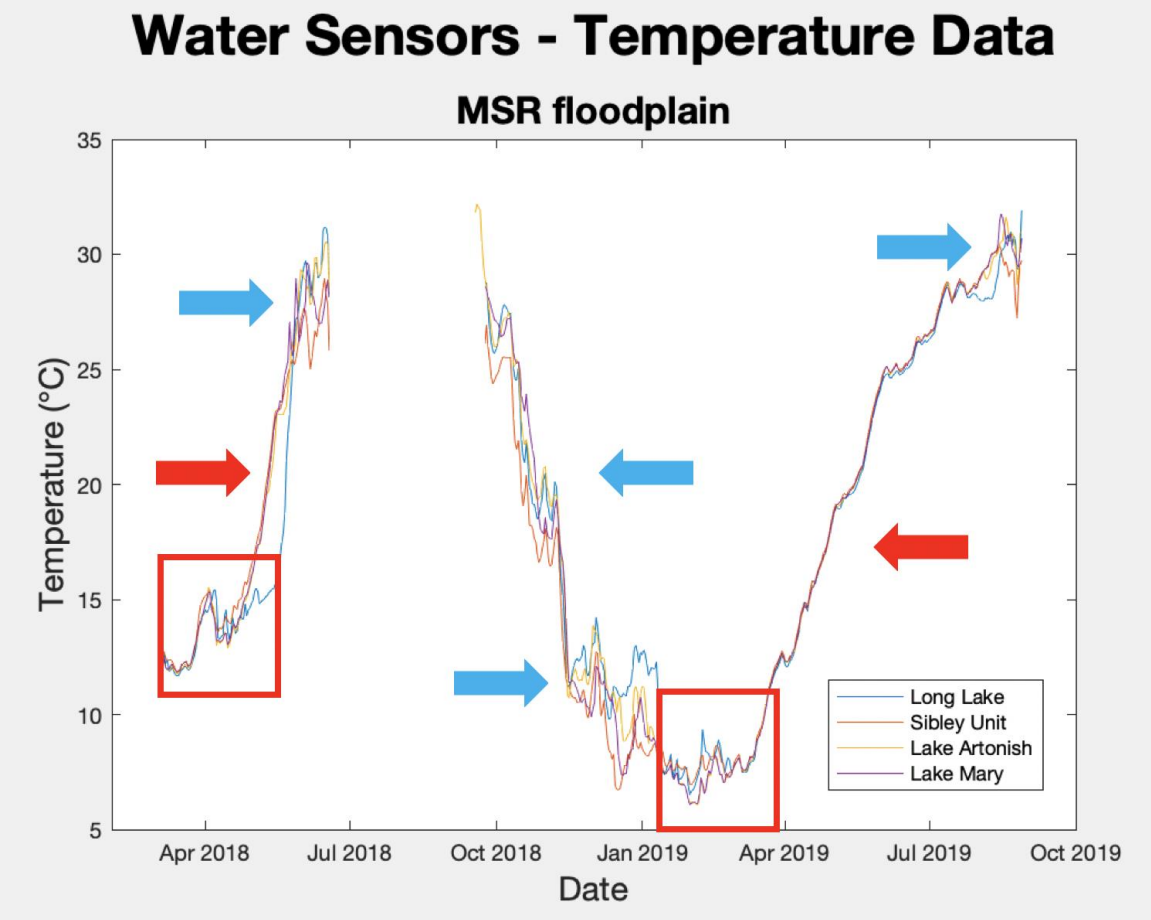

Figure 6.27 *A hydrograph for all four water gauge locations (Long Lake, Sibley Unit, Lake Artonish, and Lake Mary).*

Note: The red squares indicate the months in which stage height during the 2018 and 2019 flood were at its peak. The blue arrows indicate a separation in temperature data between all of the locations. The gaps in data are times when the water sensors were not submerged in overbank flow consistently.

6.3 SUSPENDED SEDIMENT AND WATER QUALITY IN EMBANKED FLOODPLAINS DURING THE 2019 FLOOD

6.3.1 CLOVERDALE UNIT

The Cloverdale Unit includes three water-quality sampling locations in the meander scroll sub-environment: QW06, QW07, and QW08. Depth and velocity have negative relationships with each other, with distances from the main LMR channel (Figures 6.30 and 6.31). Suspended sediment concentrations decline with overbank flow distance (Figure 6.32). D50 does not have a relationship with overbank flow distance from the channel or by the two sample dates, but turbidity increases closer to Long Lake (Figures 6.33 and 6.34).

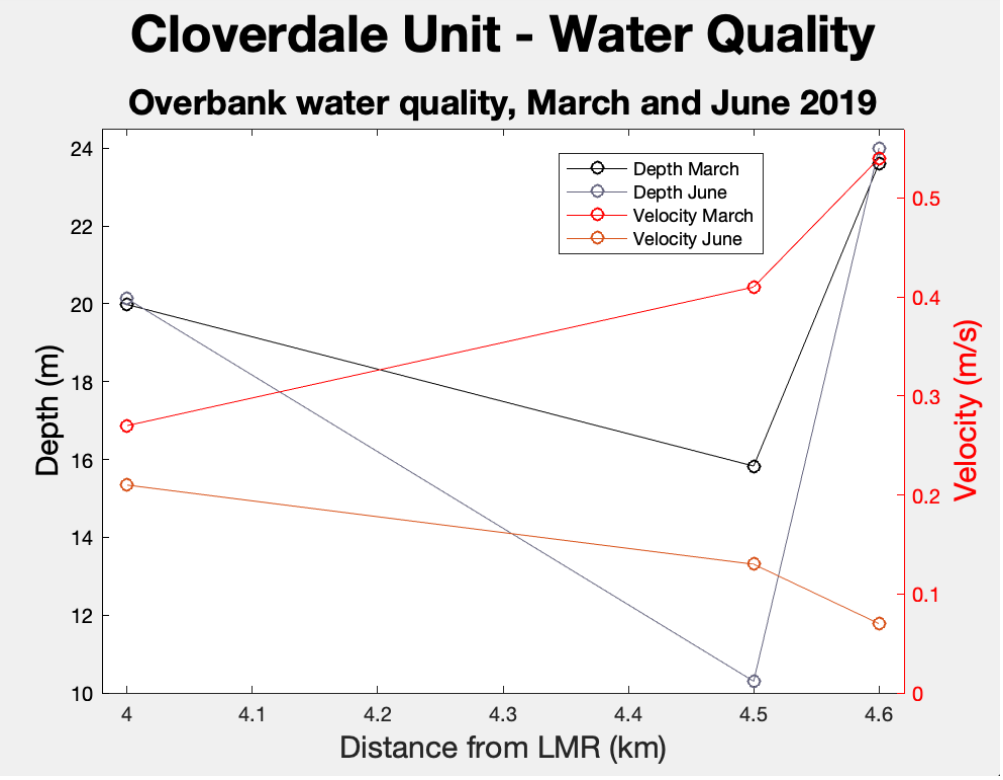

Figure 6.28 *A plot of water samples QW06 to QW08 at the Cloverdale Unit for depth (m) and velocity (m/s) during both March and June 2019.*

Note: Depth is black and gray and velocity is red and orange.

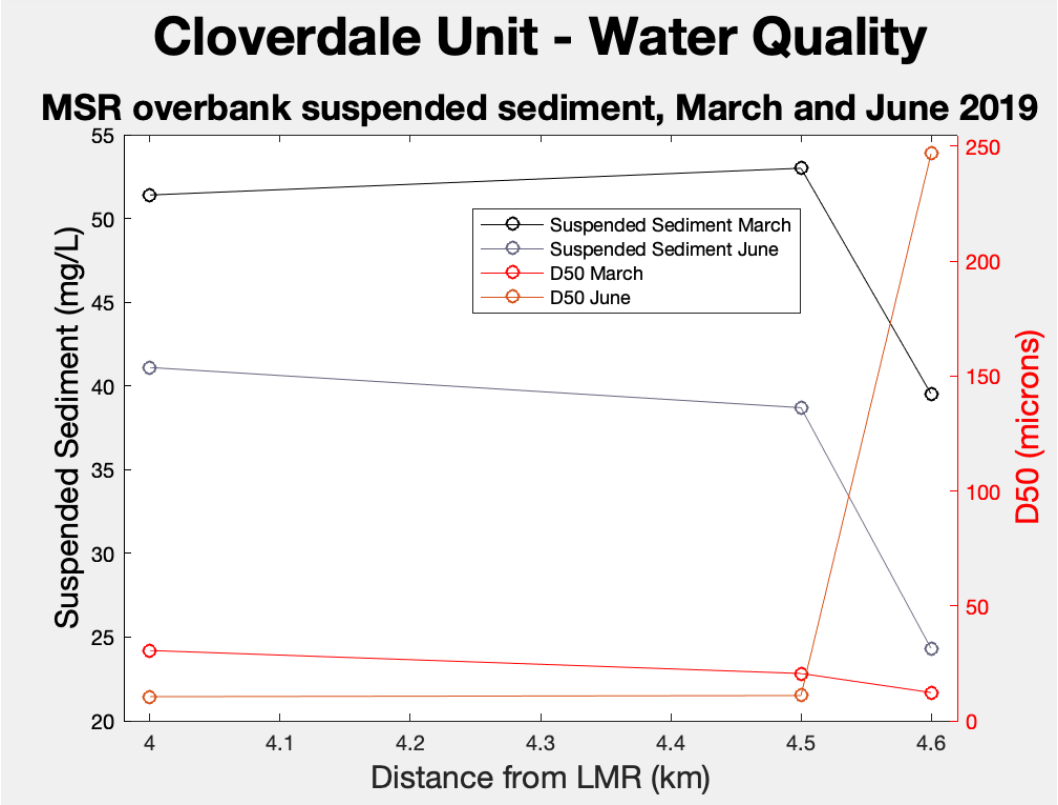

Figure 6.29 *A plot of water samples QW06 to QW08 at the Cloverdale Unit for suspended sediment (mg/L) and D50 (microns) during both March and June 2019.*

Note: Suspended sediment is black and gray and D50 is red and orange.

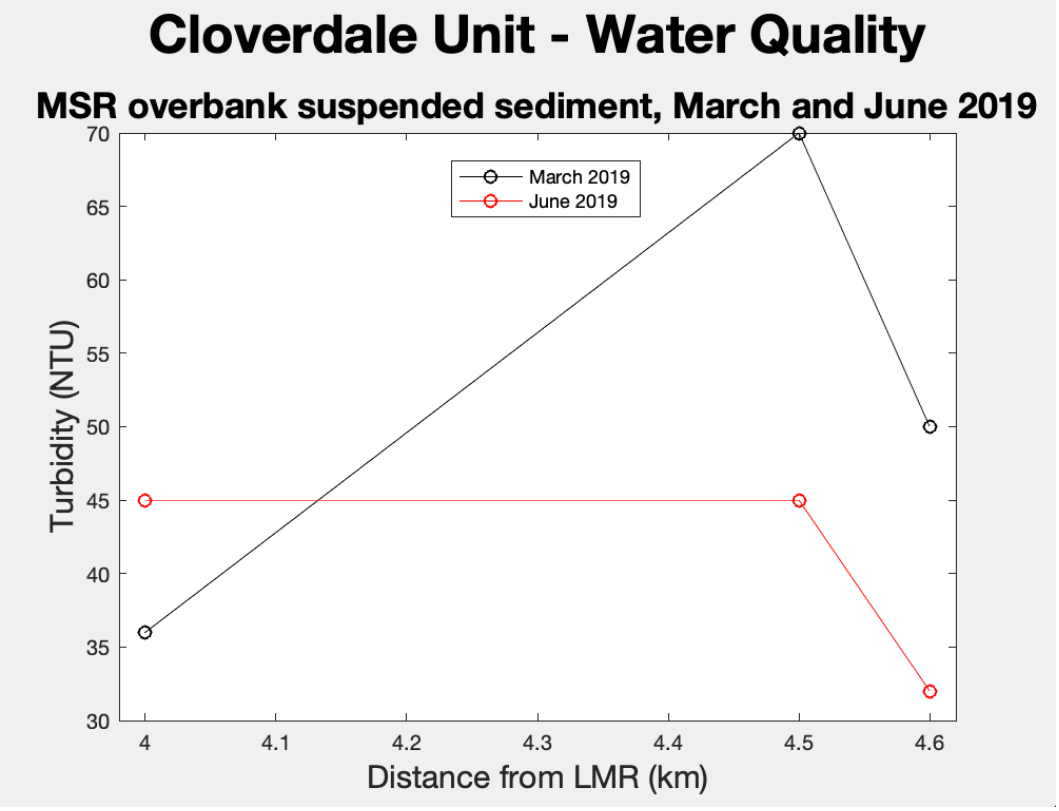

Figure 6.30 *A plot of water samples QW06 to QW08 at the Cloverdale Unit for turbidity (NTU) during both March and June 2019.*

Note: March 2019 is black and June 2019 is red.

March 2019 values for suspended sediment, nitrogen, carbon, and phosphorus have similar values among the three sample locations. Similarly, in June 2019, values for suspended sediment, nitrogen, carbon, and phosphorus have similar values among the three sample locations. In both March and June, however, a lower suspended sediment concentration occurred at QW06. QW06 is located along Long Lake and imagery (Figure 3.1) shows that relatively dense floodplain vegetation occurs between this sampling site and the upstream source of overbank flow along the LMR channel, which likely results in depositional filtering of suspended sediment along that overbank flow path. The Cloverdale samples at all locations, both nitrogen and carbon (weight by percent)

increase with distance from the LMR (Figures 6.35 and 6.36), between March and June 2019. Nitrite-nitrate and phosphorus are similar among all samples (QW_06, QW_07, and QW_08).

A

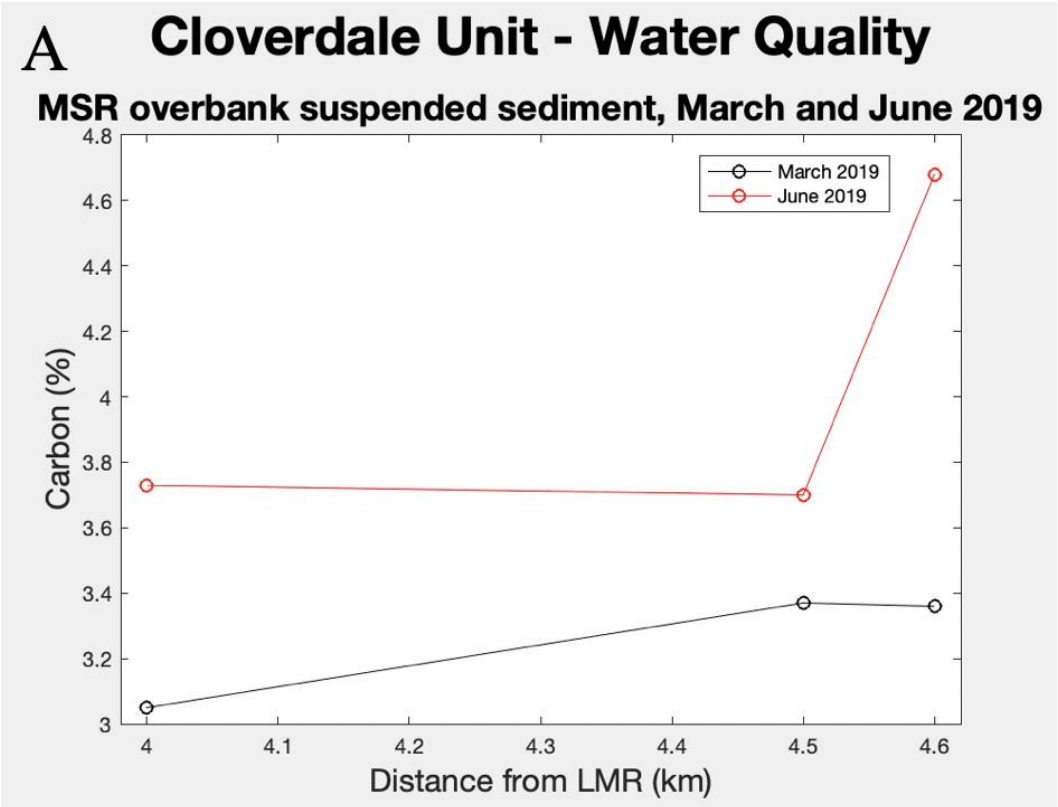
Cloverdale Unit - Water Quality
MSR overbank suspended sediment, March and June 2019
March 2019
June 2019
Carbon (%)
Distance from LMR (km)
4.8
4.6
4.4
4.2
4
3.8
3.6
3.4
3.2
3
4
4.1
4.2
4.3
4.4
4.5
4.6

B

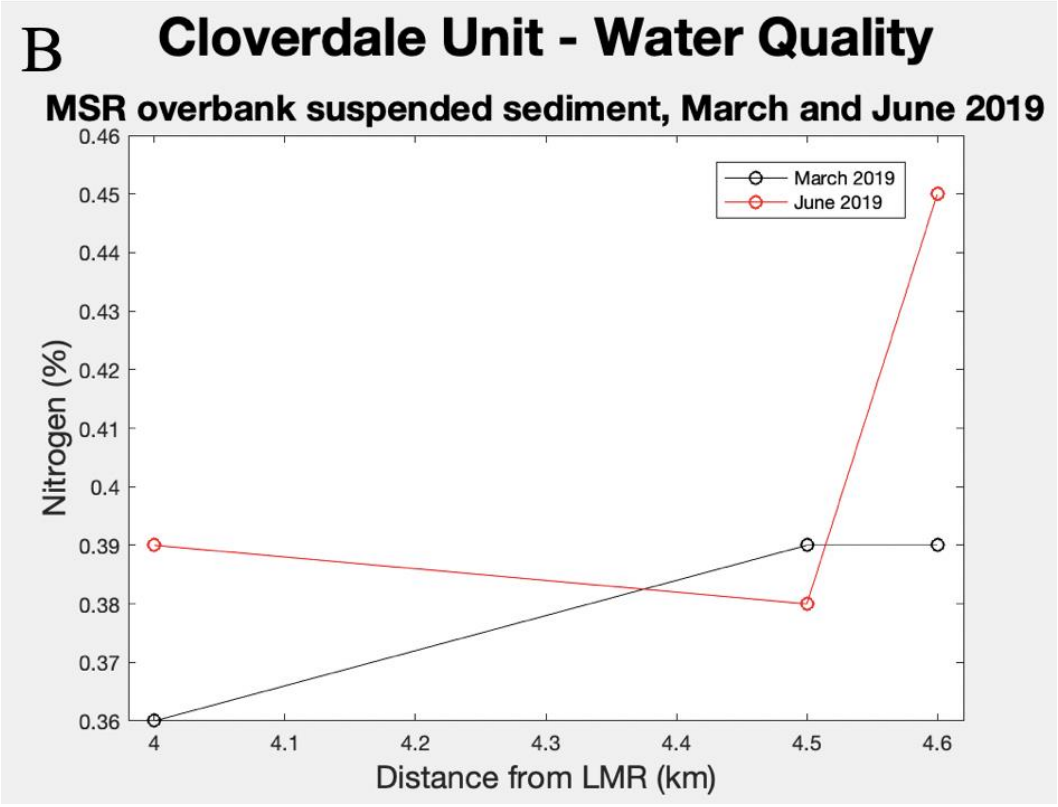
Cloverdale Unit - Water Quality
MSR overbank suspended sediment, March and June 2019
March 2019
June 2019
Nitrogen (%)
Distance from LMR (km)
0.46
0.45
0.44
0.43
0.42
0.41
0.4
0.39
0.38
0.37
0.36
4
4.1
4.2
4.3
4.4
4.5
4.6

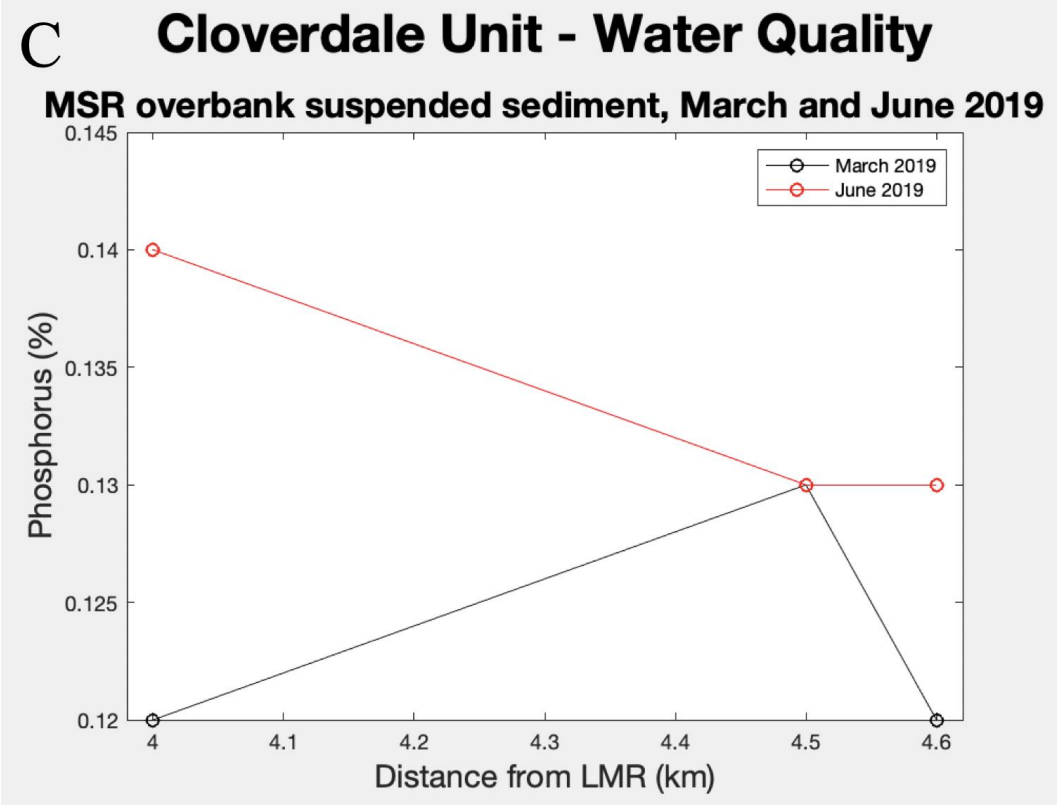

Figure 6.31 *Three plots of water samples QW06 to QW08 at the Cloverdale Unit for weight by percent during both March and June 2019.*

Note: A is carbon, B is nitrogen, and C is phosphorus. March 2019 is black and June 2019 is red.

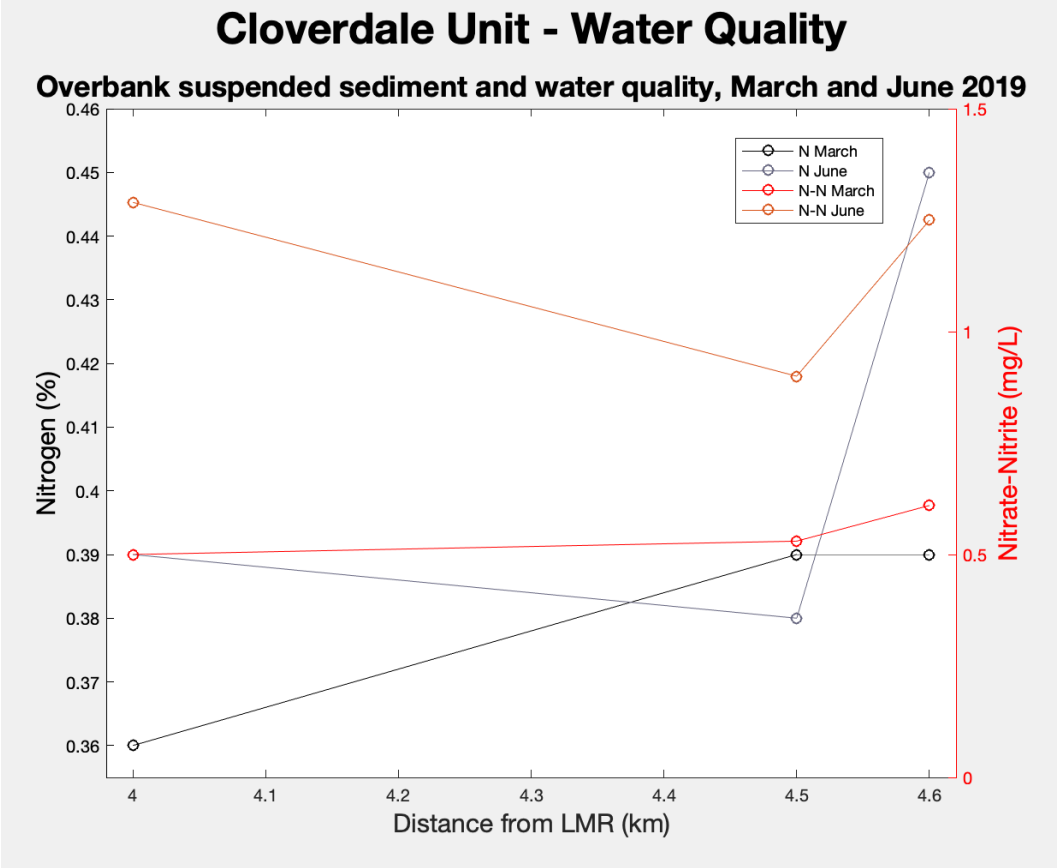

Figure 6.32 *A plot of water samples QW06 to QW08 at the Cloverdale Unit for phosphorus (%) and nitrogen (mg/L) during both March and June 2019.*

Note: Nitrogen (%) is black and gray and nitrogen (mg/L) is red and orange. Nitrogen (%) is derived from suspended sediment samples and nitrogen (mg/L) is derived from filtered water samples.

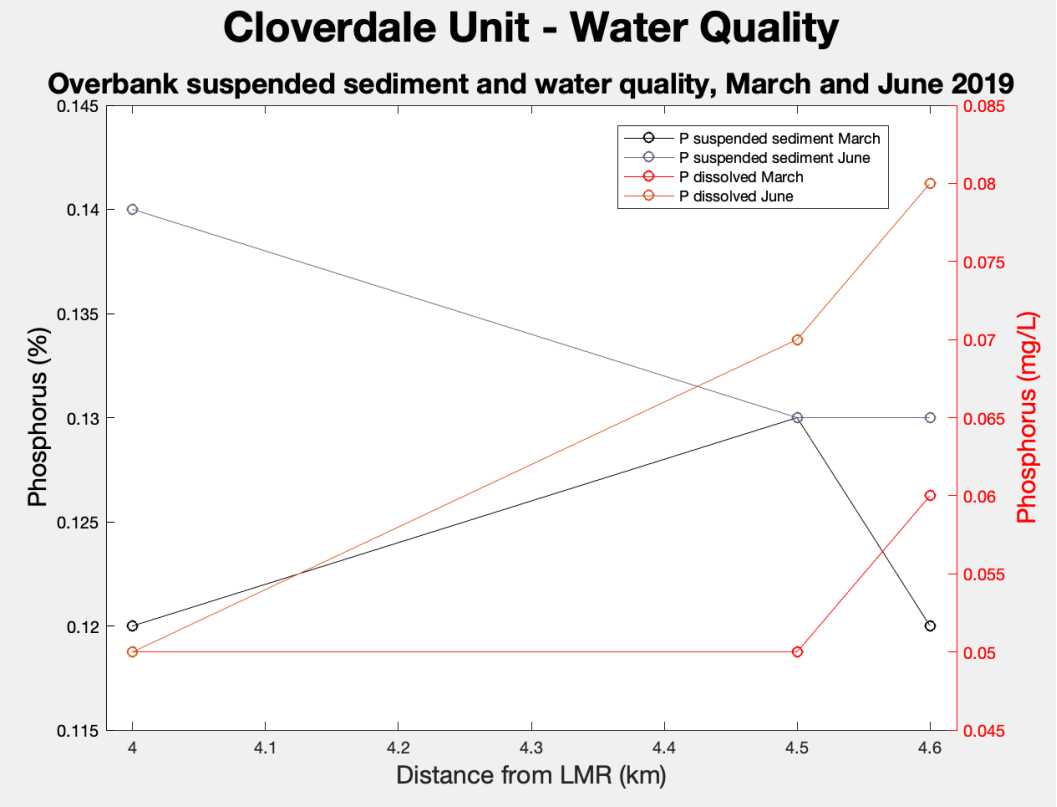

Figure 6.33 *A plot of water samples QW06 to QW08 at the Cloverdale Unit for phosphorus (%) and phosphorus (mg/L) during both March and June 2019.*

Note: Phosphorus (%) is black and gray and phosphorus (mg/L) is red and orange. Phosphorus (%) is derived from suspended sediment samples and phosphorus (mg/L) is derived from filtered water samples.

The variation of the data above indicates that the meander scroll environment does not have much of an influence on the water column above, but roughness associated with the floodplain vegetation is influential on some water-quality parameters. Meander scrolls will have little to no effect on water quality; however, the permanently ponded areas like Long Lake allow for more efficient conveyance of flood waters because of minimal vegetation. Influences from the floodplain's sub environments have more of a hydraulic influence when the overbank water column is receding (i.e., facilitates sediment deposition). There are three meanders of the LMR that are located within the study location. However, during peak inundation, these three meanders do not have a large

influence on the samples collected. This is due to the flow and movement of water within the entire floodplain. The overbank flow is directed downstream (north to south) and does not directly follow the direction of flow of the LMR during normal flow periods (along meanders). Both March and June sampling periods occurred during high stages, and overbank flow was along the longitudinal axis of the embanked floodplain (i.e., not lateral).

6.3.2 SIBLEY UNIT

The overbank water samples in the Sibley Unit are more variable than the Cloverdale Unit. Overbank water quality and suspended sediment parameters in the Sibley Unit are depicted with respect to overbank flow distance from the LMR and by perpendicular orientation to the LMR channel. The floodplain's natural boundaries and basin have more of an influence on the data, than the natural meander of the LMR (Figure 3.4).

The Sibley Unit's depth throughout the floodplain is variable because of transitions from natural levees to the backswamp; further variability is imparted by large areas cleared of vegetation and a grid of access roads. Depth and velocity are irregular and are influenced by and the degree of roughness associated with adjacent vegetation (Figures 6.39, 6.40, and 6.41). Velocity was fastest at 3.1 km (QW03) from the LMR but varied throughout in March 2019, however velocity was less variable during June 2019, likely because of additional overbank flow resistance associated with leaf growth. During the dry season, this area is maintained by SCCNWR, including vegetation clearance for roads and trails. These human-made pathways act as makeshift "channels" during times of inundation. Therefore, overbank flow velocities increase with proximity to the

"channels." An overall decrease in suspended sediment concentration with increasing distance from the LMR was observed in both March and June 2019 (Figure 6.42).

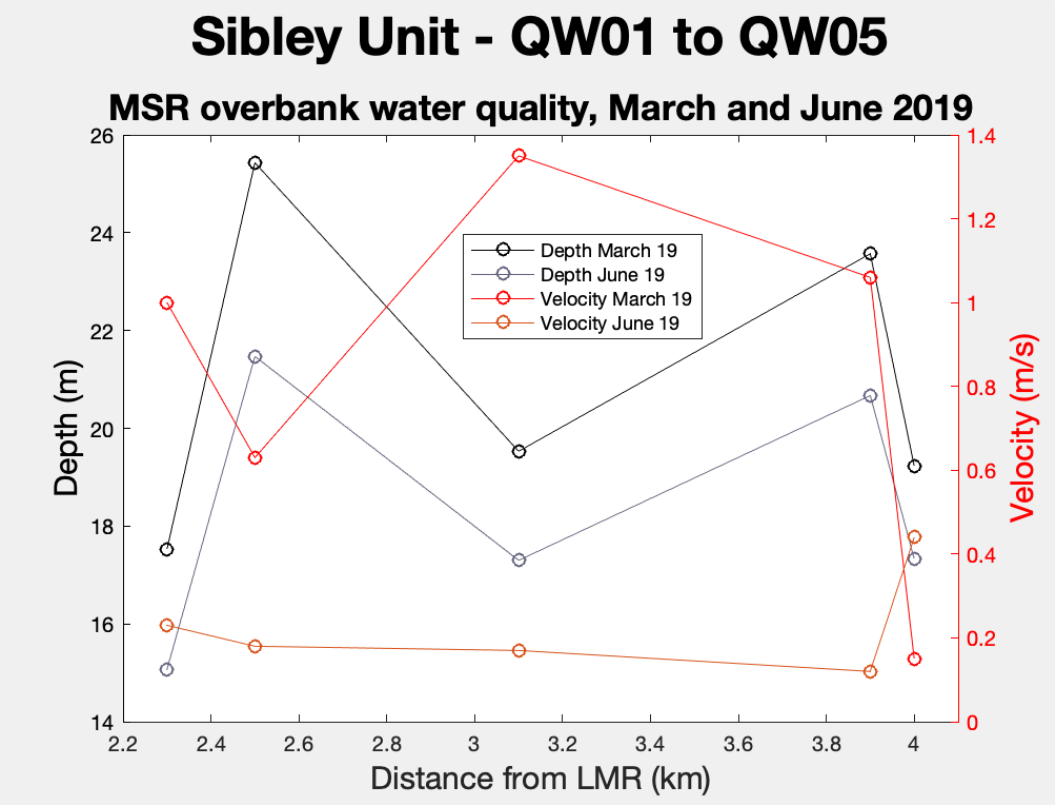

Figure 6.34 *A plot of water samples QW01 to QW05 at the Sibley for depth (m) and velocity (m/s) during both March and June 2019.*

Note: Depth is black and gray and Velocity is red and orange.

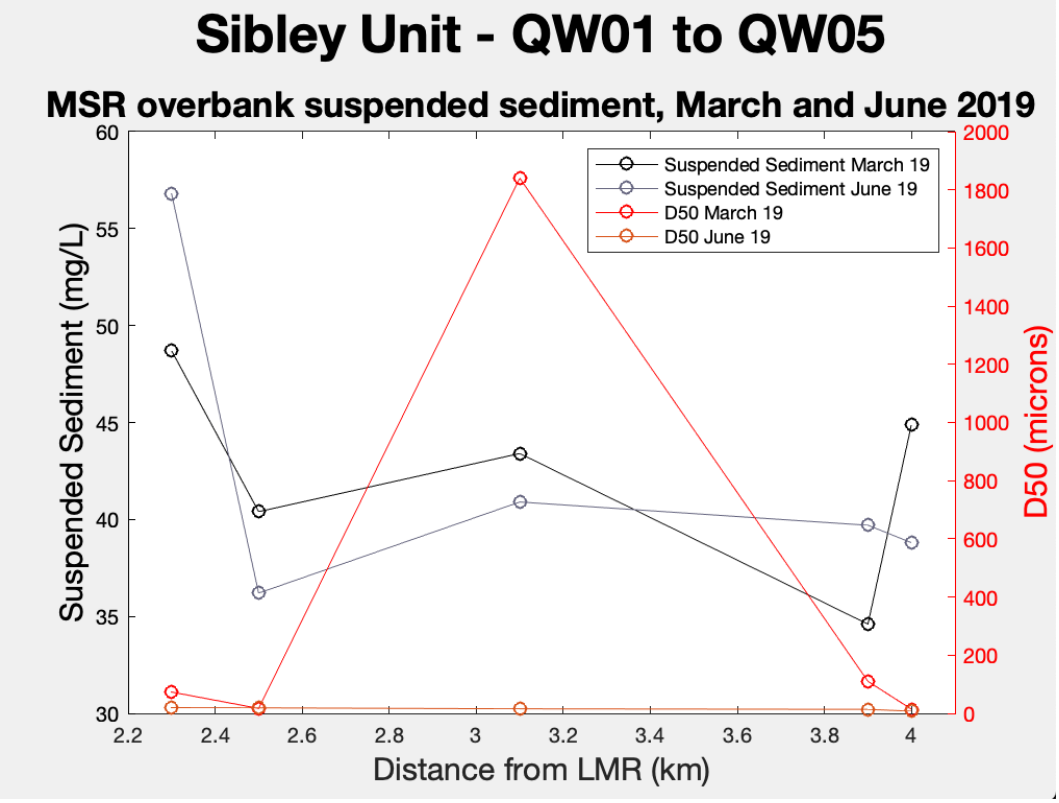

Figure 6.35 *A plot of water samples QW01 to QW05 at the Sibley for suspended sediment (mg/L) and D50 (microns) during both March and June 2019.*

Note: Suspended sediment is black and gray and D50 is red and orange.

Oppositely, an overall increase in carbon with increased distance into the floodplain was observed (backswamp) (Figure 6.45). The remaining parameters tested (nutrients, pH, etc.) are variable, with peaks at the 3.1 km distance (QW03) (location of largest ATV trail) (Figures 6.45, 6.46, 6.47, 6.48, and 6.49). The variability during March 2019 indicates that the overbank flow takes the path of least resistance though gaps in vegetation where roads are located (Figure 3.5). The flow path of overbank conditions can be seen throughout the study area where vegetation is controlled and maintained yearly (aerial imagery)(Figure 3.5). As proven in the literature vegetation has an influence on water and sediment flow. Crosato and Saleh (2010) shows that there is a

decrease in bed shear stress, sediment transport capacity (flow with areas of dense vegetation), and increase in hydraulic resistance (causing a decrease in flow velocities).

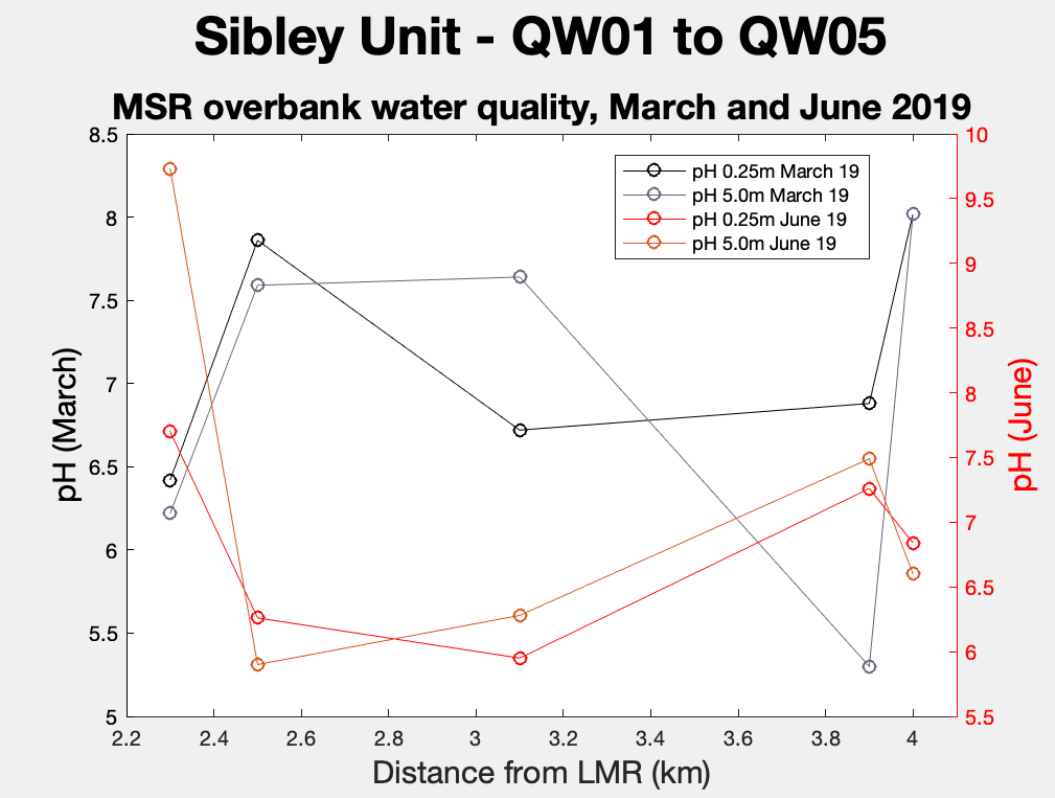

Figure 6.36 *A plot of water samples QW01 to QW05 at the Sibley for pH at both water quality depths of 0.25m and 0.5m.*

Note: March 2019 is black and gray and June 2019 is red and orange.

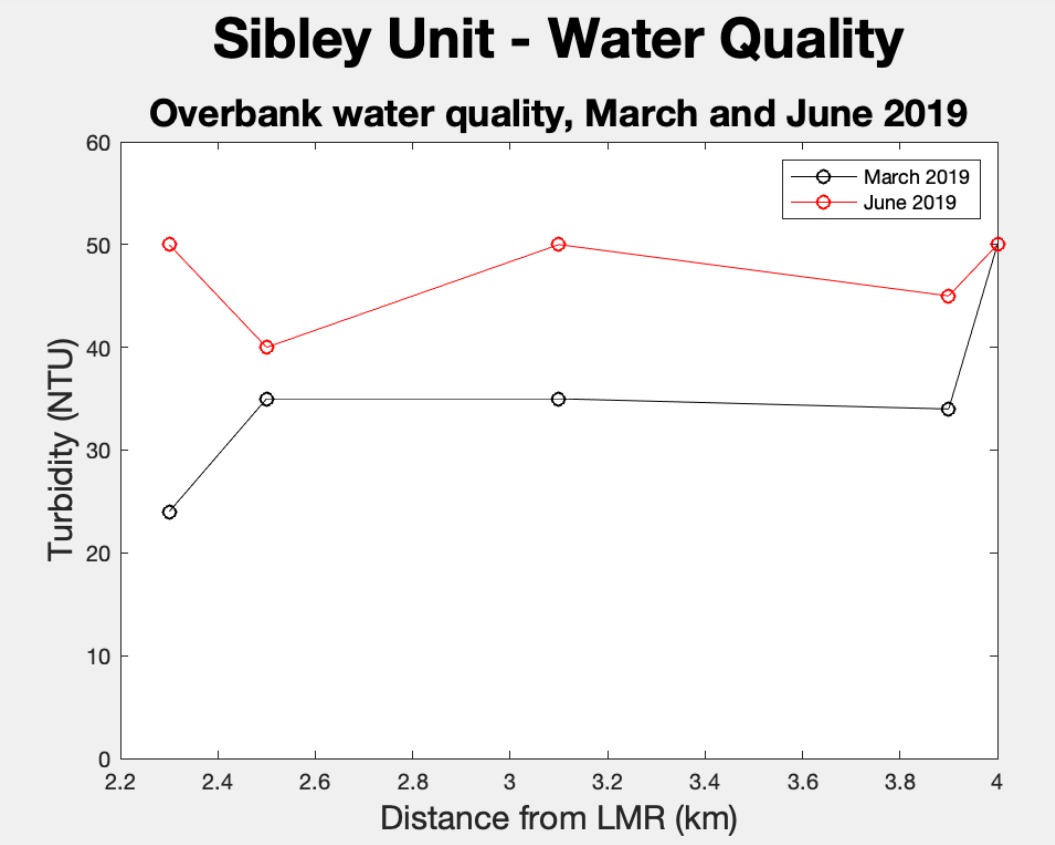

Figure 6.37 *A plot of water samples QW01 to QW05 at the Sibley for turbidity (NTU) during both March and June 2019.*

Note: March 2019 is black and June 2019 is red.

A

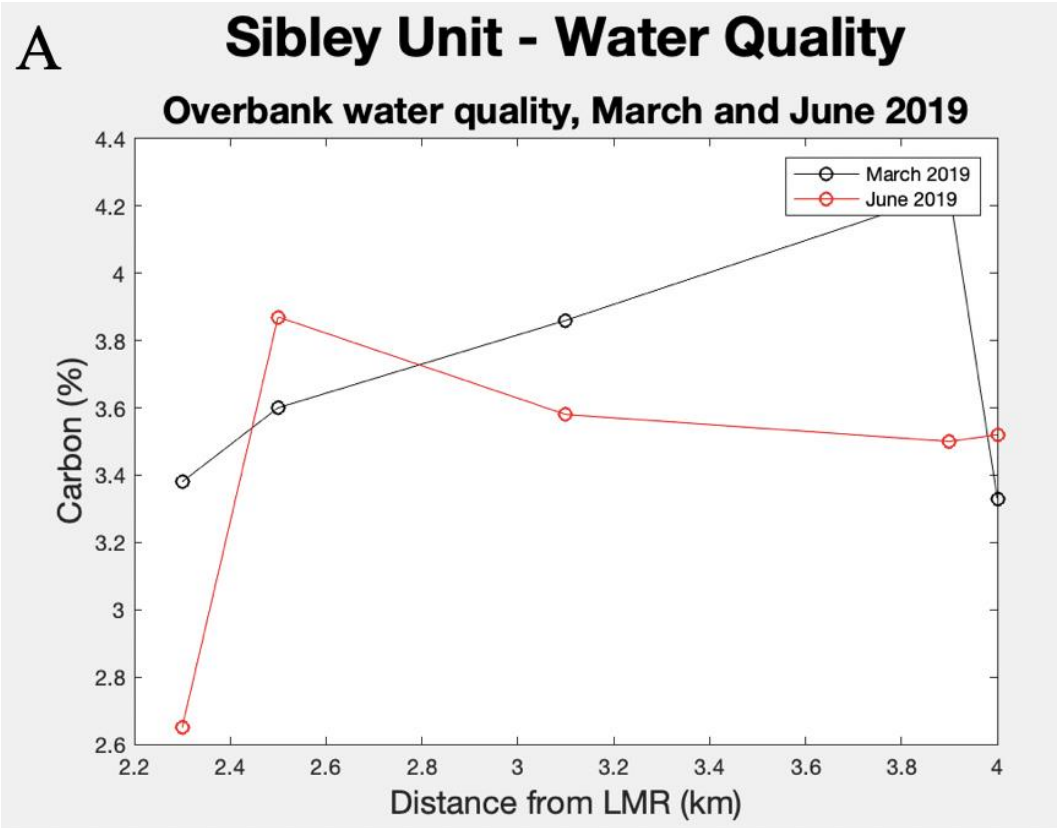
Sibley Unit - Water Quality
Overbank water quality, March and June 2019
March 2019
June 2019
Carbon (%)
Distance from LMR (km)
4.4
4.2
4
3.8
3.6
3.4
3.2
3
2.8
2.6
2.2
2.4
2.6
2.8
3
3.2
3.4
3.6
3.8
4

B

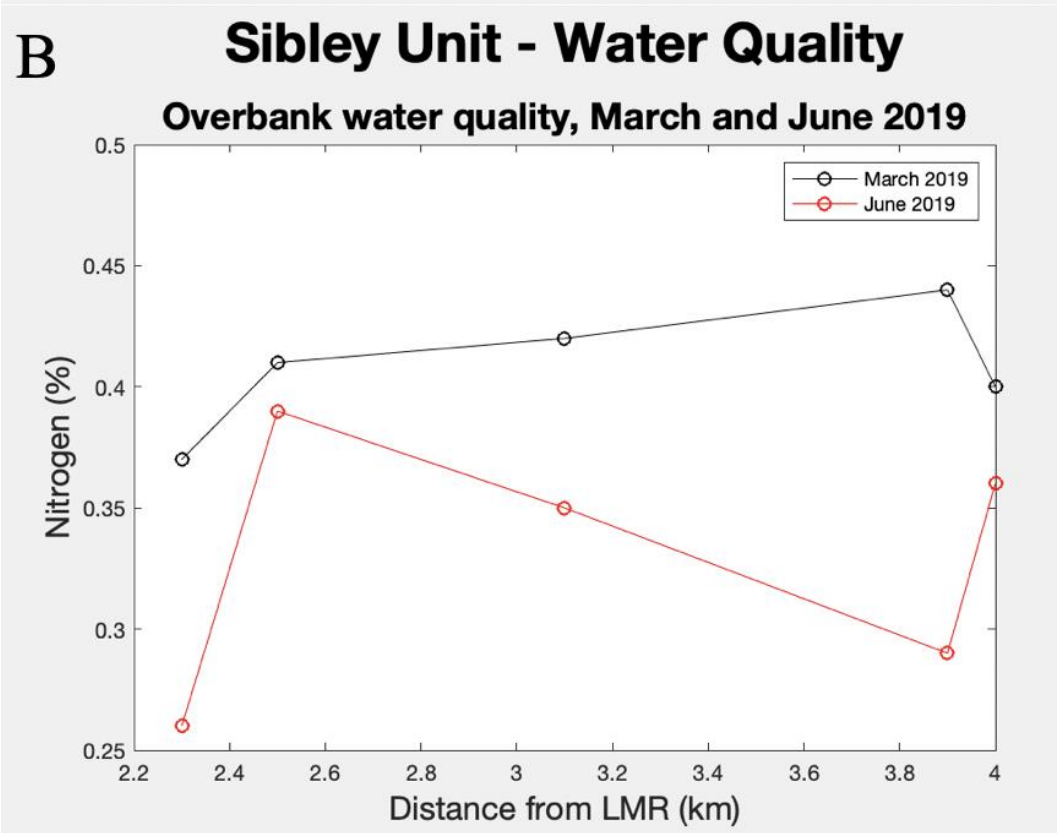
Sibley Unit - Water Quality
Overbank water quality, March and June 2019
March 2019
June 2019
Nitrogen (%)
Distance from LMR (km)
0.5
0.45
0.4
0.35
0.3
0.25
2.2
2.4
2.6
2.8
3
3.2
3.4
3.6
3.8
4

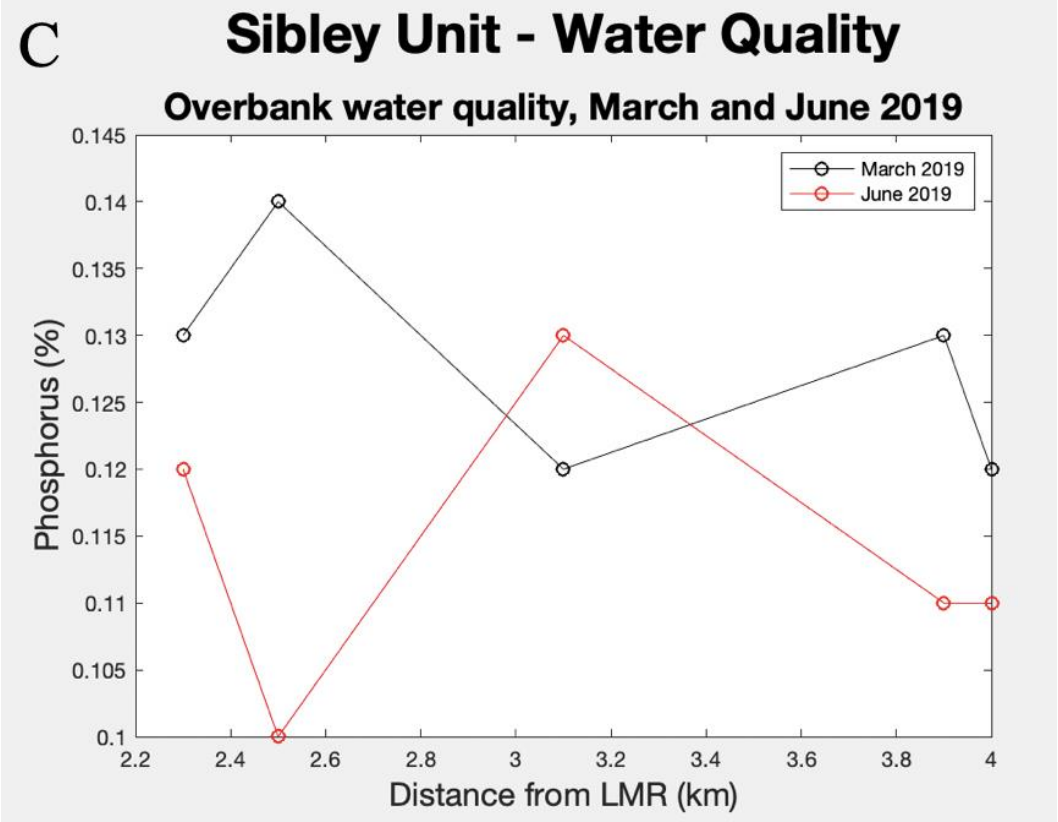

Figure 6.38 *Three plots of water samples QW01 to QW05 at the Sibley Unit for weight by percent during both March and June 2019.*

Note: A is carbon, B is nitrogen, and C is phosphorus. March 2019 is black and June 2019 is red.

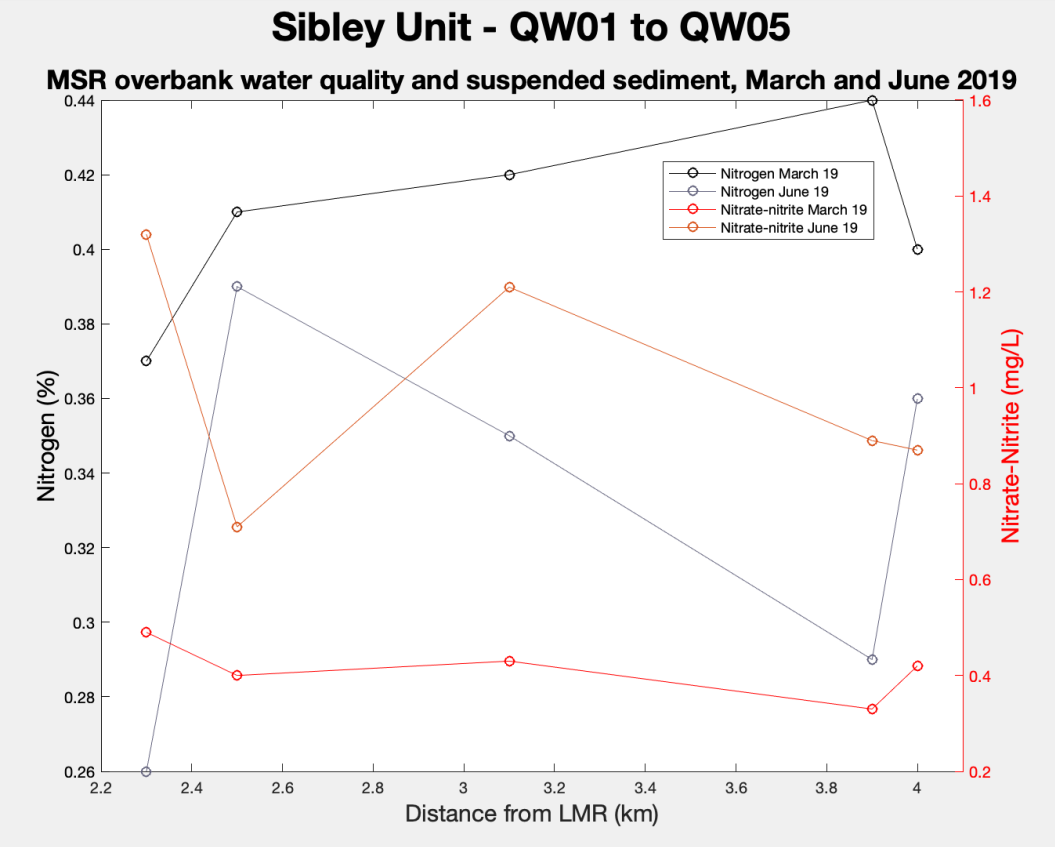

Figure 6.39 *A plot of water samples QW01 to QW05 at the Sibley Unit for phosphorus (%) and nitrogen (mg/L) during both March and June 2019.*

Note: Nitrogen (%) is black and gray and nitrogen (mg/L) is red and orange. Nitrogen (%) is derived from suspended sediment samples and nitrogen (mg/L) is derived from filtered water samples.

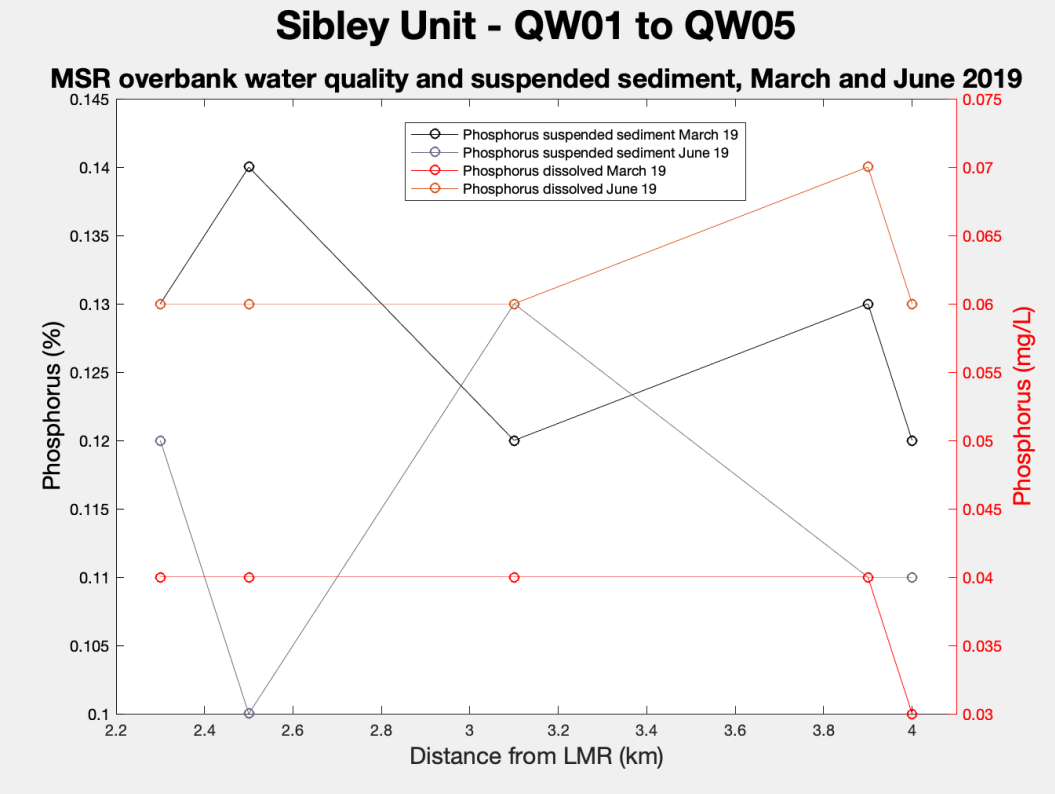

Figure 6.40 *A plot of water samples QW01 to QW05 at the Sibley Unit for phosphorus (%) and nitrogen (mg/L) during both March and June 2019.*

Note: Nitrogen (%) is black and gray and nitrogen (mg/L) is red and orange. Nitrogen (%) is derived from suspended sediment samples and nitrogen (mg/L) is derived from filtered water samples.

For this portion of the study, Sibley Unit's samples are observed as a transect from the main LMR channel (QW_02, QW_03, QW_04, QW_01, and QW_05). There is an increase in flow depth distal from the levee crest and into the backswamp. A decrease in suspended sediment concentration occurs further from the LMR in both March and June 2019. Oppositely, an overall increase in carbon and nutrients is observed with increased distance into the floodplain (backswamp). Overbank flow velocity as expected, decreases with distance from the main LMR. This decrease in velocity may be a large contributing factor to the decrease in sediment and an increase in carbon and nutrients due to a ponding effect in the backswamp. Another factor that likely influences these

patterns is that the further the distance the water in the floodplain has traveled, the more contact with soils it has (i.e., potential gains), resulting in an increase in dissolved C, N, and P.

6.3.3 WILKINSON COUNTY

Suspended sediment and water-quality values during the 2019 flood in the southern region of water sample sites between Loch Leven, Artonish Lake, and Fort Adams in Wilkinson County (QW09 to QW13) are more variable than the Cloverdale Unit and the Sibley Unit. There are no detectable trends in overbank water quality when applying a transect perpendicular from the LMR channel; however trends are observed with overbank flow distance, particularly for sample QW09QW09 is the furthest overbank water-quality sample location from the LMR and has the lowest values of multiple water-quality parameters (DO (mg/L), conductivity (μS/cm), TDS (mg/L), salinity (ppt), and pH) than the other sample locations. QW13 and QW09 both occur in the southernmost part of the study area; however QW13 is located closer to the "funnel" of the entire embanked floodplain and the LMR channel. QW09 is in a backswamp along the bluff line where the overbank flow has traversed a considerable distance with dense vegetation along the eastern edge of the floodplain.

All samples at Wilkinson County being considered as an entire floodplain basin, suspended sediment and nitrogen increase with distance from the LMR (Figures 6.51 and 6.55). Oppositely, nitrogen decreases with distance from the LMR (Figure 6.54). These trends in water-quality and suspended-sediment values in June 2019 in Wilkinson County vary because each sample site (of the 5) is relatively unique. QW09 is along the bluff line and overbank water had to flow across a long distance (continuous soil contact) of

dense vegetation; QW10 is relatively close to the LMR channel, but the flow direction was coming from Lake Mary meaning that that water was in the oxbow lake and perhaps across part of the open field at Loch Leven; QW11 was relatively close to the river and was a combination of water from QW10 and water directly from the LMR channel; QW12 basically flowed a reasonable distance across the meander scroll environment in the Artonish Lake area and was the fastest velocity because of its proximity to the "funnel" of the embanked floodplain; finally QW13 traveled a long-distance overbank flow path but is located along the edge of influence of that raging Buffalo River where its waters could easily flow into an open field just north of our sampling site and diffuse down to where the author sampled (Fig 6.51 to 6.55).

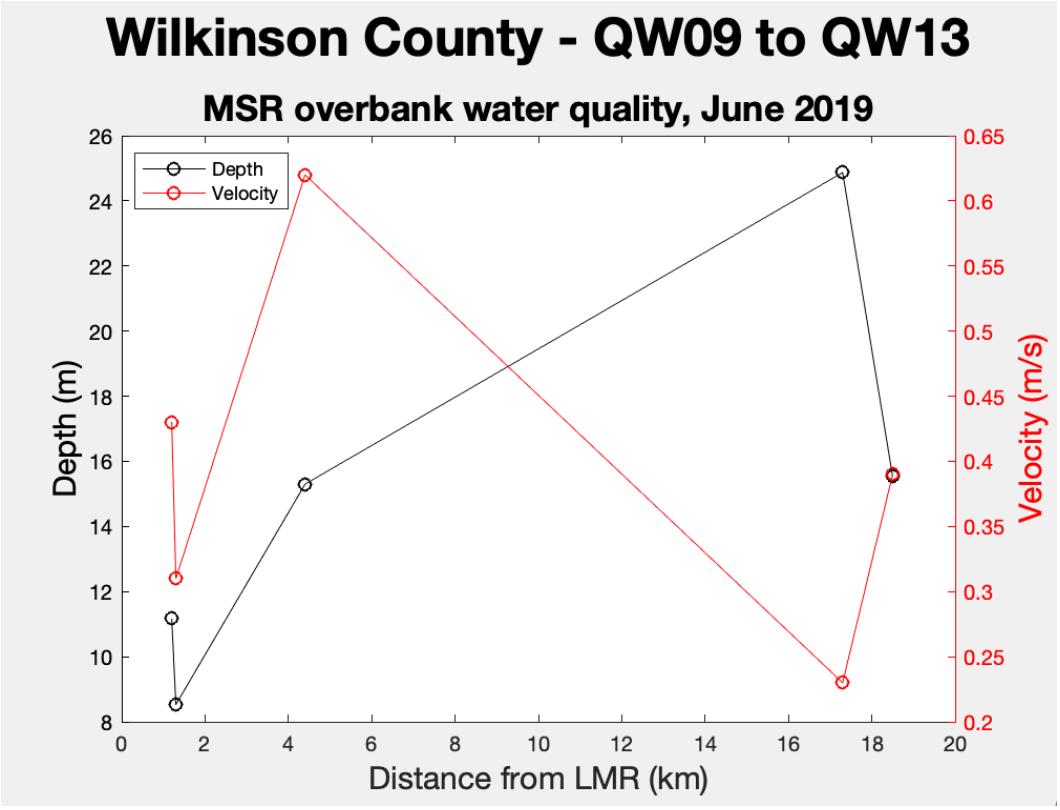

Figure 6.41 *A plot of water samples QW09 to QW13 at Wilkinson County.*

Note: Depth (m) is plotted on the left y-axis (black) and velocity is plotted on the right y-axis (red) during only June 2019.

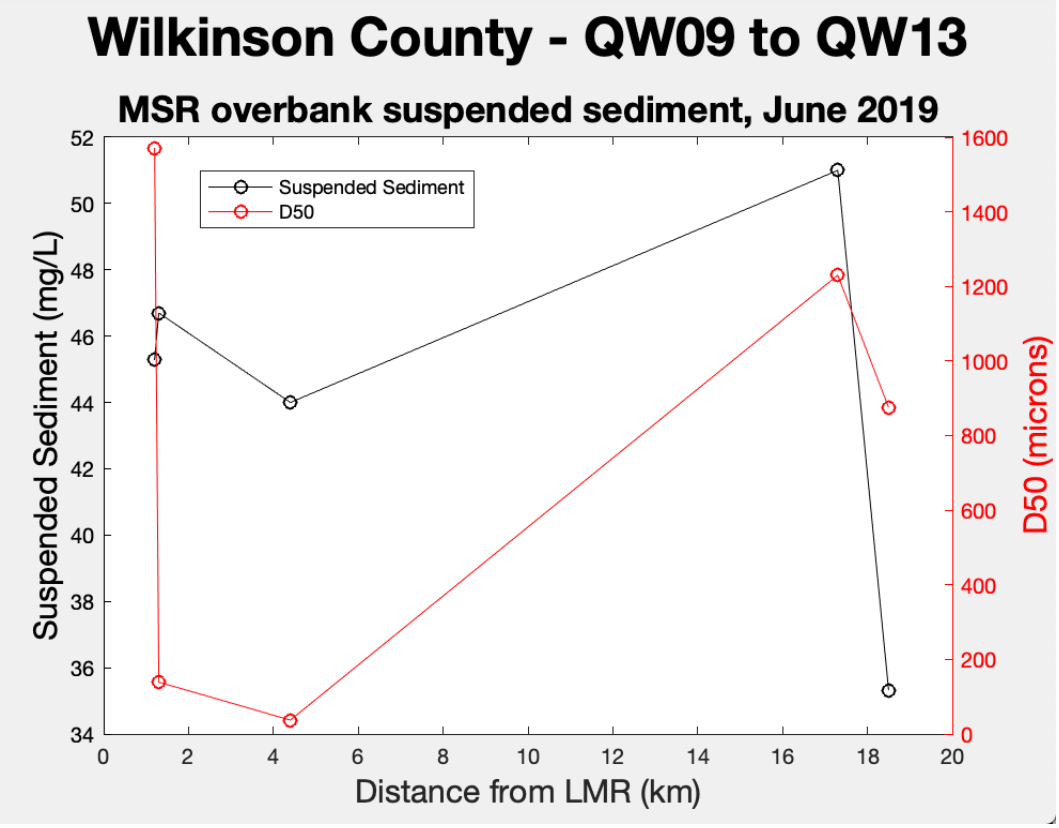

Figure 6.42 *A plot of water samples QW09 to QW13 at Wilkinson County.*

Note: Suspended sediment is plotted on the left y-axis (black) and D50 is plotted on the right y-axis (red) during only June 2019.

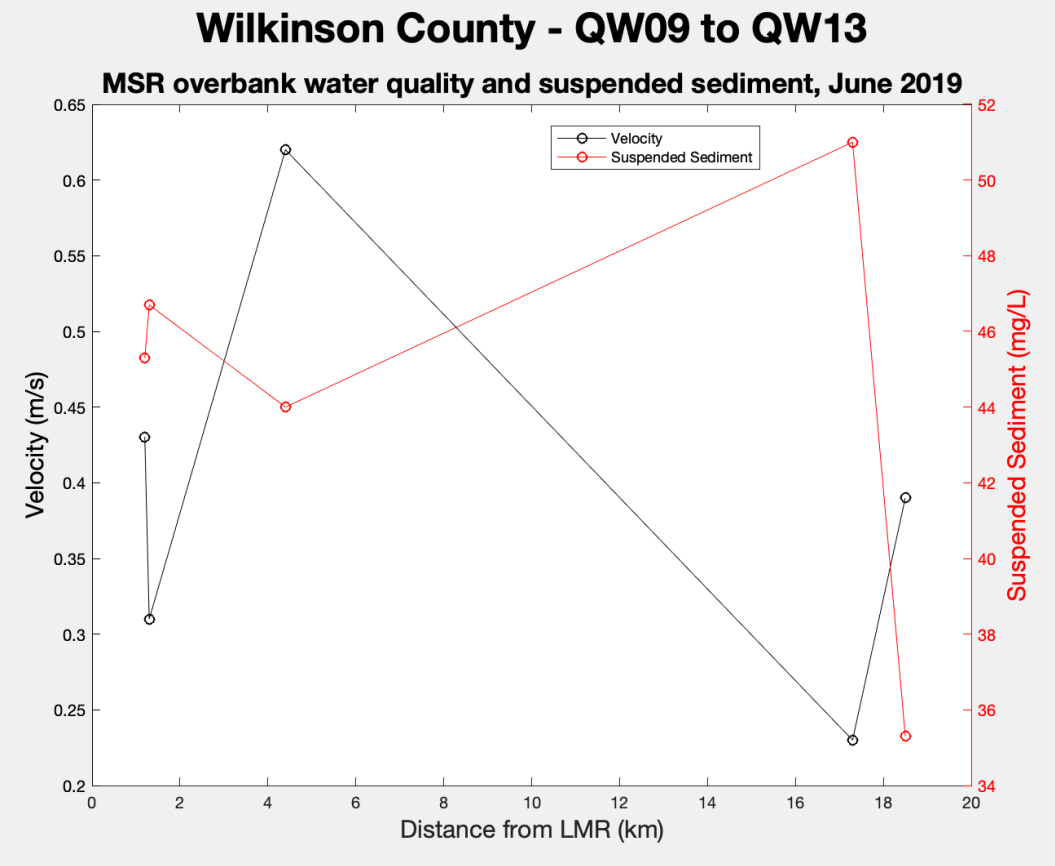

Figure 6.43 *A plot of water samples QW09 to QW13 at Wilkinson County.*

Note: Velocity is plotted on the left y-axis (black) and suspended sediment is plotted on the right y-axis (red) during only June 2019.

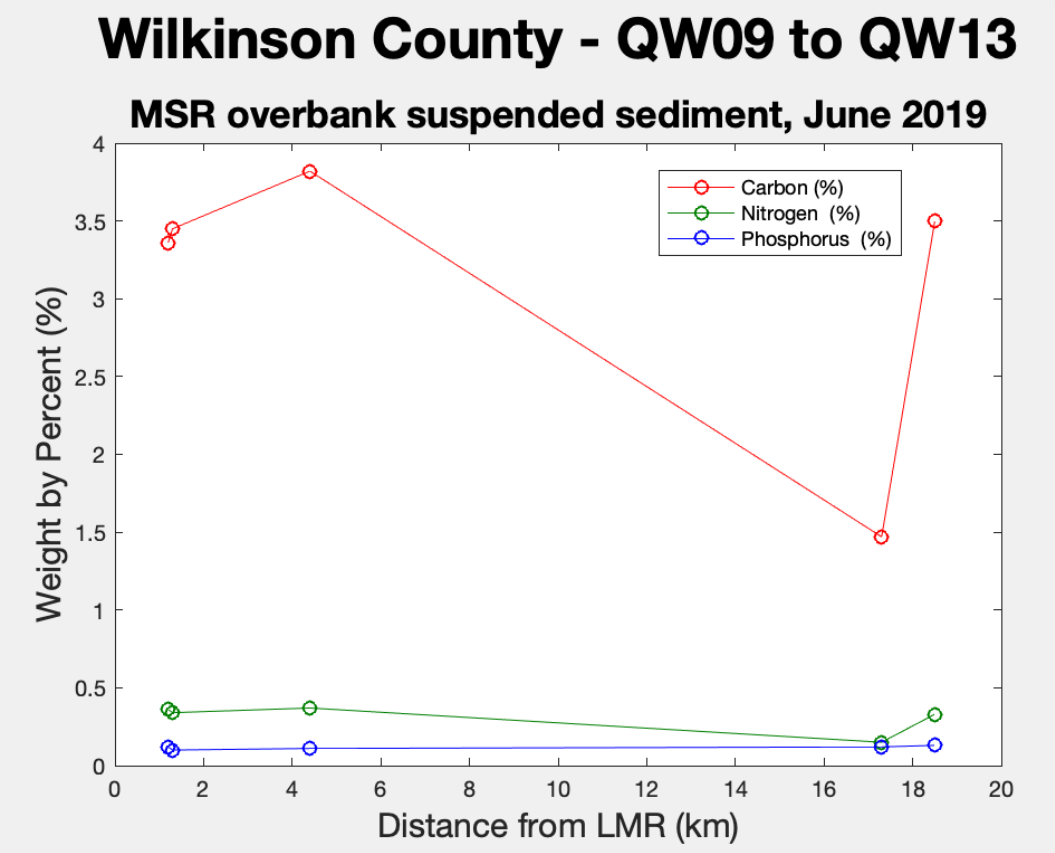

Figure 6.44 *A plot of water samples QW09 to QW13 at Wilkinson County of percent by weight.*

Note: N is nitrogen (green), C is carbon (red), and P is phosphorus (blue).

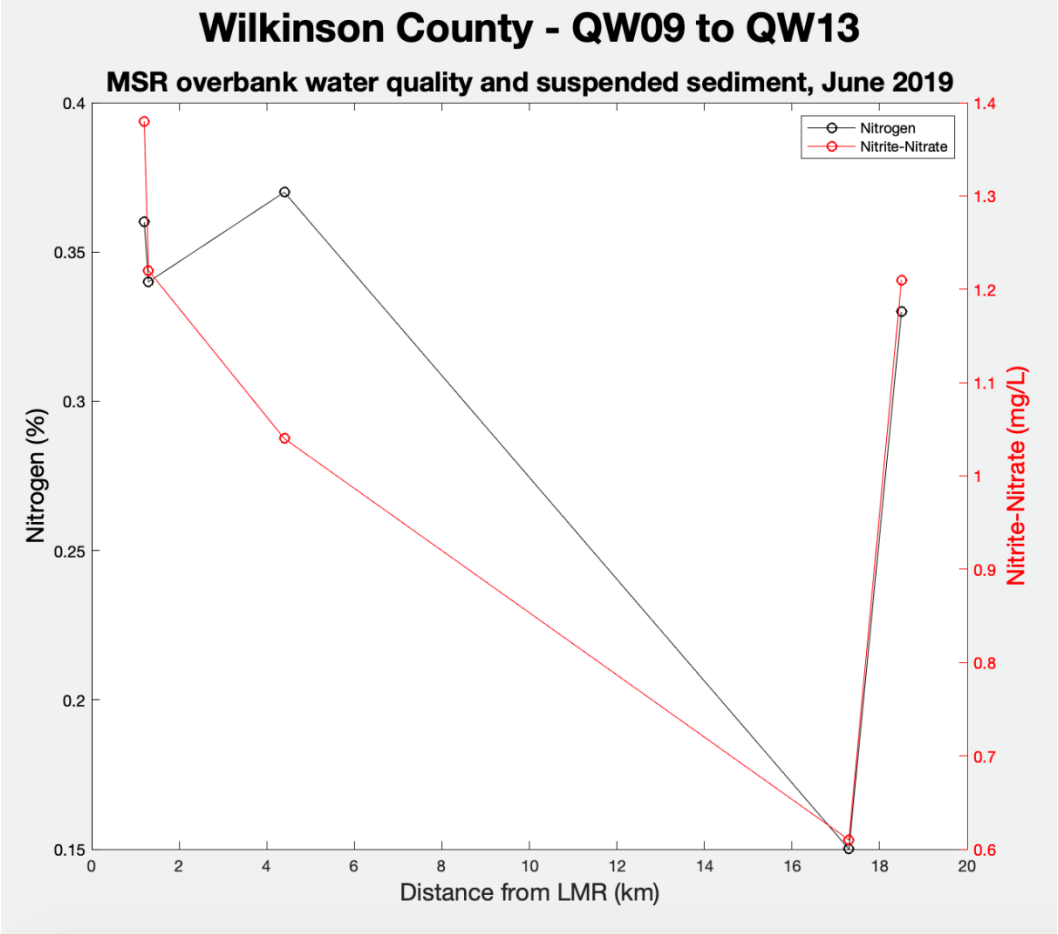

Figure 6.45 *A plot of water samples QW09 to QW13 at Wilkinson County.*

Note: Nitrogen (%) is plotted on the left y-axis (black) and Nitrite plus nitrate (mg/L) is plotted on the right y-axis (red) during only June 2019.

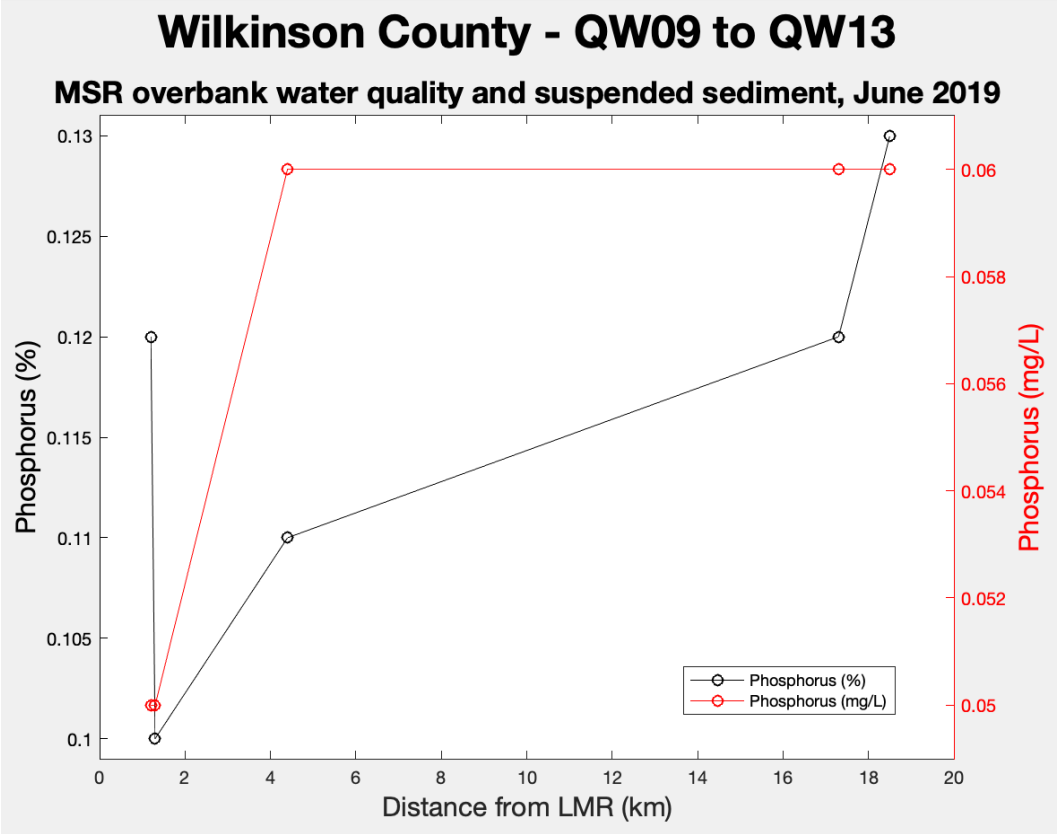

Figure 6.46 *A plot of water samples QW09 to QW13 at Wilkinson County.*

Note: Phosphorus (%) is plotted on the left y-axis (black) and phosphorus (mg/L) is plotted on the right y-axis (red) during only June 2019.

6.3.4 LMR CHANNEL

Two stations along the LMR main channel, Vicksburg, MS and St. Francisville, LA, were periodically sampled for suspended sediment and various water-quality parameters during the 2019 flood. Vicksburg had higher suspended sediment concentration (mg/L) values in comparison to St. Francisville, LA, likely because St. Francisville is located downstream of the Old River Control Structure. The Old River Control Structure diverts ~25% of the flow volume from upstream, including sediment (located between the study area and Baton Rouge). During floods, there is an expected

increase in suspended sediment (mg/L) and nutrient concentrations (N, C, P in mg/L) at both locations.

The patterns of suspended sediment and nutrient concentrations are similar for both Vicksburg and St. Francisville (the timing, shape, and symmetry of the peaks), but St. Francisville exhibits a more muted peak due to the Old River Control Structure. Both Vicksburg and St. Francisville have peak measurements of suspended sediment during the 2018 water year that coincidently occur during the 2018 flood. However, during the 2019 water year the max suspended sediment values do no coincide with the 2019 flood. At Vicksburg, the three peaks of suspended sediment during the 2018 through 2019 water years occurred on February 26, 2018 (388 mg/L), September 20, 2018 (475 mg/L), and October 17, 2019 (276 mg/L). At St. Francisville, the three peaks of suspended sediment during the 2018 through 2019 water years occurred on March 01, 2018 (289 mg/L), July 09, 2018 (215 mg/L), , and October 24, 2019 (201 mg/L). For both locations, the February 26, 2018 (388 mg/L) and the March 01, 2018 (289 mg/L) peaks occurred a few weeks before the peak stage height of the 2018 flood on March 18th. Coinciding with the period of maximum stage, however, the suspended sediment concentration declined to 142 mg/L on 3/16/18 at Vicksburg and 95 mg/L on 3/12/18 at St. Francisville. During the 2019 flood, the peaks occurring within the flood duration of the 2019 flood were very small (92 mg/L on 3/11/19), in comparison to the surrounding peaks of July, September, and October. This shows that the 2018 flood had a greater suspended sediment concentration than the 2019 flood.

During the same sampling periods (2018 and 2019 water years) at Vicksburg and St. Francisville, nutrient concentrations decreased during times of flooding, unlike

suspended sediment. At Vicksburg, near the period of maximum stage height for the 2018 flood on 3/16/2018, phosphorus (mg/L) reached the lowest concentration of 0.05 mg/L of the 2018 water year (0.12 mg/L being the highest value). At Vicksburg, during the 2019 flood, phosphorus (mg/L) during the peak stage height was 0.06 mg/L on 3/12/19, which was the lowest value recorded for the 2019 water year (0.11 mg/L being the highest value). At St. Francisville, phosphorus was 0.06 mg/L on 3/16/18, being the second lowest for the 2018 water year (0.05 mg/L for the lowest value and 0.12 mg/L being the highest value). During the 2019 flood at St. Francisville, phosphorus was 0.06 mg/L on 3/11/19, which was the lowest value recorded for the 2019 water year (0.17 mg/L on 6/17/19).

At Vicksburg, near the period of maximum stage height for the 2018 flood on 3/16/2018, nitrate plus nitrite (mg/L) reached the lowest concentration of 1.15 mg/L for the 2018 water year (2.89 mg/L being the highest value). At Vicksburg, during the 2019 flood, nitrate plus nitrite (mg/L) during the peak stage height was 1.00 mg/L on 3/12/19, which was the second lowest value recorded for the 2019 water year (0.81 mg/L being the lowest and 1.64 mg/L being the highest value). At St. Francisville, nitrate plus nitrite was 0.99 mg/L on 3/12/18, being the third lowest concentration for the 2018 water year (0.48 mg/L for the lowest value and 2.51 mg/L being the highest value). During the 2019 flood at St. Francisville, the nitrate plus nitrite was 1.05 mg/L on 3/11/19, which was the second lowest value recorded for the 2019 water year (0.95 mg/L being the lowest and 1.65 mg/L on 6/17/19).

Suspended sediment is the only variable that increases with discharge during major floods along the LMR. Nutrient concentrations for the LMR expectedly decrease

during major flood events because of dilution and re-distribution throughout the floodplain. Nutrient concentrations increase during the receding limb of the flood, possibly resulting from floodplain draining to the main LMR channel.

6.3.5 COMPARISON OF OVERBANK WATER QUALITY AND THE LMR CHANNEL

All floodplain environments (natural levee, backswamp, meander scroll) had somewhat variable suspended sediment concentrations and water quality values (including carbon and nutrients). The overbank water samples collected in March and June 2019 indicate an overall decrease in suspended sediment concentrations and flow velocities with distance from the main channel; whereas an increase in carbon and nutrients was observed. In comparison to the main LMR channel at both Vicksburg and St. Francisville, sediment concentrations ranged from 60 to 630 mg/L, whereas the samples collected in the floodplain ranged from 24.3 to 56.8 mg/L (Figure 6.56). Main channel data for phosphorus ranged from 0.05 to 0.17 mg/L, whereas concentrations in the floodplain ranged from 0.03 to 0.08 mg/L (Figure 6.57). Main channel data for nitrate plus nitrite ranged from 0.48 to 2.13 mg/L, whereas concentrations in the floodplain ranged from 0.33 to 1.29 mg/L (Figure 6.58). Phosphorus and nitrate plus nitrite samples collected in the floodplain were equal to or greater than LMR main channel data throughout multiple times of non-inundation of the 2018 and 2019 water year. Whereas, suspended sediment concentrations in the floodplain never reached the levels measured in the LMR on coinciding dates of LMR samples and author samples for both 2018 and 2019 water years. This further indicates that suspended sediment decreases and nutrients increase with distance into the floodplain.

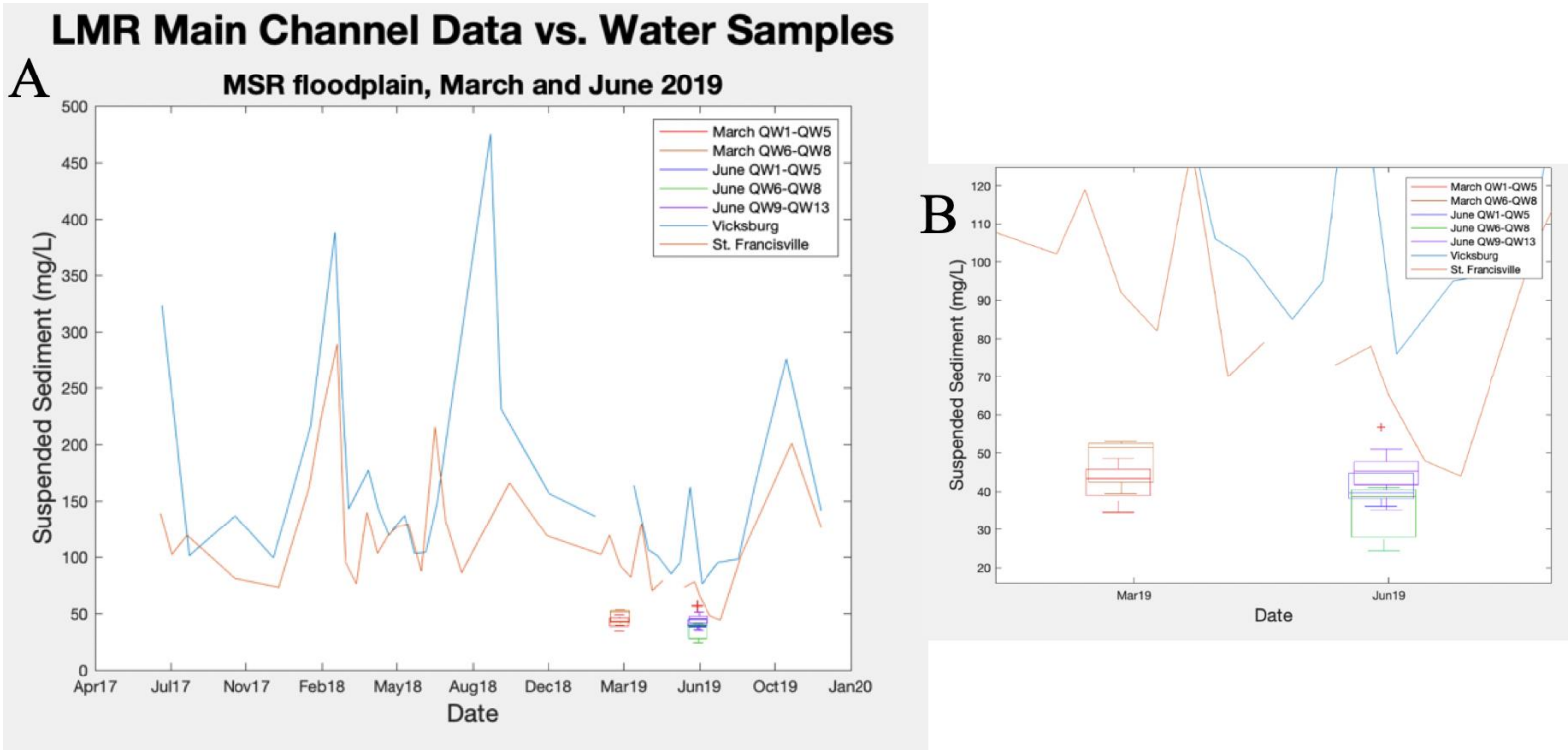

Figure 6.47 *Hydrograph of suspended sediment (mg/L) for the authors' water quality data (boxplots) plotted against the LMR main channel data (lines).*

Note: Graph A is the full dataset and graph B is a zoomed in version of the data to better view the box plots.

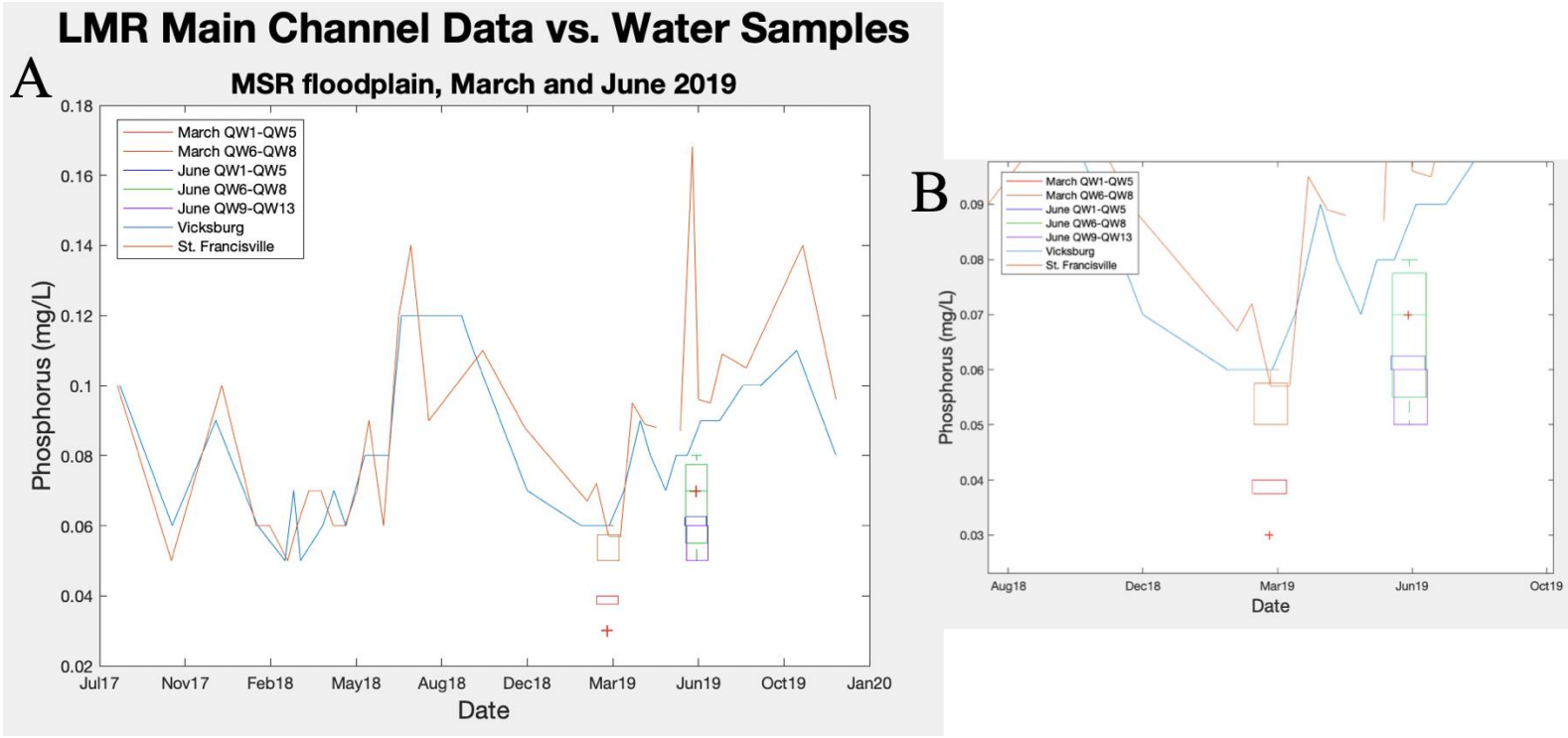

Figure 6.48 *Hydrograph of phosphorus (mg/L) for the authors' water quality data (boxplots) plotted against the LMR main channel data (lines).*

Note: Graph A is the full dataset and graph B is a zoomed in version of the data to better view the box plots.

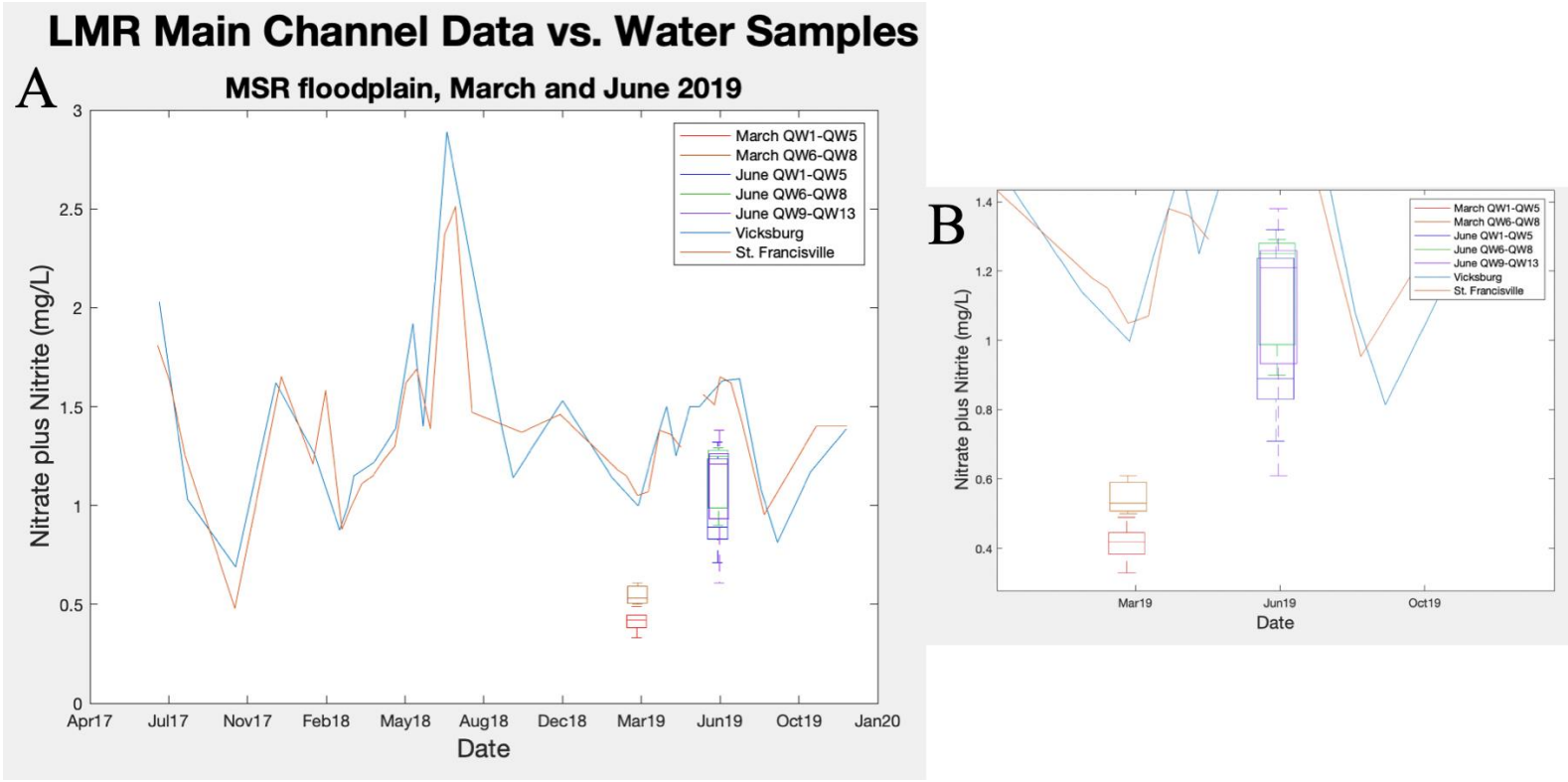

Figure 6.49 *Hydrograph of suspended nitrate plus nitrite (mg/L) for the authors' water quality data (boxplots) plotted against the LMR main channel data (lines).*

Note: Graph A is the full dataset and graph B is a zoomed in version of the data to better view the box plots.

The low values of suspended sediment during the times of overbank water sample collection can be explained due to various reasons. During the flood of 1993, the Upper Mississippi River received low rates of sediment into the floodplain. The relatively minor floodplain deposition was caused by an excess of sediment already transported earlier in the season, resulting in a lack of sediment supply during the flood (Gomez et al., 1997; Magilligan et al., 1998). This might be the case for the 2019 flood because it was the longest flood duration on record for the area. This caused the floodplain in the study areas to be inundated for a large portion the year. The previous 2018 flood might have exhausted available sediment (before the 2019 flood) and sediment loads transported by the 2019 flood were distributed over a longer duration of time.

The source areas for the 2018 and 2019 flood varied when observing the precipitation maps. Before and during the 2018 flood, precipitation originated in and around the Ohio River basin. Previous studies show that the Ohio River valley provides less sediment than the other tributaries. Before and during the 2019 flood, precipitation originated in three major tributary systems: the Ohio River, the MS River, and the Missouri River drainage basins. Each basin is known for a different type of flood. The Missouri River, provides more suspended sediment. The Arkansas River, then moderate amounts of sediment expected. The Ohio River, provides less sediment than the other tributary. The 2019 flood had large inputs from the Arkansas River, but flooding being from four tributaries, a combination of sediment and nutrients was provided.

Suspended sediment data and percent sand was observed from the main Mississippi channel of Vicksburg and St. Francisville. The fluxes of sediment was compared to differing discharge values throughout the 2018 and 2019 water year. Figure

Figure 6.49 shows that suspended sediment peaked before the 2018 flood (max discharge). The percent sand was less after the 2018 flood. Suspended sediment peaked for the 2019 flood before the peak discharge. The percent sand was greater after the 2018 flood. This showing that major floods can have a hysteresis cycle of large amounts of sediment before the main discharge peak of the flood entirety.

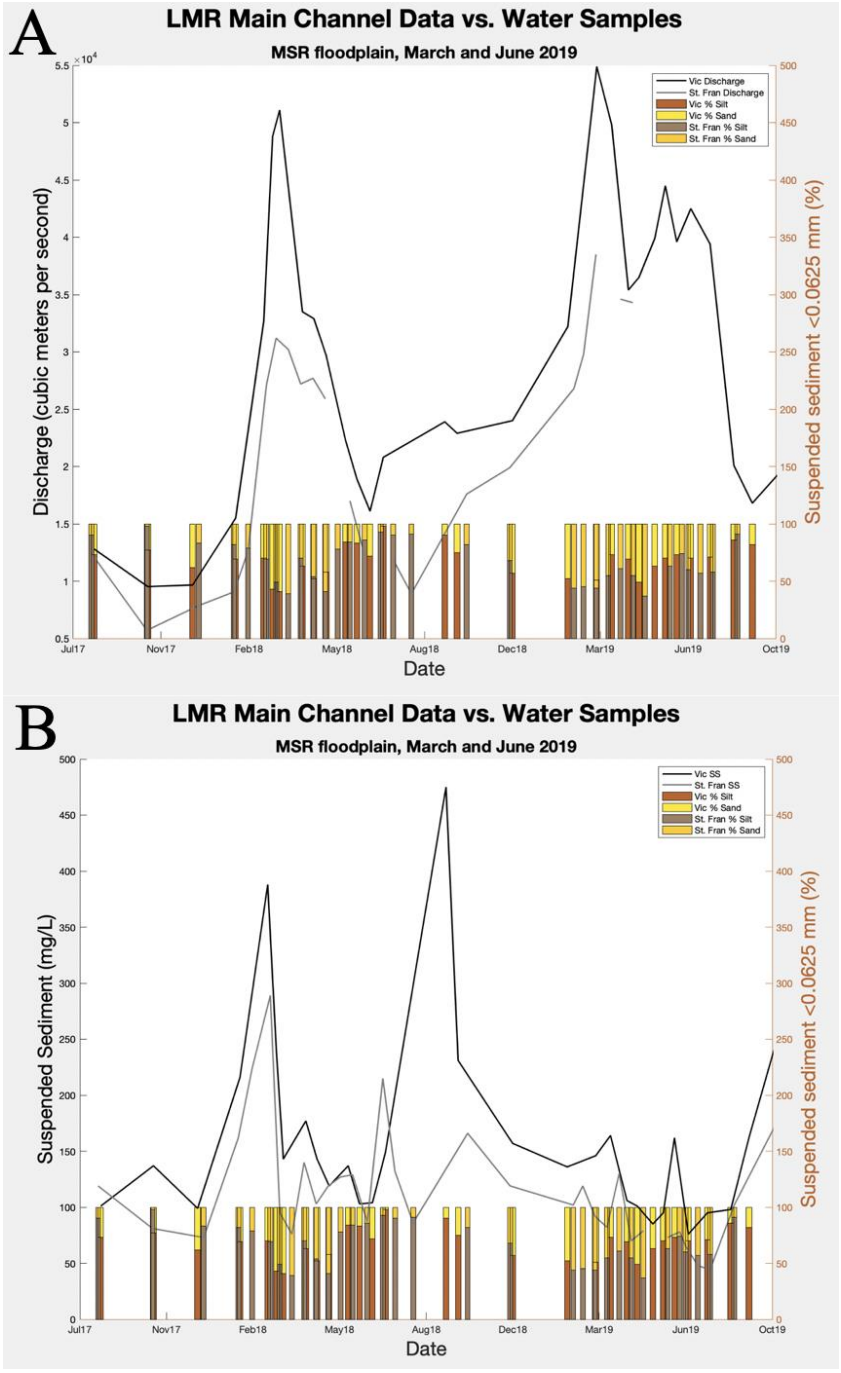

Figure 6.50 *Hydrograph of (A) discharge and percentage sand and (B) suspended sediment (mg/L) for the the LMR main channel data (US Army Corps of Engineers, 2020).*

Note: Graph A is discharge data (left) of the LMR and graph B is suspended sediment data (left) of the LMR. Both A and B have suspended sediment percentages of sand and silt/clay, where brown is silt/clay percent and yellow is sand percent.

Hysteresis cycles result in sediment concentration values that differ throughout the period of flooding. Depending on the given year, timing, and source areas of a flood, maximum concentrations of suspended sediment can occur both before and after a flood crest. Figure 6.59 depicts different patterns and peaks between the measured values of mean daily discharge and suspended sediment concentration along the Mississippi River (Mossa, 1989). These peak values often do not align with the peak stage and flood. For the 2019 flood, suspended sediment peaked before and after the peak stage height. Patterns of increased suspended sediment and nutrient values off peak of the flooding events occurred for all study locations and LMR channel data.

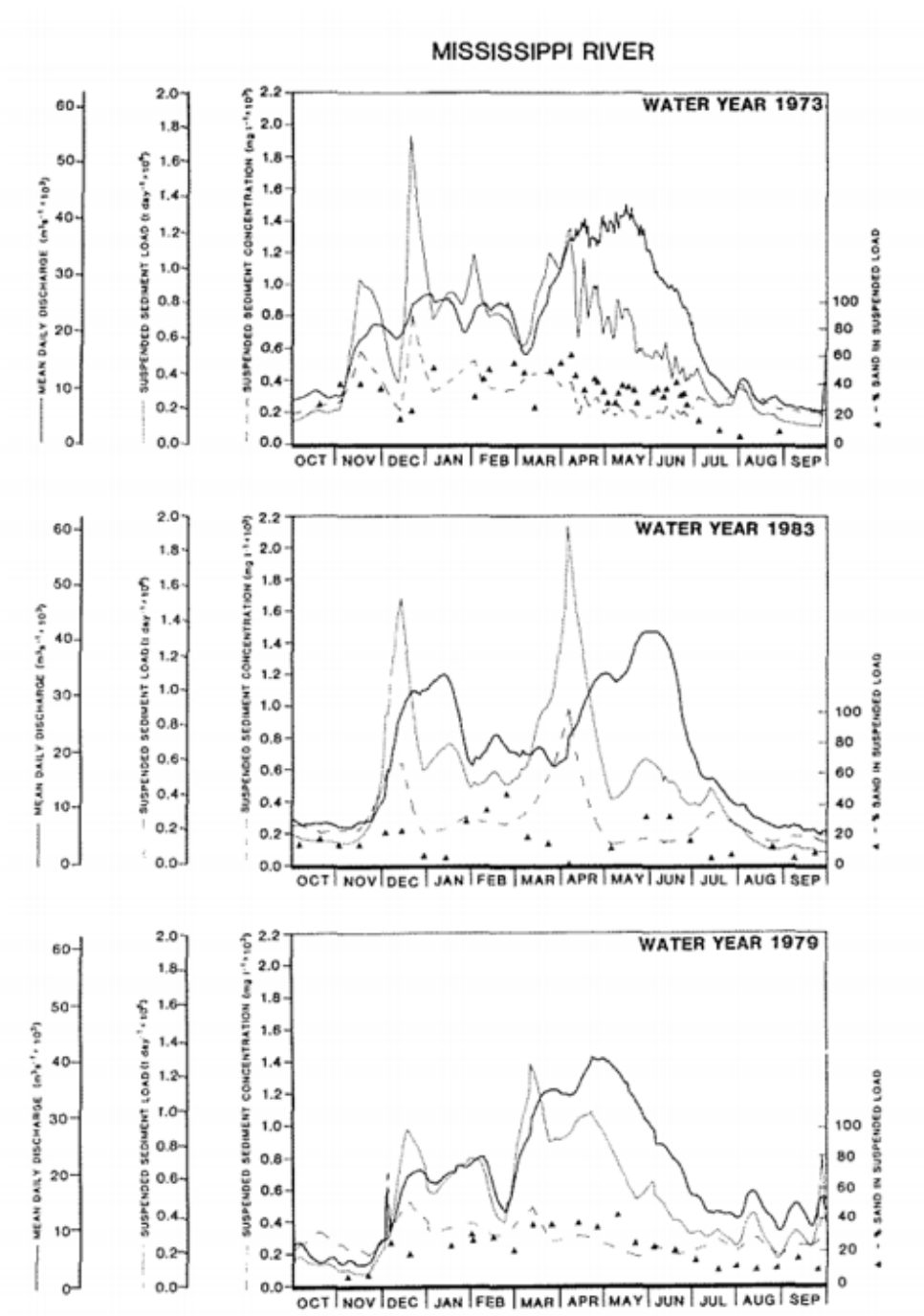

Figure 6.51 *Time series of different years of hysteresis on the LMR at Tarbert Landing. Discharge and sediment concentrations are plotted on the y-axis (from Mossa, 1989).*

CHAPTER VII – CONCLUSIONS

The Lower Mississippi River (LMR) near Natchez, Mississippi, experienced intervals of major flooding during the 2018 and 2019 water years. Analysis of floodplain-surface sediments, overbank water levels, and overbank water quality associated with the 2018 and 2019 floods has led to a better understanding of the deposition and sequestration of sediment, carbon, and nutrients in the embanked floodplain. Overall, overbank patterns associated with distance from the LMR channel indicate a decrease in grain size (in both deposited and suspended sediment), suspended sediment concentration, flow velocity, and turbidity. Opposite relations with distance from the LMR channel are apparent by increases in organic matter, carbon, and nutrients (nitrogen and phosphorus). Therefore, as a whole, physical characteristics are inversely related to adsorbed and dissolved compositions of the overbank sediment and water column, respectively.

The sediment samples collected from the floodplain surface in October 2017 and September 2018 all had environmental differences, but tended to show an anticipated pattern of fining with distance from the LMR channel. This hypothesis was supported by sediment samples in T8, T9, T3, T1, and T2 in 2017 and T8, T9, T13, T3, T1 following the 2018 flood using distance from main LMR channel. A fining of sediment an overall increase in organic matter, carbon, and nutrients was found.

When classifying each transect by environment; levee, backswamp, and meander scroll, the transects studied followed previously reported patterns of levee and ridges having a larger sediment size than backswamps and swales, with a fining transition into backswamp and ponded areas of meander scrolls. T1 and T2 best fit the previous

classifications of a floodplain transitioning from a levee into a backswamp for sediment deposition style. This included a fining sequence with increased distance into the backswamp. Along with the fining sequence, an increase in organic matter, carbon, and nutrients were found. The meander scroll subenvironment T4 had very well defined ridge and swale characteristics transitioning into longer ponding periods becoming closer to Long Lake. These areas where ponding occurs, a decrease in sediment size and an increase in organic matter, carbon, and nutrients was observed.

Floodplain surface samples and overbank water column levels indicate complete lateral connectivity across the floodplain during both the 2018 and 2019 floods, albeit downstream propagation of maximum flood stages was slightly postponed during the 2019 flood. . The 2018 flood peaks between Natchez and Wilkinson County (i.e., Lake Mary / Artonish Lake) occurred on the same day. During the 2019 flood, the maximum stage at the northern water sensors (Long Lake and Sibley Unit) occurred on 03/12/2019, six days before the southern sensors (Lake Mary and Artonish Lake) on 03/18/2019. It remains unknown if flood management actions (i.e., release schedules at the Old River Control Structure and/or the Bonnet Carré Spillway) contributed to the temporal patterns of maximum stage upstream. Overbank water temperature during both floods (2018 and 2019) had minor peaks of increased temperature during and after peak inundation (maximum stage). Ideally, overbank sequestration of nutrients will be maximized in seasonally later floods because of higher water temperatures.

Drainage basin control of the MSR has a large influence on each flood event that occurs in the LMR floodplain. The hydroclimatology and where the source of water originated has a large influence on the quantity of water, nutrients, and suspended

sediment. These different source areas effect the hydrotopography and hysteresis patterns of both the 2018 and 2019 flood. In previous studies it has been proven that the majority of suspended sediment originates from the Missouri Basin, where oppositely the Ohio area provides low suspended sediment (Mossa, 1996). Hysteresis cycles of high discharge events tend to show suspended sediment peaks 40-85 days after peak discharges (Mossa, 1996). Comparing to the author's suspended sediment data and main LMR channel data, peak discharge occurred after both the 2018 and the 2019 flood.

Overbank water-quality data collected in different floodplain subenvironments during the long-duration 2019 flood were relatively similar across space. Temperature, pH, salinity, total dissolved solids (TDS), conductivity, and dissolved oxygen (DO) were constant across space during each sample period (March 2019 and June 2019). However, a comparison of the two sampling periods indicate that the higher overbank water temperature in March was associated with differences in other parameters, including an increase in TDS and salinity and a decrease in DO and pH.

The most important control of overbank water quality is associated with distance from the LMR channel. Most data discussed accounted for distance and direction of overbank flow from the LMR, however flow direction perpendicular distances from the LMR is important to consider. These perpendicular flow patterns were especially recognized within the Sibley Unit with flow being directed from the SCCNWR. Suspended sediment concentrations and grain sizes decreased with distance from the channel. Although carbon and nutrient levels did not change much with increasing distance from the channel, dissolved carbon and nutrients generally increased with the

embanked floodplain width, possibly indicating that these constituents are incorporated from the inundated floodplain soils and submerged vegetation into the overbank column.

Future research is needed in this area in order to fully understand how flooding affects sedimentation and nutrient sequestration in the embanked floodplain. Additional transects aligned at different orientations to the LMR channel and other floodplain water bodies will support a better understanding of how water, sediment, and nutrients move throughout the floodplain. Each flood is unique and will have a different spatial pattern, suspended sediment and dissolved constituent hysteresis cycle, sediment load, discharge, and duration. These variables must be considered when collecting overbank flood and sediment data. A more comprehensive overbank flood database is needed to provide better statistical analyses of spatial and temporal trends.

Transect Samples
October 2017 Samples

Table A.1 *Transect 4 (Cloverdale Unit): Sediment Samples*

Transect ID (m)	Munsell Color (Value/Chroma)	D (10)	D (50)	D (90)	OM Wt%	MS	N Wt%	C Wt%	P Wt%
04.01.00	10YR(3/3)	4.0	92.3	442	16.34	2.10E-04	0.34	2.61	0.02
04.02.10	10YR(3/3)	3.9	44.9	216	11.11	2.16E-04	0.21	1.91	0.09
04.03.20	10YR(3/2)	4.4	58.2	249	13.39	2.32E-04	0.28	2.64	0.11
04.04.40	10YR(4/2)	5.0	105.0	453	13.63	2.24E-04	0.40	3.01	0.14
04.05.50	10YR(3/3)	5.9	113.0	443	13.45	1.84E-04	0.34	2.80	0.14
04.06.61	10YR(4/2)	3.8	47.8	242	11.50	2.29E-04	0.22	2.02	0.08
04.07.80	10YR(3/3)	3.7	43.2	215	12.50	2.38E-04	0.40	3.64	0.19
04.08.90	10YR(3/3)	5.5	96.0	421	12.33	2.34E-04	0.37	2.87	0.16
04.09.100	10YR(3/3)	3.2	26.9	139	8.42	2.33E-04	0.27	2.47	0.11
04.10.110	10YR(3/3)	10.5	101.0	229	7.64	2.14E-04	0.18	1.72	0.05
04.11.120	10YR(3/2)	2.9	25.1	127	12.70	2.08E-04	0.33	3.33	0.09
04.12.130	10YR(3/2)	7.2	116.0	454	11.65	2.41E-04	0.26	2.66	0.10

Note: Grain size percentiles (D(%)) are in microns. OM, N, C, and P percentages are from weight. Magnetic susceptibility (MS) is * 10^{-4} m^3kg^{-1}.

September 2018 Samples

Table A.2 *Transect 4 (Cloverdale Unit): Sediment Samples*

Transect ID (m)	Munsell Color (Value/Chroma)	D (10)	D (50)	D (90)	OM Wt%	MS	N Wt%	C Wt%	P Wt%
24B.00	10YR(3/2)	5.4	59.0	328	12.78	2.41E-04	0.44	3.01	0.16
25B.09	10YR(3/2)	5.9	67.5	296	16.46	2.41E-04	0.48	4.30	0.14
26B.25	10YR(3/2)	4.6	57.4	257	14.83	2.65E-04	0.35	3.27	0.12
27B.38	10YR(3/2)	5.3	51.9	266	14.11	2.18E-04	0.45	4.34	0.15
28B.58	10YR(3/3)	5.2	53.1	257	15.92	2.04E-04	0.45	4.10	0.16
29B.79	10YR(3/2)	4.6	45.5	225	15.18	2.48E-04	0.39	3.07	0.15

Note: Grain size percentiles (D(%)) are in microns. OM, N, C, and P percentages are from weight. Magnetic susceptibility (MS) is * 10^{-4} m^3kg^{-1}.

October 2017 Samples

Table A.3 *Transect 5 (Cloverdale Unit): Sediment Samples*

Transect ID (m)	Munsell Color (Value/Chroma)	D (10)	D (50)	D (90)	OM Wt%	MS	N Wt%	C Wt%	P Wt%
05.01.00A	10YR(3/3)	5.0	54.4	538	12.70	2.68E-04	0.26	2.18	0.13
05.01.00B	10YR(4/2)	6.3	101.0	434	10.92	2.12E-04	0.21	1.75	0.10
05.02.10	10YR(3/3)	3.2	24.1	162	10.11	2.50E-04	0.14	1.30	0.08
05.03.20	10YR(3/2)	6.3	112.0	478	10.52	3.27E-04	0.16	1.48	0.08

Note: Grain size percentiles (D(%)) are in microns. OM, N, C, and P percentages are from weight. Magnetic susceptibility (MS) is * 10^{-4} m^3kg^{-1}.

September 2018

Table A.4 *Transect 5 (Cloverdale Unit): Sediment Samples*

Transect ID (m)	Munsell Color (Value/Chroma)	D (10)	D (50)	D (90)	OM Wt%	MS	N Wt%	C Wt%	P Wt%
36B.00	10YR(3/2)	4.9	37.7	182	9.89	4.50E-04	0.21	2.14	0.10
36BB.00	10YR(3/2)	6.8	74.4	293	9.07	4.18E-04	0.23	2.18	0.13
37B.01	10YR(4/2)	5.6	52.6	253	8.82	3.50E-04	0.17	1.67	0.09
38B.01	10YR(3/2)	5.2	41.1	245	11.88	2.59E-04	0.25	2.45	0.11
38BB.21	10YR(3/2)	4.9	38.5	233	11.32	2.38E-04	0.26	2.51	0.13

Note: Grain size percentiles (D(%)) are in microns. OM, N, C, and P percentages are from weight. Magnetic susceptibility (MS) is * 10^{-4} m^3kg^{-1}.

Table A.5 *Transect 7 (Butler Lake): Sediment Samples*

Transect ID (m)	Munsell Color (Value/Chroma)	D (10)	D (50)	D (90)	OM Wt%	MS	N Wt%	C Wt%	P Wt%
07.01.00	10YR(3/2)	4.0	30.7	189	13.23	3.82E-04	0.27	2.61	0.10
07.02.13	10YR(3/2)	2.8	17.6	65	12.42	3.73E-04	0.25	2.65	0.10

Note: Grain size percentiles (D(%)) are in microns. OM, N, C, and P percentages are from weight. Magnetic susceptibility (MS) is * 10^{-4} m^3kg^{-1}.

October 2017 Samples

Table A.6 *Transect 8 (Salt Lake): Sediment Samples*

Transect ID (m)	Munsell Color (Value/Chroma)	D (10)	D (50)	D (90)	OM Wt%	MS	N Wt%	C Wt%	P Wt%
08.01.00	10YR(3/2)	5.2	61.9	334	17.53	3.34E-04	0.45	5.71	0.11
08.02.73	10YR(3/2)	5.3	83.3	334	15.52	3.94E-04	0.44	5.40	0.11
08.03.135	10YR(3/2)	2.8	27.3	183	15.15	3.63E-04	0.40	5.20	0.12
08.04.234	10YR(3/2)	2.6	22.4	165	13.43	2.75E-04	0.34	4.16	0.10
08.05.475	10YR(3/2)	2.8	24.1	169	17.44	2.67E-04	0.34	4.05	0.10

Note: Grain size percentiles (D(%)) are in microns. OM, N, C, and P percentages are from weight. Magnetic susceptibility (MS) is * 10^{-4} m^3kg^{-1}.

October 2017 Samples

Table A.7 *Transect 9 (Sibley Unit): Sediment Samples*

Transect ID (m)	Munsell Color (Value/Chroma)	D (10)	D (50)	D (90)	OM Wt%	MS	N Wt%	C Wt%	P Wt%
09.02.00	10YR(3/2)	4.8	28.6	107	9.90	3.79E-04	0.17	1.76	0.07
09.01.27	10YR(3/2)	5.1	37.1	174	10.08	3.99E-04	0.16	1.71	0.10
09.03.77	10YR(3/3)	5.6	44.6	203	14.73	4.80E-04	0.20	2.02	0.16
09.04.168	10YR(3/2)	4.1	28.1	132	10.09	4.78E-04	0.18	1.82	0.08
09.05.223	10YR(4/2)	4.0	24.5	113	9.02	4.06E-04	0.17	1.77	0.07

Note: Grain size percentiles (D(%)) are in microns. OM, N, C, and P percentages are from weight. Magnetic susceptibility (MS) is * 10^{-4} m^3kg^{-1}.

October 2017 Samples

Table A.8 *Transect 10 (Sibley Unit): Sediment Samples*

Transect ID (m)	Munsell Color (Value/Chroma)	D (10)	D (50)	D (90)	OM Wt%	MS	N Wt%	C Wt%	P Wt%
10.01.0	10YR(4/2)	9.3	49.1	133	4.95	4.82E-04	0.08	1.06	0.05
10.02.180	10YR(3/2)	9.8	45.0	134	6.84	3.63E-04	0.16	1.82	0.06

Note: Grain size percentiles (D(%)) are in microns. OM, N, C, and P percentages are from weight. Magnetic susceptibility (MS) is * 10^{-4} m^3kg^{-1}.

October 2017 Samples

Table A.9 *Transect 11 (Sibley Unit): Sediment Samples*

Transect ID (m)	Munsell Color (Value/Chroma)	D (10)	D (50)	D (90)	OM Wt%	MS	N Wt%	C Wt%	P Wt%
11.01.0	10YR(5/3)	118.0	186.0	289	0.58	1.44E-03	0.01	0.16	0.02
11.02.160	10YR(3/2)	5.6	32.8	89	5.77	4.13E-04	0.14	1.67	0.06
11.03.316	10YR(4/2)	4.1	26.9	98	7.55	3.66E-04	0.18	1.84	0.09

Note: Grain size percentiles (D(%)) are in microns. OM, N, C, and P percentages are from weight. Magnetic susceptibility (MS) is * 10^{-4} m^3kg^{-1}.

September 2018

Table A.10 *Transect 11 (Sibley Unit): Sediment Samples*

Transect ID (m)	Munsell Color (Value/Chroma)	D (10)	D (50)	D (90)	OM Wt%	MS	N Wt%	C Wt%	P Wt%
56B.00	10YR(3/2)	5.6	33.2	227	8.74	3.95E-04	0.17	2	0.09
57B.43	10YR(4/3)	6.0	34.5	191	8.25	3.94E-04	0.15	1.76	0.08

Note: Grain size percentiles (D(%)) are in microns. OM, N, C, and P percentages are from weight. Magnetic susceptibility (MS) is * 10^{-4} m^3kg^{-1}.

October 2017 Samples

Table A.11 *Transect 12 (Sibley Unit): Sediment Samples*

Transect ID (m)	Munsell Color (Value/Chroma)	D (10)	D (50)	D (90)	OM Wt%	MS	N Wt%	C Wt%	P Wt%
12.01.0	10YR(3/2)	3.5	26.3	164	9.26	3.33E-04	0.26	2.73	0.08
12.02.134	10YR(3/2)	4.6	41.1	291	11.59	3.20E-04	0.27	3.22	0.07
12.03.1808	10YR(3/2)	2.8	28.4	175	11.83	3.67E-04	0.27	3.14	0.10

Note: Grain size percentiles (D(%)) are in microns. OM, N, C, and P percentages are from weight. Magnetic susceptibility (MS) is * 10^{-4} m^3kg^{-1}.

September 2018

Table A.12 *Transect 13 (Sibley Unit): Sediment Samples*

Transect ID (m)	Munsell Color (Value/Chroma)	D (10)	D (50)	D (90)	OM Wt%	MS	N Wt%	C Wt%	P Wt%
12B.00	10YR(3/3)	7.9	43.5	182	6.47	4.21E-04	0.09	1.30	0.05
13B.11	10YR(3/2)	11.7	56.2	194	5.47	4.24E-04	0.085	1.44	0.05
14B.26	10YR(3/3)	27.1	65.5	135	2.91	3.47E-04	0.045	0.83	0.04
15B.44	10YR(3/3)	87.8	148.0	234	1.26	3.47E-04	0.02	0.50	0.03
16B.69	10YR(3/3)	23.5	116.0	214	3.01	6.19E-04	0.04	0.97	0.04
17B.97	10YR(3/2)	19.9	84.8	173	3.11	5.56E-04	0.035	0.65	0.04
18B.119	10YR(4/3)	17.6	76.2	163	3.58	5.53E-04	0.045	0.85	0.04
19B.142	10YR(3/2)	8.8	45.0	148	6.53	4.26E-04	0.12	1.64	0.06

Note: Grain size percentiles (D(%)) are in microns. OM, N, C, and P percentages are from weight. Magnetic susceptibility (MS) is * 10^{-4} m^3kg^{-1}.

October 2017 Samples

Table A.13 *Transect 3 (Lake Mary): Sediment Samples*

Transect ID (m)	Munsell Color (Value/Chroma)	D (10)	D (50)	D (90)	OM LOI%	MS	N Wt%	C Wt%	P Wt%
03.01.00	10YR(3/3)	78.7	163.0	281	1.39	7.56E-04	0.02	0.47	0.02
03.02.10	10YR(4/3)	21.2	71.9	183	2.52	6.32E-04	0.04	0.54	0.03
03.03.20	10YR(3/3)	18.2	67.9	201	4.20	4.48E-04	0.06	0.90	0.04
03.04.40	10YR(3/3)	10.3	48.0	177	5.98	4.15E-04	0.12	1.53	0.05
03.05.60	10YR(3/3)	14.7	54.7	178	5.80	3.86E-04	0.11	1.41	0.05
03.06.80	10YR(3/3)	12.3	59.5	264	7.17	3.67E-04	0.16	1.75	0.06
03.07.120	10YR(4/2)	5.1	31.4	127	9.84	3.62E-04	0.25	2.78	0.08
03.08.160	10YR(4/2)	4.3	27.9	134	8.56	3.14E-04	0.16	1.88	0.06
03.09.190	10YR(3/2)	6.1	38.8	214	8.67	3.40E-04	0.20	2.12	0.08

Note: Grain size percentiles (D(%)) are in microns. OM, N, C, and P percentages are from weight. Magnetic susceptibility (MS) is * 10^{-4} m^3kg^{-1}.

October 2017 Samples

Table A.14 *Transect 1 (Fort Adams): Sediment Samples*

Transect ID (m)	Munsell Color (Value/Chroma)	D (10)	D (50)	D (90)	OM Wt%	MS	N Wt%	C Wt%	P Wt%
01.01.00	2.5Y(4/4)	114.0	189.0	295	0.98	3.26E-04	0.01	0.21	0.02
01.02.10	10YR(3/2)	23.2	91.6	186	6.24	4.27E-04	0.11	2.06	0.04
01.03.20	10YR(4/3)	31.5	109.0	207	3.15	5.22E-04	0.09	1.49	0.04
01.04.40	10YR(3/4)	9.1	54.9	154	3.57	5.30E-04	0.10	1.37	0.05
01.05.60	10YR(4/2)	17.9	78.1	188	2.47	4.85E-04	0.05	0.73	0.04
01.06.80	10YR(4/2)	12.1	74.6	194	3.57	4.88E-04	0.07	0.95	0.03
01.07.120	10YR(3/3)	9.3	48.2	150	6.05	3.90E-04	0.14	1.55	0.05
01.08.160	10YR(4/2)	8.9	45.7	139	6.63	3.92E-04	0.15	1.65	0.06
01.09.190	10YR(3/3)	13.8	64.6	215	5.18	4.72E-04	0.11	1.38	0.05
01.10.347	10YR(3/2)	6.8	49.0	308	10.28	3.18E-04	0.31	3.27	0.08
01.11.524	10YR(3/2)	6.8	55.8	508	9.90	3.09E-04	0.22	2.06	0.07
01.12.652	10YR(3/2)	7.1	60.1	445	8.86	3.46E-04	0.21	2.27	0.08
01.13.830	10YR(3/3)	7.6	60.4	484	8.78	3.92E-04	0.24	3.10	0.05
01.14.1032	10YR(3/3)	16.7	59.1	221	7.13	3.41E-04	0.19	2.69	0.06
01.15.1151	10YR(3/4)	22.9	138.0	329	1.26	3.06E-04	0.01	0.13	0.01

Note: Grain size percentiles (D(%)) are in microns. OM, N, C, and P percentages are from weight. Magnetic susceptibility (MS) is * 10^{-4} m^3kg^{-1}.

September 2018

Table A.15 *Transect 1 (Fort Adams): Sediment Samples*

Transect ID (m)	Munsell Color (Value/Chroma)	D (10)	D (50)	D (90)	OM Wt%	MS	N Wt%	C Wt%	P Wt%
5B.00	10YR(3/3)	8.4	41.5	123	4.46	4.27E-04	0.075	1.08	0.10
6B.21	10YR(3/3)	10.2	50.1	142	4.62	5.05E-04	0.07	1.18	0.10
7B.59	10YR(3/2)	6.5	36.5	121	7.83	3.91E-04	0.165	2.01	0.08
8B.91	10YR(3/2)	10.9	54.9	147	7.59	4.38E-04	0.14	2.00	0.06
9B.129	10YR(3/2)	15.9	69.4	254	7.21	4.49E-04	0.14	1.97	0.06

Note: Grain size percentiles (D(%)) are in microns. OM, N, C, and P percentages are from weight. Magnetic susceptibility (MS) is * 10^{-4} m^3kg^{-1}.

October 2017 Samples

Table A.16 *Transect 2 (Fort Adams): Sediment Samples*

Transect ID (m)	Munsell Color (Value/Chroma)	D (10)	D (50)	D (90)	OM Wt%	MS	N Wt%	C Wt%	P Wt%
02.16.00	10YR(4/3)	85.6	151.0	248	1.03	6.27E-04	0.01	0.26	0.03
02.17.10	10YR(4/3)	19.5	83.9	179	3.57	5.10E-04	0.08	1.18	0.04
02.18.20	10YR(3/3)	14.4	68.5	270	4.26	4.77E-04	0.10	1.36	0.04
02.19.40	10YR(3/3)	24.7	166.0	305	3.61	3.39E-04	0.07	1.15	0.03
02.20.53	10YR(3/2)	10.4	63.7	252	6.31	3.95E-04	0.07	0.85	0.03
02.21.80	10YR(4/3)	24.6	125.0	255	2.42	5.67E-04	0.06	0.71	0.03
02.22.120	10YR(4/2)	9.5	59.0	196	5.63	4.82E-04	0.11	1.30	0.04
02.23.160	10YR(3/2)	6.3	37.8	155	8.27	4.01E-04	0.22	2.73	0.07

Note: Grain size percentiles (D(%)) are in microns. OM, N, C, and P percentages are from weight. Magnetic susceptibility (MS) is * 10^{-4} m^3kg^{-1}.

Discrete Samples
October, 2019
Table A.17 *Transect 6 (Cartharage Point Road): Sediment Samples*

Transect ID (m)	Munsell Color (Value/Chroma)	D (10)	D (50)	D (90)	OM Wt%	MS	N Wt%	C Wt%	P Wt%
06.01.00	10YR(4/3)	114.0	194.0	308	0.89	5.17E-04	0.01	0.19	0.02

Note: Grain size percentiles (D(%)) are in microns. OM, N, C, and P percentages are from weight. Magnetic susceptibility (MS) is * 10^{-4} m^3kg^{-1}.

September 2018
Table A.18 *Transect 6 (Cartharage Point Road): Sediment Samples*

Transect ID (m)	Munsell Color (Value/Chroma)	D (10)	D (50)	D (90)	OM Wt%	MS	N Wt%	C Wt%	P Wt%
40B.00	10YR(3/4)	66.3	173.0	296	1.61	1.12E-03	0.02	0.34	0.03

Note: Grain size percentiles (D(%)) are in microns. OM, N, C, and P percentages are from weight. Magnetic susceptibility (MS) is * 10^{-4} m^3kg^{-1}.

Pit Samples
September 2018
Table A.19 *Sibley Unit Trench (Sibley Unit): Sediment Samples*

Transect ID (mm)	Munsell Color (Value/Chroma)	D (10)	D (50)	D (90)	OM Wt%	MS	N Wt%	C Wt%	P Wt%
C1B.42	10YR(3/2)	8.4	54.1	203	5.63	4.71E-04	0.08	1.18	0.05
S1B.153	10YR(3/3)	84.3	159.0	263	0.82	5.41E-04	0.005	0.25	0.03
C2B.168	10YR(3/3)	10.6	57.2	173	4.12	4.98E-04	0.06	0.87	0.04
S2B.230	2.5 Y(4/4)	79.3	138.0	228	0.84	1.17E-03	0.01	0.21	0.03
C3B.259	10YR(3/3)	13.1	58.0	183	4.16	4.69E-04	0.065	0.945	0.05
S3B.461	10YR(4/4)	112.0	184.0	289	0.82	5.14E-04	0.005	0.145	0.02
C4B.N/A	10YR(3/3)	16.3	85.7	191	3.36	5.15E-04	0.06	0.975	0.04

Note: Grain size percentiles (D(%)) are in microns. OM, N, C, and P percentages are from weight. Magnetic susceptibility (MS) is * 10^{-4} m^3kg^{-1}.

Cloverdale Unit
March 2019

Table A.20 *Transect 2 (Cloverdale Unit) (Sites 6-8): Filter Papers from Water Samples (field and lab)*

Transect ID (km)	Avg. Depth (m)	Velocity (m/s)	SS (mg/L)	D (10)	D (50)	D (90)	N (%)	C (%)	P (%)	Turbidity (NTU)
QW06_4.6	7.19	0.54	39.5	2.69	12.30	891.00	0.39	3.36	0.12	50
QW07_4.5	4.82	0.41	53.0	3.60	20.60	1910.00	0.39	3.37	0.13	70
QW08_4.0	6.09	0.27	51.4	3.90	30.60	958.00	0.36	3.05	0.12	36

Note: Average depth are in meters. Percentiles are in microns. N, C, and P percentages are from weight. Suspended Sediment are in mg/L. Velocities are in m/s. Turbidities are in NTU.

Table A.21 *Transect 2 (Cloverdale Unit) (Sites 6-8): Water Quality Samples at Depth of 0.25 meters*

Transect ID (km)	Temp. (°C)	DO (%)	DO (mg/L)	Conductivity (µS/cm)	TDS (mg/L)	Salinity (ppt)	pH	ORP (mV)
QW06_4.6	8.10	89.90	10.52	175.30	168.35	0.12	6.88	-62.90
QW07_4.5	8.10	90.70	10.62	174.90	167.70	0.12	6.85	-40.40
QW08_4.0	8.20	91.10	10.62	174.20	167.05	0.12	6.98	-44.90

Note: Temperatures are in degrees Celsius. Dissolved oxygen values are listed as a percent and mg/L. Conductivities are in µS/cm. Total dissolved solids are mg/L. Salinities are in parts per trillions. Oxidation reduction potential values are in mega volts.

Table A.22 *Transect 2 (Cloverdale Unit) (Sites 6-8): Water Quality Samples at Depth of 5.0 meters*

Transect ID (km)	Temp. (°C)	DO (%)	DO (mg/L)	Conductivity (µS/cm)	TDS (mg/L)	Salinity (ppt)	pH	ORP (mV)
QW06_4.6	8.00	89.20	10.46	175.00	168.35	0.12	6.68	-36.90
QW07_4.5	8.00	90.00	10.55	174.40	167.70	0.12	6.51	-22.00
QW08_4.0	8.10	90.00	10.53	173.60	167.05	0.12	6.56	-23.50

Note: Temperatures are in degrees Celsius. Dissolved oxygen values are listed as a percent and mg/L. Conductivities are in µS/cm. Total dissolved solids are mg/L. Salinities are in parts per trillions. Oxidation reduction potential values are in mega volts.

Table A.23 *Transect 2 (Cloverdale Unit) (Sites 6-8): Water Samples Filtered (Lab)*

Transect ID (km)	P (mg/L)	Nitrite-Nitrate (mg/L)
QW06_4.6	0.06	0.61
QW07_4.5	0.05	0.53
QW08_4.0	0.05	0.50

Note: P and Nitrite-Nitrate values are in mg/L.

June 2019

Table A.24 *Transect 2 (Cloverdale Unit) (Sites 6-8): Filter Papers from Water Samples (field and lab)*

Transect ID (km)	Avg. Depth (m)	Velocity (m/s)	SS (mg/L)	D (10)	D (50)	D (90)	N (%)	C (%)	P (%)	Turbidity (NTU)
QW06_4.6	7.32	0.07	24.30	3.06	247.00	660.00	0.45	4.68	0.13	32
QW07_4.5	3.14	0.13	38.70	2.23	11.00	1620.00	0.38	3.70	0.13	45
QW08_4.0	6.14	0.21	41.10	2.91	10.50	284.00	0.39	3.73	0.14	45

Note: Average depth are in meters. Percentiles are in microns. N, C, and P percentages are from weight. Suspended Sediment are in mg/L. Velocities are in m/s. Turbidities are in NTU.

Table A.25 *Transect 2 (Cloverdale Unit) (Sites 6-8): Water Quality Samples at Depth of 0.25 meters*

Transect ID (km)	Temp. (°C)	DO (%)	DO (mg/L)	Conductivity (µS/cm)	TDS (mg/L)	Salinity (ppt)	pH	ORP (mV)
QW06_4.6	26.50	82.70	6.64	394.00	249.60	0.18	6.35	-32.40
QW07_4.5	26.30	79.00	6.38	385.40	244.40	0.18	6.15	14.60
QW08_4.0	26.50	81.90	6.57	399.90	252.20	0.18	6.22	-10.40

Note: Temperatures are in degrees Celsius. Dissolved oxygen values are listed as a percent and mg/L. Conductivities are in µS/cm. Total dissolved solids are mg/L. Salinities are in parts per trillions. Oxidation reduction potential values are in mega volts.

Table A.26 *Transect 2 (Cloverdale Unit) (Sites 6-8): Water Quality Samples at Depth of 5.0 meters*

Transect ID (km)	Temp. (°C)	DO (%)	DO (mg/L)	Conductivity (µS/cm)	TDS (mg/L)	Salinity (ppt)	pH	ORP (mV)
QW06_4.6	26.00	75.10	6.05	390.70	248.95	0.18	6.25	-17.40
QW07_4.5	26.20	78.50	6.32	391.70	248.95	0.18	6.42	9.90
QW08_4.0	26.40	81.00	6.49	399.20	252.85	0.18	6.95	39.70

Note: Temperatures are in degrees Celsius. Dissolved oxygen values are listed as a percent and mg/L. Conductivities are in µS/cm. Total dissolved solids are mg/L. Salinities are in parts per trillions. Oxidation reduction potential values are in mega volts.

Table A.27 *Transect 2 (Cloverdale Unit) (Sites 6-8): Water Samples Filtered (Lab)*

Transect ID (km)	P (mg/L)	Nitrite-Nitrate (mg/L)
QW06_4.6	0.08	1.25
QW07_4.5	0.07	0.90
QW08_4.0	0.05	1.29

Note: P and Nitrite-Nitrate values are in mg/L.

Sibley Unit
March 2019

Table A.28 *Transect 1 (Sibley Unit) (Sites 1-5): Filter Papers from Water Samples (field and lab)*

Transect ID (km)	Avg. Depth (m)	Velocity (m/s)	SS (mg/L)	D (10)	D (50)	D (90)	N (%)	C (%)	P (%)	Turbidity (NTU)
QW01_3.9	7.18	1.06	34.6	3.14	110.00	1910.00	0.44	4.24	0.13	34
QW02_2.3	5.34	1.00	48.7	3.44	73.20	840.00	0.37	3.38	0.13	24
QW03_3.1	5.95	1.35	43.4	3.03	184.00	584.00	0.42	3.86	0.12	35
QW04_4.0	5.86	0.15	44.9	2.90	14.30	734.00	0.40	3.33	0.12	50
QW05_2.5	7.75	0.63	40.4	3.06	17.00	761.00	0.41	3.60	0.14	35

Note: Average depth in meters. Percentiles are in microns. N, C, and P percentages are from weight. Suspended sediment in mg/L. Velocity in m/s. Turbidity in nephelometric turbidity units (NTU).

Table A.29 *Transect 1 (Sibley Unit) (Sites 1-5): Water Quality Samples at Depth of 0.25 meters (field)*

Transect ID (km)	Temp. (°C)	DO (%)	DO (mg/L)	Conductivity (µS/cm)	TDS (mg/L)	Salinity (ppt)	pH	ORP (mV)
QW01_3.9	7.90	90.50	10.67	174.70	168.35	0.12	6.88	101.00
QW02_2.3	7.90	90.40	10.63	176.70	170.30	0.13	6.42	127.80
QW03_3.1	7.90	90.30	10.60	175.90	169.65	0.12	6.72	19.00
QW04_4.0	8.10	90.30	10.54	176.20	169.00	0.12	8.02	25.00
QW05_2.5	8.20	90.60	10.53	177.20	169.65	0.12	7.86	-27.40

Note: Temperature in degrees Celsius. Dissolved oxygen listed as a percent and mg/L. Conductivity in µS/cm. Total dissolved solids in mg/L. Salinity in parts per thousand. Oxidation reduction potential values in millivolts.

Table A.30 *Transect 1 (Sibley Unit) (Sites 1-5): Water Quality Samples at Depth of 5.0 meters (field)*

Transect ID (km)	Temp. (°C)	DO (%)	DO (mg/L)	Conductivity (µS/cm)	TDS (mg/L)	Salinity (ppt)	pH	ORP (mV)
QW01_3.9	7.90	89.90	10.59	175.60	169.65	0.12	5.30	83.90
QW02_2.3	7.90	89.70	10.57	175.80	169.65	0.12	6.22	92.10
QW03_3.1	7.90	90.00	10.61	175.80	169.65	0.12	7.64	13.40
QW04_4.0	7.90	89.60	10.54	176.00	169.65	0.12	8.02	-3.70
QW05_2.5	8.20	90.00	10.50	176.80	169.65	0.12	7.59	-21.60

Note: Temperatures are in degrees Celsius. Dissolved oxygen values are listed as a percent and mg/L. Conductivities are in µS/cm. Total dissolved solids are mg/L. Salinities are in parts per trillions. Oxidation reduction potential values are in mega volts.

Table A.31 *Transect 1 (Sibley Unit) (Sites 1-5): Water Samples Filtered (Lab)*

Transect ID (km)	P (mg/L)	Nitrite-Nitrate (mg/L)
QW01_3.9	0.04	0.33
QW02_2.3	0.04	0.49
QW03_3.1	0.04	0.43
QW04_4.0	0.03	0.42
QW05_2.5	0.04	0.40

Note: P and Nitrite-Nitrate values in mg/L.

June 2019

Table A.32 *Transect 1 (Sibley Unit) (Sites 1-5): Filter Papers from Water Samples (field and lab)*

Transect ID (km)	Avg. Depth (m)	Velocity (m/s)	SS (mg/L)	D (10)	D (50)	D (90)	N (%)	C (%)	P (%)	Turbidity (NTU)
QW01_3.9	6.30	0.12	39.70	2.65	13.70	1250.00	0.29	3.50	0.11	45
QW02_2.3	4.59	0.23	56.80	2.91	19.70	1460.00	0.26	2.65	0.12	50
QW03_3.1	5.27	0.17	40.90	2.77	15.60	1290.00	0.35	3.58	0.13	50
QW04_4.0	5.28	0.44	38.80	1.03	7.50	507.00	0.36	3.52	0.11	50
QW05_2.5	6.54	0.18	36.20	3.18	18.90	763.00	0.39	3.87	0.10	40

Note: Average depth are in meters. Percentiles are in microns. N, C, and P percentages are from weight. Suspended Sediment are in mg/L. Velocities are in m/s. Turbidities are in NTU.

Table A.33 *Transect 1 (Sibley Unit) (Sites 1-5): Water Quality Samples at Depth of 0.25 meters*

Transect ID (km)	Temp. (°C)	DO (%)	DO (mg/L)	Conductivity (µS/cm)	TDS (mg/L)	Salinity (ppt)	pH	ORP (mV)
QW01_3.9	26.20	79.60	6.41	375.90	238.55	0.17	7.26	1.70
QW02_2.3	25.80	75.40	6.12	373.50	238.55	0.17	7.70	309.80
QW03_3.1	25.90	75.60	6.13	376.00	240.50	0.18	5.95	65.10
QW04_4.0	26.90	75.30	6.10	375.20	239.85	0.18	6.84	43.80
QW05_2.5	26.50	80.20	6.43	396.10	250.25	0.18	6.26	-11.50

Note: Temperatures are in degrees Celsius. Dissolved oxygen values are listed as a percent and mg/L. Conductivities are in µS/cm. Total dissolved solids are mg/L. Salinities are in parts per trillions. Oxidation reduction potential values are in mega volts.

Table A.34 *Transect 1 (Sibley Unit) (Sites 1-5): Water Quality Samples at Depth of 5.0 meters*

Transect ID (km)	Temp. (°C)	DO (%)	DO (mg/L)	Conductivity (µS/cm)	TDS (mg/L)	Salinity (ppt)	pH	ORP (mV)
QW01_3.9	25.90	75.00	6.08	373.20	238.55	0.17	7.49	7.80
QW02_2.3	26.70	74.30	6.04	373.90	239.85	0.18	9.73	61.20
QW03_3.1	25.80	75.00	6.08	376.10	240.50	0.18	6.28	42.70
QW04_4.0	25.80	74.90	6.09	374.90	239.85	0.18	6.60	48.80
QW05_2.5	26.50	79.50	6.38	395.20	250.25	0.18	5.90	25.80

Note: Temperatures are in degrees Celsius. Dissolved oxygen values are listed as a percent and mg/L. Conductivities are in µS/cm. Total dissolved solids are mg/L. Salinities are in parts per trillions. Oxidation reduction potential values are in mega volts.

Table A.35 *Transect 1 (Sibley Unit) (Sites 1-5): Water Samples Filtered (Lab)*

Transect ID (km)	P (mg/L)	Nitrite-Nitrate (mg/L)
QW01_3.9	0.07	0.89
QW02_2.3	0.06	1.32
QW03_3.1	0.06	1.21
QW04_4.0	0.06	0.87
QW05_2.5	0.06	0.71

Note: P and Nitrite-Nitrate values are in mg/L.

Wilkinson County, MS
June 2019

Table A.36 *Transect 3 (Fort Adams) (Sites 9-13): Filter Papers from Water Samples (field and lab)*

Transect ID (km)	Avg. Depth (m)	Velocity (m/s)	SS (mg/L)	D (10)	D (50)	D (90)	N (%)	C (%)	P (%)	Turbidity (NTU)
QW09_17.3	7.58	0.23	51.00	0.07	9.64	1230.00	0.15	1.47	0.12	28
QW10_1.2	3.40	0.43	45.30	2.46	15.1	1570.00	0.36	3.36	0.12	50
QW11_1.3	2.60	0.31	46.70	2.38	7.46	139.00	0.34	3.45	0.10	55
QW12_4.4	4.66	0.62	44.00	0.08	5.72	37.20	0.37	3.82	0.11	50
QW13_18.5	4.73	0.39	35.30	0.06	6.33	875.00	0.33	3.50	0.13	45

Note: Average depth are in meters. Percentiles are in microns. N, C, and P percentages are from weight. Suspended Sediment are in mg/L. Velocities are in m/s. Turbidities are in NTU.

Table A.37 *Transect 3 (Fort Adams) (Sites 9-13): Water Quality Samples at Depth of 0.25 meters*

Transect ID (km)	Temp. (°C)	DO (%)	DO (mg/L)	Conductivity (µS/cm)	TDS (mg/L)	Salinity (ppt)	pH	ORP (mV)
QW09_17.3	26.70	70.10	5.59	340.80	214.50	0.16	6.47	92.60
QW10_1.2	26.00	79.10	6.39	390.50	247.00	0.18	6.50	17.10
QW11_1.3	25.90	78.40	6.34	347.00	243.10	0.18	6.24	12.70
QW12_4.4	26.10	78.70	6.36	381.10	243.10	0.18	6.60	-41.20
QW13_18.5	26.70	75.60	6.10	363.00	230.75	0.17	6.91	-43.20

Note: Temperatures are in degrees Celsius. Dissolved oxygen values are listed as a percent and mg/L. Conductivities are in µS/cm. Total dissolved solids are mg/L. Salinities are in parts per trillions. Oxidation reduction potential values are in mega volts.

Table A.38 *Transect 3 (Fort Adams) (Sites 9-13): Water Quality Samples at Depth of 5.0 meters*

Transect ID (km)	Temp. (°C)	DO (%)	DO (mg/L)	Conductivity (µS/cm)	TDS (mg/L)	Salinity (ppt)	pH	ORP (mV)
QW09_17.3	26.60	68.30	5.46	344.3	217.1	0.16	6.18	87.00
QW10_1.2	26.00	78.60	6.36	376.5	245.7	0.18	6.83	-2.40
QW11_1.3	25.90	78.00	6.32	381.3	243.75	0.18	6.5	-2.30
QW12_4.4	26.00	78.40	6.34	381.2	243.1	0.18	6.8	-46.60
QW13_18.5	26.10	74.70	6.03	362.9	230.75	0.17	7.21	-41.80

Note: Temperatures are in degrees Celsius. Dissolved oxygen values are listed as a percent and mg/L. Conductivities are in µS/cm. Total dissolved solids are mg/L. Salinities are in parts per trillions. Oxidation reduction potential values are in mega volts.

Table A.39 *Transect 3 (Fort Adams) (Sites 9-13): Water Samples Filtered (Lab)*

Transect ID (km)	P (mg/L)	Nitrite-Nitrate (mg/L)
QW09_17.3	0.06	0.61
QW10_1.2	0.05	1.38
QW11_1.3	0.05	1.22
QW12_4.4	0.06	1.04
QW13_18.5	0.06	1.21

Note: P and Nitrite-Nitrate values are in mg/L.

LMR main channel data

Table A.40 *Vicksburg, MS LMR data at Mile 438 (Field and Lab)*

Date	Discharge (m3/s)	Temp (C)	pH	Nitrate + nitrite (mg/L) (Filtered)	Phosphorus (mg/L) (filtered)	Turbidity (NTRU)	SS (mg/L)	Total Carbon (mg/L)(SS)
2/7/19	32200	6.3	7.7	1.14	0.06	58	136	1.4
3/12/19	54900	7.4	7.6	0.997	0.06	53	A 146	1.47
3/29/19	49800	11.7	7.7	1.25	0.07	92	164	3.14
4/17/19	35400	14.9	7.5	1.5	0.09	45	106	2.22
4/29/19	36500	17	7.7	1.25	0.08	31	101	1.57
5/17/19	39900	19.5	7.5	1.5	0.07	37	85	1.69
5/29/19	44500	23.6	7.5	1.5	0.08	43	95	1.77
6/11/19	39600	24.4	7.5	1.56	0.08	88	162	2.31
6/27/19	42500	25.9	8	1.63	0.09	33	76	1.77
7/19/19	39400	28.4	7.8	1.64	0.09	36	95	2.08

Note: Nitrite+nitrate, phosphorus, suspended sediment, and total carbon values are in mg/L.

Table A.41 *St. Francis, LA LMR data (Field and Lab)*

Date	Gage Ht. (m)	Discharge (m3/s)	Temp (C)	pH	Nitrate + nitrite (mg/L) (Filtered)	Phosphorus (mg/L) (filtered)	SS (mg/L)	Total Carbon (mg/L)(suspended sediment)
2/14/19	12.88	26800	7.1	8	1.18	0.067	102	1.4
2/25/19	14.07	29800	8.3	7.9	1.15	0.072	119	1.06
3/11/19	15.84	38500	8.3	7.2	1.05	0.057	92	1.48
3/25/19	15.76	N/A	11.7	7.8	1.07	0.057	82	1.65
4/8/19	14.87	34600	13	7.7	1.38	0.095	130	2.3
4/22/19	14.73	34300	16.2	7.7	1.36	0.089	70	1.41
5/6/19	15.01	N/A	19.2	7	1.29	0.088	79	1.14
5/20/19	13.45	38800	20.8	7.5	N/A	N/A	N/A	N/A
6/3/19	15.61	N/A	24.9	7.7	1.56	0.087	73	1.7
6/17/19	15.77	N/A	25.1	7.1	1.51	0.168	78	2.07
6/24/19	15.4	N/A	26.2	7.7	1.65	0.096	65	1.36
7/8/19	15.3	N/A	27.7	7.5	1.62	0.095	48	1.29
7/22/19	14.73	N/A	28.6	7.4	1.42	0.109	44	2.04

Note: Nitrite+nitrate, phosphorus, suspended sediment, and total carbon values are in mg/L

REFERENCES

Anding, M.G., Pierce, P.W. and Elliott, C.M. 1968. Hydraulic Analysis of Channels and Evaluation of Dike Systems, Report 1-2 (Mile 541.5-550 AHP), Upper Greenville Reach, US Army Corps of Engineers, Vicksburg, Mississippi.

Angel, J.R., and Huff, F.A., 1997, Changes in heavy rainfall in Midwestern United States: Journal of Water Resources Planning and Management, doi: 10.1061/(ASCE)0733-9496(1997)123:4(246).

Allison, M.A., Demas, C.R., Ebersole, B.A., Kleiss, B.A., Little, C.D., Meselhe, E.A., Powell, N.J., Pratt, T.C., and Vosburg, B.M., 2012, A water and sediment budget for the lower Mississippi-Atchafalaya River in flood years 2008-2010: Implications for sediment discharge to the oceans and coastal restoration in Louisiana: Journal of Hydrology, doi: 10.1016/j.jhydrol.2012.02.020.

Allen, J.R.L., 1965, A Review of the Origin and Characteristics of Recent Alluvial Sediments: Sedimentology, doi: 10.1111/J.1365-3091.1965.tb01561.x.

Alexander, R.B., Smith, R.A., and Schwarz, G.E., 2000, Effect of stream channel size on the delivery of nitrogen to the Gulf of Mexico: Nature, doi: 10.1038/35001562.

Aslan, A., and W. J. Autin. 1999. "Evolution of the Holocene Mississippi River Floodplain, Ferriday, Louisiana; Insights on the Origin of Fine-Grained.

Autin, W.J., Burn, S.F., Miller, B.J., Saucier, R.T., and Snead, J.I., 1991, Quaternary geology of the lower Mississippi Valley, in Morrison, R.B., ed., Quaternary nonglacial geology: Conterminous U.S.: Boulder, Colorado, Geological Society of America, Geology of North America, v. K-2, p. 547–582.

Bluck, B.J., 1971, Sedimentation in the meandering river Endrick: Scottish Journal of Geology, doi: 10.1144/sjg07020093.

Blum, M.D., and Roberts, H.H., 2009, Drowning of the Mississippi Delta due to insufficient sediment supply and global sea-levelrise: Nature Geoscience, doi: 10.1038/ngeo553.

Bourne, J., 2000, Louisiana's vanishing wetlands: Going, going: Science, doi: 10.1126/science.289.5486.1860.

Brady NC, Weil RR. 1999. The Nature and Property of Soils. Upper Saddle Hall, NJ: Prentice Hall

Brierley, G.J., Ferguson, R.J., and Woolfe, K.J., 1997, What is a fluvial levee? Sedimentary Geology, doi: 10.1016/S0037-0738(97)00114-0.

Brinson, M.M., Lugo, A.E., and Brown, S., 1981, Primary Productivity, Decomposition and Consumer Activity in Freshwater Wetlands: Annual Review of Ecology and Systematics, doi: 10.1146/annurev.es.12.110181.001011.

Cahoon, D.R., Perez, B.C., Segura, B.D., and Lynch, J.C., 2011, Elevation trends and shrink-swell response of wetland soils to flooding and drying: Estuarine, Coastal and Shelf Science, doi: 10.1016/j.ecss.2010.03.022.

Camillo, C. A. (2012). Divine providence: The 2011 flood in the Mississippi River and tributaries project. Mississippi River Commission.

Changnon, S.A., 2001, Thunderstorm rainfall in the conterminous United States: Bulletin of the American Meteorological Society, doi: 10.1175/1520-0477(2001)082<1925:TRITCU>2.3.CO;2.

Church, J. A., Gregory, J. M., Huybrechts, P., Kuhn, M., Lambeck, K., Nhuan, M. T., ... & Woodworth, P. L. (2001). Changes in sea level. In , in: JT Houghton, Y. Ding, DJ Griggs, M. Noguer, PJ Van der Linden, X. Dai, K. Maskell, and CA Johnson (eds.): Climate Change 2001: The Scientific Basis: Contribution of Working Group I to the Third Assessment Report of the Intergovernmental Panel (pp. 639-694).

Coleman, J.M., 1966, Ecological Changes in Massive Fresh-Water Clay Sequence: ABSTRACT: AAPG Bulletin, doi: 10.1306/5d25b737-16c1-11d7-8645000102c1865d.

Coleman, J.M., 1969, Brahmaputra river: Channel processes and sedimentation: Sedimentary Geology, doi: 10.1016/0037-0738(69)90010-4.

Coleman, J.M., Huh, O.K., and Braud, D.W., 2008, Wetland loss in world deltas: Journal of Coastal Research, doi: 10.2112/05-0607.1.

Collinson, J. D. 1996. Alluvial sediments. In Sedimentary environments: Processes, facies and stratigraphy, -third edition. ed. H.G. Reading, 37-82. Oxford: Blackwell Science.

Cooper, C.M., and McHenry, J.R., 1989, Sediment accumulation and its effects on a Mississippi River oxbow lake: Environmental Geology and Water Sciences, doi: 10.1007/BF01666569.

Costa, J. E., & Jarrett, R. D. (2008). An evaluation of selected extraordinary floods in the United States reported by the US Geological Survey and implications for future advancement of flood science.

Costanza, R., D'Arge, R., De Groot, R., Farber, S., Grasso, M., Hannon, B., Limburg, K., Naeem, S., O'Neill, R. V., Paruelo, J., Raskin, R.G., Sutton, P., and Van Den Belt,

M., 1997, The value of the world's ecosystem services and natural capital: Nature, doi: 10.1038/387253a0.

Cuffney, T.F., 1988, Input, Movement and Exchange of Organic Matter within a Subtropical Coastal Black Water River-Flood Plain System: Freshwater Biology, doi: 10.1111/j.1365-2427.1988.tb00353.x.

Cayan, D.R., Kammerdiener, S.A., Dettinger, M.D., Caprio, J.M., and Peterson, D.H., 2001, Changes in the Onset of Spring in the Western United States: Bulletin of the American Meteorological Society, doi: 10.1175/1520-0477(2001)082<0399:CITOOS>2.3.CO;2.

Davis, Broderick E. "A Guide to the Proper Selection and Use of Federally Approved Sediment and Water-Quality Samplers." U.S. Geological Survey Open-File Report 2005-1087, 2005.

Enfield, D.B., Mestas-Nuñez, A.M., and Trimble, P.J., 2001, The Atlantic multidecadal oscillation and its relation to rainfall and river flows in the continental U.S: Geophysical Research Letters, doi: 10.1029/2000GL012745.

Fagherazzi, S., Edmonds, D.A., Nardin, W., Leonardi, N., Canestrelli, A., Falcini, F., Jerolmack, D.J., Mariotti, G., Rowland, J.C., and Slingerland, R.L., 2015, Dynamics of river mouth deposits: Reviews of Geophysics, doi: 10.1002/2014RG000451.

Farrell, K.M., 1987, Sedimentology and Facies Architecture of Overbank Deposits of the Mississippi River, False River Region, Louisiana, in Recent Developments in Fluvial Sedimentology, doi: 10.2110/Pec.87.39.0111.

Fisk, H.N., 1944, Geological investigations of the alluvial valley of the lower Mississippi River: Vicksburg, Mississippi, U.S. Army Corps of Engineers, Mississippi River Commission.

Fisk, H.N., 1947. Fine grained alluvial deposits and their effects on the Mississippi River activity. U.S. Waterways Experimental Station.

Forshay, K.J., and Stanley, E.H., 2005, Rapid nitrate loss and denitrification in a temperate river floodplain: Biogeochemistry, doi: 10.1007/s10533-004-6016-4.

Gagliano, S.M.; Kwon, H.J., and Van Beek, J.L., 1970. Deterioration and restoration of coastal wetlands. Twelfth International Conference on Coastal Engineering, Sept. 13-17, Washington D.C.

Gagliano, S.M., Meyer-arendt, K.J., and Wicker, K.M., 1981, Land loss in the Mississippi River Deltaic Plain: Gulf Coast Associaction of Geological Societies Transactions,.

Gambrell, R.P., and Patrick Jr, W.H., 1978, Chemical and microbiological properties of anaerobic soils and sediments, *in* Plant Life in Anaerobic Environments.

Gomez, B., Phillips, J.D., Magilligan, F.J., James, L.A., 1997. Floodplain sedimentation and sensitivity: summer 1993 flood, Upper Mississippi River Valley. Earth Surface Processes and Landforms 22, 923–936.

Groisman, P.Y., Knight, R.W., and Karl, T.R., 2001, Heavy precipitation and high streamflow in the contiguous United States: Trends in the twentieth century: Bulletin of the American Meteorological Society, doi: 10.1175/1520-0477(2001)082<0219:HPAHSI>2.3.CO;2.

Groisman, Pavel Ya, et al. "Contemporary climate changes in high latitudes of the Northern Hemisphere: Daily time resolution." 14th Symposium on Global Change and Climate Variations. 2003.

Gutreuter, S., Bartels, A.D., Irons, K., and Sandheinrich, M.B., 1999, Evaluation of the flood-pulse concept based on statistical models of growth of selected fishes of the Upper Mississippi River system: Canadian Journal of Fisheries and Aquatic Sciences, doi: 10.1139/f99-161.

Heitmuller, F.T., Hudson, P.F., and Kesel, R.H., 2017, Overbank sedimentation from the historic A.D. 2011 flood along the Lower Mississippi River, USA: Geology, doi: 10.1130/G38546.1.

Horowitz, A.J., 2010, A quarter century of declining suspended sediment fluxes in the Mississippi River and the effect of the 1993 flood: Hydrological Processes, doi: 10.1002/hyp.7425.

Howarth, R.W., Billen, G., Swaney, D., Townsend, A., Jaworski, N., Lajtha, K., Downing, J.A., Elmgren, R., Caraco, N., Jordan, T., Berendse, F., Freney, J., Kudeyarov, V., Murdoch, P., et al., 1996, Regional nitrogen budgets and riverine N & P fluxes for the drainages to the North Atlantic Ocean: Natural and human influences: Biogeochemistry, doi: 10.1007/BF02179825.

Hudson, P. F., and R. H. Kessel. 2000. "Channel Migration and Meander-Bend Curvature in the Lower Mississippi River prior to Major Human Modification." Geology 28 (6): 531-34. doi:10.1130/0091-7613(2000)282.0.CO;2.

Hudson, P.F., and Heitmuller, F.T., 2003, Local- and watershed-scale controls on the spatial variability of natural levee deposits in a large fine-grained floodplain: Lower Pánuco Basin, Mexico: Geomorphology, doi: 10.1016/S0169-555X(03)00155-7.

Hudson, P.F., Heitmuller, F.T., and Leitch, M.B., 2012, Hydrologic connectivity of oxbow lakes along the lower Guadalupe River, Texas: The influence of geomorphic

and climatic controls on the “ flood pulse concept”: Journal of Hydrology, doi: 10.1016/j.jhydrol.2011.10.029.

Hudson, P.F., Middelkoop, H., and Stouthamer, E., 2008, Flood management along the Lower Mississippi and Rhine Rivers (The Netherlands) and the continuum of geomorphic adjustment: Geomorphology, v. 101, p. 209–236.

Hudson, P. F., M. A. Sounny-Slittine, and M. Lafevor. 2013. "A New Longitudinal Approach to Assess Hydrologic Connectivity: Embanked Floodplain Inundation along the Lower Mississippi River." Hydrological Processes 27 (15): 2187-96. doi:10.1002/hyp.9838.

Iseya F, Ikeda H. 1989. Sedimentation in coarse-grained sand-bedded meanders: distinctive deposition of suspended sediment. In Sedimentary Facies in the Active Plate Margin, Taira A, Masuda F (eds). Terra Scientific Publishing (TERRAPUB): Tokyo.

Junk, W.J., Bayley, P.B., and Sparks, R.E., 1989, The flood pulse concept in river-floodplain systems, in Dodge, D.P., ed., Proceedings of the International Large River Symposium: Canadian Special Publication of Fisheries and Aquatic Sciences 106, p. 110–127.

Justić, D., Rabalais, N.N., Eugene Turner, R., and Wiseman, W.J., 1993, Seasonal coupling between riverborne nutrients, net productivity and hypoxia: Marine Pollution Bulletin, doi: 10.1016/0025-326X(93)90620-Y.

Karl, T.R., Knight, R.W., Easterling, D.R., and Quayle, R.G., 1996, Indices of climate change for the United States: Bulletin of the American Meteorological Society, doi: 10.1175/1520-0477(1996)077<0279:IOCCFT>2.0.CO;2.

Kerr, R.A., 2000, A North Atlantic climate pacemaker for the centuries: Science, doi: 10.1126/science.288.5473.1984.

Kesel, R.H., Dunne, K.C., McDonald, R.C., Allison, K.R., and Spicer, B.E., 1974, Lateral erosion and overbank deposition on the Mississippi River in Louisiana caused by 1973 flooding: Geology, doi: 10.1130/0091-7613(1974)2<461:LEAODO>2.0.CO;2.

Kesel, R.H., 2003, Human modifications to the sediment regime of the Lower Mississippi River flood plain: Geomorphology, doi: 10.1016/S0169-555X(03)00159-4.

Khan, N.S., Horton, B.P., McKee, K.L., Jerolmack, D., Falcini, F., Enache, M.D., and Vane, C.H., 2013, Tracking sedimentation from the historic A.D. 2011 Mississippi River flood in the deltaic wetlands of Louisiana, USA: Geology, doi: 10.1130/G33805.1.

Kleinhans, M.G., Ferguson, R.I., Lane, S.N., and Hardy, R.J., 2013, Splitting rivers at their seams: Bifurcations and avulsion: Earth Surface Processes and Landforms, doi: 10.1002/esp.3268.

Kleinhans, M.G., Jagers, H.R.A., Mosselman, E., and Sloff, C.J., 2008, Bifurcation dynamics and avulsion duration in meandering rivers by one-dimensional and three-dimensional models: Water Resources Research, doi: 10.1029/2007WR005912.

Knox, J. C. (2000). Sensitivity of modern and Holocene floods to climate change. Quaternary Science Reviews, 19(1-5), 439-457.

Knox, R.L., and Latrubesse, E.M., 2016, A geomorphic approach to the analysis of bedload and bed morphology of the Lower Mississippi River near the Old River Control Structure: Geomorphology, doi: 10.1016/j.geomorph.2016.05.034.

Kraus, M.J., and Aslan, A., 1993, Eocene hydromorphic paleosols: significance for interpreting ancient floodplain processes: Journal of Sedimentary Petrology, doi: 10.1306/D4267B22-2B26-11D7-8648000102C1865D.

Leopold, L.B., Wolman, M.G., and Miller, J.P., 1964, Fluvial processes in geomorphology: San Francisco, W.H. Freeman.

Leming, T.D., and Stuntz, W.E., 1984, Zones of coastal hypoxia revealed by satellite scanning have implications for strategic fishing: Nature, doi: 10.1038/310136a0.

Lettenmaier, D.P., Wood, E.F., and Wallis, J.R., 1994, Hydro-climatological trends in the continental United States, 1948-88: Journal of Climate, doi: 10.1175/1520-0442(1994)007<0586:HCTITC>2.0.CO;2.

Lohrenz, S.E., Redalje, D.G., Cai, W.J., Acker, J., and Dagg, M., 2008, A retrospective analysis of nutrients and phytoplankton productivity in the Mississippi River plume: Continental Shelf Research, v. 28, n. 12, p. 1,466–1,475.

Magilligan, F.J., Phillips, J.D., James, A.J., Gomez, B., 1998. Geomorphic and sedimentological controls on the effectiveness of an extreme flood. The Journal of Geology 106, 87–95.

McFarlan, E., JR., 1961, Radiocarbon dating of Late Quaternary deposits, south Louisiana: Geological Society of America, Bulletin, v. 72, p. 129–158.

Meade, R.H., and Moody, J.A., 2010, Causes for the decline of suspended-sediment discharge in the Mississippi River system, 1940-2007: Hydrological Processes, doi: 10.1002/hyp.7477.

Meyers, P.A., 1997, Organic geochemical proxies of paleoceanographic, paleolimnologic, and paleoclimatic processes, *in* Organic Geochemistry, doi: 10.1016/S0146-6380(97)00049-1.

Miall, A.D., 1985, Architectural-element analysis: A new method of facies analysis applied to fluvial deposits: Earth Science Reviews, doi: 10.1016/0012-8252(85)90001-7.

Middelkoop, H., and Asselman, N.E.M., 1998, Spatial variability of floodplain sedimentation at the event scale in the Rhine-Meuse Delta, the Netherlands: Earth Surface Processes and Landforms, doi: 10.1002/(SICI)1096-9837(199806)23:6<561::AID-ESP870>3.0.CO;2-5.

Mississippi Department of Environmental Quality, Surface Geology:, https://www.mdeq.ms.gov/geology/work-areas/surface-geology/

Moody, R.H., and Meade, J.A., 2010, Causes for the decline of suspended-sediment discharge in the Mississippi River system, 1940–2007: Hydrological Processes, v. 24, p. 35–49.

Moore, N.R. 1972. Improvement of the Lower Mississippi River and Tributaries, 1931-1972. Vicksburg, MS: U.S. Army Corps of Engineers, Mississippi River Commission.

Mossa, J., 1996, Sediment dynamics in the lowermost Mississippi River: Engineering Geology, v. 45, n. 1–2, p. 457–479.

Mossa, J., 1989: Hysteresis and nonlinearity of discharge-sediment relationships in the Atchafalaya and lower Mississippi. In: Hadley, R.F and ongley, E.D. (eds): Sediment and the environment (Proceedings of the Baltimore symposium, May 1989). IAHS Publication 184: 105-112.

Nanson, G.C., and Croke, J.C., 1992, A genetic classification of floodplains: Geomorphology, doi: 10.1016/0169-555X(92)90039-Q.

Noe, G.B., and Hupp, C.R., 2005, Carbon, nitrogen, and phosphorus accumulation in floodplains of Atlantic Coastal Plain rivers, USA: Ecological Applications, doi: 10.1890/04-1677.

North, C.P., and Davidson, S.K., 2012, Unconfined alluvial flow processes: Recognition and interpretation of their deposits, and the significance for palaeogeographic reconstruction: Earth-Science Reviews, doi: 10.1016/j.earscirev.2011.11.008.

Olsen, J.R., Stedinger, J.R., Matalas, N.C., and Stakhiv, E.Z., 1999, Climate variability and flood frequency estimation for the Upper Mississippi and Lower Missouri

Rivers, *in* Journal of the American Water Resources Association, doi: 10.1111/j.1752-1688.1999.tb04234.x.

Pavela, J.S., Ross, J.L., and Chittenden, M.E., 1983, Sharp Reductions in Abundance of Fishes and Benthic Macroinvertebrates in the Gulf of Mexico Off Texas Associated with Hypoxia: Northeast Gulf Science, doi: 10.18785/negs.0602.11.

Peierls, B.L., Caraco, N.F., Pace, M.L., and Cole, J.J., 1991, Human influence on river nitrogen [5]: Nature, doi: 10.1038/350386b0.

Pinay, G., Fabre, A., Vervier, P., and Gazelle, F., 1992, Control of C,N,P distribution in soils of riparian forests: Landscape Ecology, doi: 10.1007/BF00130025.

Pizzuto, J.E., 1987, Sediment diffusion during overbank flows: Sedimentology, doi: 10.1111/j.1365-3091.1987.tb00779.x.

Poff, N.L., Allan, J.D., Bain, M.B., Karr, J.R., Prestegaard, K.L., Richter, B.D., Sparks, R.E., and Stromberg, J.C., 1997, The natural flow regime: a paradigm for river conservation and restoration: BioScience. 47(11), 769–784.

Pokryfki, L., and Randall, R.E., 1987, Nearshore hypoxia in the bottom water of the northwestern gulf of Mexico from 1981 to 1984: Marine Environmental Research, doi: 10.1016/0141-1136(87)90081-X.

Rabalais, Nancy N., R. Eugene Turner, Dubravko Justić, Quay Dortch, William J. Wiseman, Barun K. Sen Gupta, and Dubravko Justic. 1996. "Nutrient Changes in the Mississippi River and System Responses on the Adjacent Continental Shelf." Estuaries 19 (2): 386. doi:10.2307/1352458.

Rabalais, N.N., Turner, R.E., and Wiseman, W.J., 2001, Hypoxia in the Gulf of Mexico: Journal of Environmental Quality, doi: 10.2134/jeq2001.302320x.

Rabalais, Nancy N., R. Eugene Turner, and William J. Wiseman. 2002. “Gulf of Mexico Hypoxia, A.K.A. ‘The Dead Zone.’” Annual Review of Ecology and Systematics. doi:10.1146/annurev.ecolsys.33.010802.150513.

Renaud, M.L., 1983, Hypoxia in Louisiana Coastal Waters during 1983: Implications for Fisheries: Fishery Bulletin,.

Roberts, J.D., 1997, Geographic variation in calls of males and determination of species boundaries in tetraploid frogs of the Australian genus Neobatrachus (Myobatrachidae): Australian Journal of Zoology, doi: 10.1071/ZO96006.

Rosenqvist, Å., Forsberg, B.R., Pimentel, T., Rauste, Y.A., and Richey, J.E., 2002, The use of spaceborne radar data to model inundation patterns and trace gas emissions in

the central Amazon floodplain: International Journal of Remote Sensing, doi: 10.1080/01431160110092911.

Salo, J., Kalliola, R., Häkkinen, I., Mäkinen, Y., Niemelä, P., Puhakka, M., and Coley, P.D., 1986, River dynamics and the diversity of Amazon lowland forest: Nature, doi: 10.1038/322254a0.

Saucier, R.T., 1994, Geomorphology and Quaternary geologic history of the lower Mississippi

Scavia, D., Rabalais, N.N., Turner, R.E., Justić, D., and Wiseman, W.J., 2003, Predicting the response of Gulf of Mexico hypoxia to variations in Mississippi River nitrogen load: Limnology and Oceanography, doi: 10.4319/lo.2003.48.3.0951.

Schramm, H.L., Cox, M.S., Tietjen, T.E., and Ezell, A.W., 2009, Nutrient dynamics in the lower Mississippi river floodplain: Comparing present and historic hydrologic conditions: Wetlands, doi: 10.1672/08-62.1.

Schramm, A., De Beer, D., Gieseke, A., and Amann, R. (2000) Microenvironments and distribution of nitrifying bacteria in a membrane-bound biofilm. Environ Microbiol 2: 680–686

Shen, Z., Törnqvist, T.E., Mauz, B., Chamberlain, E.L., Nijhuis, A.G., and Sandoval, L., 2015, Episodic overbank deposition as a dominant mechanism of floodplain and delta-plain aggradation: Geology, doi: 10.1130/G36847.1.

Sloff, K., and Mosselman, E., 2012, Bifurcation modelling in a meandering gravel-sand bed river: Earth Surface Processes and Landforms, doi: 10.1002/esp.3305.

Smith, Lawson M. 1996. "Fluvial Geomorphic Features of the Lower Mississippi Alluvial Valley." Engineering Geology 45: 139-65. doi:10.1016/S0013-7952(96)00011-7.

Smith, L.M., and Winkley, B.R., 1996, The response of the Lower Mississippi River to river engineering: Engineering Geology, v. 45, p. 433–455.

Syvitski, J.P.M., Kettner, A.J., Overeem, I., Hutton, E.W.H., Hannon, M.T., Brakenridge, G.R., Day, J., Vörösmarty, C., Saito, Y., Giosan, L., and Nicholls, R.J., 2009, Sinking deltas due to human activities: Nature Geoscience, doi: 10.1038/ngeo629.

Turner, R.E., and Rabalais, N.N., 1991, Changes in Mississippi River Water Quality This Century: BioScience, doi: 10.2307/1311453.

U.S. Army Corps of Engineers, The Mississippi Drainage Basin:, https://www.mvn.usace.army.mil/Missions/Mississippi-River-Flood-Control/Mississippi-River-Tributaries/Mississippi-Drainage-Basin/

U.S. Army Corps of Engineers, 2020, RiverGages.com: Mississippi River @ Natchez, MS: https://rivergages.mvr.usace.army.mil/WaterControl/stationinfo2.cfm?sid=CE4103F4&fid=NTZM6&dt=S

U.S. Army Corps of Engineers, 2020, RiverGages.com: Mississippi River nr St. Francisville (01145): https://rivergages.mvr.usace.army.mil/WaterControl/stationinfo2.cfm?sid=01145&fid=&dt=S

U.S. Army Corps of Engineers, 2020, RiverGages.com: Mississippi River @ Vicksburg, MS: https://rivergages.mvr.usace.army.mil/WaterControl/stationinfo2.cfm?sid=CE40FF58&fid=VCKM6&dt=S

USGS, 2020, National Water Information System: Web Interface: USGS 322023090544500 MISSISSIPPI RIVER ABOVE VICKSBURG AT MILE 438, MS: https://nwis.waterdata.usgs.gov/nwis/qwdata?site_no=322023090544500&agency_cd=USGS&inventory_output=0&rdb_inventory_output=file&TZoutput=0&pm_cd_compare=Greater%20than&radio_parm_cds=all_parm_cds&format=html_table&qw_attributes=0&qw_sample_wide=wide&rdb_qw_attributes=0&date_format=YYYY-MM-DD&rdb_compression=file&submitted_form=brief_list

USGS, 2020, National Water Information System: USGS 07295100 Mississippi River at TarbertLanding,MS: https://waterdata.usgs.gov/nwis/inventory/?site_no=07295100

USGS, 2020, National Water Information System: Web Interface: USGS 07373420 MISSISSIPPI R NR ST. FRANCISVILLE, LA: https://waterdata.usgs.gov/nwis/inventory/?site_no=07373420

Walling, D.E., and He, Q., 1998, The spatial variability of overbank sedimentation on river floodplains: Geomorphology, doi: 10.1016/S0169-555X(98)00017-8.

Ward, J.V., and Stanford, J.A., 1995, Ecological connectivity in alluvial river ecosystems and its disruption by flow regulation: Regulated Rivers: Research and Management, v. 11, n. 1, p. 105–119.

Welch, H. L., & Barnes, K. K. (2013). Streamflow characterization and summary of water-quality data collection during the Mississippi River flood, April through July 2011. US Department of the Interior, US Geological Survey.

Welcomme RL. 1979. Fisheries ecology of floodplain rivers. New York: Longman.

Welder, F. A. 1959. Processes of Deltaic Sedimentation in the Lower Mississippi River. Technical Report 12, Coastal Studies Institute, Louisiana State University, Baton Rouge, Louisiana.

Willis, B.J., and Behrensmeyer, A.K., 1994, Architecture of Miocene overbank deposits in northern Pakistan: Journal of Sedimentary Research B: Stratigraphy & Global Studies, doi: 10.1306/d4267f46-2b26-11d7-8648000102c1865d.

Wiseman, W.J., Rabalais, N.N., Turner, R.E., Dinnel, S.P., and Macnaughton, A., 1997, Seasonal and interannual variability within the Louisiana coastal current: Stratification and hypoxia: Journal of Marine Systems, doi: 10.1016/S0924-7963(96)00100-5.

Wolman, M.G., and Gerson, R., 1978, Relative scales of time and effectiveness of climate in watershed geomorphology: Earth Surface Processes, doi: 10.1002/esp.3290030207.

Wolman, M.G., and Miller, J.P., 1960, Magnitude and frequency of forces in geomorphic processes: Journal of Geology, v. 68, p. 54–74.

Yuill, B.T., Khadka, A.K., Pereira, J., Allison, M.A., and Meselhe, E.A., 2016, Morphodynamics of the erosional phase of crevasse-splay evolution and implications for river sediment diversion function: Geomorphology, doi: 10.1016/j.geomorph.2016.02.005.